Synthesis, Characterization and Application of Pyrimidopteridine based Photocatalysts

Dissertation

in monographischer Form

zur Erlangung des akademischen Grades

Doctor rerum naturalium (Dr. rer. nat.)

der Mathematisch-Naturwissenschaftlichen Fakultät

der Universität Rostock

vorgelegt von

Richy Hauptmann

Geboren am 15.04.1992 in Berlin

Rostock, den 16.10.2020

https://doi.org/10.18453/rosdok_id00002964

Die vorliegende Arbeit entstand in der Zeit von September 2017 bis Oktober 2020 am Leibniz-Institut für Katalyse e.V. an der Universität Rostock unter der Betreuung von Dr. Jola Pospech.

1. Gutachter: Prof. Johannes Gerardus de Vries, Leibniz-Institut für Katalyse e. V. an der Universität Rostock

2. Gutachter: Jun.-Prof. Dr. Ivana Fleischer, Eberhard Karls Universität Tübingen

Jahr der Einreichung: 2020

Jahr der Verteidigung: 2021

Erklärung

Hiermit versichere ich an Eides statt, dass ich die vorliegende Arbeit selbständig angefertigt und ohne fremde Hilfe verfasst habe. Dazu habe ich keine außer den von mir angegebenen Hilfsmitteln und Quellen verwendet. Die aus den benutzten Werken inhaltlich und wörtlich entnommenen Stellen sind als solche kenntlich gemacht.

Richy Hauptmann

Rostock, den 16.10.2020

Danksagung

Hiermit möchte ich mich zunächst bei Dr. Jola Pospech bedanken, dass ich meine Dissertation in ihrer Gruppe anfertigen durfte. Darüber hinaus möchte ich mich für die Möglichkeit bedanken, dass ich mein Wissen auf diversen Konferenzen erweitern und vertiefen konnte. Prof. Johannes Gerardus de Vries möchte ich für die Übernahme der Erstgutachten und insbesondere der Betreuung danken. Außerdem möchte ich der gesamten analytischen Abteilung des LIKATs danken ohne diese wäre es nicht möglich gewesen die hier präsentierten Ergebnisse zu erzielen. Jabor, Haijun, Annette und Miguel möchte ich für die Kooperation in den verschiedenen Projekten danken. Nils Rockstroh möchte ich hier ebenfalls noch namentlich nennen.

Am meisten möchte ich aber meiner Familie meinen Freunden und meinen Kollegen danken. Firas und Tobi möchte ich für die großartige Arbeitsatmosphäre danken, es war immer spaßig mit euch und ich habe sehr viel dank euch dazu gelernt. Chris möchte ich danken, dass er mich stehts motiviert hat und immer ein offenes Ohr für mich hatte. Ohne die emotionale Unterstützung und die fachlichen Diskussionen mit Lars wäre ich nicht in der Lage gewesen diese Arbeit anzufertigen. Danke Lars, für alles. Meinen Eltern möchte ich für das in mich gesetzte Vertrauen und ihre Unterstützung danken. Natalie, Elias, Gigi und Giusy möchte ich auch vom ganzen Herzen danken. Egal wie schlecht es mir geht ihr schafft es immer ein Lächeln auf mein Gesicht zu zaubern.

Kurzfassung

Die Entwicklung von neuen Photokatalysatoren ist ein attraktiver Weg, um bisher nicht erschlossene Reaktionspfade zu entdecken. Insbesondere das Entwickeln von günstigen und einfach zugänglichen organischen Photokatalysatoren ist wichtig. Üblicherweise werden Übergangsmetall basierte Katalysatoren verwendet. Diese Katalysatoren sollten aufgrund ihres hohen Preises durch günstigere Alternativen ersetzt werden. Diese Dissertation beschäftigt sich mit der Synthese, Charakterisierung und Anwendung von Pyrimidopteridin *N*-Oxid (PPTNO) basierten organischen Photokatalysatoren. Zuerst wurden verschieden substituierte PPTNOs synthetisiert und anschließend wurde eine gründliche Charakterisierung dieser Verbindungen mittels verschiedenster analytischer Methoden durchgeführt. Dies diente der Bestimmung der photophysikalischen und elektrochemischen Eigenschaften.

PPTNOs sind strukturell verwandt mit den Flavinen und teilen deren Reaktivität in bestimmten Maßen. Diese Ähnlichkeit wurde in Isomerisierungs- und Oxidationsreaktionen gezeigt. PPTNOs sind sehr potente Photokatalysatoren die die Umsetzung von schwer zu oxidieren Verbindungen, wie einfach substitutierten Aminen, ermöglichen. Diese Eigenschaft wurde in einer photokatalytischen Hydroaminierung von Stilbenen mit einfach substituierten Aminen gezeigt. Zuletzt wurde eine photokatalytische Trifluormethylierung untersucht, um die Anwendbarkeit dieser Katalysatoren zu unterstreichen. Kernpunkt dieses Projektes war die Verwendung von Trifluoressigsäureanhydrid als Trifluormethylierungsreagenz, da dieses günstig und einfach zugänglich ist.

Abstract

The development of new photocatalysts is an attractive way to access new reactivities. Especially the employment of inexpensive and easily accessible organic photocatalysts is important. Commonly used transition-metal based catalysts suffer from a high price and should therefore be replaced by cheaper alternatives. The present thesis describes the synthesis, characterization, and application of pyrimidopteridine *N*-oxide (PPTNO) based organic photocatalysts. Multiple types of PPTNOs were synthesized showing a change in substitution pattern. A thorough characterization using different analytical methods was performed to evaluate the photophysical and electrochemical properties.

PPTNOs are structurally related to flavins and share their reactivity to a certain degree. This similarity was shown in isomerization and oxidation reactions. PPTNOs are very potent photocatalysts that even enable oxidation reactions of mono substituted amines. These amines have a high oxidation potential and their application in photochemical transformations is therefore underexplored. The potency of the PPTNOS was revealed in a photocatalytic hydroamination using stilbenes and mono substituted amines. Subsequently a photocatalytic trifluoromethylation was investigated to further show the applicability of these photocatalysts. The focus of this project was the use trifluoroacetic anhydride as cheap and easily accessible trifluoromethylation agent.

List of Abbreviation

Ac	Acetyl	LAH	Lithium aluminium hydride
BET	Back electron transfer	LED	Light-emitting diode
CAA	Cyanoacetic acid	LUMO	Lowest unoccupied molecular orbital
CT	Charge-transfer	mCPBA	Meta-chloroperoxybenzoic acid
CV	Cyclic voltammetry	MS	Mass spectroscopy
DCA	Dicyanoanthracene	MTO	Methyltrioxorhenium
DCM	Dichloromethane	NCR	nitrogen-centered radical
DMF	N,N-Dimethylformamide	PCET	Proton coupled electron transfer
DMA	Dimethyl aniline	PC	Photocatalyst
DMSO	Dimethylsulfoxid	PET	Photoinduced electron transfer
DPV	Differential pulse voltammetry	PIDA	phenyliodine (III) diacetate
DFT	Density functional theory	PPT	Pyrimidopteridine
EDG	Electron donating group	PPTNO	Pyrimidopteridine *N*-oxide
EI	Electron ionization	RFTA	Riboflavine tetraacetae
EPR	Electron paramagnetic resonance	SET	Single electron transfer
EWG	Electron withdrawing group	TDDFT	Time dependent density functional theory
FID	Flame ionization detector	TEMPO	2,2,6,6-Tetramethylpiperidinyloxyl
GC	Gas chromatography	TFA	Trifluoroacetic acid
HAT	Hydrogen atom transfer	TFAA	Trifluoroacetic anhydride
HFIP	Hexafluoroisopropanol	TLC	Thin layer chromatography
HOMO	Highest occupied molecular orbital	THF	Tetrahydrofuran
IC	Internal conversion	TPT	Triphenylpyrillium
ISC	Intersystem crossing	UV-Vis	Ultraviolet-visible

Table of contents

1 Introduction **1**

1.1 The development of photochemistry 1

1.2 Photochemical processes 3

1.3 Photoredox catalysis: Background and Application 5

1.4 Pyrimidopteridine *N*-oxides as oxygen atom transfer reagent 8

1.5 Design and characterization of photocatalysts 13

2 Motivation and aim **19**

3 Synthesis, characterization and first application of PPTNO based photocatalysts **20**

3.1 Synthesis 20

3.2 Photophysical, electrochemical and computational characterization 21

3.3 Evaluation of PPTNO based photocatalysts 25

3.4 Photoisomerization of cinnamic acid derivatives 26

3.5 Photooxidative cyclization of biphenylcarboxylic acid 28

3.6 Extension of the catalyst library, CyPPTNO 29

3.7 Oxidative decarboxylation of Boc-Proline 30

3.8 Extension of the catalyst library, PPT 33

3.9 Oxidation of PPT based compounds to obtain PPTNOs 36

3.10 Extension of the catalyst library, synthesis of sulfur containing PPTNOS 38

4 Photocatalytic, intermolecular hydroamination of stilbenes with monosubstituted amines **44**

4.1 Introduction 44

4.2 Results and discussion 48

4.3 Reaction scope for the hydroamination of stilbenes using monosubstituted amines 53

4.4 Stern-Volmer quenching studies 58

4.5 EPR measurements 60

4.6 Stability of α-chiral centers 61

4.7 DFT calculations 62

4.8 Proposed mechanism. 63

4.9 Deprotection of hydroamination products 64

4.10 Summary and Outlook 65

5 Photocatalytic trifluoromethylation of aromatic compounds **66**

5.1 Introduction 66

5.2 Photocatalytic trifluoromethylation of arenes. Optimization of the reaction conditions. 69

5.3 Mechanistic Consideration 73
5.4 Substrate scope for the photocatalytic trifluoromethylation of arenes 77
5.5 Summary and Outlook 82
6 Experimental Section 84
6.1 General Remarks 84
6.2 Solvents 84
6.3 Chromatography 84
6.4 Vacuum 84
6.5 Infrared Spectroscopy 84
6.6 Nuclear Magnetic Resonance Spectroscopy 85
6.7 Mass spectrometry 85
6.8 Melting Points 85
6.9 Crystallographic Data 85
6.10 Optical Rotations 86
6.11 Cyclovoltammetric and DPV measurements 86
6.12 DFT calculations 86
6.13 UV-Vis spectroscopy 87
6.14 Fluorescence spectroscopy 87
6.15 Determination of quantum yield of fluorescence 87
6.16 Chiral HPLC 88
6.17 Experimental Procedures 88
6.18 General Procedures 88
6.19 Synthesis and Characterization of PPT based Photocatalysts 89
6.20 Oxidative cyclization of 2-phenylbenzoic acid 94
6.21 Oxidative decarboxylation of Boc-proline 99
6.22 Photocatalytic hydroamination of stilbenes using monosubstituted amines 104
6.23 Photocatalytic trifluoromethylation of arenes 128
6.24 Geometries obtained by DFT methods 133
7 References 135
8 Anhang 140

1 Introduction

1.1 The development of photochemistry

The utilization of light in chemistry can be tracked back to more than 180 years ago.[1] One of the first photochemical transformations was reported in 1834 by Trommerdorff. He observed that irradiating a sample of crystallin santonin lead to a color change from colorless to yellow and the "explosion" of the material. He even correlated these transformations to the color of the light namely blue and purple whereas red and green light lead to no observable transformation. In the end of the 19th and the beginning of the 20th century Ciamician investigated many chemical transformations triggered by light. He was the first pioneer in this field.[2] Not only did he dedicate his research to photochemistry but especially the link between photochemistry and nature. He was arguing about the importance of mild reaction conditions and the importance of waste produced under thermal conditions. He hypothesized in 1908 that plants are forming compounds under seemingly mild conditions and he reasoned it is because plants are utilizing light as energy source. One can argue he was the first chemist to connect photochemistry and what is today considered as "green" chemistry. One field Ciamician investigated was the excited state chemistry of carbonyls (Scheme 1). He was interested in the photochemical addition of alcohols to ketones (Scheme 1, a). Ciamician stated this reaction could be likened to the aldol reaction one of the fundamental C–C-bond formation reactions, yet no heat or additional base is needed. Another reminiscent example is the dimerization of ethyl-methyl-ketone (Scheme 1, b). The obtained 1,4-diketone is an important chemical intermediate since it gives direct access to heterocycles like pyrroles (Scheme 1, c).

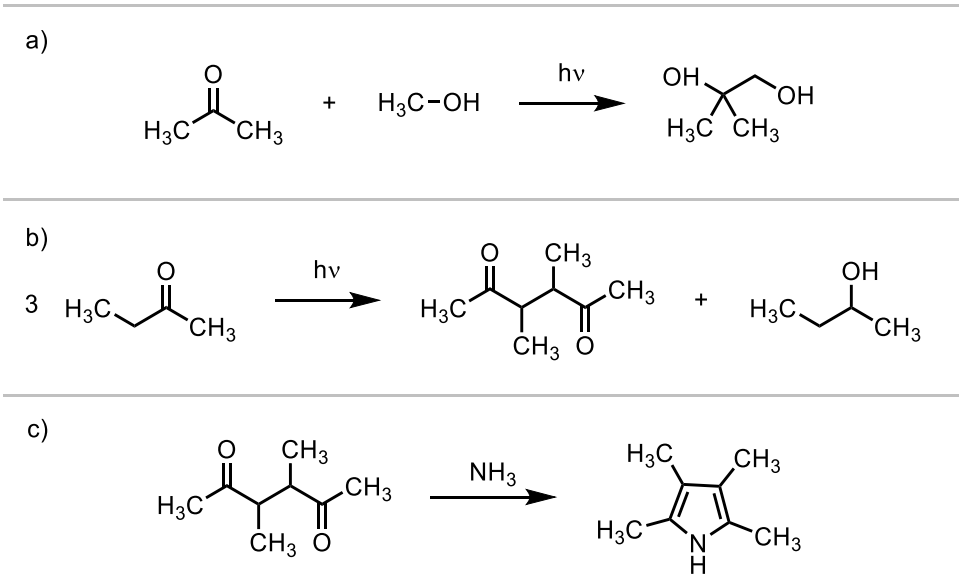

Scheme 1. Photochemistry of carbonyls. a) Addition of methanol to acetone. b) Synthesis of 1,4-diketones c.) Utilization of 1,4-diketones in the synthesis of pyrroles.

Even though Ciamicians opinions were generally accepted by the chemical society and he showcased the value of photochemistry in many reactions, it took decades before photochemistry was thoroughly investigated in research.[3] Presumably this was due to lack of knowledge and missing models to understand the interaction between light and matter. Important findings that eventually lead to the utilization of photochemistry in laboratories include: Plancks discovery of the quantization of energy (1911), Einsteins discovery of the photoelectric effect (1919), Millikans work on the elementary charge (1923) and De Broglies explanation on the wave nature of electrons (1924).

Norrish adopted the strategies of Cimician in the 1930s and evaluated the photo reactivity of aldehydes and ketones in solution. The major difference between these two investigations is the use of a new technology e.g. a mercury lamp instead of sunlight.[4] The results of these experiments were later to be known as Norrish type reactions. In 1950 Kurt Alder and Otto Diels received their Nobel price on the diene synthesis and related reactions. The focus of this work was on the cyclization reaction of dienes with dienophiles. The work of Diels and Alder was expanded by Woodward and Hoffmann in 1965 introducing rules for thermal and photochemical cyclization reactions. With this knowledge the mystery of the reaction of santonin with light was finally solved in 1968 (Scheme 2).[5]

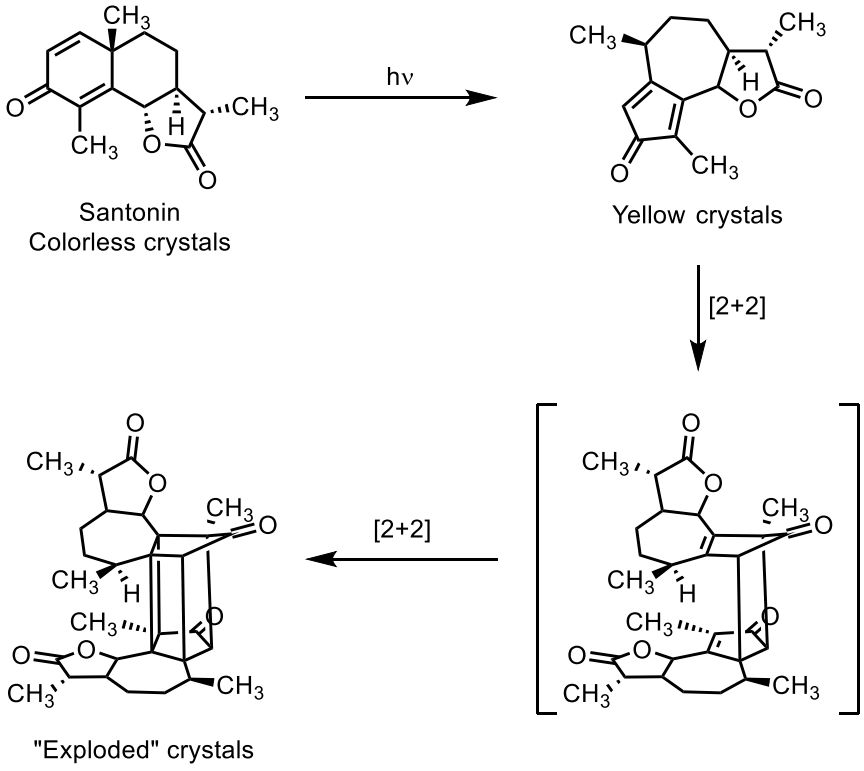

Scheme 2. Solid state reactivity of santonin towards light.

Parallelly the development of many spectroscopic tools like flash photolysis or time-resolved spectroscopy were introduced. These tools are important to get mechanistic

insight in photoreactions. Eventually, to secure the proper exchange of scientific information the terminology in the field of photochemistry was defined by IUPAC in 1996.[6]

1.2 Photochemical processes

When a molecule in its ground state is irradiated with light of a specific wavelength the molecule absorbs the energy and is changing from the ground state (S_0) to an excited state ($S_{n>0}$). Assuming that there are only single photon processes involved the molecule is in its first excited state (S_1). This excited state S_1 is divided in multiple vibrational states which leads to the more precise description $S_{1,m}$. These excited states undergo relaxation to the lowest vibrational, first excited state $S_{1,0}$ as stated by Kashas rule.[7] From this state multiple processes can occur: i) the relaxation back to the ground state involving emission of the energy in form of light, called fluorescence ii) non-radiative relaxation to S_0, typically involving dissipation, called internal conversion (IC) iii) intersystem-crossing (ISC) to the first triplet state (T_1). The radiative relaxation from T_1 to S_1 is called phosphorescence and the non-radiative process is also called intersystem crossing. To visualize these processes a Jabłoński diagram is used (Figure 1).[8]

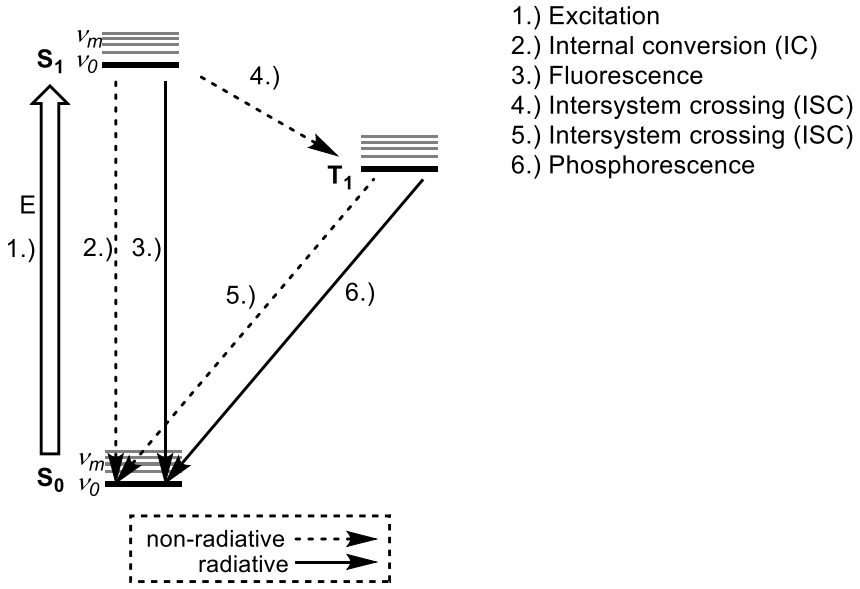

Figure 1. Illustration of electronic states using a Jabłoński Diagram.

These processes generally occur when a molecule is irradiated. When a suitable substrate (S) is added new actions can be observed (Scheme 3). The excited state of the reactant (R*) can interact with the substrate and transfer the energy leaving the substrate in the excited state while the reactant is back in its ground state. This process is an energy transfer from an excited state molecule to a ground state molecule and is called *photosensitization* and is a redox neutral process. Another possibility is the reaction of an excited state molecule with a ground state molecule to furnish a new molecule (or molecules), called *photochemical reaction*. The excited state molecule can also give an electron to the ground

state molecule or vice versa, called electron transfer photosensitization or photoinduced electron transfer (PET). This feature is the basis for the field of photo redox chemistry.[9]

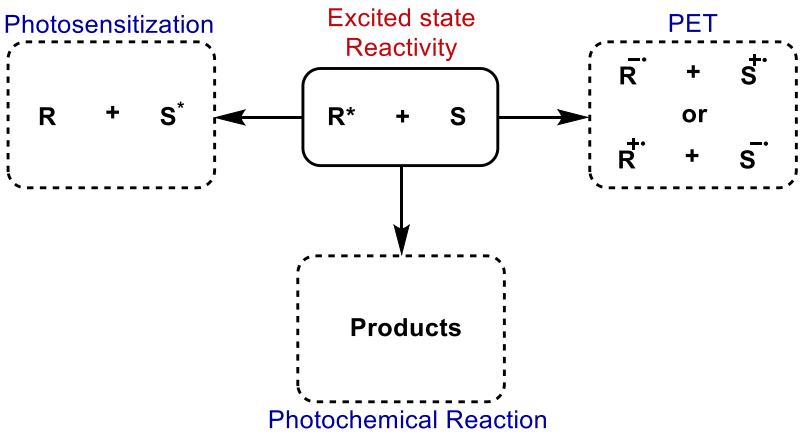

Scheme 3. Reactivity of an excited state molecule.

The excited state reactivity gives access to transformations that are often not achievable by thermal means.[10] The mechanistic difference is shown in Figure 2. A thermal reaction of a reactant (R) through intermediate (I) to product (P) has certain energy barriers (Figure 2, a).

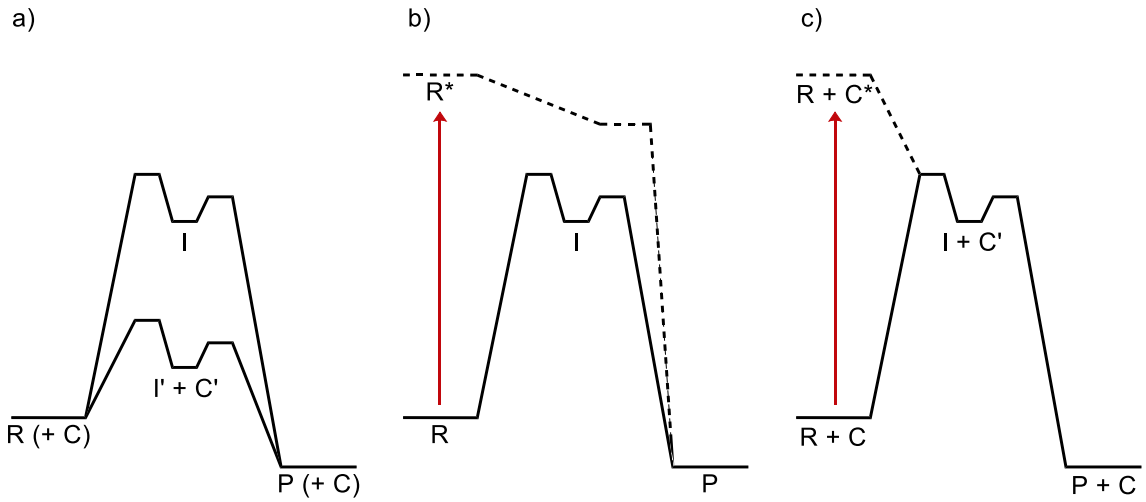

Figure 2. Comparison between a thermal a), photochemical b) and photocatalyzed reaction c). Ground state surface in solid lines excited state surface in dashed lines.[10]

These barriers can be lowered when the reaction is catalyzed, since the involved intermediates (I') lay lower in energy. Noteworthy reactant (R) and catalyst (C) react through their ground state. The photochemical reaction (Figure 2, b) is distinctive because of the unique properties of the excited state. The S_1 or T_1 state lay high in energy so overcoming certain activation barriers is easily achieved. In this case the reactant goes through the excited state of the reactant (R*). This is the major difference to a photocatalyzed reaction (Figure 2, c). An excited state catalyst (C*) will react with a ground state reactant through intermediates (I). These intermediates are radicals for photo redox reactions.

When a ground state molecule is reduced, the lowest unoccupied molecular orbital (LUMO) is the molecular orbital participating in the reaction. Since the highest occupied molecular orbital (HOMO) is fully occupied an additional electron can only occupy the higher laying LUMO. Conclusively, oxidation processes involve the relatively low lying HOMO since it is the highest in energy being occupied by electrons. In the excited state these properties swap. The former LUMO is now reactive in oxidation processes since the electron is higher in energy and therefore more easily removed from the molecule. The same reasoning applies for the former HOMO which is now connected to reduction processes. The former HOMO lays lower energy which eventually leads to a higher energy gain when this molecule is being reduced. In conclusion the S_1 and T_1 state are not only more easily reduced but also more easily oxidized then their ground state counterpart, rendering excited state molecules attractive for redox chemistry (Figure 3).[11]

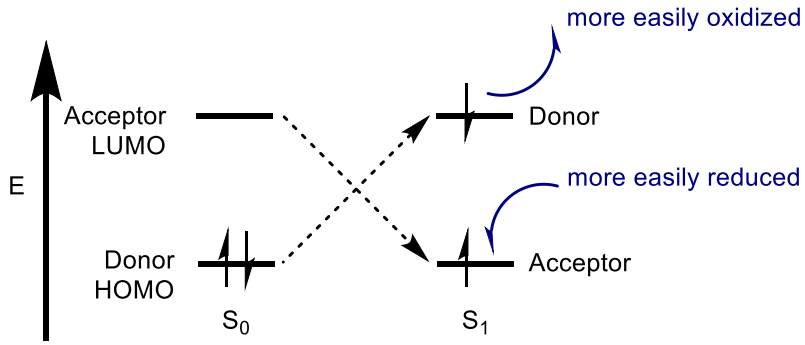

Figure 3. Comparison of ground and excited state redox properties.

1.3 Photoredox catalysis: Background and Application

Over the last few decades, the field of photocatalysis gained a lot of interest. This is because photocatalysis is seen as a mild and green alternative to conventional/thermal reactions.[10, 12] The generalized mechanism for a photocatalyzed redox reaction is depicted in Scheme 3.

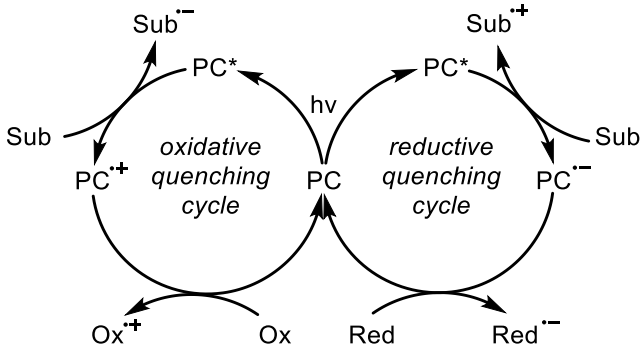

Scheme 3. Generalized mechanism of a photocatalyzed reaction.

A suitable photocatalyst (PC) is irradiated forming the excited state photocatalyst (PC*). This excited state can now undergo oxidative or reductive PET with a substrate (Sub)

forming the radical cation or anion of the substrate and the corresponding radical cation or anion of the photocatalyst. Importantly to close the catalytic cycle (called turnover) a suitable oxidant or reductant is necessary. These can be for example the formerly formed radical intermediates of the substrate, this process is called *back electron transfer* (BET). The back electron transfer is typically considered an unwanted side reaction. To get a productive pathway the reaction of the substrate radicals must be faster then back electron transfer.

In 2011 Zeitler published the utilization of different organic dyes as photocatalysts in the enantioselective α-alkylation of aliphatic aldehydes (Scheme 4).[13] Zeitler was merging different ideas that made this work so important it is considered as one of the fundaments of organic photocatalysis.

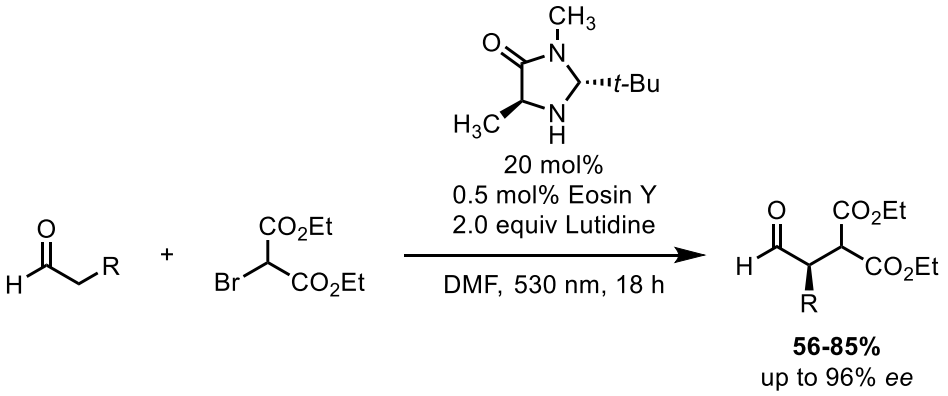

Scheme 4. Enantioselective α-alkylation of aliphatic aldehydes.

Beforehand, mostly iridium and ruthenium based photocatalysts bearing pyridyl ligands were used. These catalysts are very well understood and show promising properties like a long excited state lifetime.[14] Since these catalysts are expensive and not sustainable the need for purely organic photocatalysts raised.[15] The authors were arguing further that these transition metal photocatalysts should also be avoided due to the limited availability in the future. Additionally, the authors merged photocatalysis with enantioselective (ground state) organocatalysis. And lastly, they decided to use any given orange colored molecule as photocatalysts because excitation of green light is attractive since it is the most abundant part in sunlight. At this point, terms like excited state redox potential were not well established and only the local absorption maximum and the ground state reduction potentials were taken into consideration. After this publication the characterization of organic photocatalysts became more important and was put more into focus to predict exited state transformations.[9, 15-16] But even with this information in hand, the question still arises: When should one choose a photocatalytic reaction over a thermal variant if the same transformation is possible? Albini attempted to shed some light on this difficult question. He did so by using the AETOS (environmental assessment tool for organic

syntheses) procedure.[12] This procedure considers the price and "greenness" of a given reaction by evaluating factors like price, waste, environmental impact and social cost.

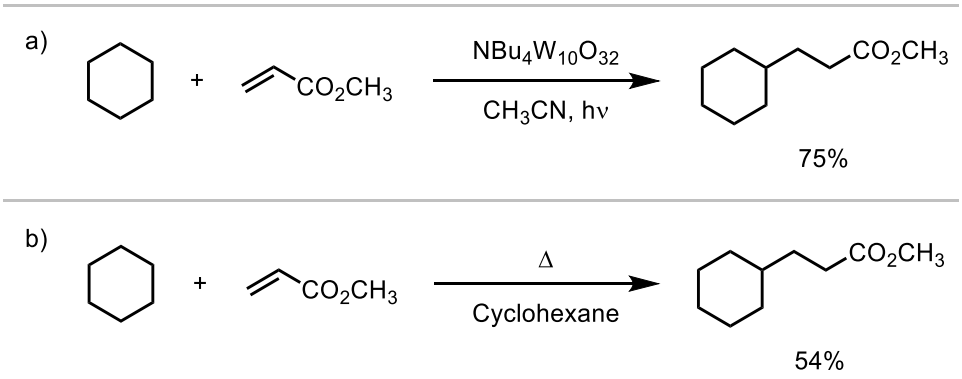

Scheme 5. Synthesis of methyl cyclohexylpropanoate under a) photocatalytic and b) thermal conditions.[12]

In Scheme 5 the C–C-bond formation of cyclohexane and methacrylate is shown. The photocatalytic reaction is presented using $NBu_4W_{10}O_{32}$ as photocatalyst and acetonitrile as solvent. As comparison the reaction under thermal conditions (pyrolysis) using cyclohexane as solvent is shown. The yield of the photocatalytic reaction is higher but when the price per kg is calculated the photocatalytic reaction costs 1300€/kg vs. 200€/kg for the thermal reaction. This is mostly because acetonitrile is an expensive solvent and for photocatalysis special solvents need to be used that must be transparent for the wavelength used. Additionally, photoreactions are characteristically run under dilute conditions (see Lambert-Beer-Law). This means that for this photocatalytic reaction a large amount of expensive solvent is necessary which renders the reaction not only expensive but also highly impacting on the environment.

Noteworthy if this reaction would be attempted using isopropanol instead of cyclohexane as substrate only the photocatalytic approach would lead to product formation. There is no direct thermal alternative. Albini draw the conclusion that for simple transformations classic thermal reaction are indeed greener and often cheaper than their photochemical counterparts. When it comes to more complex transformations the photocatalytic approach may be superior. This especially can be seen for arylation of an alkyne using a more complex substrate (Scheme 6).

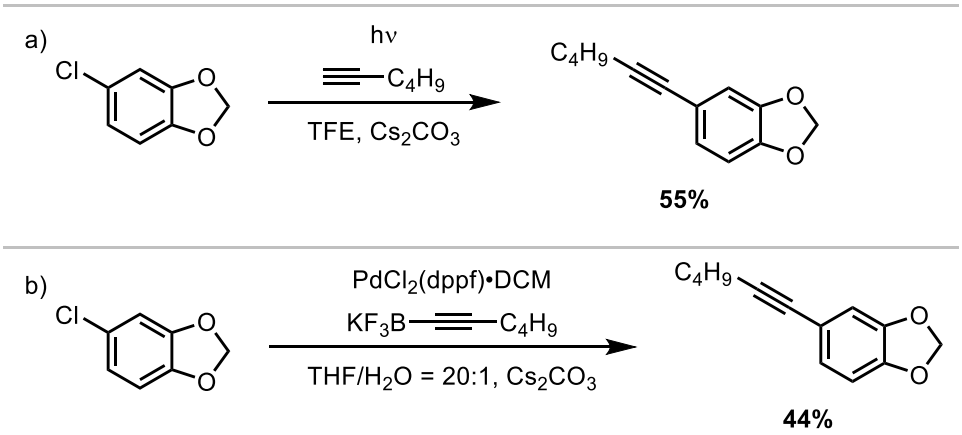

Scheme 6. Arylation of an alkyne using a) photocatalytic or b) thermal conditions.[12]

The major advantage of the photocatalytic conditions is that the alkyne can directly be converted. For the palladium catalyzed reaction, the potassium trifluoroborate salt needs to be used and the synthesis of this reagent is expensive and the environmentally burden is increased considerably. The photocatalytic conditions have the major disadvantage of using the expensive and environmentally impacting trifluoroethanol as solvent. The price for the photocatalytic reaction turns out to be 18000€/kg while the classical palladium catalyzed reaction costs 35000€/kg, so almost double the price. Albini summarized that both reactions turn out to be as polluting, but the photocatalytic reaction costs less and should therefore be preferred.

Notably, the major contribution of the solvent to the cost and environmental impact lead Albini to suggest that it is necessary to attempt recycling experiments like distillation of the solvent to reduce the environmental impact if upscaling to industry is wanted.

1.4 Pyrimidopteridine *N*-oxides as oxygen atom transfer reagent

In 1971 Maki reported the novel synthesis of pyrimidopteridine-*N*-oxides (PPTNO).[17] The PPTNOs were obtained after oxidative dimerization of 6-amino-5-nitroso uracil **1** using lead tetraacetate (Scheme 7). The first step involves a H abstraction to form a nitroxyl radical **1-a** which will tautomerize to give the iminyl radical **1-b**. This radical will react with another molecule of **1** giving the dimerized product **1-c**. Tautomerization leads to **1-d**, H-atom abstraction by an acetoxy radical delivers **1-e** which will undergo cyclization to **1-f**. Further oxidation by lead tetraacetate will lead to an unstable intermediate **1-g** which collapses under the extrusion of N_2O, leaving radical intermediate **1-h**. **1-h** cyclizes to give **2-b** and a final H-atom abstraction furnishes the PPTNO (**2**). Maki successfully conducted ^{18}O labelling experiments to verify that the oxygen of the former nitroso group ends in the *N*-oxide moiety and EPR experiments revealed the presence of nitrogen centered radicals. Formation of certain side products (not depicted) and the former mentioned experiments lead to the proposed mechanism.[18]

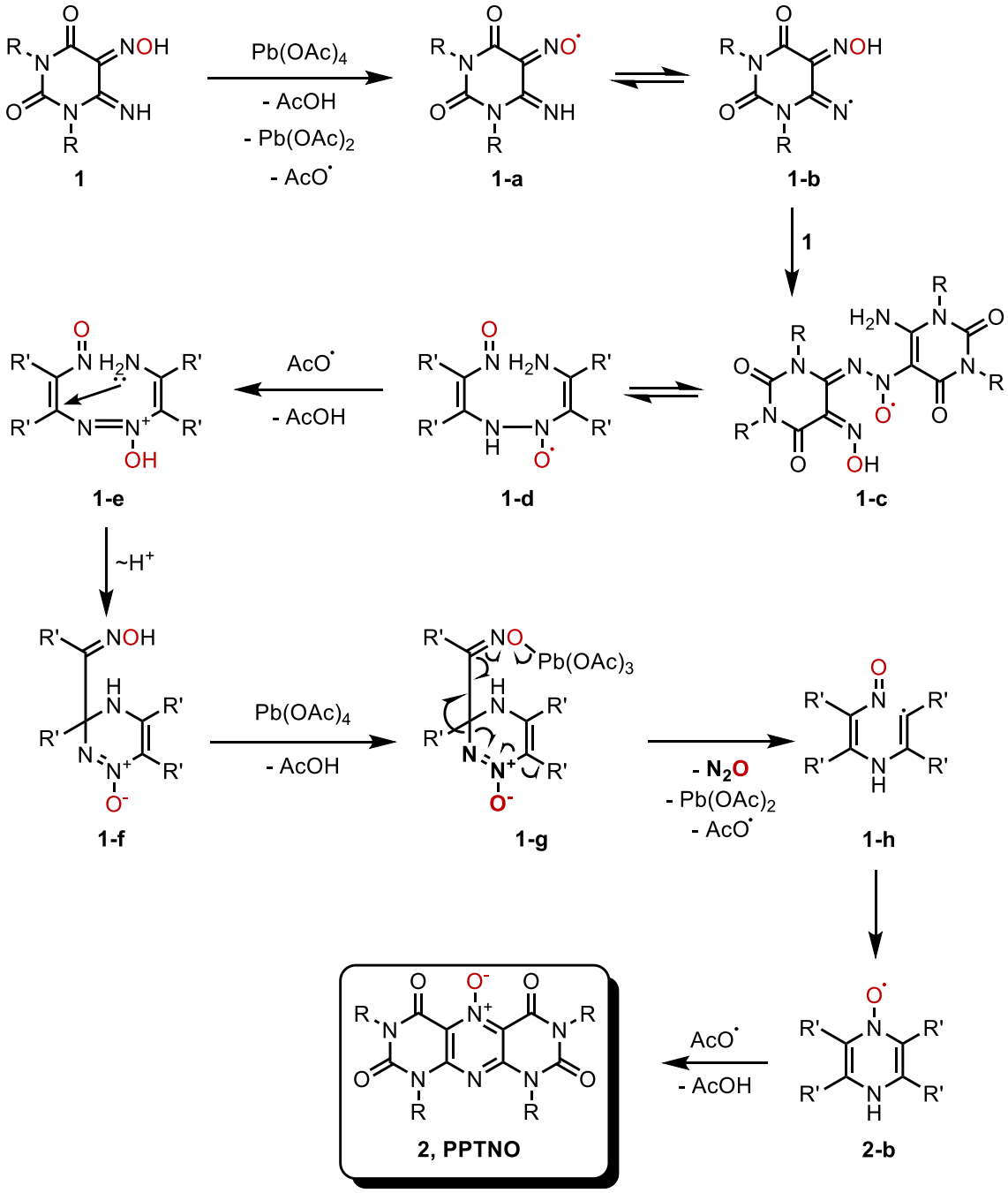

Scheme 7. Oxidative formation of PPTNOs by lead tetraacetate. Reaction conditions: For R = Bu, a mixture of 1a (0.21 mmol), AcOH (5 ml) and $Pb(OAc)_4$ (0.25 mmol) was stirred at room temperature for 1d. 66% isolated yield after purification by column chromatography [18-19]

PPTNOs are structural related to flavins and to isoalloxazines (Scheme 8). Within the next 20 years after the published synthesis of the PPTNOs the photochemical application of these compounds was evaluated by Maki and coworkers. The focus of this investigation was on the photochemical oxygen transfer of the *N*-oxide moiety to different substrates.

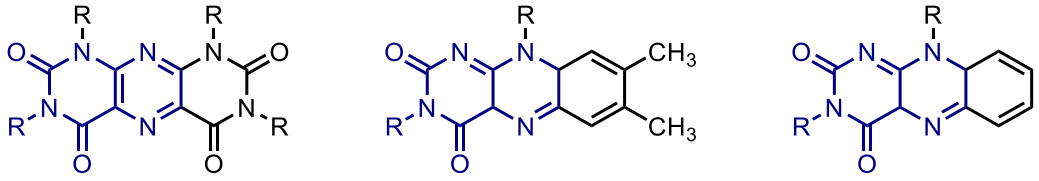

Scheme 8. Structural relationship of PPTNO, flavin and isoalloxazine.

The aim was to get insight on a hypothesis that photochemical oxygen transfer might play a role in variety of biological oxidations like those performed by cytochrome P-450. The reactions that were investigated included C–C bond cleavage[20], C–N bond cleavage[20b, 21], C–O bond cleavage[22], dehydrogenations[23], and oxygenation of sp^3 and sp^2 C–H bonds[24]. Notably, the proposed mechanisms were different for some of these reactions showcasing the versatility of the PPTNOs.

For example the reaction of the butyl substituted pyrimidopteridine-*N*-oxide **2b** (BuPPTNO) with dimethyl aniline **3a** (DMA) lead to mono demethylation (Scheme 9).[21] Differential UV-Vis spectroscopy revealed a charge-transfer complex **3a-a** (CT complex) that is responsible for this reactivity. Excitation of the CT-complex lead to SET from the DMA to the BuPPTNO delivering a radical pair **2a-c** and **3a-b**. The BuPPTNO radical (**2a-c**) then deprotonates the radical cation of DMA (**3a-b**) giving two neutral radicals **2a-b** and **3a-c** that will combine, forming **3a-d** with a new C–O bond. **3a-d** will collapse giving the aminal of DMA (**3a-f**) and the deoxygenated pyrimidoteridine (PPT). Since aminals are unstable intermediates the release of formaldehyde furnishes the demethylated product monomethyl aniline (**4a**). Noteworthy this proposed mechanism shows the bifunctional character of PPTNO based compounds to participate in SET processes and acting as base in deprotonation steps.

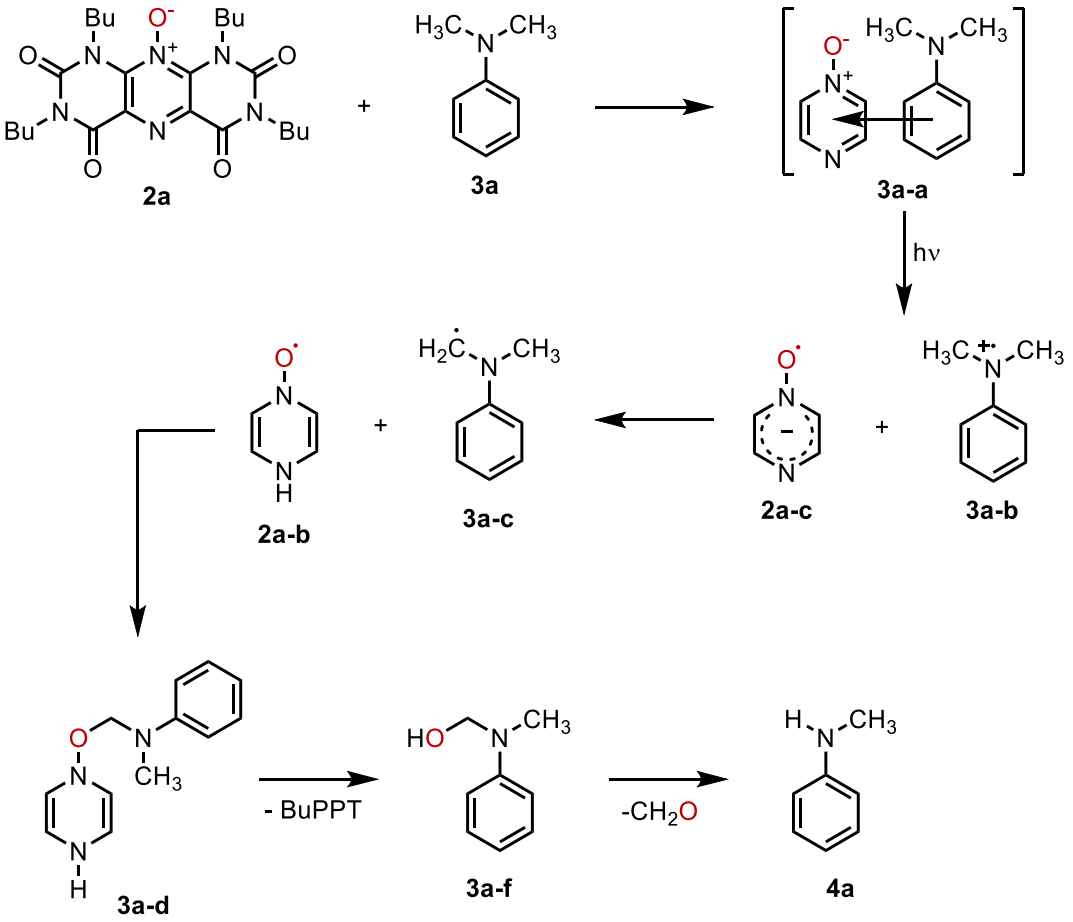

Scheme 9. Oxidative C–N bond cleavage of DMA using BuPPTNO.[21]

Another reaction investigated by Maki was the photochemical oxidation of benzene to form phenol (Scheme 10).[22] In contrast to the beforementioned reaction no CT complex **4a-a** was found. The authors argued that a single-electron transfer from benzene (**4a**) to BuPPTNO (**2a**) occurs. Like in the reaction of DMA first a radical pair form (**2a-c** and **4a-b**). This pair combines to give an unstable intermediate **4a-d** with a newly formed C–O bond that collapses to release the products BuPPT **5a** and phenol **6a**. Here the bifunctional character of PPTNOs, acting as SET reagent and base, was also suggested.

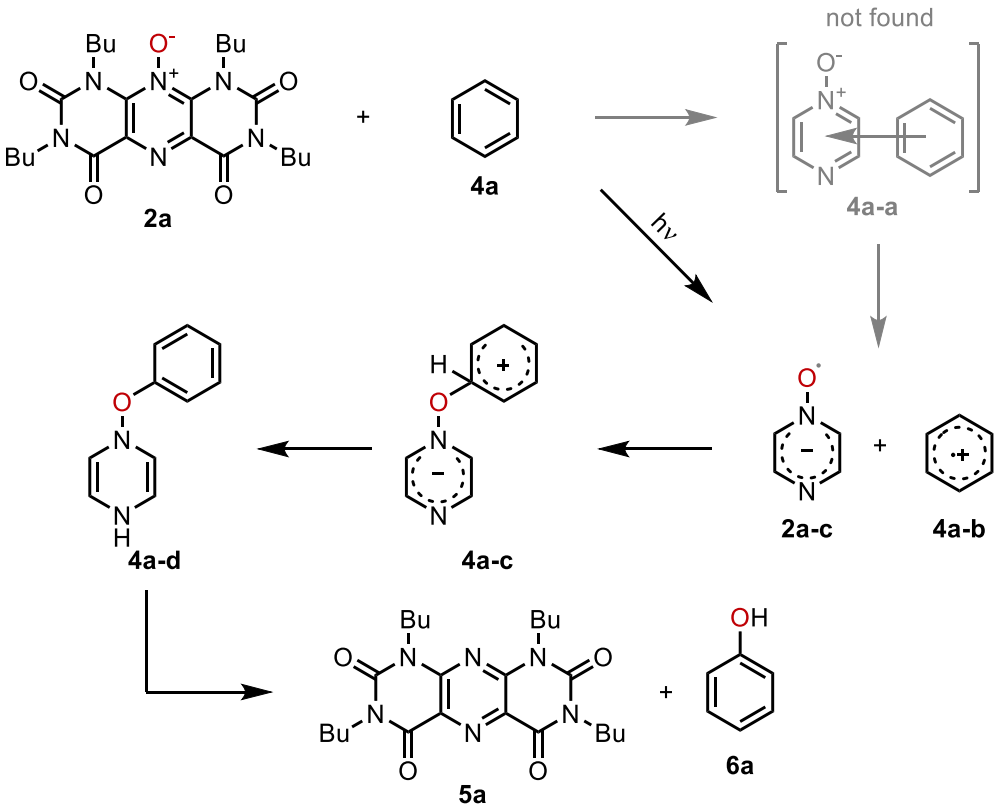

Scheme 10. Oxidation of benzene to phenol by BuPPTNO.[22]

Remarkably, the oxygen atom in BuPPTNO can also be used in photochemical dehydrogenation reactions.[23] When using BuPPTNO, 2-hydroxychalcones can cyclize to form the flavones (Scheme 11). For this reaction, a charge-transfer complex between the chalcone (**7**) and BuPPTNO (**2a**) was found (**7-a**). Varying the wavelength used in this reaction showed that the CT complex only contributes to a small degree for the product formation. Consequently, the first step in the reaction is likely a SET process from the chalcone to BuPPTNO forming the radical-cation intermediate **7-a** and the BuPPTNO radical anion (**2a-c**). Subsequently **7-a** will cyclize to form **7-b** and is then deprotonated by **2a-c** forming **2a-b**. The flavone **8** is then formed after proton coupled electron transfer (PCET) **2a-b**. Eventually release of water and rearomatization forms the BuPPT (**5a**). This reaction is very distinctive because it showcases that in principle BuPPTNO based compounds might also undergo reactions involving (PCET).[25]

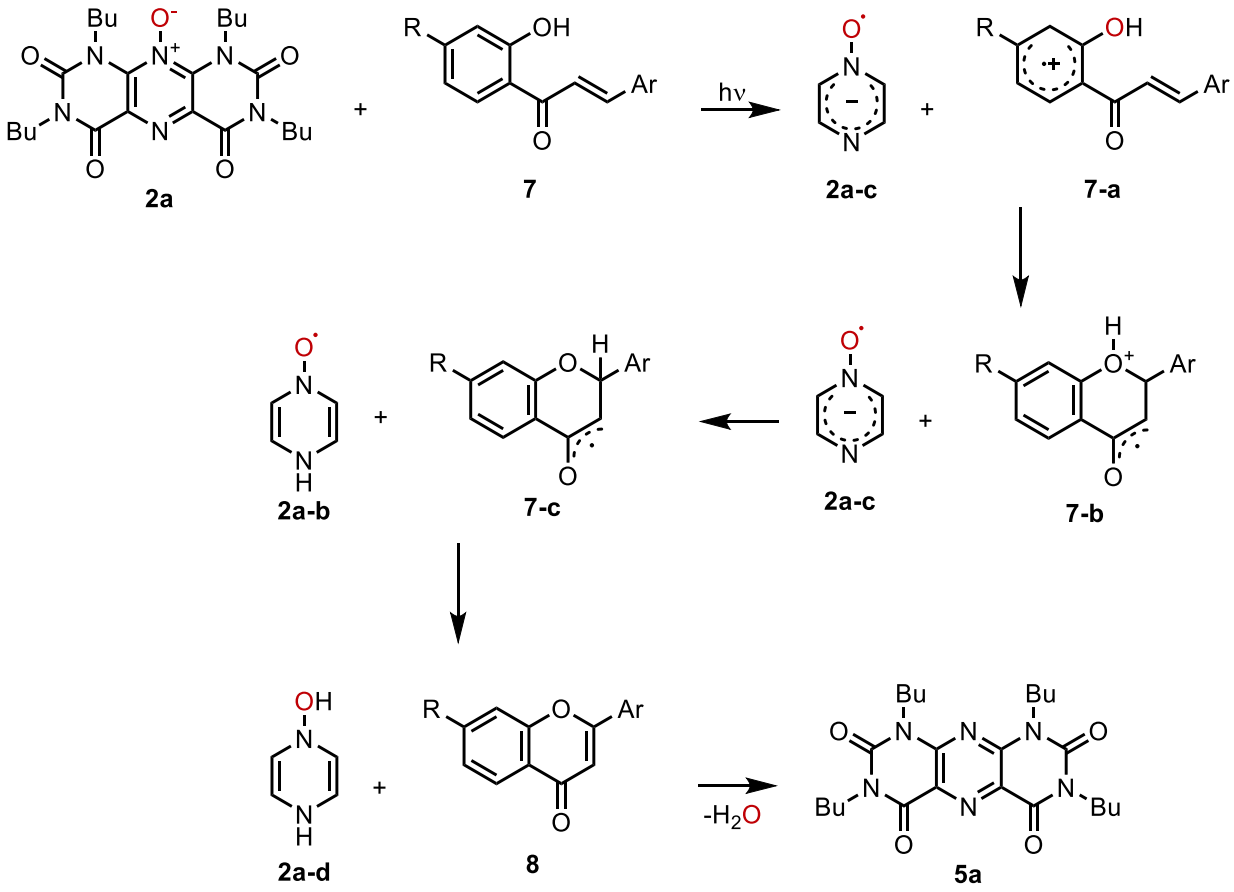

Scheme 11. Dehydrogenative cyclization of 2-hydroxychalcone to flavones.[23]

In the first months of conducting this PhD thesis an intensive literature research was performed and a review was written on the oxygen atom transfer of heteroaromatic *N*-oxides like the PPTNO based compounds.[26]

1.5 Design and characterization of photocatalysts

Knowing that photocatalysis is an attractive field that gives access to reactions not achievable by classical ground state chemistry it is important to understand what makes a molecule a suitable photocatalyst. Therefore, a thorough catalyst design and characterization is very important.

In principle any given molecule can be used as an excited state reactant. Certain ground state and excited state properties render some molecule better candidates for photocatalysis. In the upcoming paragraphs methods to determine important characteristics are listed and explained why and how these influence reactivity.[9, 15a, 27]

To promote a given molecule into the excited state, light with a very defined energy and therefore wavelength is necessary. This wavelength is determined by measuring an UV-Vis spectrum. The UV-Vis spectrum contains much information, the most important one being the *absorption maximum* ($\lambda_{abs,max}$). This value is necessary in the evaluation which light

source can and should be used when attempting excited state chemistry. The normalized UV-Vis spectrum of rhodamine G6 and the normalized emission spectra of two different LED light sources is shown in Figure 3. The emission spectrum of the blue LED clearly shows no overlap with any absorption band of rhodamine G6. In contrast, the emission spectrum of the green LED shows a satisfying overlap with the absorption band rendering this light source suitable for excited state chemistry.

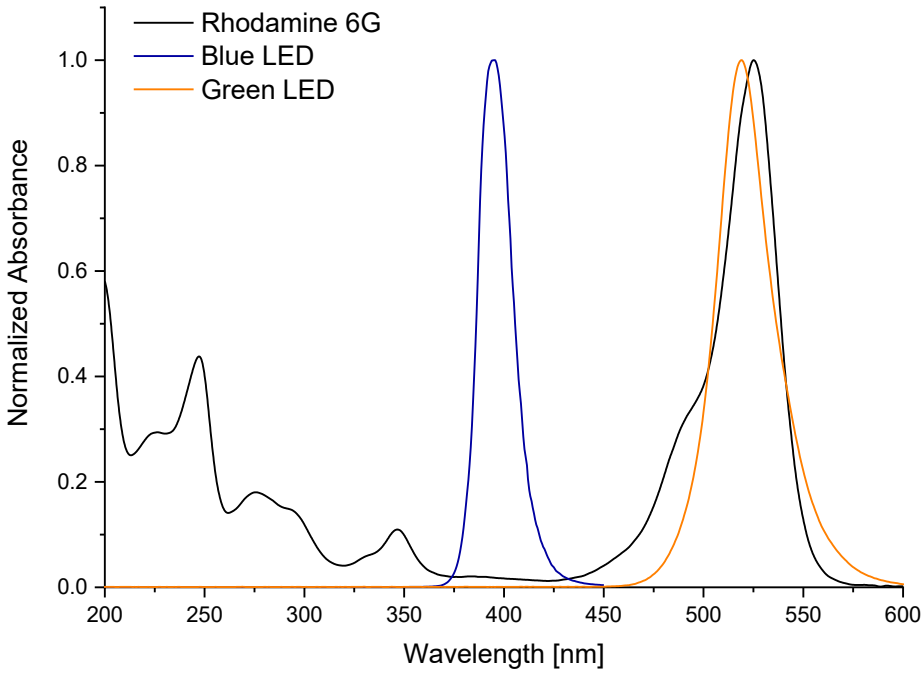

Figure 3. Absorption spectrum of rhodamine 6G (black) and emission spectrum of a blue and greed LED.

The shape, intensity and position of an absorption band can additionally give information to the structure of the molecule and the position of the chromophore. This important feature should be mentioned but is not further discussed here.[28]

When aiming for photo redox catalysis the most important values are the *excited state redox potentials* $E^*_{ox}(S_1)$ and $E^*_{red}(S_1)$. These characteristic values can be used to predict which substrates can be oxidized or reduced when performing excited state chemistry. Unfortunately, this value cannot be measured directly therefore it needs to be estimated using other characteristic values (Figure 4).

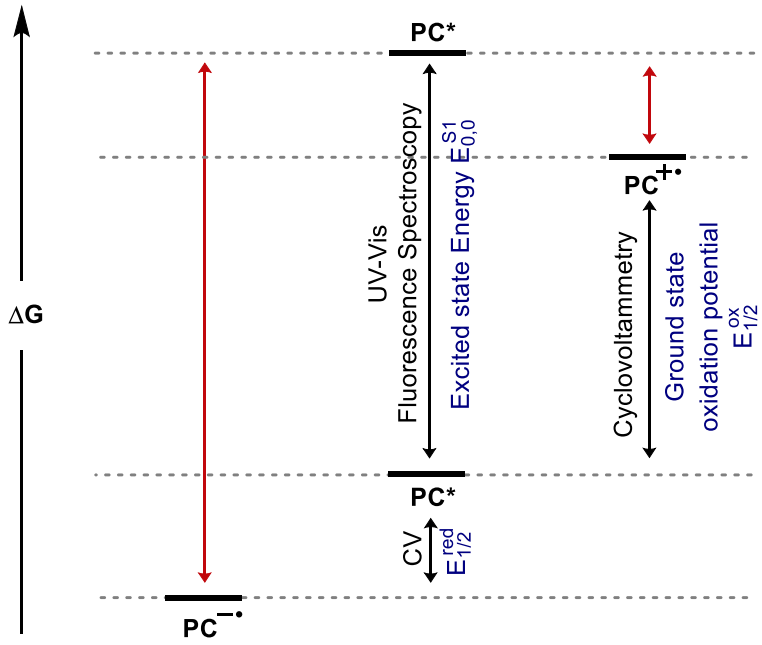

Figure 4. Determination of the excited state redox potentials (red arrows).

To obtain the excited state redox potentials it is necessary to determine the *excited state energy* ($E_{0,0}^{S1}$) and the *ground state redox potentials* (E_{ox} and E_{red}). These values can then be used to determine the excited state redox potentials using formula 1 and 2.

$$E_{red}^{*} = E_{0,0}^{S1} - E_{1/2}^{ox} \quad (1)$$

$$E_{ox}^{*} = E_{0,0}^{S1} + E_{1/2}^{red} \quad (2)$$

The energy that is necessary to promote an electron from $S_{0,0}$to $S_{1,0}$ is called the excited state energy. This is the value that is used to compare organic compounds and their potency to be used in a *photochemical* reaction. This value needs to be estimated and cannot be obtained directly from the UV-Vis spectrum (see Frank-Condon-Principle). In theory it is possible to use the fluorescence spectrum or more precisely the *emission maximum* ($\lambda_{em,max}$) to determine the excited state energy but this is typically an underestimation. It is also possible to use the earliest onset of the fluorescence, however this generally leads to overestimated values. More reliable results are obtained when both the UV-Vis spectrum and the fluorescence spectrum are used. Here the intersection of normalized absorption and emission is used.[9] For compounds not having an intersection point half of the Stokes shift is used.

Theoretically, the excited state energy can be fully transferred to another molecule. This leads to the conclusion that a high excited state energy is wanted to be able to convert as many different molecules as possible. A high excited state energy on the other hand might also lead to unwanted side reactions. An efficient catalyst design is achieved by evaluating this value thoroughly (selectivity vs reactivity).

The ground state redox potentials are determined by cyclovoltammetry (CV) and differential pulse voltammetry (DPV). The major advantage of DPV measurements over CV measurements is a higher sensitivity.[29] Unless otherwise noted, all reported and discussed redox potentials were determined in acetonitrile and referenced against SCE.

With both the excited state energy and the ground state redox potentials in hand the excited state redox potentials can now be determined (Equation 1 and 2). Furthermore, to determine if an electron transfer is thermodynamically feasible the Gibbs free energy of photoinduced electron transfer can be calculated (Equations 3 and 4).[9]

$$\Delta G_{PET} = -F(E^*_{red} - E^{ox}_{1/2}) \quad (3)$$

$$\Delta G_{PET} = -F(E^{red}_{1/2} - E^*_{ox}) \quad (4)$$

Not only the prediction of suitable substrates is now possible but also a direct comparison to other photocatalysts (Figure 5). For example, 10-mesityl-9-methylacridinium catalysts ($MesAcrMe^+$) have an excited state reduction potential of +2.18 V vs SCE and can therefore oxidize a whole variety or organic molecules like styrenes, phenols and amines. While benzophenone (BP) can oxidize a smaller spectrum of compounds in its excited state, it is a very strong excited state reductant. BP can reduce alkyl and aryl halides and both aryl aldehydes and ketones.

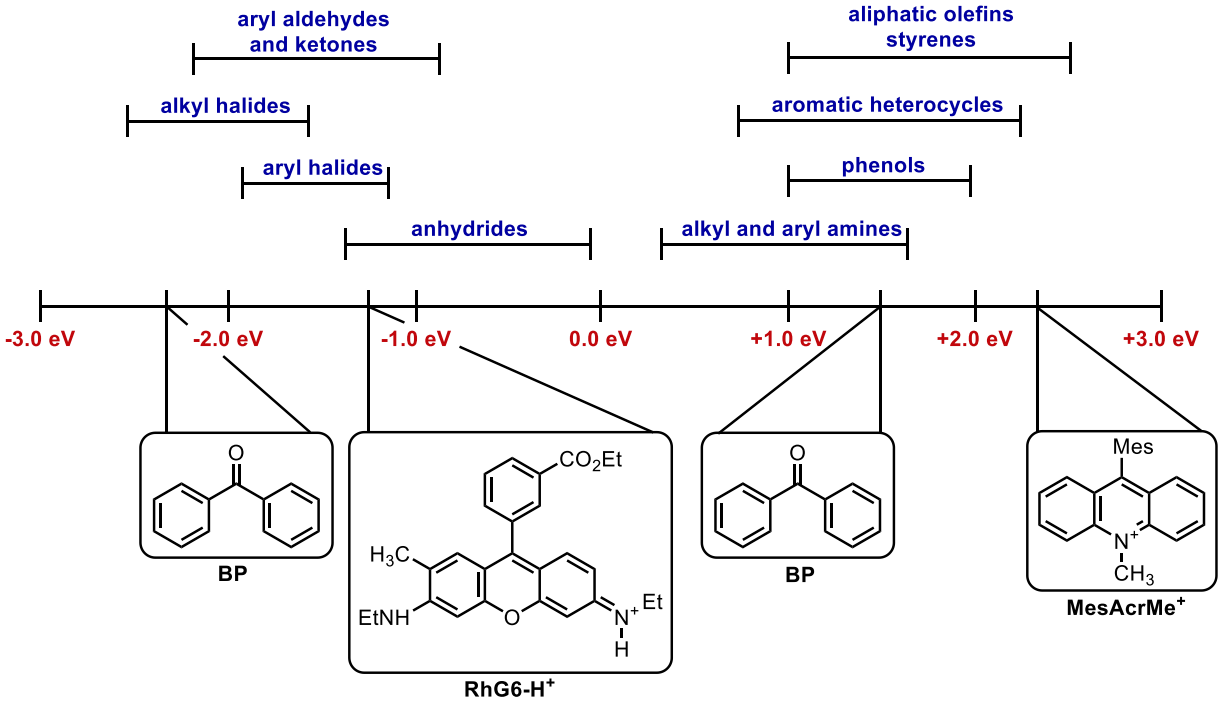

Figure 5. Electrochemical series of organic molecules and photocatalysts. Potentials are reported against SCE.[30]

Other crucial parameters that need to be evaluated when performing excited state chemistry are the *lifetime of the excited state* (τ_f) and the *quantum yield of fluorescence*

(Φ_f). The lifetime of the excited state can be determined by using time-resolved fluorescence spectroscopy e.g. by measuring the fluorescence decay. This value gives information on how long lived the excited state is and therefore how likely a chemical reaction is. A long excited state lifetime is beneficial because it ensures that there is enough time that the substrate can diffuse to the excited state molecule and undergo the chemical reaction. By comparing τ_f with the diffusion constant a chemical reaction involving the excited state can be ruled out if τ_f is smaller than the diffusion constant. The quantum yield of fluorescence is the fraction of the number of photons emitted by a compound divided by the number of photons absorbed. This value is typically obtained by relative measurements e.g. by evaluating the fluorescence intensity compared to a fluorescence standard. What this parameter describes is how many of the absorbed photons are used for fluorescence and in conclusion how many are used in other processes like ISC or IC. This means that a low quantum yield of fluorescence is desired when exploring reaction employing triplet states. Furthermore, a low quantum yield can also indicate a long excited state lifetime, but determination of the fluorescence decay is necessary to distinguish between a long lifetime and a high degree of ISC.

Knowing what photophysical properties a molecule should have to be used efficiently in photo redox catalysis it is now possible compare these properties. In Table 1 an overview of commonly used photocatalysts including their ground and excited state properties are listed.

Table 1. Comparison of excited and ground state properties from commonly used photocatalyst [9, 31] Structures are depicted in Figure 5 and 6.

Compound	$E_{1/2}^{red}$ [V vs. SCE]	$E_{1/2}^{ox}$ [V vs. SCE]	E_{red}^{*} [V vs. SCE]	E_{ox}^{*} [V vs. SCE]	ϕ_f [%]
BP	-1.72	+2.39	+1.50	-0.83	-
DCA	-0.91	-	+1.99	-	0.76
MesAcrMe$^+$	-0.49	-	+2.18	-	0.10
Rh6G-H$^+$	-1.14	+1.23	+1.18	-1.09	0.90
RFTA	-0.60	-	+1.50	-	0.2–0.6[a]
TPT$^+$	-0.32	-	+2.55	-	0.58

[a]For the tetrabutyrat, high solvent dependency.[32]

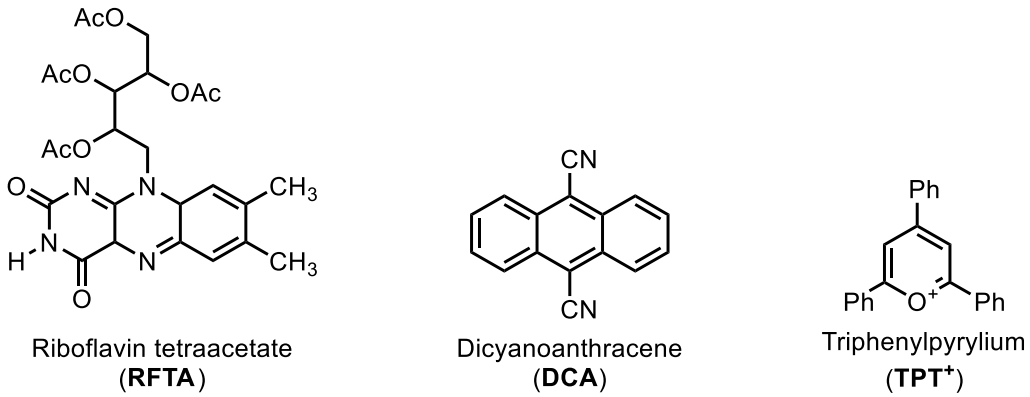

Riboflavin tetraacetate (**RFTA**) | Dicyanoanthracene (**DCA**) | Triphenylpyrylium (**TPT$^+$**)

Figure 6. Structure of commonly used photocatalysts.

Out of these photocatalysts, MesAcrMe$^+$ and TPT$^+$ are very strong excited state oxidants. Notably, the ground state reduction potential is very high with -0.49 V and -0.32 V (vs SCE) respectively. This makes it very difficult to close the catalytic cycle without the help of an additionally added reductant. For this reason, many reported methods employing acridinium catalysts add thiophenols to assist catalyst turnover.[33] On the other hand, Rh6G-H$^+$ shows a broad redox window. While the excited state reduction potential is not as high (+1.18 V vs SCE) the ground state reduction potential is very low (-1.14 V vs SCE) this ensures a selective oxidation while turnover of many intermediate species is likely. Additionally, the high quantum yield of fluorescence ensures that side reactions that involve triplet sensitization are unlikely. Benzophenone and its derivatives are typically used as strong excited state reductants involving triplet state chemistry.

2 Motivation and aim

PPTNO based compounds were used by Maki in photoinduced oxygen atom transfer reactions showing very promising results. It is desirable to run these reactions under catalytic conditions using PPTNOs as catalyst in combination with a cheap terminal oxidant. Therefore, a small library of PPTNO based compounds was synthesized in our group. Having these compounds in hand, initial screening experiments were performed. It was quickly shown that the oxygen transfer reactions cannot be run catalytically, but these compounds showed very promising photophysical properties and revealed a possible application in photo redox catalysis. The aim of this thesis was to follow this lead and synthesize a broader variety of PPTNO based compounds to check the influence of the substituents on the relevant photophysical properties. First it was necessary to improve the reported synthesis since this procedure suffers from low yields and usage of toxic reagents. Then a thorough characterization of the synthesized compounds would be necessary to investigate their suitability as organic photocatalysts. This characterization would include the determination of the ground and excited state redox potentials, measurement of the quantum yield of fluorescence and DFT calculations. With the fully characterized photocatalysts a comparison to commonly used photocatalysts would be possible. Of high interest would be the direct comparison with riboflavin due to its similar structure. Subsequently, the application of the PPTNOs in more challenging transformations should be realized. Therefore, a photocatalytic hydroamination and a photocatalytic trifluoromethylation reaction should be investigated.

3 Synthesis, characterization and first application of PPTNO based photocatalysts

3.1 Synthesis

Maki reported the use of PPTNOs in the photo mediated oxygen transfer to various organic molecules. Since these PPTNOs are structurally related to flavins, which are commonly used in organic photocatalysis, we hypothesized that the PPTNOs might also be used in similar reactions. Especially, since the reactivity of flavins is well understood, this knowledge might be profitable for the evaluation of the PPTNOs as photocatalysts. First, a library of PPTNO based compounds was synthesized. The substituents were varied but the heterocyclic core remained unchanged. Since the reported route to access these compounds has several drawbacks like low yields and a small scale it was necessary to optimize the synthesis. An overview of the synthesis can be found in Scheme 12.

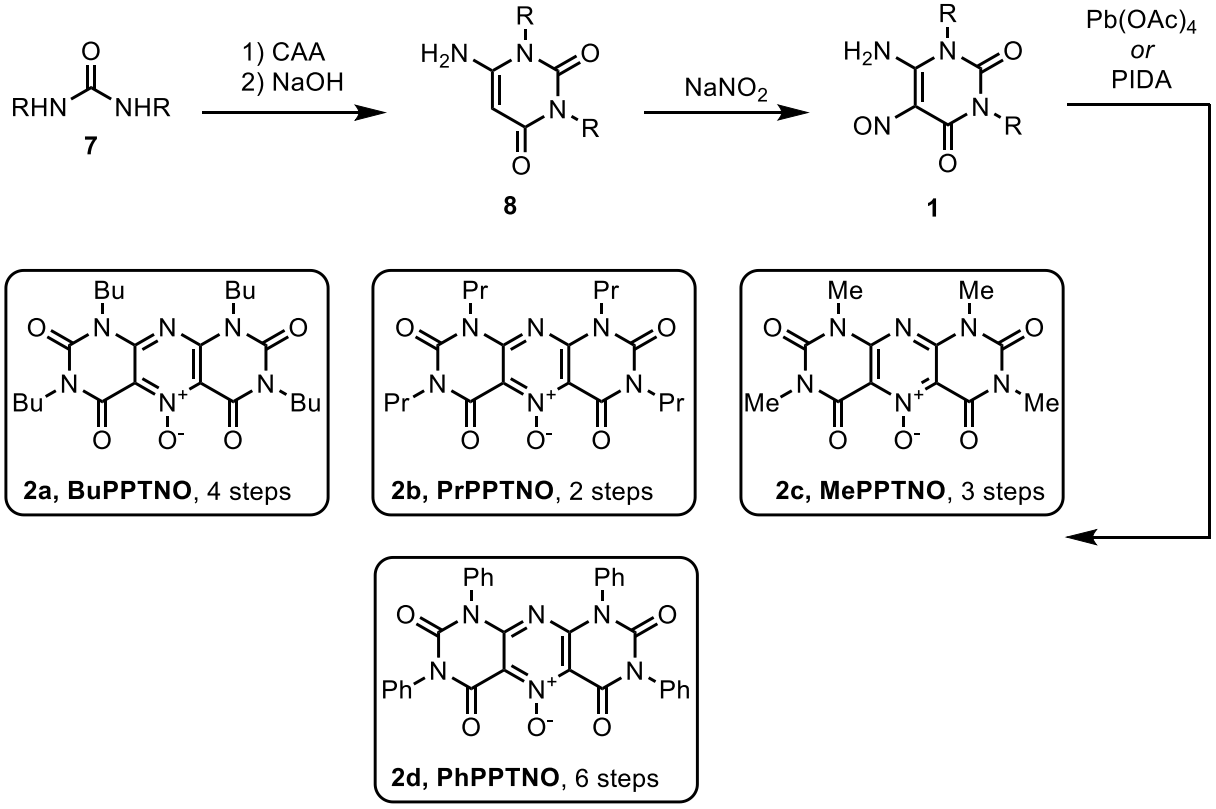

Scheme 12. Synthetic route for the synthesis of PPTNO based compounds.

Depending on which starting material is commercially available and if the substituent is an alkyl or aryl group the synthesis takes 2 to 6 steps. For the synthesis of alkyl bearing PPTNOs the first step is a cyclization of a urea (**7**) using cyanoacetic acid (CAA) giving the 6-amino-uracil (**8**) in up to 76% yield. Next an electrophilic substitution using sodium nitrite is performed giving the 6-amino-5-nitroso uracil (**1**) in yields exceeding 90%. Of special

interest is the last step, were **1** is dimerized oxidatively under extrusion of N_2O. This step was reported using lead tetraacetate, a very toxic and hygroscopic compound. To avoid the usage of this oxidant, the utilization of phenyliodine(III) diacetate (PIDA) was chosen as a bench stable, crystalline, and nontoxic compound. The yield of the obtained PPTNO varies strongly depending on the substituent but can reach up to 65% using a gram scale synthesis. The purification is done by recrystallization and the more tedious and expensive column chromatography can be avoided. At this point, the library contained the methyl, propyl, butyl, and phenyl substituted PPTNO and was later expanded. With the compounds in hand it was necessary to evaluate the ground and excited state properties.

3.2 Photophysical, electrochemical and computational characterization

To determine the excited state energy and therefore the excited state redox potentials it is necessary to first record and analyze the UV-Vis spectra (Figure 7).

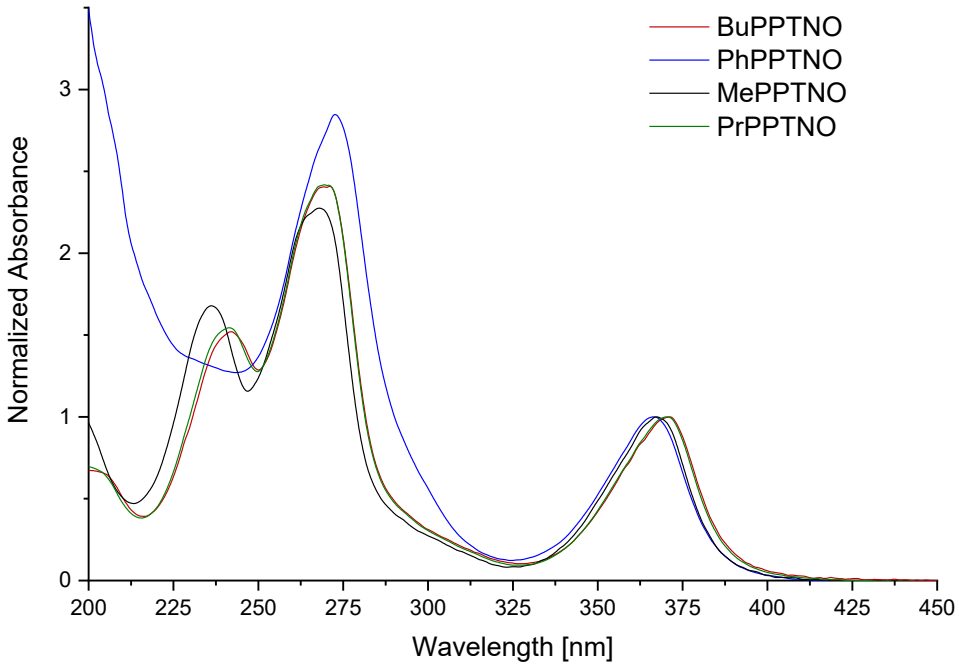

Figure 7. Normalized UV-Vis spectra of PPTNO based compounds.

A weak and broad absorption band can be seen from 325 to 400 nm. This band was prior correlated by Maki to be an n–>pi* transition using DFT methods.[34] The local absorption maximum $\lambda_{abs,max}$ for this band is approximately 370 nm and is not influenced by the substituents. This suggests that the chromophore is solely located on the heterocycle and not influenced by the substituents.

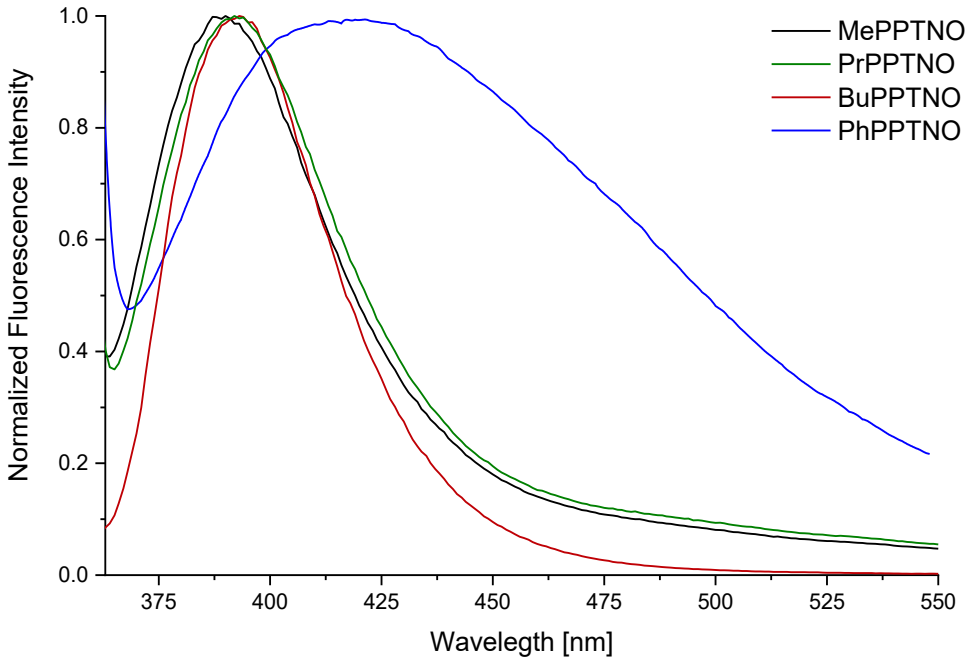

Figure 8. Normalized fluorescence spectra of substituted PPTNO compounds.

When characterizing the excited state redox properties of a molecule, fluorescence measurements need to be performed. For the PPTNOs the maximum of the fluorescence signal for the alkyl bearing compounds shows no dependency on the chainlength with $\lambda_{em,max}$ being approximately 398 nm (Figure 8). For the phenyl bearing compound a broadening of the fluorescence signal can be seen which is indicative for charge-transfer (CT) character.[35] If this CT band originates from a local excited state was not further investigated but this could be done measuring the fluorescence in solvents of different polarity.[36] The PPTNOs generally show a small Stokes shift of 30 nm. The PhPPTNO shows a bigger Stokes shift of 55 nm with $\lambda_{em,max}$ = 423 nm. With both the UV-Vis and fluorescence spectra measured the excited state energy can be determined to be +3.2 eV for the PPTNOs. Since neither the absorption nor the emission of these compounds is dependent on the substituents the excited state energy derived from this is also independent from the substituent. A value of +3.2 eV is very high and indicates that in theory many transformations should be accessible when considering photochemical transformation. Importantly, this high reactivity also has its downsides since high reactivity is often connected with a low selectivity.

Next, the ground state redox properties were investigated by CV (Figure 9) and DPV (Figure 10) measurements. For all PPTNO compounds two reduction events can be observed. The first one at -1.35 V which is not reversible and the second at -1.60 V which is reversible. The first reduction process might be irreversible due to a chemical transformation of the compound. Likely, the compound is reduced to the PPT based compound under loss of oxygen. The oxidation signal is barely seen at around +2.0 V and is not reversible. A

polymeric film was observed on the electrodes after the attempt of oxidizing PPTNO compounds. This chemical decomposition is likely the reason why this process is not reversible. Since reversible processes are necessary to get reliable ground state redox potentials from CV measurements, we opted to perform DPV measurements.

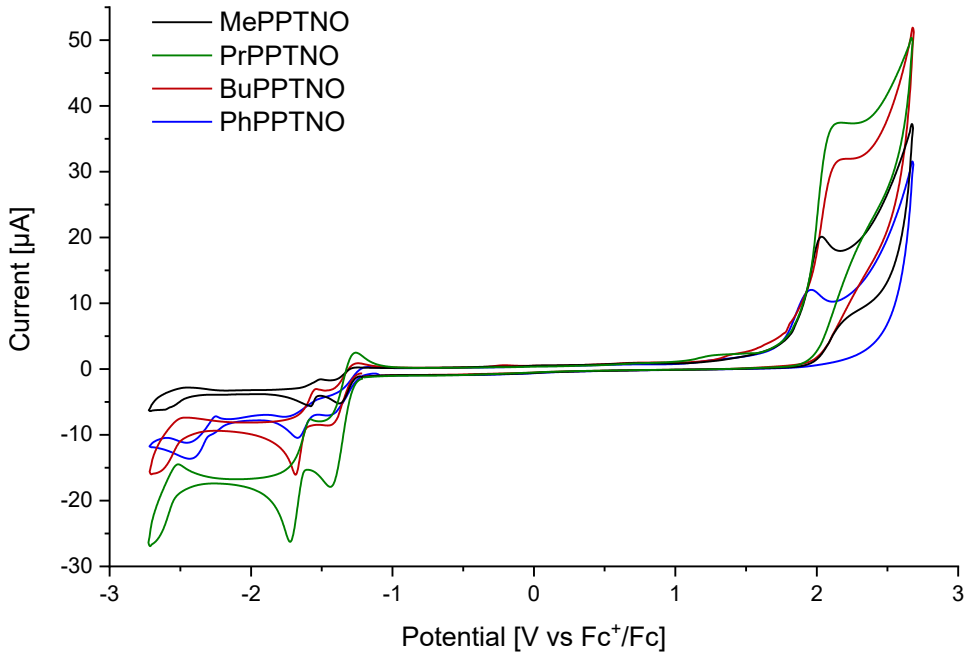

Figure 8. CV measurements of substituted PPTNOs.

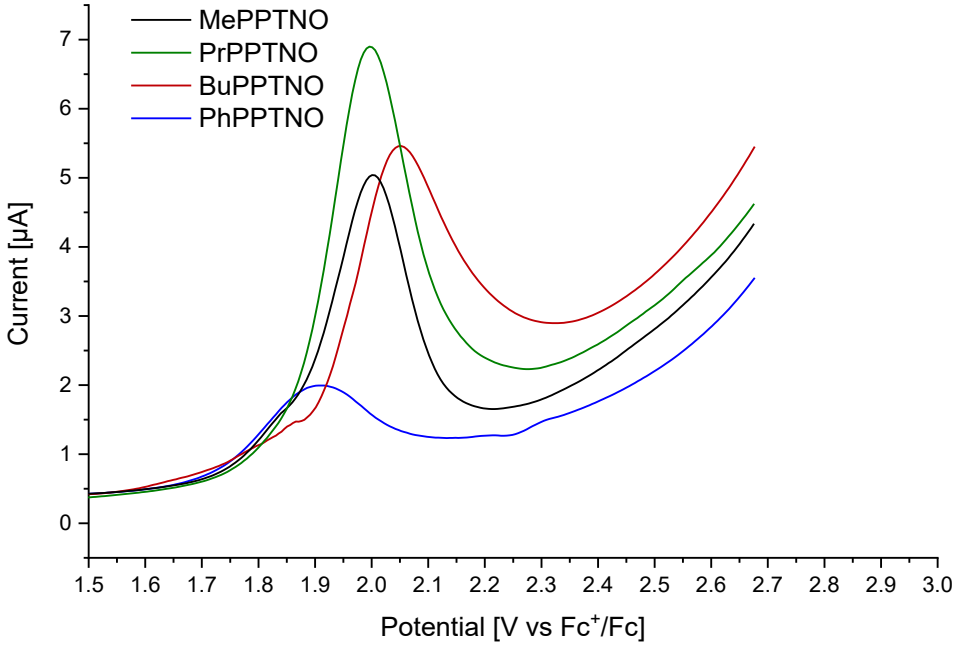

Figure 9. DPV measurement of substituted PPTNOs

As for the UV-Vis spectra and the emission spectra, also here the substituents do not seem to have an effect, further proving the assumption that the chromophore is solely located on

the heterocycle. Having the excited state energy and the ground state redox potentials in hand the excited state redox potentials can be calculated. The excited state reduction potential is determined to be approximately +2.3 V. This value is one of the highest reported for organic photocatalysts.[9] A whole variety of different molecules can in theory be oxidized (Figure 5). This result is very promising for the possible application of PPTNO based compounds as photocatalysts. The excited state oxidation potential is calculated to be approximately -0.9 eV. This value is rather low and the utilization of the PPTNOs as excited state reductant is rather limited.

Next, the quantum yield of fluorescence was determined for the PPTNOs. Values in the range of 0.2 to 0.7% were obtained. These values are very low and indicate a either a high degree of ISC or IC or a long lifetime of the excited state. Again, the values obtained for differently substituted PPTNOs are very similar. To understand why the substituents have no influence in any of these redox and optical properties DFT calculations were performed to visualize the HOMO and LUMO (Figure 10). The HOMO and LUMO are the frontier orbitals that are relevant when considering single electron oxidation or reduction including the first excited state.

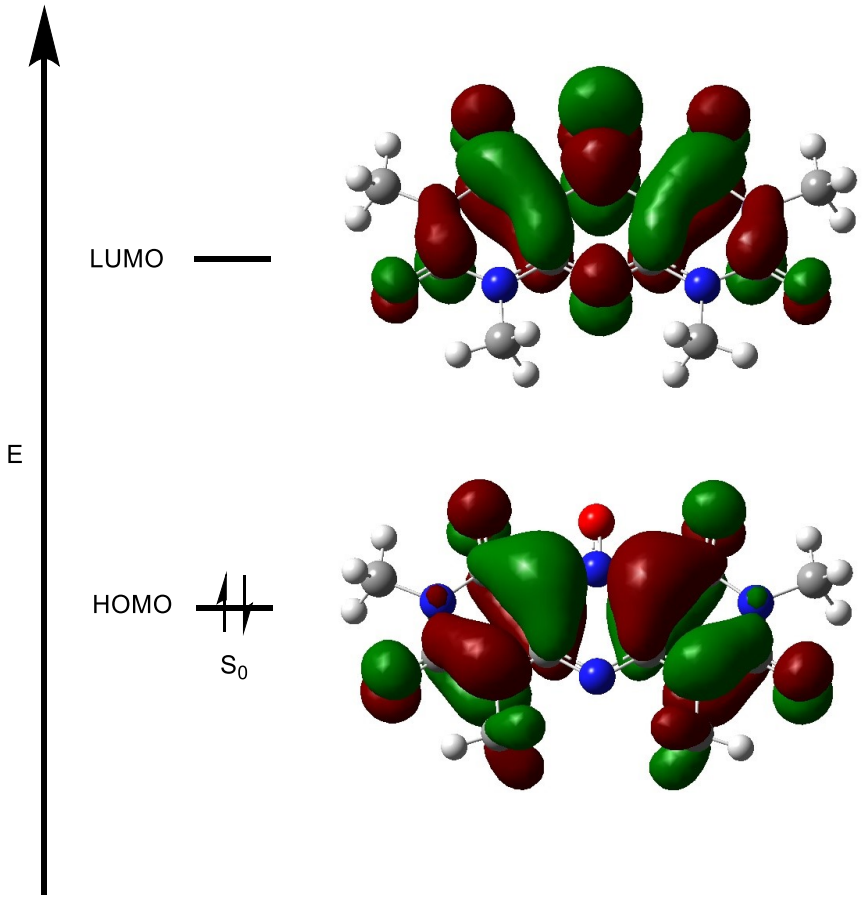

Figure 10. DFT calculations of MePPTNO. Top: LUMO, bottom: HOMO. B3LYP 6-31g(d,p) was used.

From the calculated frontier orbitals, it can clearly be seen that the substituent contribution is negligible in both the HOMO and the LUMO. Noteworthy the *N*-oxide functionality does not contribute to the HOMO but to the LUMO. This feature was discussed by Maki to be responsible for the oxygen atom transfer properties of these compounds.[34] In the LUMO the N–O bond has antibonding properties, therefore exciting an electron into the LUMO or reducing the PPTNO to the radical anion leads to a weakening of this bond and an oxygen atom transfer is facilitated.

In conclusion, a change in the substituent pattern is not expedient when looking for new properties and reactivities within the class of PPTNOs. If new properties are wanted its necessary to change atoms that contribute to the chromophore e.g. changing the amid to thioamide or phosphamide.

3.3 Evaluation of PPTNO based photocatalysts

When investigating photocatalysts it is important to compare new candidates to already established photocatalysts and judge their advantages and. A summary of all previously determined and discussed properties are in Table 2 and compared to commonly used organic photocatalysts. For this comparison acridinium based MesAcrMe$^+$ and flavin based RFTA were chosen. These catalysts are frequently used and are structurally related e.g. tricyclic *N*-heterocycle (Figure 11).[9]

Table 2. Comparison of commonly used photocatalysts [9, 31]

Compound	$E_{1/2}^{red}$ [V vs. SCE]	$E_{1/2}^{ox}$ [V vs. SCE]	E_{red}^{*} [V vs. SCE]	E_{ox}^{*} [V vs. SCE]	ϕ_f [%]
MePPTNO	-0.91	+2.42	+2.33	-0.82	0.7
PrPPTNO	-0.95	+2.42	+2.30	-0.83	1.9
BuPPTNO	-0.92	+2.47	+2.33	-0.78	0.4
PhPPTNO	-0.93	+2.33	+2.32	-0.92	0.2
MesAcrMe$^+$	-0.49	-	+2.18	-	0.1
RFTA	-0.60	-	+1.50	-	0.2-0.6[a]

[a] For the tetrabutyrat, high solvent dependency.[32]

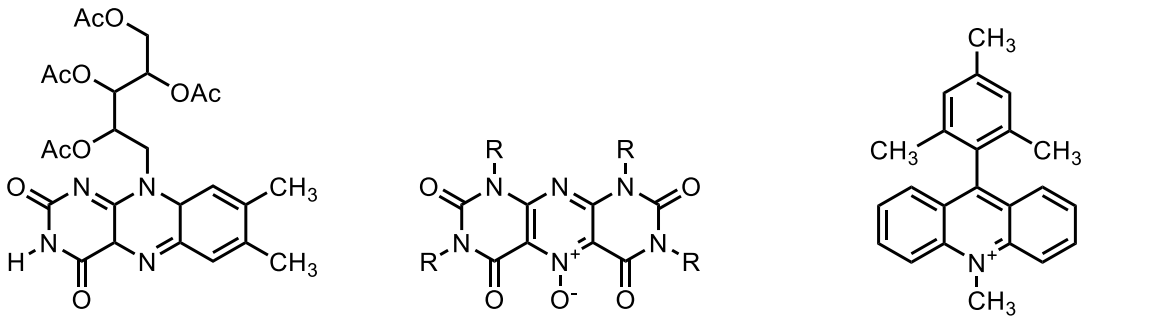

Riboflavin tetraacetate (RFTA) | Pyrimidopteridine (PPTNO) | 10-mesityl-9-phenylacridinium ($MesAcrMe^+$)

Figure 11. Structure of tricyclic photocatalysts containing an *N*-heterocycle.

With respect to the quantum yield the PPTNOs are very comparable to the commonly used $MesAcrMe^+$ and RFTA. A low quantum yield was determined which is generally considered to be a good characteristic for a photocatalyst. There are no excited state oxidation potentials reported for both the acridinium and flavin catalyst, possibly due to problems when measuring the CV/DPV. As already discussed, using the PPTNOs as excited state reductant is not very promising due to limited transformations possible. Importantly, the excited state reduction potential is very high, even higher than that of $MesAcrMe^+$. Since it is very promising to use the PPTNOs as excited state oxidants, the ground state reduction potential should be as low as possible to ensure that as many intermediates as possible can close the catalytic cycle. In other words, the gap between E^*_{red} and $E^{red}_{1/2}$ should be as big as possible. For RFTA and $MesAcrMe^+$ this window is smaller than that of the PPTNOs. This again showcases that the PPTNOs are very promising candidates to be used in photo redox catalysis. Not only a broad spectrum of compounds can be oxidized but also many species can close the catalytic cycle.

Importantly, these considerations are all theoretical and there are more parameters to consider when evaluating a photocatalyst. For example, some compounds might show promising excited state redox potentials but might decompose under irradiation. So, the photostability is another factor that needs to be considered. Noteworthy, the parameters discussed before, e.g. ground state and excited state redox potentials are only parameters that can predict the thermodynamic view on a reaction. Sometimes, a reaction is very exergonic but still no product is found after conducting the reaction. This might be because one or many steps in the catalytic cycle are too slow or back electron transfer is too fast, so a careful kinetic evaluation is also very important.

3.4 Photoisomerization of cinnamic acid derivatives

After the theoretical considerations it is important to show the applicability of the newly synthesized PPTNOs in a photocatalyzed reaction. The structurally related riboflavin was

chosen as a benchmark. Gilmour reported the *E-Z* isomerization of cinnamic acids derivatives using riboflavin (Scheme 13).

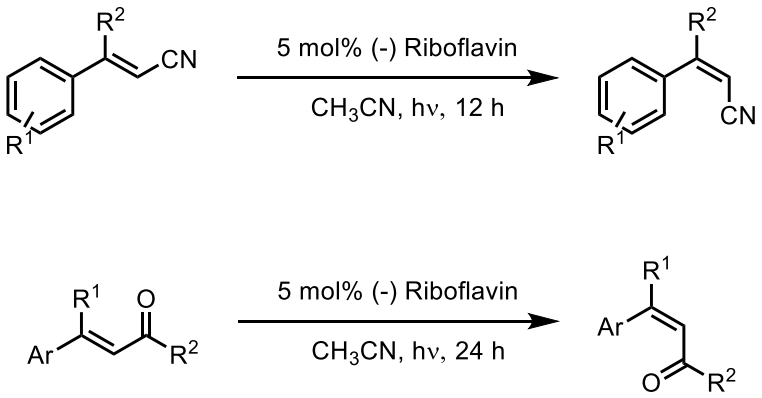

Scheme 13. E-Z isomerization of cinnamic acid derivatives by riboflavin.

The mechanism was proposed to be an energy transfer of the triplet excited state from RFTA to the cinnamic acid derivative. Due to the low quantum yield of fluorescence of the PPTNOs they might also be able to participate in ISC to form the triplet excited state. The PPTNOs were irradiated under the same conditions as those used by Gilmore and unsubstituted methyl cinnamate was chosen as model substrate. The results are shown in Table 3.

Table 3. Photocatalytic isomerization of methyl cinnamate.

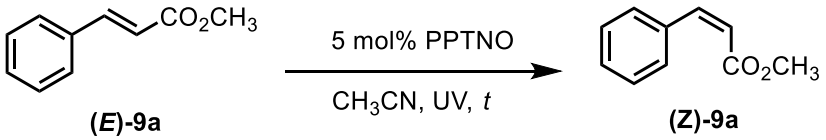

(*E*)-9a **(*Z*)-9a**

		16 h		24 h	
Entry	**Catalyst**	**Yield [%]**	**Ratio *E*:*Z***	**Yield [%]**	**Ratio *E*:*Z***
1	MePPTNO	95	69:31	90	55:45
2	PrPPTNO	99	68:32	96	70:30
3	BuPPTNO	99	76:24	96	67:33
4	PhPPTNO	99	77:23	98	55:45
5	-	-	-	99	95:5
6	Riboflavin	-	-	quant.	41:59

All four PPTNOs (Me, Pr, Bu, Ph) can isomerize (*E*)-methyl cinnamate **(*E*)-9a** to (*Z*)-methyl cinnamate **(*Z*)-9a** up to an E:Z ratio of 68:32 using PrPPTNO (Entry 2). Increasing the

reaction time from 16 h to 24 h was beneficial especially for MePPTNO and PhPPTNO reaching an E:Z ratio of 55:45 (Entry 1 and 4). To rule out a background reaction triggered by light but not by the catalyst the reaction was performed at the same wavelength without photocatalyst. No isomerization was observed proving the necessity of the PPTNOs. Gilmore reported an E:Z ratio of 41:59 favoring the Z isomer. Unfortunately, the PPTNOs are not as potent as riboflavin in this reaction. As a proof of concept this reaction was important, showing the possible application of PPTNOs as photocatalyst. The mechanism was not investigated for the PPTNO catalyzed photoisomerization of (*E*)-cinnamic acid. While a triplet energy transfer might be possible other pathways like a SET followed by isomerization and BET cannot be ruled out.

3.5 Photooxidative cyclization of biphenylcarboxylic acid

To further evaluate the applicability of the PPTNOs another model reaction was chosen. Here an oxidative cyclization of biphenyl carboxylic acid using molecular oxygen as terminal oxidant was evaluated (Table 4). Gilmour reported this reaction using riboflavin as photocatalyst. Importantly every 12 h 5 mol% of catalyst was added due to photodecomposition of the catalyst (12-36 h reaction time). A low photostability is a parameter that cannot be predicted when evaluating the beforementioned photophysical and electrochemical parameters. Here the photodecomposition was addressed by adding more catalyst. Using a more stable catalyst would certainly be a better choice. Using the PPTNOs in this reaction gave the wanted product using only 5 mol% of catalyst. Here the BuPPTNO showed to be the most promising catalyst (53% yield) and the MePPTNO being the least promising (30%). Slightly changing the reaction conditions from using acetonitrile to acetonitrile:MeOH = 1:1 and using a more powerful light source drastically increased the yield. Using these conditions PhPPTNO provided the product in 86% isolated yield. This is higher than the yield reported by Gilmour (84%) by using only 5 mol% instead of 2 x 5mol%. For this reason, PPTNOs are promising photocatalysts, while giving the same reactivity the catalyst is more stable. Importantly the only photodecomposition product of the PPTNO found was the corresponding PPT.

Table 4. Photocatalytic oxidation of 2-phenylbenzoic acid to form 3,4-benzocoumarin.

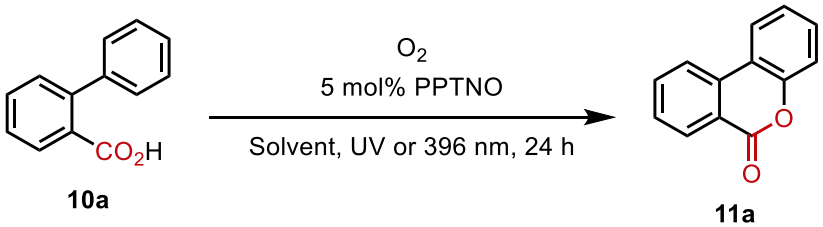

10a **11a**

	CH_3CN	CH_3CN/CH_3OH (1:1)

Entry	Catalyst	Yield [%][a]	Yield [%][b]
1	MePPTNO	30	65
2	PrPPTNO	44	77
3	BuPPTNO	53	80
4	PhPPTNO	49	86
5	-	6	-
6	Riboflavin	84	-

[a] Reactions performed using UVA lamps. [b] Reactions performed using LEDs (λ = 396 nm).

3.6 Extension of the catalyst library, CyPPTNO

Knowing that the PPTNOS are promising photocatalysts an extension of the library is important. Primary alkyl chains (Me, Pr, Bu) and aryl ring (Ph) bearing PPTNOs were synthesized. We rationalized that a cyclohexyl group might change the reactivity of the PPTNO. No change in the optical and redox properties was expected yet the stability might change due to the sterical demand of the cyclohexyl group. The synthetic route was different than that of the other alkyl substituted PPTNOs (Scheme 14). The direct synthesis to the 6-amino uracil was not possible because the dicyclohexyl urea is less reactive and very poorly soluble.

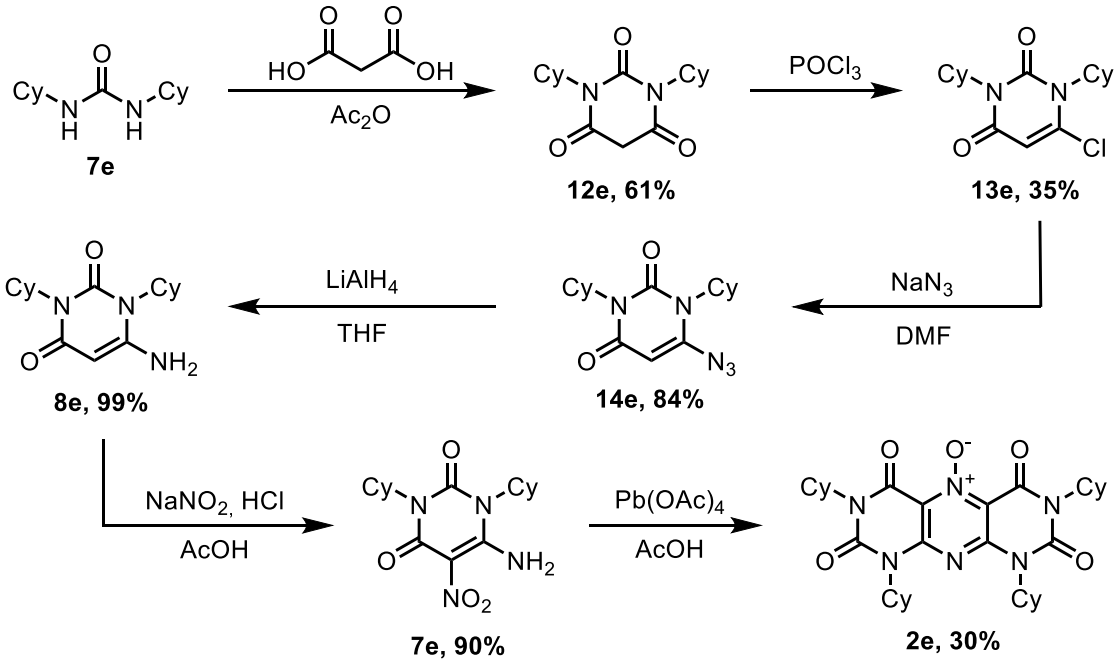

Scheme 14. Route for the synthesis of CyPPTNO.

The first step was the synthesis of the barbituric acid (**12e**) from the dicyclohexyl urea (**7e**) using malonic acid and acetic anhydride. The product was obtained in a moderate yield of

61%. Intermediate **12e** is then converted using phosphorous oxychloride giving chlorinated product **13e** in a poor yield of 35%. Main problem for this reaction was the poor conversion of the substrate. Increasing the reaction time and/or the temperature will likely increase the yield. After nucleophilic substitution using sodium azide the azido uracil (**14e**) is obtained in 84%. Reduction using LAH furnished the amino uracil (**8e**) in quantitative yield. Next, an electrophilic addition using sodium nitrite gave the nitroso uracil (**7e**) in 90% yield. The oxidative dimerization of **7e** using lead tetraacetate gave the product **2e** in poor yield of 30%. Many uncharacterized side products were formed as observed by TLC. This reaction should be performed again using PIDA as oxidant and maybe the yield can be increased using this milder oxidant.

Furthermore, the characterization of the ground and excited state properties of **2e** was performed. The results are presented in Table 5 and compared to MePPTNO and PhPPTNO. No influence of the substituent on these properties was found, as expected. Also, neither the shape nor the position of the UV-Vis and the fluorescence signals were affected.

Table 5. Electrochemical and photophysical comparison of MePPTNO and PhPPTNO with CyPPTNO.

Compound	$E_{0,0}^{S1}$ [eV]	$E_{1/2}^{red}$ [V vs. SCE]	$E_{1/2}^{ox}$ [V vs. SCE]	E_{red}^{*} [V vs. SCE]	E_{ox}^{*} [V vs. SCE]
MePPTNO	+3.24	-0.91	+2.42	+2.33	-0.82
PhPPTNO	+3.25	-0.93	+2.33	+2.32	-0.92
CyPPTNO	+3.26	-0.91	+2.37	+2.35	-0.89

3.7 Oxidative decarboxylation of Boc-Proline

Due to the promising results in the oxidative cyclization of biphenyl carboxylic acid it might be possible to use alkyl carboxylic acids as substrates. Radicals formed after single electron oxidation of aryl carboxylic acids do not undergo decarboxylation. This is attributed to the fact that the decarboxylation is very slow, and BET is in most cases faster. In comparison aliphatic carboxylic acids quickly undergo decarboxylation once the carboxyl radical is formed.[37]

Table 6. Screening for the oxidative decarboxylation of Boc-proline.

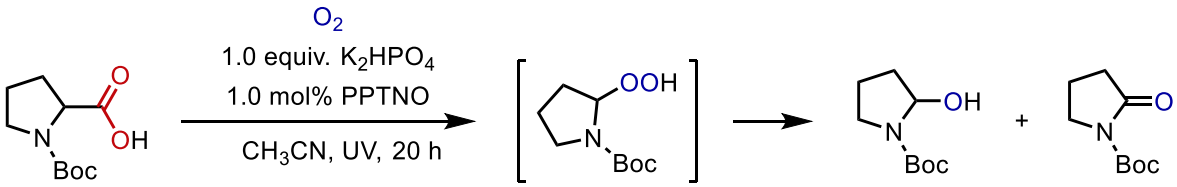

15a **16a** **17a** **18a**

Entry	Catalyst	Solvent (Ratio)	Yield [%][a]
1	BuPPTNO	CH_3CN/H_2O (9:1)	62
2	BuPPTNO	CH_3CN/H_2O (9:1)	<5[b]
3	BuPPTNO	CH_3CN	68
4	PhPPTNO	CH_3CN	59
5	MePPTNO	CH_3CN	77
6	CyPPTNO	CH_3CN	36
7	PrPPTNO	CH_3CN	80

[a] Mixture of 17a and 18a. [b] No irradiation.

Therefore, an oxidative decarboxylation of Boc-Proline was envisioned (Table 6). BuPPTNO was initially chosen as photocatalyst in combination with K_2HPO_4 as base. K_2HPO_4 was chosen based on a publication of MacMillan on a decarboxylative arylation.[38] Starting with an acetonitrile water mixture (9:1) gave the aminal **17a** and the amid **18a** products as a mixture in 62% isolated yield (Entry 1 and 2). Noteworthy analysis of the product mixture is challenging due to formation of the aminal which exists in its ring-closed and open chained form. Additionally, all products show rotamers, due to the bulk of the Boc group, when analyzing by NMR spectroscopy. Analysis by GC/MS lead to dehydration of **17a**. Therefore, precise determination of the ration of **17a** to **18a** was not possible. Further evaluation revealed that acetonitrile without addition of water gave a slightly higher yield (Entry 3) showing that the solubility of the base is not as important. PhPPTNO also gave the product in a satisfactory but decreased yield of 59% (Entry 4). MePPTNO gave a yield of 77% which is higher than that of BuPPTO (Entry 5). This is a surprising result because MePPTNO is very poorly soluble in common organic solvents and therefore a reduced yield was expected. Then the CyPPTNO was first tested in a photocatalytic reaction (Entry 6). While the oxidation products were found the yield was low (30%) showing that the bulk on

the substituent of the PPTNO might play a crucial role in the product formation. The best results were achieved using PrPPTNO giving 80% isolated yield (Entry 7).

A plausible mechanism for the oxidative decarboxylation of Boc-proline is shown in Scheme 15. In the first step Boc-proline (**15a**) forms the carboxylate (**15a-a**) by either deprotonation or autoprotolysis[39]. This step is necessary to reduce the oxidation potential because the acid cannot be oxidized by the excited state PPTNO (E_{ox} (Boc-proline) = +2.66 V vs SCE).[40] The PPTNO in its excited state will oxidize the carboxylate **15a-a** to the carboxyl radical **15a-b**. This radical is unstable and will form the C-centered radical **15a-c** under the extrusion of CO_2. Addition of molecular oxygen delivers peroxyradical **15a-d**. Oxygen will close the catalytic cycle under formation of a hydroperoxyradical. The formed peroxy radicals will undergo homocoupling (Scheme 15, b) forming an unstable tetraoxide intermediate **15a-e**. This intermediate will decompose in one of two possible pathways (Scheme 15, c). Either the **17a** and **18a** are formed under the extrusion of singlet oxygen, or the excited state amide **18a-a**, the **17a** and triplet oxygen are formed. Observation on fatty acid based tetraoxide intermediates favor the route that include the formation of singlet oxygen.

Since the selectivity towards one oxidation product is very low the investigation on oxidative decarboxylation of carboxylic acids was discontinued. Noteworthy, the utilization of C-centered radicals formed by photocatalytic decarboxylation was later showcased by our group in a C–C coupling with electron deficient olefins.[41]

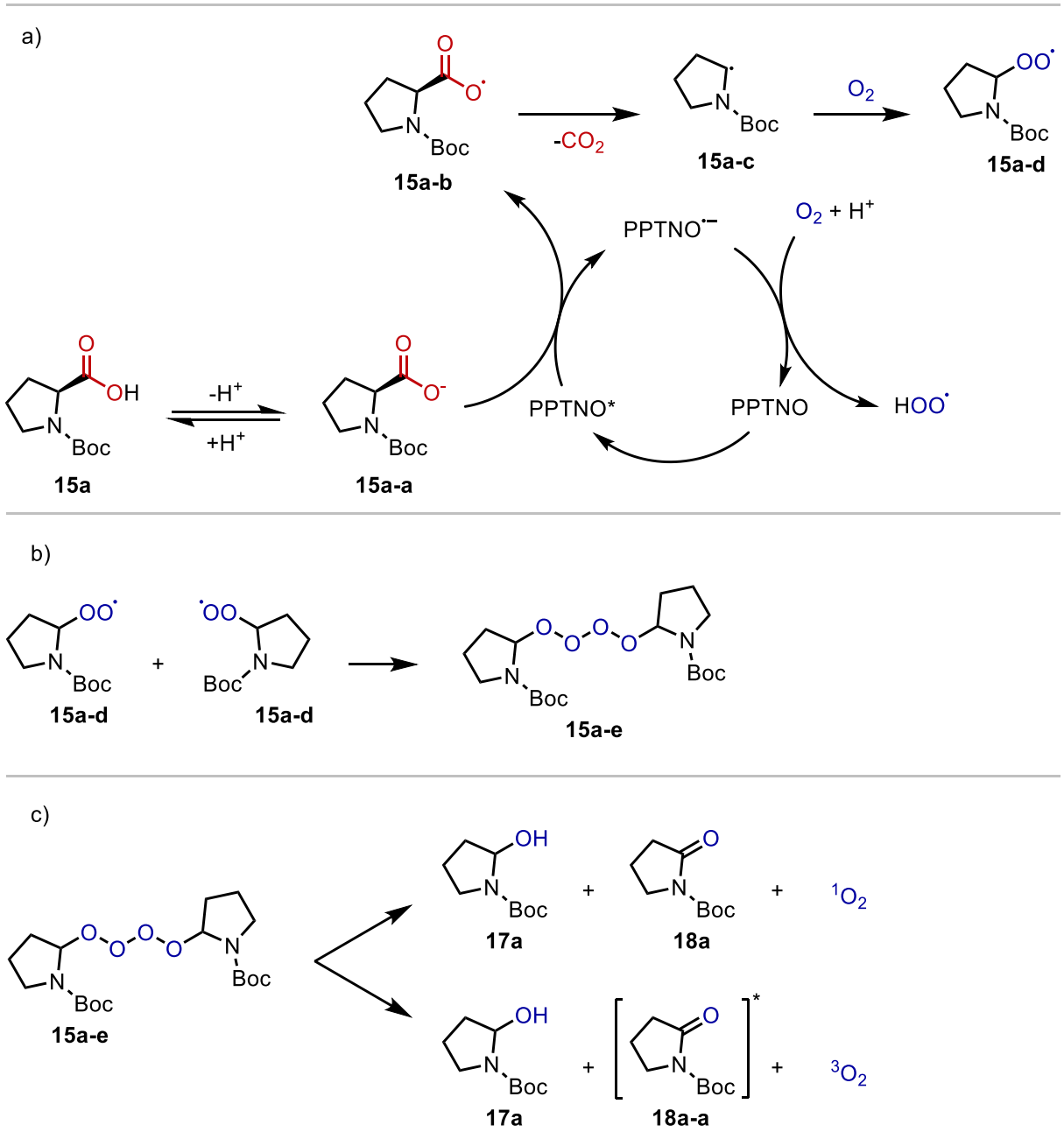

Scheme 15. Plausible mechanism for the oxidative decarboxylation of BOC-proline. a.) Photocatalytic formation of peroxyradicals. b) Homocoupling of the peroxyradicals. c) Decomposition of the tetraoxy species forming the products.

3.8 Extension of the catalyst library, PPT

Seeing the PPT being the only photodecomposition product in different reactions, the hypothesize arose that the PPTNO might act as a pre catalyst for these reactions. The PPTNO might undergo deoxygenation releasing the PPT as catalytically active species. To verify this hypothesis, it is important to synthesize and characterize these compounds. My task was the evaluation of the ground and excited state properties by UV-Vis and fluorescence spectroscopy followed by CV and DPV measurements and finally the determination of the quantum yield of fluorescence. For all determined properties there

was almost no correlation with the substituent, so the PPT behave very similar to the PPTNOs. For the UV-Vis spectra the shape of the n–>π* band changes and becomes more structured. The comparison of MePPTNO and MePPT is shown in Figure 12.

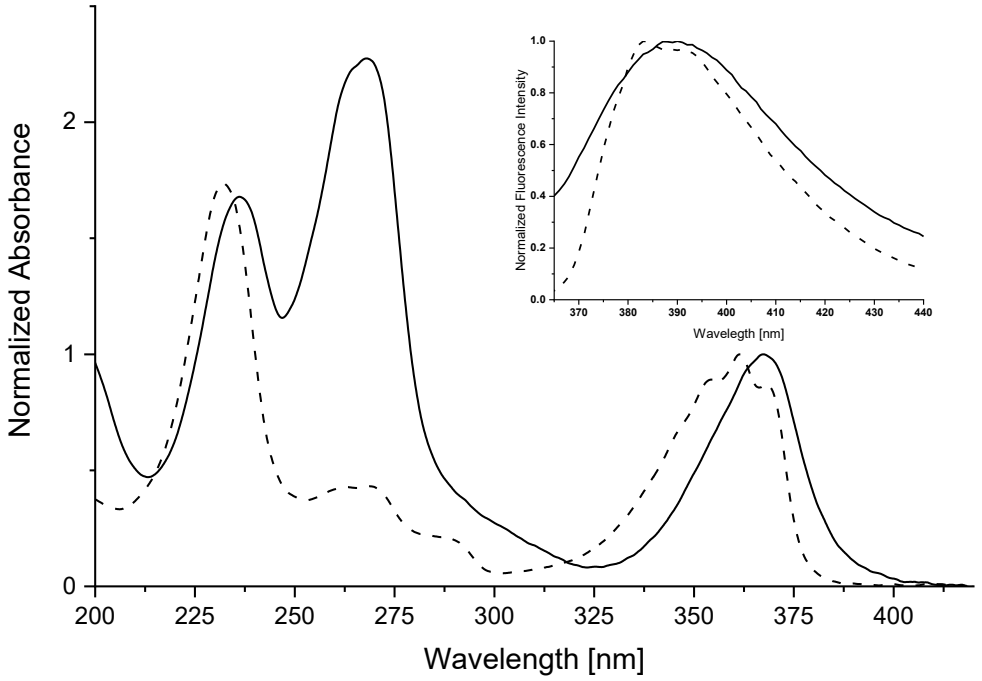

Figure 12. Normalized UV-Vis spectrum and fluorescence spectrum (inset) of MePPTNO (solid line) and MePPT (dotted line)

Additionally, a small hypsochromic shift for both the local absorption and emission maximum can be seen. Remarkable is the absorption band at 270 nm which is strong for the PPTNO and almost vanishes for the PPT compounds. Likely the *N*-oxide functionality contributes to this band.

When comparing the CV (Figure 13) and DPV (Figure 14) measurements of PPTNO and PPT only one reduction signal can be found for the PPTs compared to two for PPTNOs. This underlines the statement that the first reduction event for the PPTNOs is the deoxygenation to get the PPT which is reversible reducible. Furthermore, both the reduction and the oxidation signal are slightly shifted to more negative values. Like for the PPTNOs for the PPTs an irreversible oxidation signal can be found.

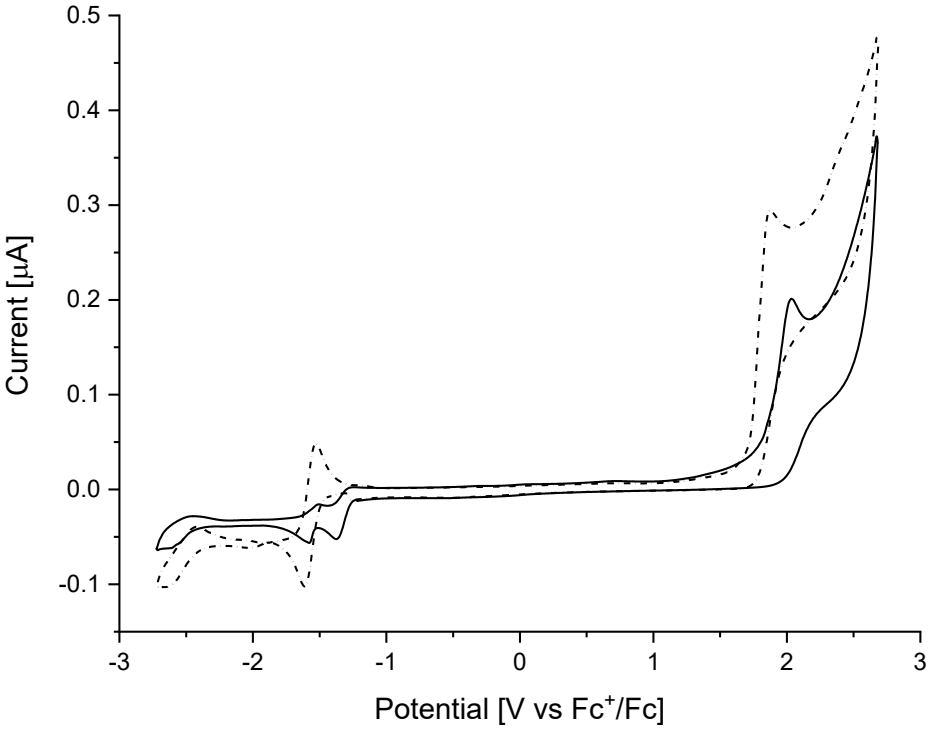

Figure 13. Cyclic voltammogram of MePPTNO (solid line) and MePPT (dotted line).

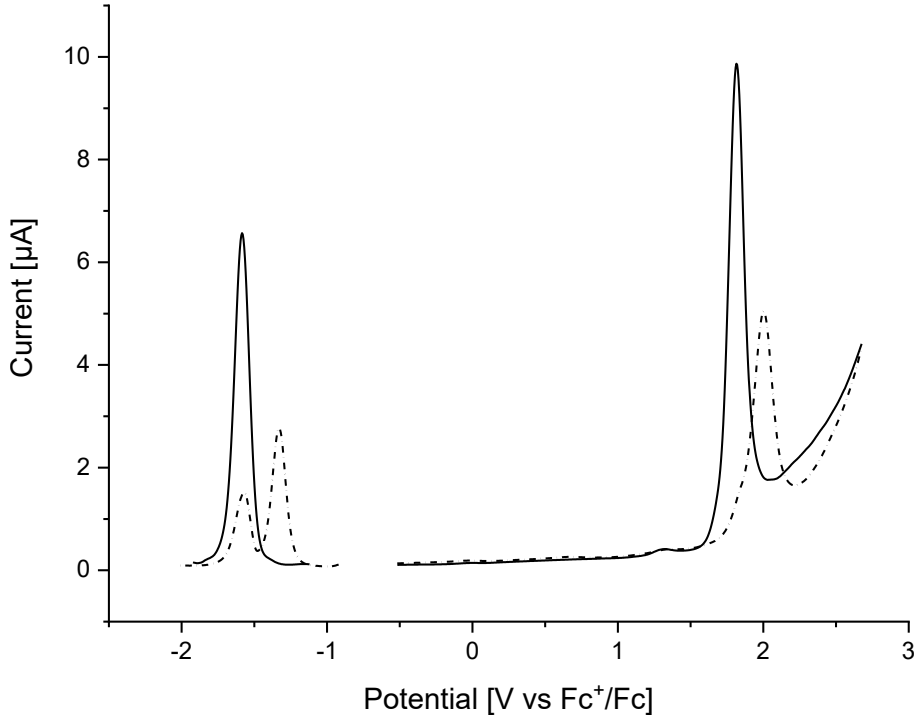

Figure 14. Differential pulse voltammogram of MePPTNO (solid line) and MePPT (dotted line).

Lastly, the quantum yields of fluorescence were determined. Here, unexpectedly, high quantum yields were found. The alkyl PPTs showed quantum yields of 60 to 70%. The PhPPT, on the other hand, showed a quantum yield of fluorescence of 10%. This is lower than for the alkyl PPTs but still much higher than for the PPTNOs. All results for the PPTs are shown in Table 7 and compared to PPTNO. The high quantum yield of fluorescence shows

that the PPTs might react in a different way from the PPTNOs. Whereas the PPTNOs might be prone to triplet excited state chemistry the PPTs are more likely to undergo singlet excited state chemistry. The low quantum yield for PhPPT compared to the alkyl PPTs is probably also explained by a charge transfer complex.

Table 7. Comparison of photophysical and electrochemical properties of PPTs and PPTNOs

Compound	$E_{1/2}^{red}$ [V vs. SCE]	$E_{1/2}^{ox}$ [V vs. SCE]	E_{red}^{*} [V vs. SCE]	E_{ox}^{*} [V vs. SCE]	ϕ_f [%]
MePPTNO	-0.91	+2.42	+2.33	-0.82	0.7
PhPPTNO	-0.93	+2.33	+2.32	-0.92	0.2
MePPT	-1.16	+2.24	+2.17	-1.09	66
PhPPT	-1.12	+2.29	+2.18	-1.01	10

3.9 Oxidation of PPT based compounds to obtain PPTNOs

Maki reported the use of the PPTNOs as stochiometric oxidants in a variety of reactions. Performing these reactions in a catalytic fashion is of course an opportunity. Since the sole photodecomposition product is the PPT a reoxidation to get the PPTNO might be possible. This would give access to a reaction using catalytic amount of the PPTNOs and a stochiometric amount of an oxidant (Scheme 16).

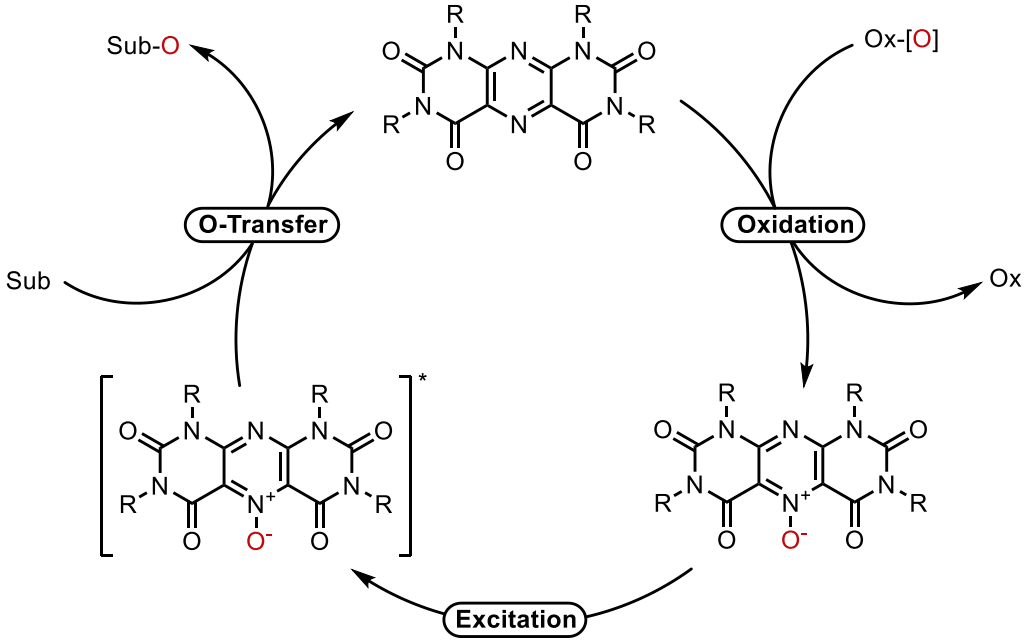

Scheme 16. Catalytic oxygen atom transfer using PPTNOs.

From the viewpoint of atom economy and price this reaction would be very promising. Therefore, different commonly used methods for the oxidation of pyridines to pyridine-*N*-

oxides were tested to reoxidize the PPT to the PPTNO. For this reaction TLC was chosen as analytical method to evaluate product formation since the PPTs are highly fluorescent and the PPTNOs strongly absorbing they can be distinguished very easily on TLC. Using GC/MS is problematic due to the high mass of these compounds and the instability towards electron ionization (EI). PPTNOs form PPTs under EI conditions which is especially problematic for this reaction.

First the oxidation of PPT by mCPBA in the presence of potassium carbonate was tested (Scheme 17).

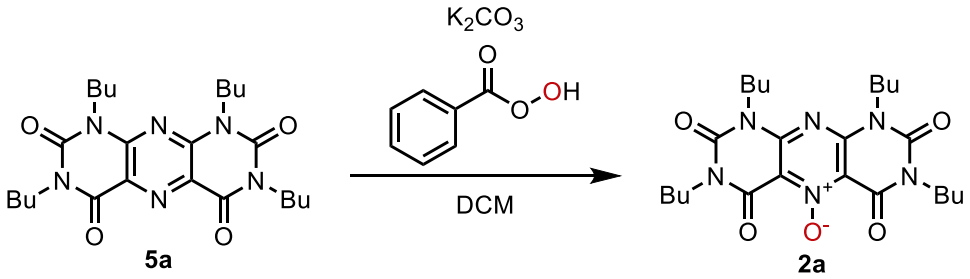

Scheme 17. Oxidation of BuPPT to BuPPTNO using mCPBA.

No PPTNO spot was found on the TLC. Assuming that a stronger (more electrophilic) oxidant is necessary, the methyl trioxo rhenium (MTO, **19a**) method was chosen (Scheme 18).[42] Here a rhenium oxo species (**19a-a**) is formed in the reaction of MTO with hydrogen peroxide. This species can transfer its oxygen to electron deficient *N*-heterocycles.[43] Unfortunately MTO suffers from low reactivity with sterically demanding substrates. Here no PPTNO was found, likely due to steric reasons.

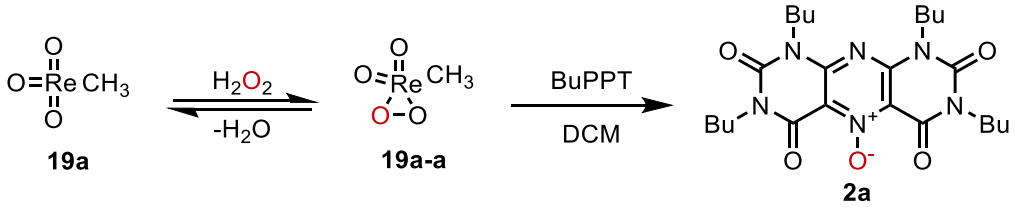

Scheme 18. Oxidation of BuPPT to BuPPTNO using MTO and H_2O_2.

Assuming that the PPTs are very electron deficient on the pyridazine heterocycle, a strongly electrophilic oxidant is necessary (Scheme 19). Therefore, trifluoroperacetic acid (**20b**) was prepared in situ by a reaction of a urea hydrogen peroxide (UHP) adduct with trifluoroacetic acid anhydride (**20a**).[44] Due to the electron withdrawing CF_3 group this reagent is more electrophilic then for example mCPBA. Unfortunately, no product was found.

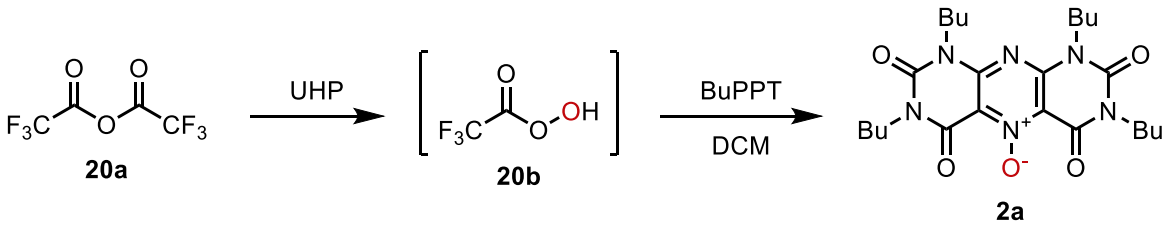

Scheme 19. Oxidation of BuPPT to BuPPTNO using in situ generated trifluoroperacetic acid.

Seeing no product formation in any of these reactions and remarkably no side reactions no further attempts were conducted. It is not clear if the reoxidation is not occurring because of steric or electronic reasons (or both). There are protocols for the oxidation of very electron deficient *N*-heterocycles to the *N*-oxides and bis-*N*-oxides using in situ generated hypofluoric acid.[45] While this might be a promising route to realize the reoxidation of PPT to PPTNO it is not applicable in a catalytic reaction due to the reactivity of hypofluoric acid towards the substrate.

To summarize, the utilization of PPTNOs in a catalytic oxygen atom transfer might not be possible due to problems in the reoxidation of PPT to PPTNO. Furthermore, there might be an additional problem concerning the position of the oxygen in the newly formed PPTNO (Scheme 20). It is possible to obtain the regioisomeric PPTNO (**2f**) which might have very different properties then **2a**.

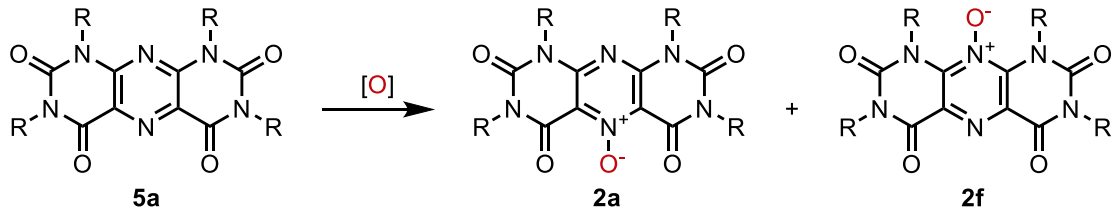

Scheme 20. Regioisomers of PPTNOs.

3.10 Extension of the catalyst library, synthesis of sulfur containing PPTNOS

To change the optical properties of the PPTNO compounds, sulfur based PPTNOs were set as a target structure. Since the calculation of the frontier orbitals revealed the participation of the carbonyl groups in the HOMO and LUMO an exchange to a thiocarbonyl group might alter the optical properties. First a reaction of BuPPTNO with Lawessons reagent (LR) was conducted in hope to get a 4-fold exchange of the carbonyl groups to thiocarbonyl groups. Interestingly the isolated product contained only two thiocarbonyl groups and the PPTNO was deoxygenated to PPT (Scheme 21).

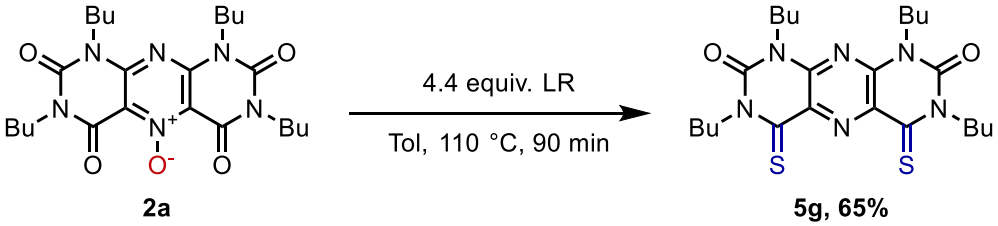

Scheme 21. Reaction of BuPPTNO with Lawessons reagent.

The deoxygenation of the *N*-Oxide should have been expected since Lawessons reagent is a strong reducing reagent.[46] The structure of this compound was verified by X-ray analysis (Figure 14).

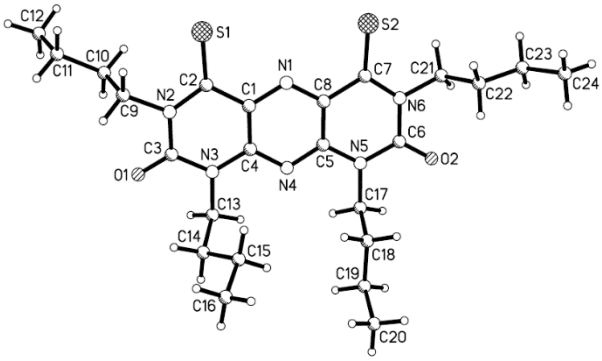

Figure 14. X-Ray analysis of **5g**.

Lawessons reagent is most reactive with compounds bearing electron rich carbonyl groups. The more electron deficient the carbonyl group is the more difficult the transformation to the thiocarbonyl group is.[47] For the PPTNOs we have two different types of carbonyl groups. One is best described as an amidic group the other as a urea. The amidic group is more electron rich and was indeed the group that was converted in this reaction. Converting a urea type carbonyl is challenging due to its electronic situation, therefore a strategy was chosen to start from the dibutyl thiourea **7g** which is commercially available.

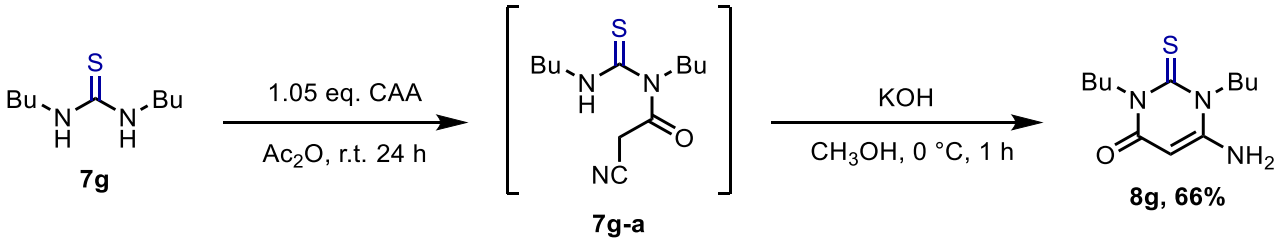

Scheme 22. Synthesis of thiocarbonyl containing 6-amino uracil.

The synthesis of the sulfur containing 6-aminouracil **8g** worked well in a promising 66% yield by slightly changing the procedure used for the BuPPTNO route (Scheme 22). Using an inert atmosphere seems to be crucial for this reaction as is decreasing the temperature to room temperature to avoid very colorful side products that cannot be removed easily using column chromatography. Despite having colorful side products there were also side

reactions that decreased the yield when using higher temperature like the formation of the carbodiimide. The formation of the carbodiimide is also profound in the reaction using *O*-ureas.

Next the reaction of **8g** with LR was performed (Scheme 23) to get the 6-aminouracil with two thiocarbonyl groups (**8h**). This reaction turned out to be challenging. If the colorful side products from the prior step are not removed properly a gray almost black side product formed in this reaction. Even after 3-fold column chromatography this black side product could not be removed. Considering that the final product is a photocatalyst and needs to be optically pure it is necessary to remove those impurities as early as possible. Purification of **8g** prior to this reaction by recrystallization obtaining colorless crystals solved this problem. Using 2.2 equivalents of LR in toluene gave the product **8h** in 67% yield. Using pyridine as solvent completely inhibits the reaction and no product is found.

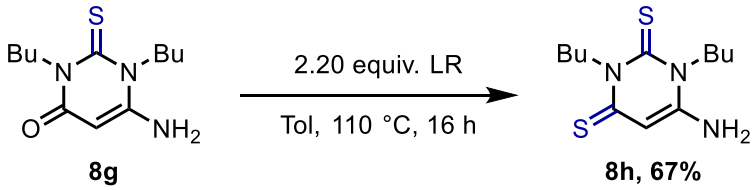

Scheme 23. Reaction of **8g** with Lawessons Reagent.

Next the nitrosylation of **8h** was attempted (Scheme 24). Using the employed reaction conditions for this reaction was not successful. While full conversion was observed (TLC) many different compounds were found. This reaction is characteristically very fast and accompanied by a distinctive purple color. Here the reaction turned black and insoluble compounds were found. Likely these conditions are too harsh and side reactions like polymerization occur. Decreasing the equivalents of sodium nitrite from 2.0 to 1.2 was not beneficial. Here the conversion was not complete, but the side products remained. The acidic conditions might be causing side reactions and a different reaction using nitrosyl tetrafluoroborate in acetonitrile was attempted. These non-acidic conditions that also deliver a nitrosyl cation were also not successful. Again, many side products were observed. Likely the low selectivity arises from the nitrosyl cation itself and therefore directly converting **8h** to **1h** cannot be achieved easily.

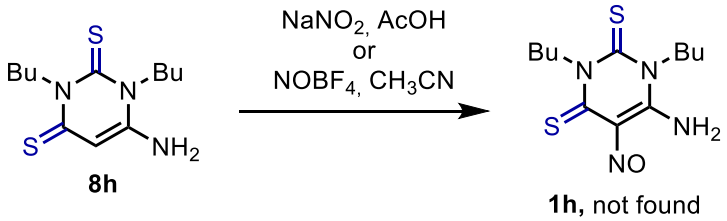

Scheme 24. Synthesis of the 5-nitroso-6-aminouracil containing two thiocarbonyl groups.

Therefore, the synthesis of the 5-nitroso-6-amino uracil containing one thiocarbonyl group **1h** was attempted (Scheme 25). After changing the solvent from using acetic acid to a mixture of hexafluoro isopropanol (HFIP) and acetic acid, **1g** could be obtained in 79% yield. In contrast to the route for the oxygen containing compounds a recrystallization of the nitroso compound is suggested again to remove colored side products.

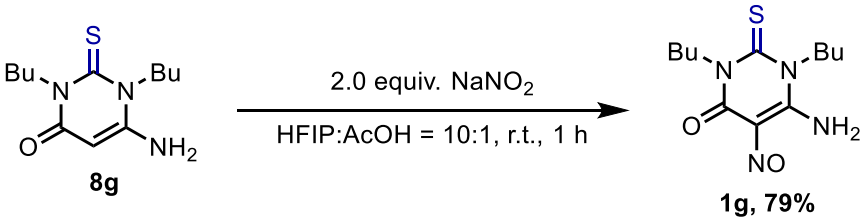

Scheme 25. Electrophilic nitrosylation of **8g**.

Attempts of converting **1f** using LR were not successful and a broad spectrum of products was obtained. Probably due to the newly introduced oxygen in the nitroso group. Fortunately, the oxidative dimerization of this compound to access the BuPPTNO with two thiocarbonyl groups (**1f**) was successful. Both the PIDA and lead tetraacetate route were successful, although in low yields (Scheme 26).

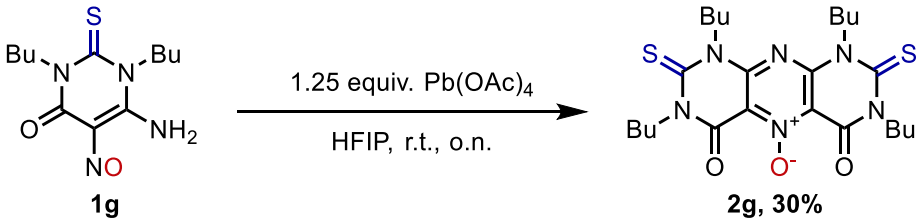

Scheme 26. Oxidative dimerization of **1g** using lead tetraacetate.

Like for most of the previously discussed reactions a broad spectrum of side products was found, and optimization of this step certainly is necessary. Noteworthy **2g** decomposes when stored under bench conditions which makes its application as photocatalyst challenging. Due to the instability further attempts in synthesizing the BuPPT containing four thiocarbonyl groups were stopped. In principle converting **2g** with LR should give this product.

To prove the alteration of the optical properties UV-Vis spectra were recorded for **5g** and **2g** (Figure 15).

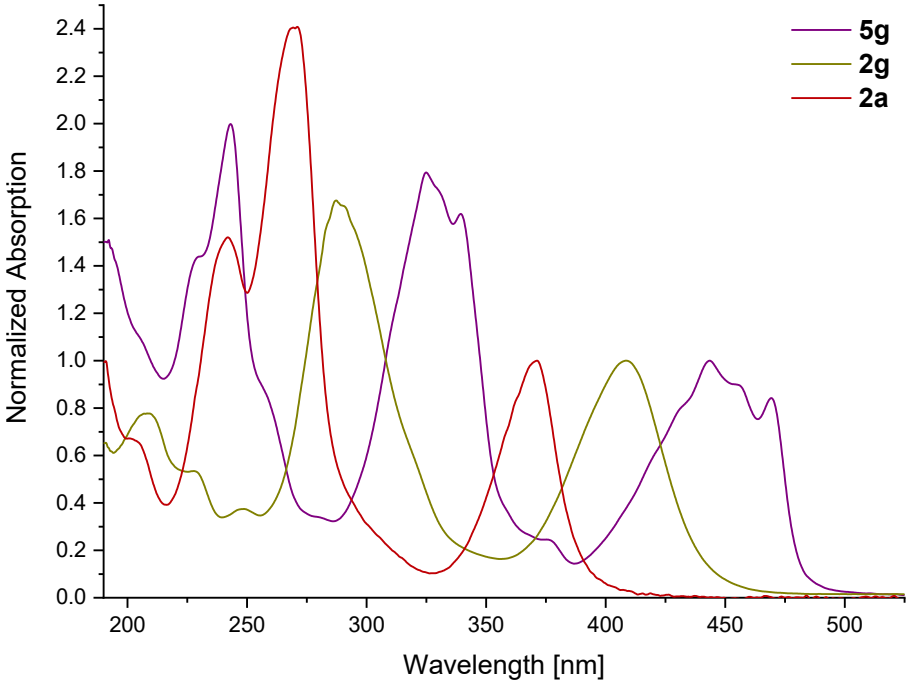

Figure 15. Normalized UV-Vis spectrum of BuPPTNO, **5g** and **2g**.

For both compounds a bathochromic shift of the lowest energy band can be seen when comparing to BuPPTNO (**2a**). This shift is very pronounced for **5g**. To verify if these low energy bands are still n–>π* in character DFT analysis would be necessary. But the low intensity compared to the other bands is an indicator that the band is indeed a n–>π* due to symmetry forbidden transitions that decrease the intensity of n–>π* bands.[28] Furthermore **5g** shows structured absorption bands, but the reason for this is not clear.

For **5g** fluorescence spectra were recorded (Figure 16). A small stokes shift of 39 nm was found. Interestingly the mirror shape behavior of fluorescence signal to absorption signal is not given for this compound. While the absorption band shows a structure, the emission response is structureless. The reason for this result might be because the emission arises from two states. Evaluation using solvents of different polarity might help get further information.[36] The excited state energy was calculated to be $E_{0,0}^{S1}$ = 2.62 eV. Due to the bathochromic shift of the absorbance band a lower excited state energy compared to BuPPTNO was expected.

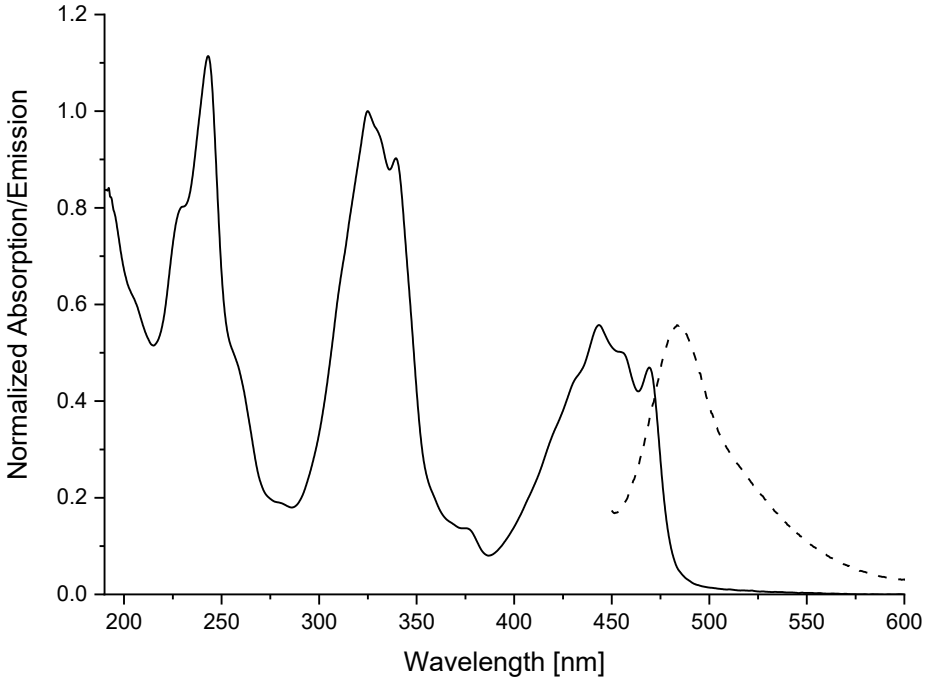

Figure 16. Absorption (solid line) and fluorescence (dotted line) spectrum of **2g**.

Further characterization of these compounds was not conducted due to the low likeliness of them being used in photocatalysis. Thiocarbonyl groups are very labile under irradiation and can undergo many different transformations.[48] For example a photocyclization with an alkene would likely lead to catalyst deactivation. Synthesizing these compounds was important to verify that it is in principle possible to alter the optical properties of PPT based compounds. Noteworthy not by variation of the substituents but by changing the heterocyclic core structure as it is predicted by DFT calculations.

I want to thank Dr. Andranik Petrosyan for the optimization of synthesis of the PPTNOs. My contribution to this was the reproduction of the synthesis of BuPPTNO and PrPPTNO. Furthermore, I want to express my appreciation to M.Sc. Miguel A. Argüello Cordero for the opportunity to reproduce and finish his results on the oxidative decarboxylation. I also want to thank Dr. Franziska Fennel (Institut für Physik, Dynamik molekularer Systeme Universität Rostock) and M.Sc. Miguel A. Argüello Cordero for the collaboration in the determination of the quantum yield of fluorescence. I want to thank Dr. Annette-E. Surkus for the collaboration in the measurement of the CV and CPV. Lastly, I want to express my gratitude to Dr. Jola Pospech for assisting me in the isomerization of methyl cinnamate and her findings that the cyclization of 2-phenylbenzoic acid is improved by a different light source and the utilization of methanol.

4 Photocatalytic, intermolecular hydroamination of stilbenes with monosubstituted amines

4.1 Introduction

Molecules containing carbon-nitrogen bonds are ubiquitous. The biological activity of these compounds is of much interest due to the possible application in drug molecules. As a result, there is a rising interest in the development of mild and safe conditions to form these nitrogen containing compounds.[49] Especially the reactivity of *N*-centered radicals (NCR) and their application in the formation of C–N bonds was developed intensively over the last decade.[50] The formation of NCRs can be difficult to achieve by thermal means. Characteristically, an N–X bond is cleaved homolytically under harsh reaction conditions. A reaction employing this type of reactivity is the Hofmann-Löffler-Freytag reaction (Scheme 26).[51]

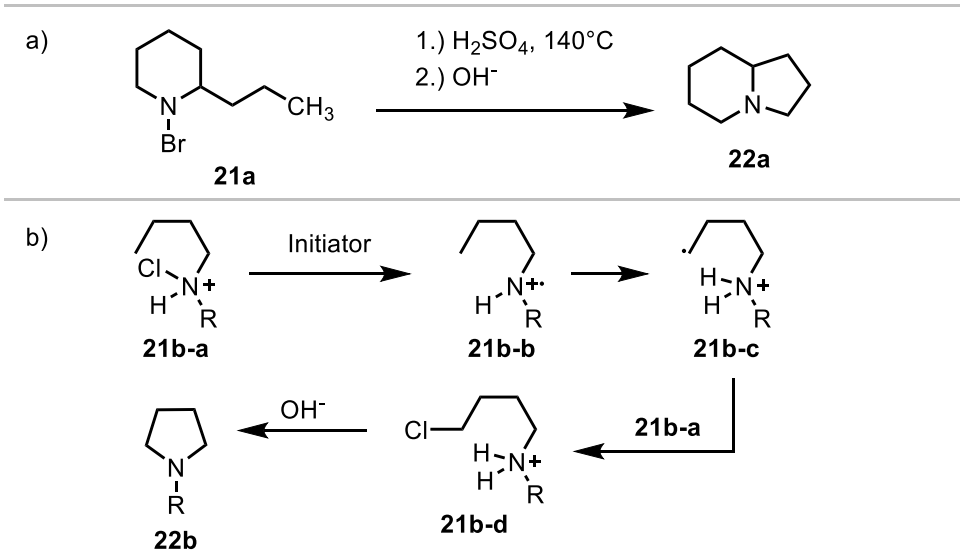

Scheme 26. a.) Hofmann reaction. B.) Extension of the Hofmann reaction by Löffler and Freytag.

Hofmann found that treatment of trisubstituted *N*-bromo amine **21a** with hot sulfuric acid followed by basic workup lead to the formation of a trisubstituted amine (Scheme 26, a). Later the product was confirmed to be **22a**. Löffler and Freytag expanded this reaction to *N*-chloro amines in the formation of pyrrolidines. The mechanism of the reaction was later found to be a free chain reaction mechanism (Scheme 26, b). The protonated *N*-chloro amine (**21b-a**) undergoes homolytic N–Cl bond cleavage to form the N centered radical cation (**21b-b**). 1-5 hydrogen atom abstraction gives a C centered radical cation **21b-c**. **21b-c** reacts with another molecule of **21b-a** which gives cation **21b-d** and regenerates **21b-b**. Basic workup furnishes the product in a nucleophilic ring closure.

Later milder reaction conditions were employed, for example the homolytic N–X bond cleavage of *N*-hydroxy-pyridine-2-thione carbamates (PTOC, Scheme 27).[52] After irradiation of the PTOC (**21c**) homolytic N–O bond scission leads to the formation of S centered radical **21c-a** and O centered carbamyl radical **21c-b.** The carbamyl radical will undergo decarboxlation releasing CO_2 and giving the NCR **21c-d**. While this reaction employs mild photolytic conditions a lot of waste is produced.

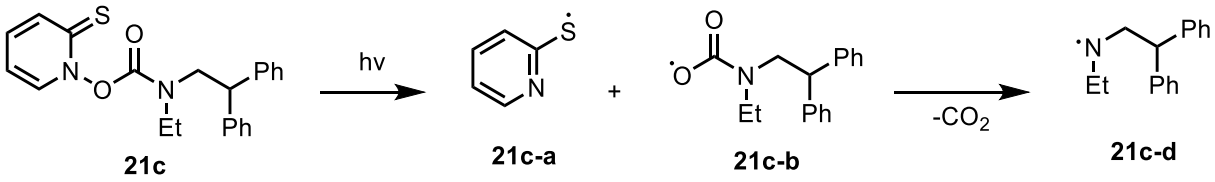

Scheme 27. Photolytic generation of aminyl radicals from PTOCs

A major disadvantage for both of the shown methods to generate NCRs is the formation of the utilized N–X bond. Generation of *N*-halo amines typically employs the utilization of *N*-chloro succinimide (NCS) or sodium hypochlorite solutions.[53] Both NCS and hypochlorites are strong oxidants and chlorination reagents. If an *N*-chloro amine containing functional group in the sidechain of a heterocycle is wanted, the introduction of the N–Cl bond might be challenging due to the low selectivity of these reagents. The synthesis of PTOCs takes several steps (Scheme 28). The commercially available sodium salt of *N*-hydroxypyridine-2-thione is first precipitated using hydrochloric acid giving **21c-e**. Reaction of the thione with very toxic phosgene gives access to pyridinium salt **21c-f**. Conversion of the pyridinium salt with an amine in the presence of triethylamine will then give access to the PTOC (**21**).

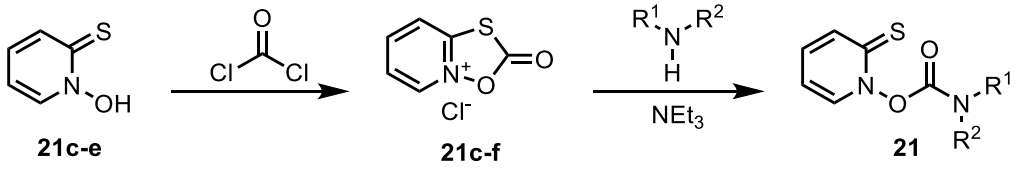

Scheme 28. Synthesis of PTOCs using phosgene.

While the homolytic cleavage of an N–X bond generally seems to be a good possibility to access NCRs the introduction of the N–X bond is tedious, expensive, and dangerous.

The introduction and development of photoredox catalysis opened a new pathway to the mild formation of NCRs avoiding the necessity of prefunctionalization. Many different types of NCRs were reported recently employing photocatalytic conditions. Notably, the reactivity of an NCR is heavily influenced by the substituents and can range from electrophilic to nucleophilic (Figure 8).

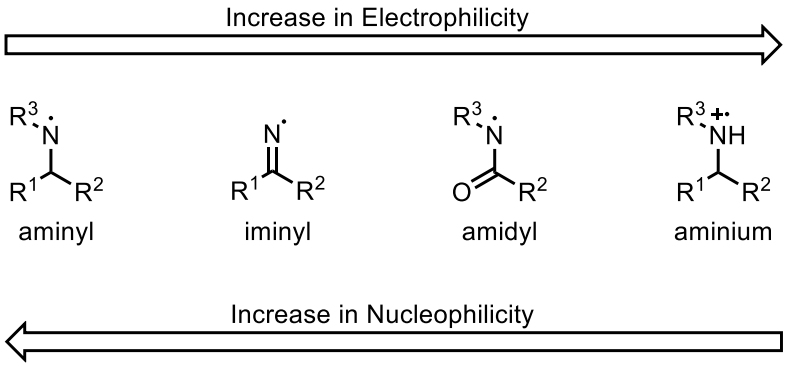

Figure 8. Types of NCRs.

The NCRs formed in photocatalytic reactions were used for a variety of transformations, the most important one being the hydroamination. In a hydroamination reaction an amine is directly added to an alkene to form a C–N bond in a fully atom economic manner. The biggest advantage is that no prefunctionalization is necessary. This reaction is thermodynamically feasible but is kinetically disfavored due to a high reaction barrier. Therefore, catalytic methods are necessary to realize such a reaction. Hydroamination reactions employing conventional ground state catalysts characteristically suffer from harsh reaction conditions like the usage of very strong bases and/or elevated temperatures. Beller reported the hydroamination of industrially important olefins (Scheme 29).[54] The direct addition of aniline (**24a**) to β-methyl styrene (**(*E*)-23a**) to access *N*-aryl amphetamines (**25a**) is a remarkable example of the utilization of easily accessible substrates to form valuable products. The reaction was performed at 160°C in THF using potassium tert-butoxid as a base giving the product in 50% yield. These are very harsh conditions that probably are not suitable for more functionalized substrates. This can be seen when stilbene (**(*E*)-26a**) was converted with piperidine (**26a**) to give α-phenyl phenethylamine **25b** in a very low 10% yield. Here the reaction was done at lower temperatures but using the even stronger base *n*-butyl lithium. It seems that the conversion of conjugated olefins remains a challenge for this type of reaction.

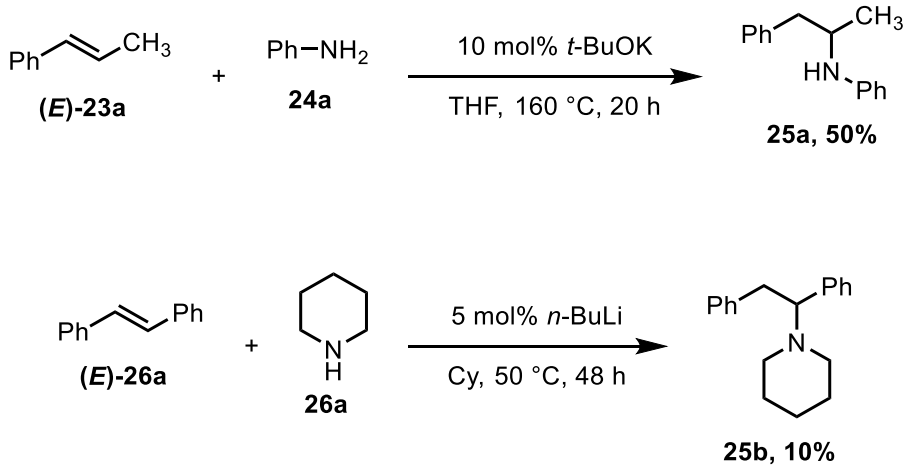

Scheme 29. Ground state catalyzed hydroamination, employing harsh reaction conditions.

To avoid these harsh reaction conditions photocatalytic methods should be preferred due to their intrinsic mildness. Leonori reported the photocatalytic intramolecular hydroamidation of aryloxy-amides employing the electrophilic reactivity of amidyl radicals (Scheme 30).[50e] In this reaction an organic excited state catalyst (Eosin Y) reduces an aryloxy-amide (**21d**) which releases the phenolate and generates the amidyl radical (**21d-a**). This amidyl radical is scavenged in an intramolecular cyclization by an electron rich olefin. After hydrogen atom transfer from a sacrificial reductant the desired product **28a** is formed. This method gives easy access to substituted pyrrolidinones under mild conditions. Tedious substrate synthesis to form the reducible N–X bond, necessity of sacrificial reductant and the restriction to intramolecular transformations are the major disadvantages for this system.

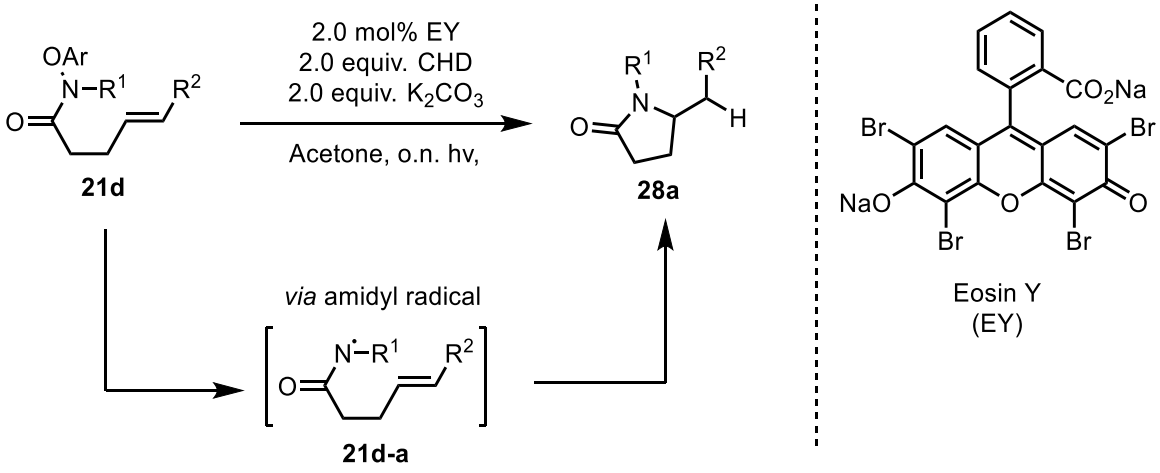

Scheme 30. Leonoris intramolecular hydroamidation employing amidyl radical reactivity.

Knowles reported a photocatalytic intermolecular hydroamination of disubstituted amines with electron rich alkenes (Scheme 31).[50c] After SET from the amine (**26b**) to an iridium based photocatalyst the aminium radical (**26b-a**) of a disubstituted amine is formed, which electrophilically attacks an electron rich alkene. After reduction followed by proton transfer

the pyrrolidine product **22b** is formed. The system of Knowles has two major advantages over that from Leonori, no sacrificial reductant and no pre functionalization is necessary.

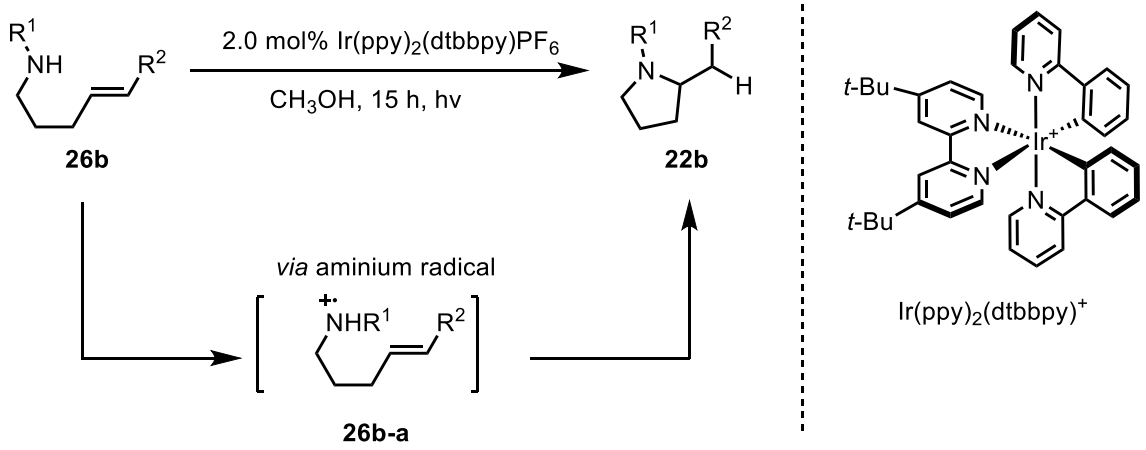

Scheme 31. Knowles intramolecular hydroamination employing aminium radical reactivity.

Besides the fact that the utilization of iridium based photocatalyst are problematic, tedious substrate synthesis and the limitation to intramolecular reactions using electron rich olefins remain a problem. Knowles and Leonori later improved this methodology by employing intermolecular versions of their reaction but converting electron deficient and conjugated olefins was not possible. Additionally, reactions using monosubstituted amines in an intermolecular fashion remain a formidable challenge due to their high oxidation potentials.

The high excited state reduction potential of the PPTNO based photocatalysts should allow the formation of aminium and/or aminyl radicals from monosubstituted amines. This feature makes these photocatalysts attractive candidates for the evaluation of a hydroamination reaction using monosubstituted amines.

4.2 Results and discussion

Irradiating a mixture of benzylamine, PrPPTNO and (*E*)-1-fluoro-4-(4-methylstyryl)benzene (**26b**) gave the hydroamination product as a mixture of regioisomers in 73% isolated yield. The regioselectivity of this transformation was rather low (61:39). To increase the yield and improve the regioselectivity a catalyst screening was performed (Table 8).

Table 8. Photocatalytic hydroamination of stilbenes. Optimization of the photocatalyst.

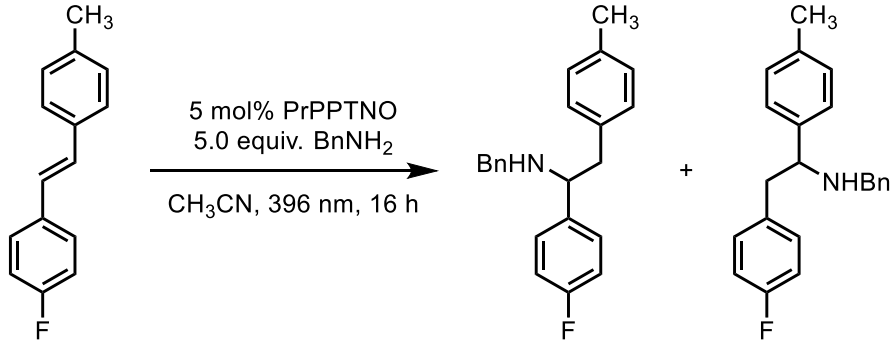

26b **73%, 61:39**

Entry	Photocatalyst	Yield[a]	Ratio of regioisomers[b]
1	**PrPPTNO**	**73**	**61:39**
2	PrPPTN	73	65:35
3	BuPPTNO	49	65:35
4	BuPPTN	66	68:32
5	MePPTNO	43	65:35
6	MePPTN	51	68:32
7	PhPPTNO	14	78:22
8	$[Ir(dFCF_3ppy)_2(bpy)]PF_6$	<5%	-
9	$Ru(bpy)_3(PF_6)$	<5%	-
10	$MesAcrMeBF_4$	<5%	-

[a]Isolated yields are shown. [b] Determined by ^{19}F NMR Spectroscopy.

Within the class of PPTNO based photocatalysts use of PrPPTNO resulted in the highest yield albeit giving a low regioselectivity. Using the deoxygenated PrPPT gave the same yield and almost the same regioselectivity as PrPPTNO (Entry 2). This indicates that either both PrPPTNO and PPT have the same activity in this reaction or more likely PrPPT is formed from PrPPTNO. When analyzing the reaction mixture by GC/MS, traces of stilbene oxide were found. Maki reported the reaction of PPTNOs with (*E*)-stilbene giving the stilbene oxide.[20b] This underlines the statement that for this reaction PrPPTNO is a precatalyst giving access to PrPPT. The best ratio of regioisomers was obtained using PhPPTNO (78:22), unfortunately the yield is too low (14%) to consider using this catalyst in further experiments (Entry 7). Commonly used photocatalysts (Entry 8–10) were not suitable for this transformation showing the unique properties of PPTNO based photocatalysts.

Next, a solvent screening was performed (Table 9). Nitrile containing solvents like aceto-, propio-, and benzonitrile showed the best results in this reaction (Entry 1–3). Using mixtures of acetonitrile and protic solvents decreased the yield (Entry 4–7 and 9) showing the general negative effect of protic solvents in this reaction. This was verified by using methanol without acetonitrile (Entry 16) the yield dropped to a very low 8%. Using unpolar solvents like *n*-hexane and toluene (Entries 14 and 15) had a very negative effect on the yield but surprisingly the ratio of regioisomers was positively affected. Using *n*-hexane, one regioisomer was dominantly formed. Since the yield is synthetically not useful it was not further investigated. Notably, pivalonitrile while bearing a nitrile functionality lead to a low yield of 25% (Entry 8).

Table 9. Photocatalytic hydroamination of stilbenes. Solvent screening. Reaction scheme depicted in Table 8.

Entry	Solvent	Yield[a]	Ratio of Regioisomers[b]
1	**CH_3CN**	**73**	**61:39**
2	PhCN	60	61:39
3	PrCN	57	61:39
4	CH_3CN/DMSO 4:1	40	61:39
5	CH_3CN/HFIP 9:1	36	61:39
6	Propylene carbonate	33	61:39
7	CH_3CN/H_2O 9:1	30	64:36
8	*t*-BuCN	25	62:38
9	CH_3CN/CH_3OH 4:1	25	62:38
10	$PhCF_3$	23	65:35
11	DMSO	18	61:39
12	DCM	18	65:35
13	THF	13	61:39
14	*n*-Hexane	10	95:5
15	$PhCH_3$	9	78:22
16	CH_3OH	8	59:41
17	DMF	<5	64:36

[a]Isolated yields are shown [b] Determined by ^{19}F NMR.

Unfortunately, the yield was not improved after the solvent optimization since the best solvent was already used, namely acetonitrile. After this it was important to find out the influence of the equivalents of amine used (Table 10).

Table 10. Photocatalytic hydroamination of stilbenes. Optimizing the ratio of amine to stilbene. Reaction scheme depicted in Table 8.

Entry	Equiv. Amine	Equiv. Stilbene	Yield[a]	Ratio of Regioisomers[b]
1	10	1	56	62:38
2	5	1	73	61:39
3	3	1	70	61:39
4	2.5	1	61	64:36
5	2	1	55[c]	62:38
6	1	1	47[c]	64:36
7	0	1	n.r.[d]	-
8	1	2	65	62:38
9	1	3	59	63:37

[a]Isolated yields are shown [b] Determined by ^{19}F NMR.[c] Average of 2 Experiments.
[d] Isomerization of stilbene E:Z = 13:1, determined by GC/MS.

Increasing the equivalents of amine from 3 to 5 slightly increases the yield (Entry 2 and 3) further raising the equivalents from 5 to 10 reduced the yield from 73% to 56% (Entry 1). Decreasing the equivalents expectedly decreased the yield (Entry 4–6). This led to the conclusion that either 3 or 5 equivalents should be used for this reaction. Noteworthy it is also possible to run this reaction with inverse stoichiometry (Entry 8 and 9) using the stilbene in excess. Giving 65% yield when using 2 equivalents of stilbene. The ratio of regioisomers was not influenced by the amine to stilbene ratio.

Since many photoreactions that employ NCRs use additives that assist the reaction in the HAT processes, deprotonation steps etc. an additive screening was conducted (Table 11).

Table 11. Photocatalytic hydroamination of stilbenes. Additive screening. Reaction scheme depicted in Table 8.

Entry	Additive	Yield[a]	Ratio of Regioisomers[b]
1	**-**	**70**	**61:39**
2	BF_3	65	63:37
3	p-Dicyanobenzene	63	63:37

4	TEMPO	56	61:39
5	Diphenylphosphate	52	65:35
6	Molecular sieves[c]	48	61:39
7	Hexamethylenetetramine	46	62:38
8	$(PhS)_2$	37	64:36
9	*i*-$PrNEt_2$	31	63:37
10	K_3PO_4	9	75:25
11	PPh_3	n.r.	-
12	*t*-BuOK	n.r.	-

[a]Isolated yields are shown. [b] Determined by ^{19}F NMR.

Heteroaromatic *N*-oxides form adducts with Lewis acids like BF_3. This adduct shows a change in hybridization on oxygen which leads to elongation of the N–O bond.[55] This elongated bond might lead to a quicker deoxygenation, releasing the active catalyst PPT more quickly. The yield and ratio of regioisomers was almost not influenced by this additive (Entry 2) indicating that the deoxygenation step is relatively fast. Dicyanobenzene was used in a work by Yasuda in the photochemical amination of stilbenes with ammonia.[56] Here stoichiometric amounts of this reagent were used. We hypothesized that adding a catalytic amount of this SET reagent might assist this reaction. The yield dropped to 63% (Entry 3) showing that PrPPT is the superior SET reagent. TEMPO[57] (Entry 4), diphenyl disulfide[50f] (Entry8) and tertiary amines[58] (Entry 9) are reagents that assist in HAT processes. The employment of these additives reduced the yield significantly. With this result the hypothesis arises that the mechanism either does not involve HAT steps or that the PPT is also the superior HAT reagent. In the screening of the solvents the negative impact of water on the yield was shown. Therefore, the addition of molecular sieves to further dry the reaction mixture might have a positive influence on the yield. The yield dropped to 31% using molecular sieves (Entry 6). The reaction mixture was heterogenous due to grinding of the sieves. This might lead to a worse transparency for the light used and therefore reducing the yield. Since the mechanism of this reaction might involve protonation and or deprotonation steps the influence of Brönsted acid (Entry 5) and Brönsted base (Entry 10 and 12) was investigated both acids and bases reduce the yield significantly. Triphenylphosphine as reducing agent was also tested (Entry 11). Here the aim was, as for the BF_3, a faster deoxygenation of the PPTNO. The reaction was completely inhibited, likely due to competitive quenching of the phosphine (E_{ox} = +1.06 V vs SCE)[59].

4.3 Reaction scope for the hydroamination of stilbenes using monosubstituted amines

With the optimized conditions in hand the substrate scope of the reaction was investigated. Symmetrical (*E*)-stilbene (**(*E*)-26a**) was chosen as model substrate for the amine scope (Scheme 32). First alkylamines were investigated. *n*-, *iso*-, and *tert*- butylamine (**29a**–**29c**) are well tolerated giving the product in up to 63% yield. Sterically demanding adamantylamine (**29e**) and cyclohexylamine (**29d**) were successfully converted in 51% and 60% yield showing that the bulk on the used amine is not a limiting factor. This method is especially powerful for the conversion of benzylamines. Unsubstituted benzylamine (**29f**) gave the product in 67% yield when using only 3 equivalents. 4-substituted benzylamines gave high yields independent if electron accepting groups like CF_3 (**29g**) or Cl (**29h**) or an electron donating CH_3 group was used (**29i**). Only when employing the strong electron donating methoxy group the yield dropped to 37% (**29j**). Allylamine is tolerated under these conditions, albeit giving the product (**29l**) in a low 34% yield. Noteworthy α-chiral amines **29m** and **29n** were converted successfully. For (*R*)-α-methyl benzylamine (**29n**) enantiomeric pure diastereomers were isolated showing that no racemization occurs under the employed reaction conditions. The absolute configuration was assigned after X-Ray analysis of one diastereomer. Since radical cations of amines show an enhanced α-C–H acidity leading to racemization these intermediates can be ruled out in the mechanism of the reaction.[60]

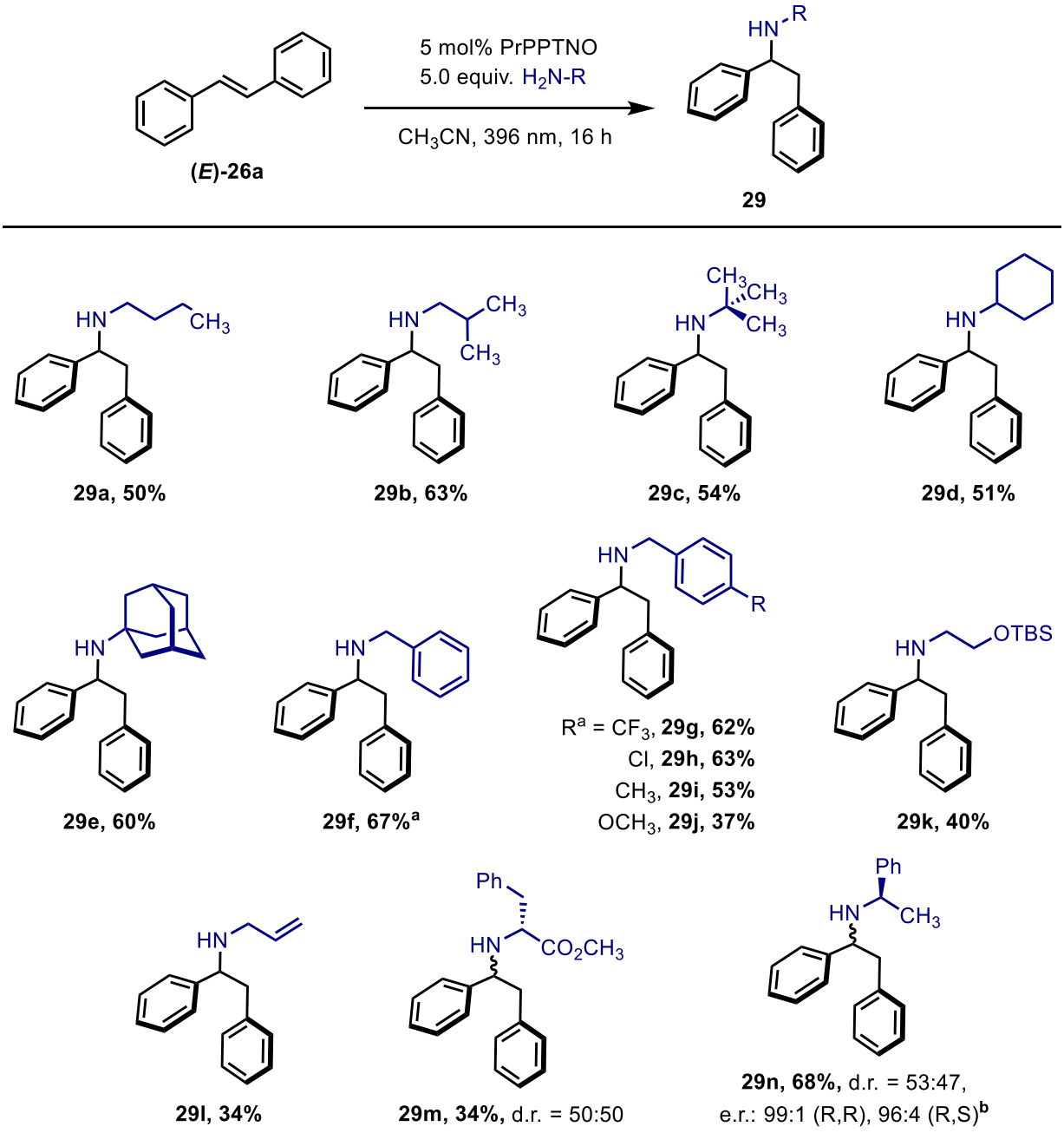

[a] 3.0 eq. amine was used. [b] The reaction time was 24 h.

Scheme 32. Substrate scope: Amines.

In the process of evaluating the substrate scope many different classes of amines were tested unfortunately many of these did not lead to any product formation (Figure 9).

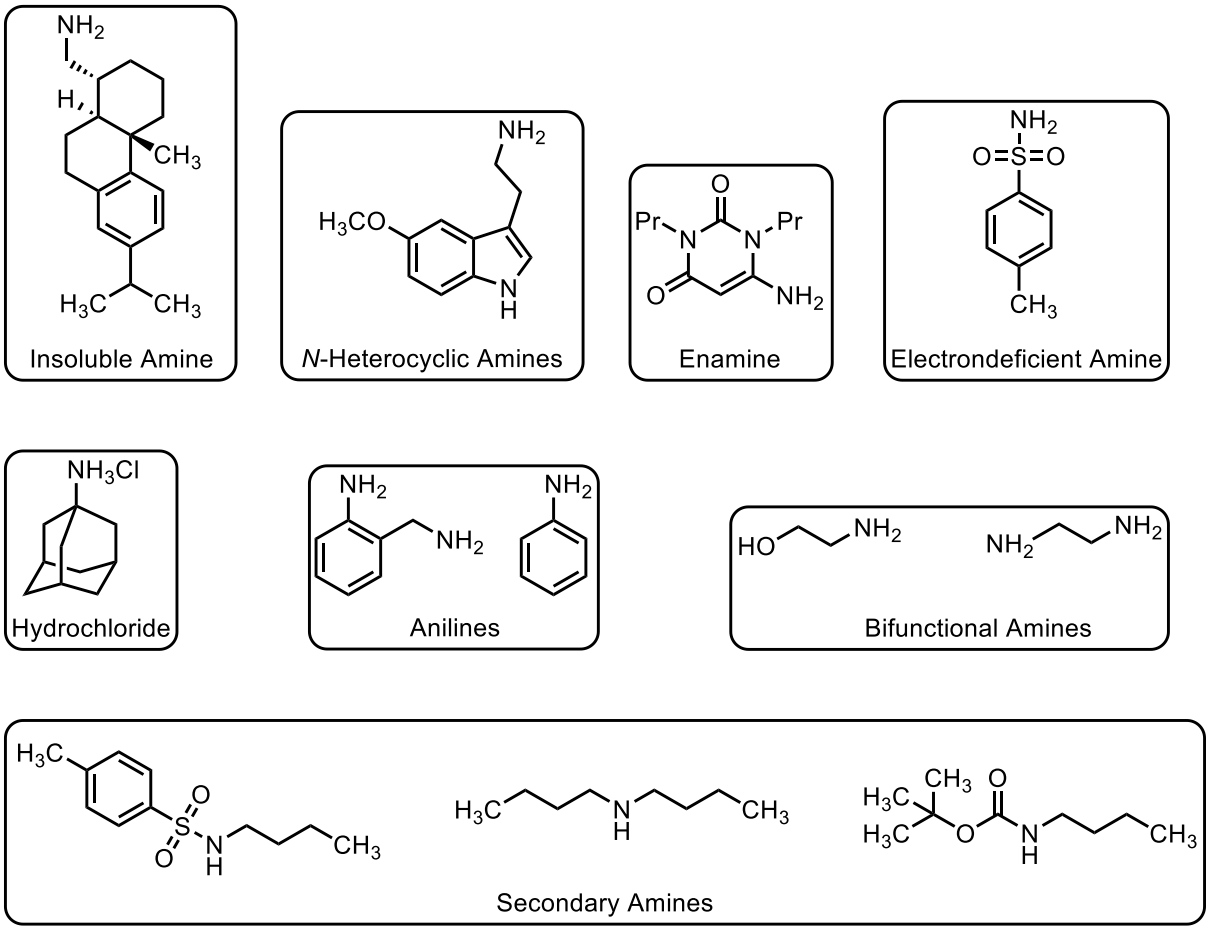

Figure 9. Substrate scope: Unsuccessful Amines.

Abietylamine showed no conversion under these reaction conditions, likely due to its low solubility in acetonitrile. Attempts using benzonitrile as solvent for abietylamine were not successful either. 5-Methoxytryptamine and the propyl substituted 6-aminouracil might act as a competitive quencher blocking the productive pathway. The oxidation of tosylamine is not possible using PrPPT (E_{ox} *(tosylamine)* = +2.56 V vs SCE).[61] Therefore, no NCR can be formed. This suggests that NCR formation is indeed necessary for product formation. Using adamantylamine hydrochloride also gave no product since oxidation is not possible without addition of a base. Anilines are easily oxidized by PrPPT (E_{ox} = +1.01 V vs SCE).[62] Aniline radical cations are highly reactive and undergo side reactions like polymerizations.[62-63] This is mostly due to the stabilization of the positive charge in the 4-position. The formally positive charged carbon atom is prone to nucleophilic attacks.[64] Using aminoethanol and ethylene diamine was also not effective. Here competitive quenching and formation of polymers might explain that no products were detected. Electron deficient and electron rich disubstituted amines were also not successfully converted. This might be due to fast BET of the formed amine that competes with the productive pathway. If BET is indeed the problem with this reaction certain strategies can be applied to overcome this problem. For

example a change in solvent polarity might lead to more separated ion pairs or the addition of a redox relay might enhance the efficiency of PET.[65]

When examining the olefin scope, we started using unsymmetric 4-substituted stilbenes (Scheme 33). Benzylamine was chosen as substrate due to its high yield on the amine scope. Electron withdrawing groups on the stilbene only have a small effect on the regioselectivity, but the yield was affected immensely. While the weakly withdrawing fluorine atom resulted in 54% yield (**30c**), stronger withdrawing groups like cyano (**30d**), ethylcarboxylate (**30e**) and CF_3 (**30f**) resulted in lower yields (32-40%). The yield of this reaction seems to directly correlate with the polarization of the introduced substituent. Gilmour investigated the E-Z isomerization of polarized alkenes and found that a more polarized double bonds leads to a higher degree of isomerization. He argued that a decrease in π-conjugation leads to a C–C bond elongation which itself leads to a lower rotation barrier.[66] This led to the conclusion that the isomerization of the stilbene might be a competitive reaction that can decrease the yield. Weakly electron releasing methyl group (**30g**) gave 67% yield but strongly donating methoxy group (**30h**) decreased the yield to 22%. Likely competitive oxidation of the electron rich stilbene instead of the amine diminishes the yield (E_{ox} = +0.84 V vs SCE)[56]. Using (*Z*)-stilbene lead to a very low yield of 22% (**29f**). The big difference in yield of *E*- and *Z*-isomer is an indication that *E*-*Z* isomerization is a major competing reaction. Adding both a 4-CF_3 and a 4-MeO group in the same molecule (**30i**) to obtain a strong push-pull system led to a low yield of 26% but a single isomer was isolated. If the push-pull system is weaker like in **30b** a high yield is obtained but a low regioselectivity. Aromatic phenanthrene gave the hydroamination product using both benzylamine (**30j**) and adamantylamine (**30k**) in 29% and 24% yield, respectively. The estrone derived stilbene (**19l**) was giving the hydroamination product **30l** in 59% when changing from CH_3CN to PhCN as solvent due to poor solubility of the stilbene in CH_3CN. Interestingly no side reactions on the carbonyl group were observed. A THC derived stilbene underwent deacetoxylation giving the phenol product (**30m**) in a high 69% yield.

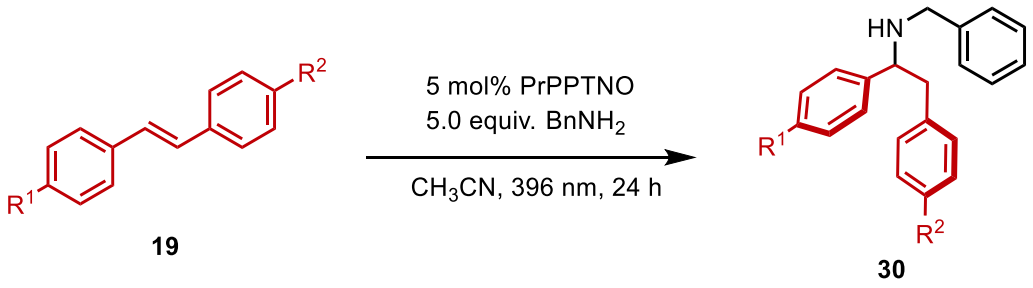

19 **30**

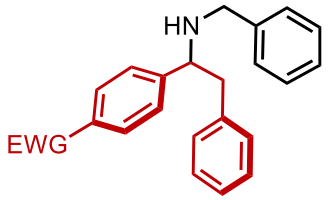

EWG = F, **30c, 54%**, (61:39)
CN, **30d, 29%,** (74:26)
EtO_2C, **30e, 41%,** (66:34)
F_3C, **30f, 28%,** (69:31)

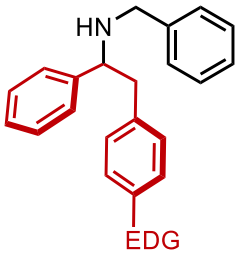

EDG = CH_3, **30g, 67%**, (61:39)
OCH_3, **30h, 21%,** (84:16)

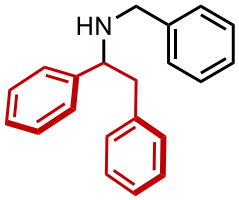

29f, 22%[a]

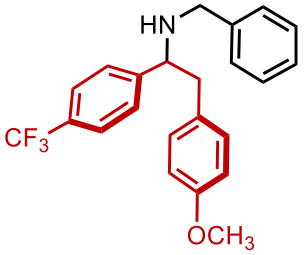

30i, 26%, (95:5)

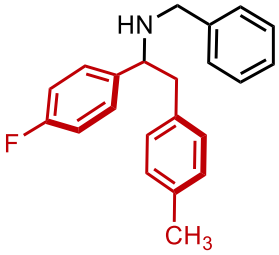

30b, 73%, (61:39)

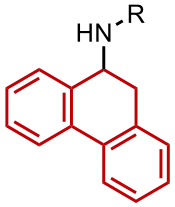

R = Bn, **30j, 29%**
Ad, **30k, 24%**

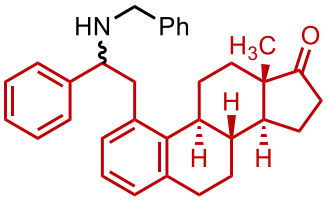

30l, 59%, (74:26)[b]

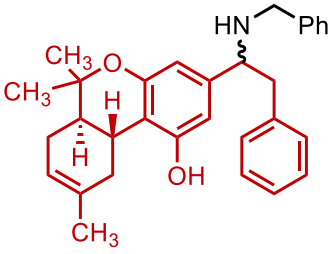

30m, 69%, (68:32)[c]

[a] Z-Stilbene was used. [b] PhCN instead of MeCN was used. [c] Substrate was the acetate.

Scheme 33. Substrate scope: Olefins.

The major regioisomer that is formed in this reaction is the one in which the C–N bond is formed on the side of the more electron deficient aryl ring (Figure 10). This indicates that a nucleophilic NCR is present in this reaction. Since aminium radicals are excluded due to lack of racemization of α-chiral amines and aminyl radicals are nucleophilic these seem to be the key intermediates in this reaction.

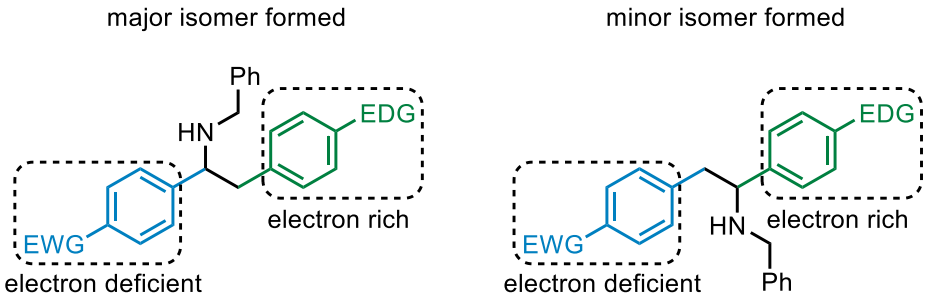

Figure 10. Formed regioisomers.

A list of olefins that were not successfully converted is shown in Figure 11. Attempts in converting cinnamic acid derivatives was not successful. For theses derivatives the double bond is likely so strongly polarized that *E-Z* isomerization is the predominant process completely surpassing product formation. The stilbene containing the very activating dimethylamino group likely undergoes competing oxidation suppressing the formation of the NCR. Due to the donating properties of the methyl group in α- and β-methyl styrene the intermediate formed in the reaction with the NCR might have a reduction potential that is too low to turnover with the PrPPT therefore not closing the catalytic cycle.

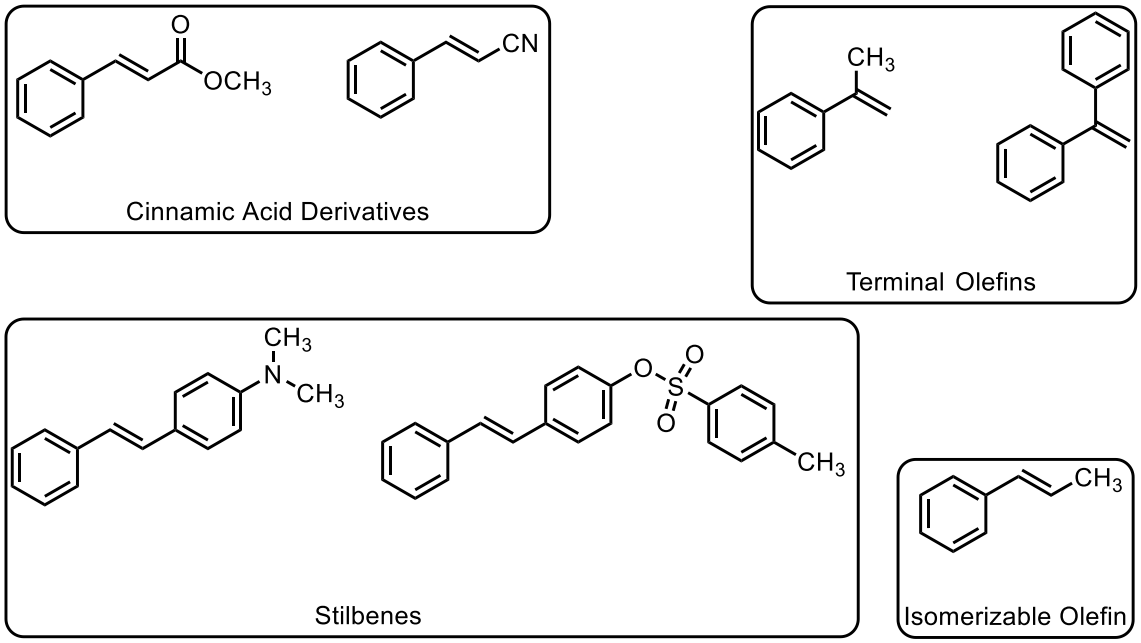

Figure 11. Substrate scope: Unsuccessful olefins.

To understand why certain substrates were not tolerated and if an NCR really participates in this reaction thorough mechanistic investigations were performed.

4.4 Stern-Volmer quenching studies

Verification of the NCR formation is the most crucial task. PrPPT in the excited state can in principle undergo both SET with (*E*)-stilbene (E_{ox} = +1.49 V vs SCE)[67] and a monosubstituted amine (E_{ox} app. +1.4 V vs SCE)[68]. Stern-Volmer quenching studies were

conducted to get insight if the excited state of PrPPT is quenched by the either stilbene or the amine. In Stern-Volmer quenching studies, the fluorescence of the photocatalyst is measured and the maximal fluorescence intensity is determined (I_0). Then a varying amount of potential quencher is added and the decrease in the maximal fluorescence intensity is measured (I). After plotting I_0/I against the quencher concentration (Q) a linear plot is obtained. The slope of this curve is the quenching constant, a kinetic value of how fast the quenching process takes place.

Interestingly both substrates are competitive quenchers for the excited state of PrPPT. For (*E*)-stilbene a quenching constant of 40.0 M^{-1} was obtained (Figure 12).

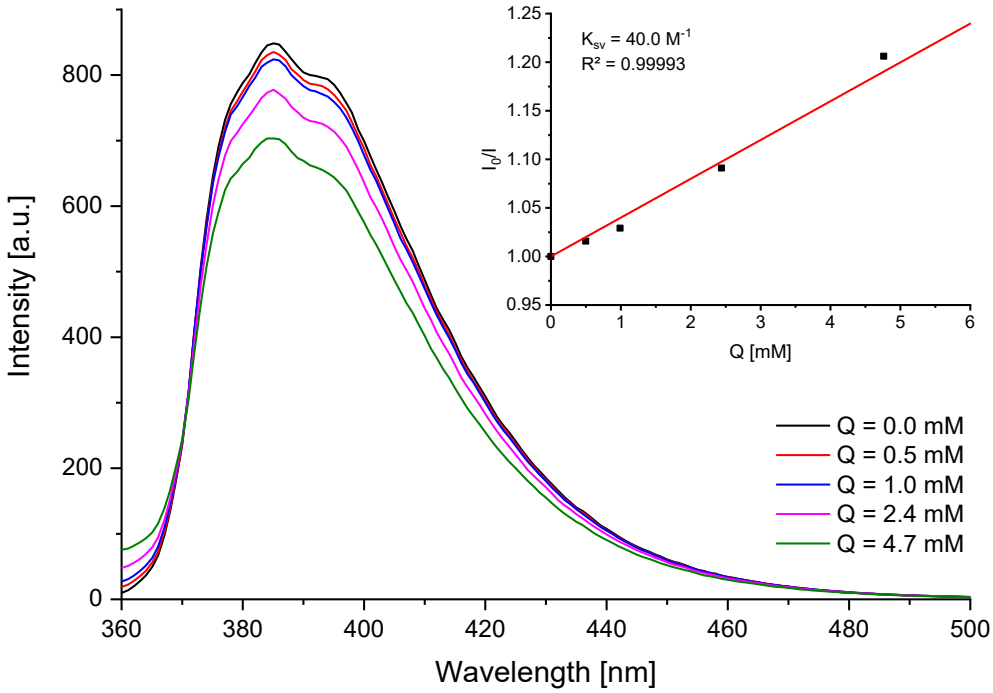

Figure 12. Quenching of luminescence and Stern-Volmer plot (inset) of PrPPT with varying concentration of (*E*)-stilbene.

For benzylamine a quenching constant of 27.8 M^{-1} was obtained (Figure 13). While (*E*)-stilbene is the stronger quencher delivering the higher quenching constant both amine and stilbene oxidation are possible. To verify if the observed excited state quenching is indeed a single electron transfer, EPR studies were conducted.

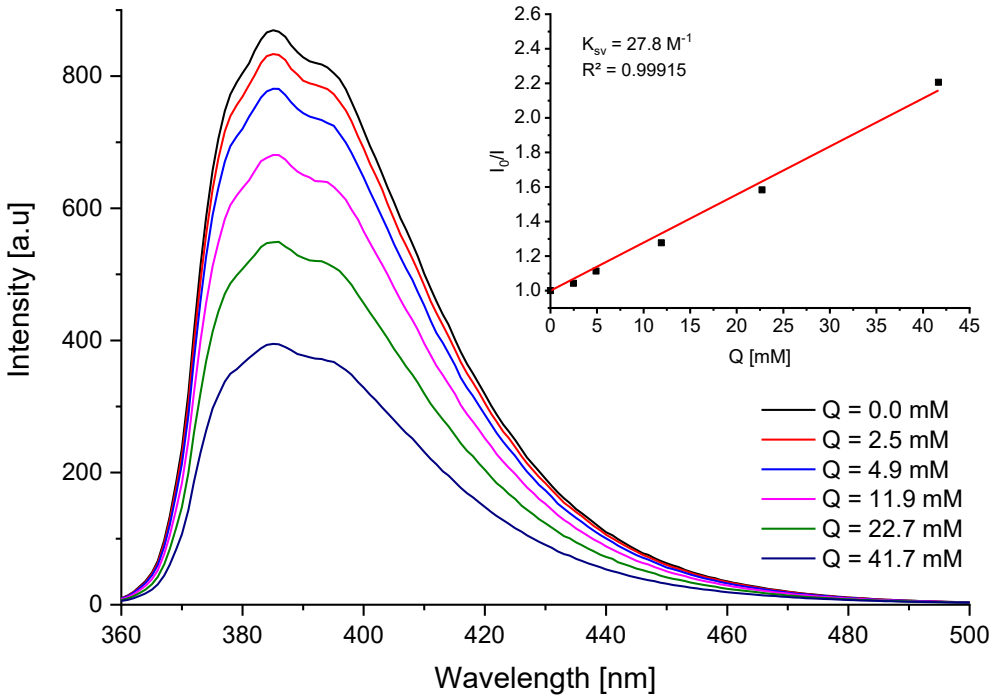

Figure 13. Quenching of luminescence and Stern-Volmer plot (inset) of PrPPT with varying concentration of benzylamine.

4.5 EPR measurements

EPR experiments were conducted in cooperation with Dr. Jabor Rabeah. A solution containing PrPPT, (*E*)-stilbene and acetonitrile was irradiated at 396 nm. No EPR signal was found. This indicates that while (*E*)-stilbene is a suitable quencher of the excited state of PrPPT, the quenching involves an energy transfer and not electron transfer, otherwise an EPR signal would have been found. Since the isomerization of the (*E*)-stilbenes was observed in all of the reported reactions and a SET mechanism is excluded, this isomerization likely follows a singlet photosensitization mechanism.[69]

When a solution of benzylamine and PrPPT in acetonitrile was irradiated an EPR signal showing a nine-line signal was found. This splitting can be explained by a radical interacting with two nonequivalent nitrogen nuclei. A comparison between a simulated and the measured EPR spectra is shown in Figure 14. The coupling of two nitrogen atom suggest that detected radical derives from the PPT. The radical is likely centered on the nitrogen that prior was part of the *N*-oxide moiety. Assignment to the nitrogen para to the aforementioned is not possible because a 12-line signal would be expected due to additional splitting with the nitrogen of the urea moiety. Evaluation of the hyperfine coupling is inconclusive. This means, that the detected EPR signal is either from the radical anion of PrPPT or from a protonated HPrPPT radical. While the radical anion would derive from a single electron oxidation of benzylamine forming the aminium radical, the PrPPTH

would derive from a PCET forming the aminyl radical. Unfortunately, the corresponding NCR signal was not found, and a certain assignment cannot be done.

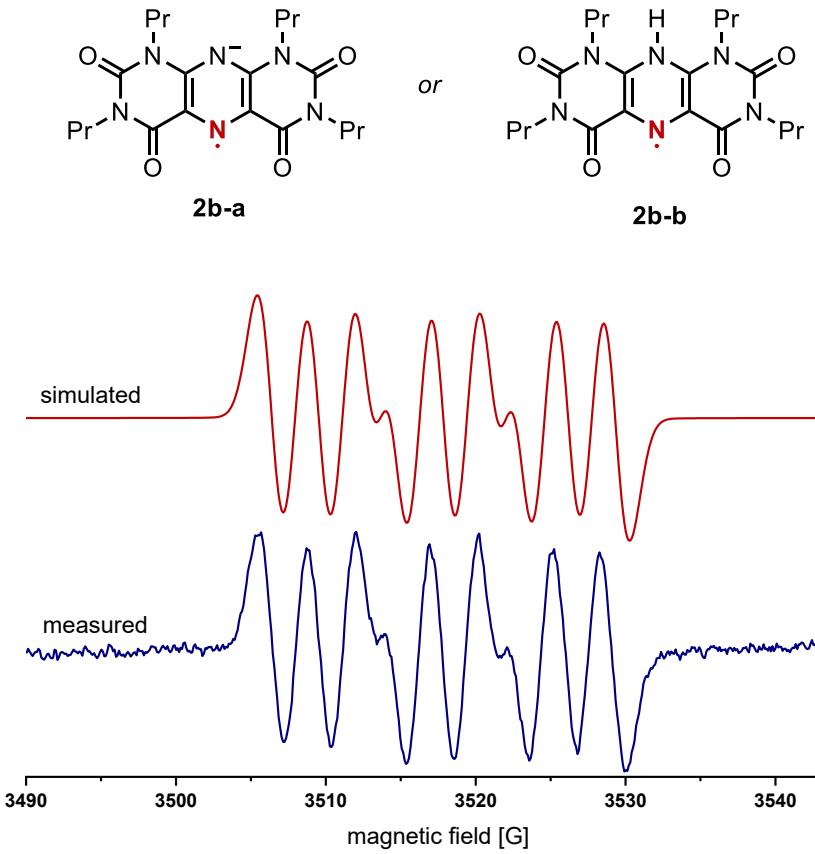

Figure 14. EPR signal derived from a solution containing benzylamine and PrPPT, after irradiation (blue). Simulated EPR spectrum of PrPPT or PrPPTH (red).

4.6 Stability of α-chiral centers

As already explained single electron oxidation of alkyl amines to aminium radicals leads to acidification of the C–H bond of the α-carbon which leads to racemization of α-chiral compounds. No racemization was observed under reaction conditions. Either no aminium radical is formed or the reaction is faster than deprotonation of the α-carbon. While the latter is very unlikely, a reaction was conducted were enantiomeric pure α-methyl benzylamine was irradiated with PrPPTNO in the absence of stilbene (Scheme 34). Stern-Volmer quenching studies and the EPR experiments verified that quenching of benzylamine involves radical formation. If the aminium radical would form after single electron transfer, racemization should be observed and if the aminyl radical is formed after PCET no racemization should be seen. After conducting the reaction and measuring chiral HPLC it was verified that no racemization occurs which excludes the formation of aminium radicals and verifies that the first step in the reaction is a PCET from the amine to the excited state catalyst.

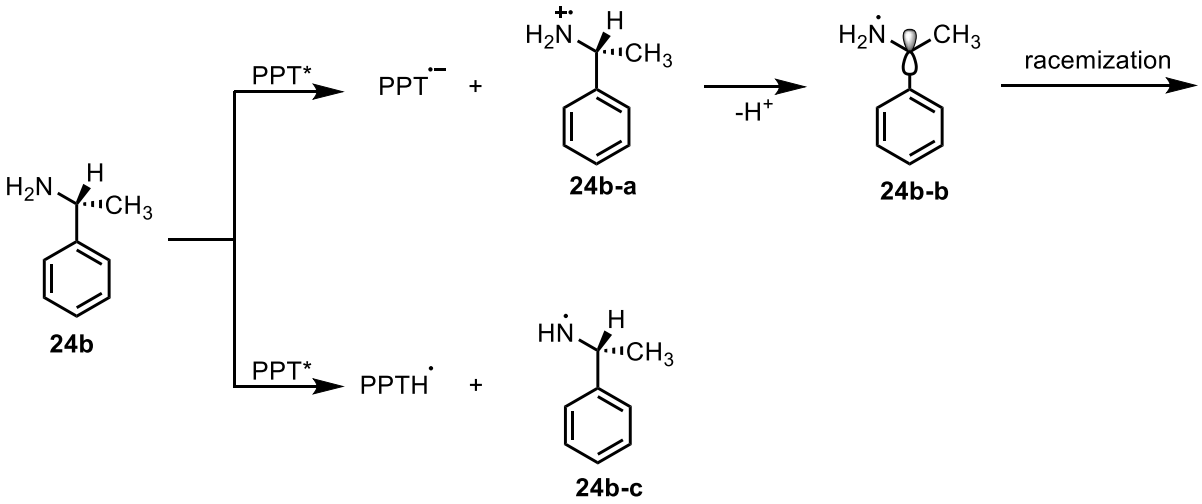

Scheme 34. Formation of aminium (top) or aminyl (bottom) radicals by reaction of amine with excited state PPT.

4.7 DFT calculations

To further underline that a PCET step is leading for the formation of an aminyl radical DFT calculations were performed in cooperation with Dr. Haijun Jiao. Utilizing time dependent DFT calculations the excited state energy of MePPT was determined to be 85.9 kcal/mol. This value is much higher compared to the experimental result (76.1 kcal/mol). This is likely due to the difficulty in determining the excited state properties of PPTNO based compounds.[34] In conclusion all absolute values are likely overestimated yet relative values can still be discussed. Next the SET and PCET reaction of excited state MePPT with benzylamine was calculated (Figure 15). It was found that both steps are exergonic but the PCET reaction is more exergonic then the SET reaction by 18.1 kcal/mol. This further proves that PCET is the key step in an aminyl radical formation.

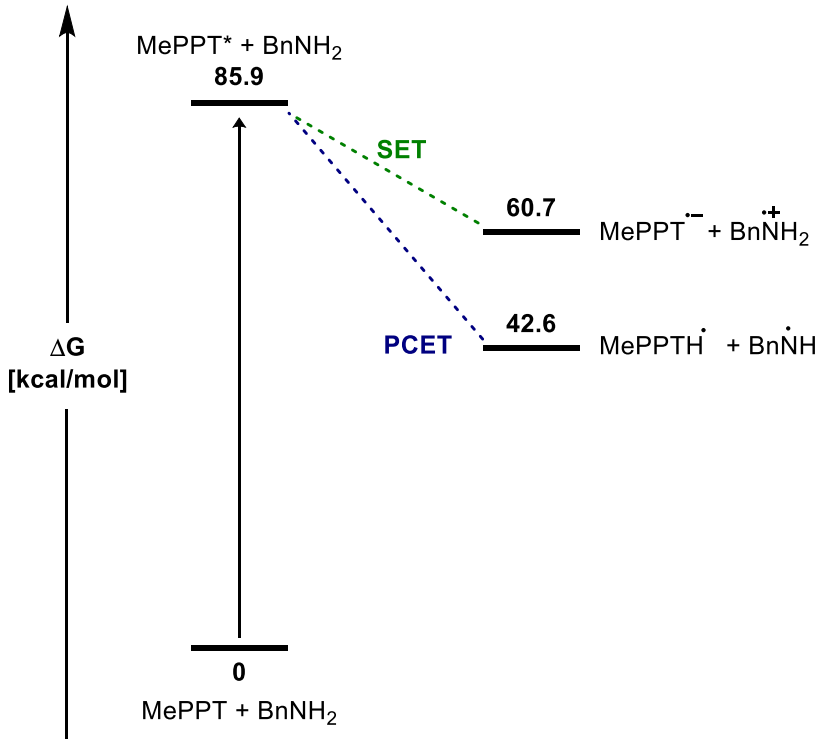

Figure 15. Free energy profile of the reaction of benzylamine with MePPT. B3PW91 and TZVP was used.

4.8 Proposed mechanism.

Additionally, to the shown experiments on-off experiments were conducted showing that this reaction is not following a chain propagation mechanism. Furthermore, the kinetic profile of the reaction was investigated and found that the hydroamination reaction of ethyl carboxylate substituted stilbene is slower than the reaction using unsubstituted (*E*)-stilbene while the isomerization to the (*Z*)-stilbene is faster. This further shows that the low yield of substituted stilbenes is due to competitive isomerization that inhibits the reaction.

The results of the aforementioned experiments lead to the proposal of a mechanism (Scheme 35). After excitation of PrPPTNO (**2b**) a reaction with (*E*)-stilbene (**(*E*)-26a**) happens, delivering the stilbene oxide (**31a**) and the active catalyst PrPPT (**5b**). The PrPPT is then excited to the strong excited state oxidant **5b-c**. PCET with the benzylamine (**24c**) delivers the aminyl radical (**24c-a**) and PrPPTH (**5b-b**). The aminyl radical reacts with (*E*)-stilbene forming the C-centered radical **29f-a**. A second PCET rearomatizes the PrPPTH back to the PrPPT closing the catalytic cycle and furnishing the product (**29f**).

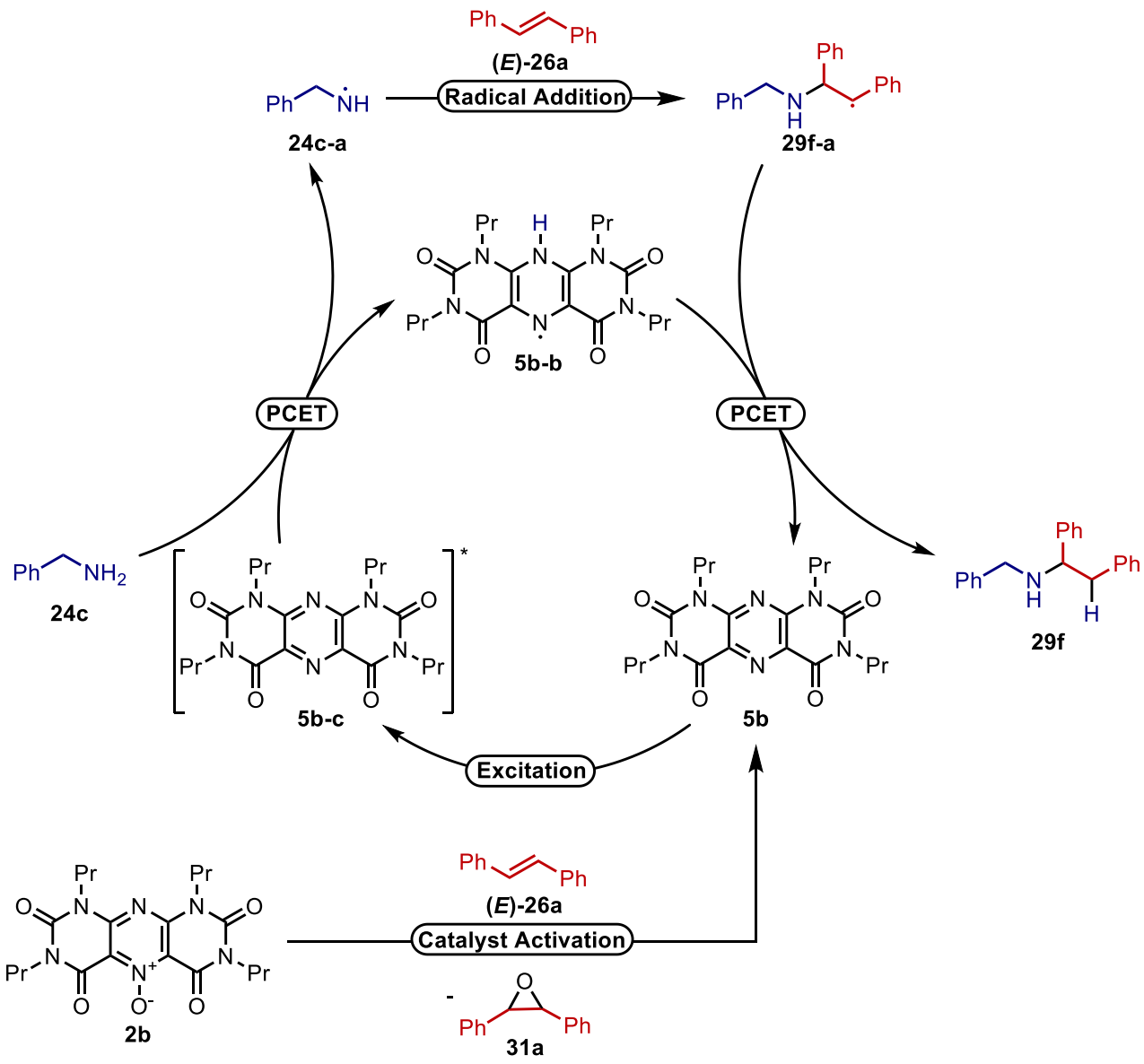

Scheme 35. Proposed mechanism for the photocatalytic hydroamination employing central PCET steps.

4.9 Deprotection of hydroamination products

To further showcase the value of this method further derivatization of the hydroamination products was evaluated. Products derived from benzylamine give access to the monosubstituted amines when deprotected under reductive conditions (Scheme 36).

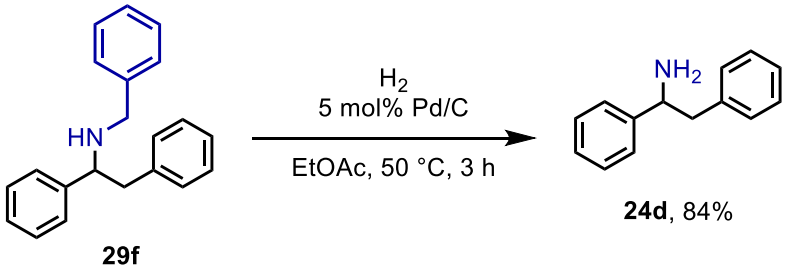

Scheme 36. Deprotection of **29f** using palladium on charcoal.

Under unoptimized conditions using a palladium on charcoal system with hydrogen the deprotected product was isolated in 84% yield.

4.10 Summary and Outlook

A protocol for the photocatalytic intermolecular hydroamination of stilbenes using monosubstituted amines was developed. The unique excited state properties of PPT based photocatalysts made this transformation possible. A variety of different substituted monosubstituted amines were converted in moderate to good yield. Investigation of the stilbene scope revealed that substitution on the stilbene leads to a significant drop in yield. This is likely due to the polarization of the double bond that eventually leads to a competitive isomerization as side reaction. The regioselectivity for most cases was poor unless a strong push-pull system is present in the substrate molecule. Mechanistic investigations revealed that the key step is a proton-coupled electron transfer from the amine to the catalyst delivering an aminyl radical. Further investigations on the mechanism certainly are necessary. While the presence of aminyl radicals are conclusive, a direct observation of this species would be worthwhile. This could be done by further EPR experiments including trapping of these species by nitroso compounds.[70] The hydroamination of stilbenes leads to the formation of a chiral product.

I want to thank Dr. Jola Pospech for converting estrone and THC derived stilbene giving the hydroamination products **30l** and **30m**. Furthermore, I want to express my gratitude to Firas el-Hage who conducted the On-Off experiments and the investigation of the kinetic profile.

5 Photocatalytic trifluoromethylation of aromatic compounds

5.1 Introduction

The synthesis of organofluorine compounds has gained much attention over the last decades.[71] Due to their unique properties they have become important key structures in pharmaceuticals, agrochemicals and functional materials.[72] Fluorine containing substituents have a profound effect on the physical and biological properties of the target molecules. They show enhanced binding interactions, bioavailability, lipophilicity and metabolic stability when introduced into drug molecules.[73] The increase in lipophilicity is distinct for aromatic compounds bearing a trifluoromethyl group and is typically accompanied by a strong polarization of the parent molecule. These effects are not limited to trifluoromethyl groups but also apply to different fluoroalkyl groups like $-CF_2H$ and $-CF_2CF_3$. The introduction of a CF_3 group can be realized via an electrophilic or a nucleophilic intermediate. These species can have different reactivities. Both the formal CF_3 cation and the CF_3 radical are electrophilic reaction partners but are utilized in different types of reactions (Scheme 37).[74]

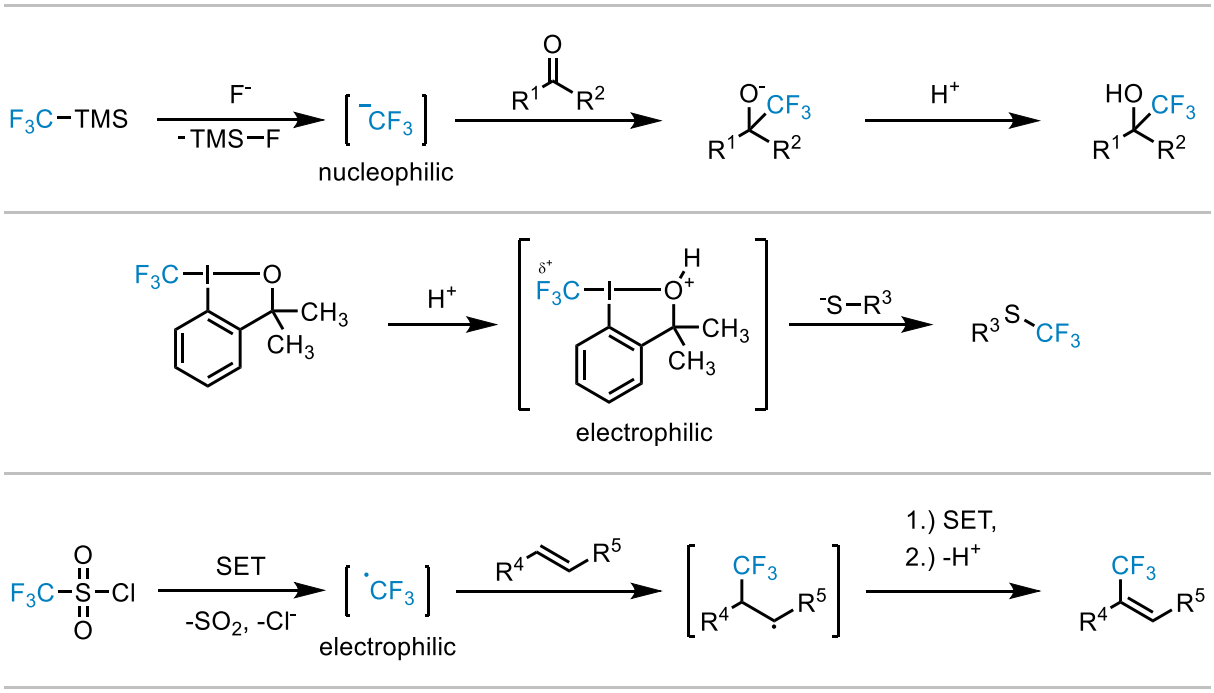

Scheme 37. Utilization of nucleophilic (top) and electrophilic (middle and bottom) trifluoromethylation agents.

The introduction of a CF_3 group to an aromatic compound characteristically employ the reactivity of an electrophilic radical intermediate. Especially the field of photocatalysis is attractive for the generation of radical intermediates and many approaches for the photocatalytic generation of CF_3 radicals are reported.[75] There are different reagents

known to efficiently generate CF_3 radicals. Notably, most trifluoromethylation agents suffer from a very high price per mole (Table 12).

Table 12. Prices of commonly used trifluoromethylation reagents.[76]

Entry	Compound	Price [€/mol] by Sigma Aldrich
1	TFA	36
2	TFAA	82
3	Tf_2O	760
4	CF_3I	950
5	CF_3SO_2Na	1200
6	$TMSCF_3$	2030
7	Togni II	27.900
8	Togni I	50.600
9	UmeOTf	54.400
10	Mes-UmeOTf	100.000

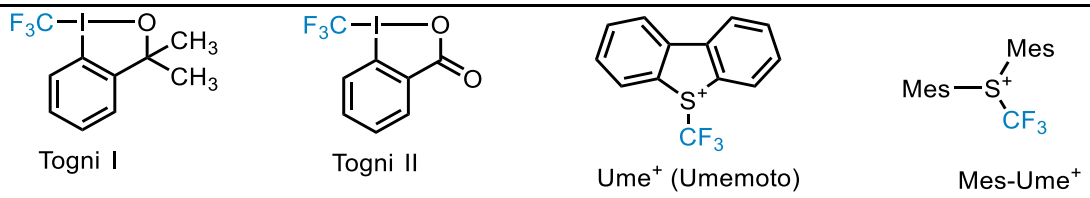

Figure 16. Structure of commonly used trifluoromethylation reagents.

The Umemoto reagents are very expensive and considering large scale application there is a need for cheaper reagents. Triflyl anhydride (Tf_2O), Trifluoroacetic anhydride (TFAA), and Trifluoroacetic acid (TFA) are the cheapest (nongaseous) trifluoromethylation reagents, yet their application is rather limited. To form a CF_3 radical using TFA it is necessary to oxidize the carboxylate. Since the oxidation potential (E_{ox} (TFA) > 2.24 V vs SCE)[77] is higher than that of most organic solvents this reaction is very hard to realize. In one example TFA was used as a source of CF_3 radicals but TFA was used as solvent. [78] Due to the corrosive properties of TFA using it as solvent intrinsically narrows the scope and applicability of such a reaction. There are reports on using Tf_2O and TFAA as trifluoromethylation agents in a photocatalytic reaction, but these methodologies suffer from using stoichiometric amounts of pyridines or pyridine-*N*-oxides as activating agents. These additional reagents increase the overall price of the reaction and end up as waste. Stephenson reported in 2015 the decarboxylative trifluoromethylation of electron rich aromatic compounds. The key feature was the utilization of an adduct from TFAA and a pyridine-*N*-oxide. After excitation of a ruthenium based photocatalyst the adduct is reduced and fragmentation delivers the CF_3

radical (Scheme 38, a). Later in 2018 Qing used triflyl anhydride as cheap trifluoromethylation reagent. Here pyridine as activating reagent was necessary to form a reducible intermediate that after single-electron transfer releases a CF_3 radical under SO_2 extrusion (Scheme 38, b). Both methods are operational simple, use cheap reagents and a broad spectrum of compounds can be converted. It would be desirable to find a protocol that does not need activating reagents - since these eventually end up as waste - while maintaining the utilization of a cheap source for CF_3 radicals. The direct reduction of TFAA should be possible without any additional reagent using most photocatalysts because of the high reduction potential (E_{red} = -0.20 V vs. SCE) to form the radical anion of TFAA.[30] This radical anion might then fragment to the trifluoroacetate and the trifluoroacyl radical. The trifluoroacyl radical would undergo decarbonylation to provide a CF_3 radical[79] (Scheme 38, c) which can then be captured by an electron rich aromatic compound. Since a decarbonylative generation (in a synthetical useful amount) of CF_3 radicals is not known in literature this system would provide access to a new pathway to generate CF_3 radicals in organic synthesis. Due to the reactive nature of the CF_3 radical the utilized photocatalyst needs to be chosen wisely. Since many organofluorine compounds are used as drugs, transition metal-based catalysts should be avoided due to their potential toxic effects in vivo.[80] An organic photocatalysts needs to be stable towards the highly electrophilic CF_3 radical and TFAA. Since the PPT core is very electron deficient these catalysts are possible candidates for this reaction.

a.) Stephenson 2015, Decarboxylation:

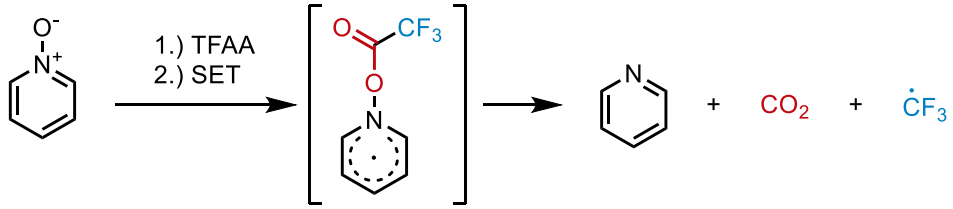

b.) Qing 2018, SO_2 extrusion

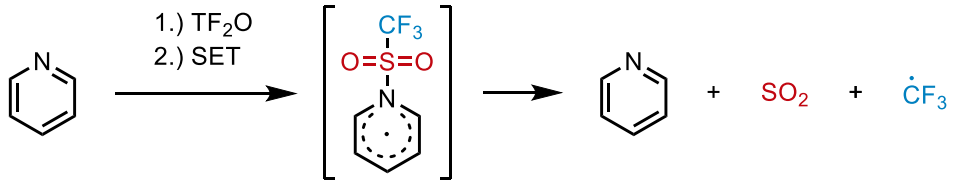

c.) Hypothesis: Decarbonylation

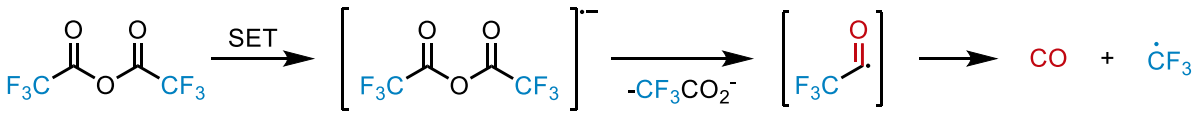

Scheme 38. Generation of CF_3 radicals after initial SET under extrusion of a) CO_2 b) SO_2 c) CO.

5.2 Photocatalytic trifluoromethylation of arenes. Optimization of the reaction conditions.

First experiments were conducted using caffeine (**32a**) as model substrate, TFAA as trifluoromethylation reagent, cesium carbonate as base, PrPPTNO as photocatalyst and acetonitrile as solvent (Scheme 39).

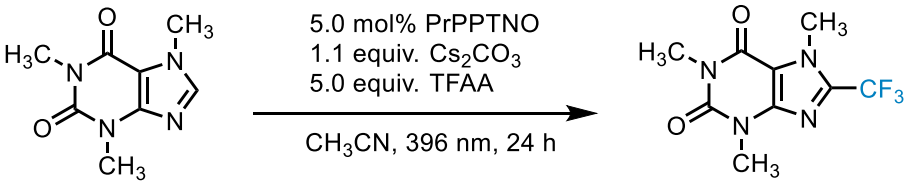

32a **33a, 36%**

Scheme 39. Initial results for the photocatalytic trifluoromethylation of caffeine. Yield determined by ^{19}F-NMR spectroscopy.

Optimization of the base (Table 13) revealed that inorganic bases are superior to organic bases, especially those containing cesium (Entry 1–3). This can be seen when directly comparing sodium and cesium carbonate (Entry 1 and 6). Likely, the reason is the very high basicity of cesium salts in acetonitrile. Both cesium fluoride and cesium carbonate show basicity comparable to potassium tert-butoxide in acetonitrile.[81] The reason for this is the big radius, the polarizability, and the low charge density of the cesium cation. This effect is profound for aprotic dipolar solvents with a high dielectric constant, like acetonitrile.[82] Clearly, addition of base is crucial to improve the yield (Entry 9).

Table 13. Photocatalytic trifluoromethylation of arenes. Base screening. Reaction depicted in Scheme 39.

Entry	Base	Yield[a]
1	**Cs_2CO_3**	**36%**
2	CsF	32%
3	Cs_2SO_4	26%
4	$NaHCO_3$	23%
5	K_3PO_4	22%
6	Na_2CO_3	22%
7	NaOAc	17%
8	CaH_2	17%
9	-	17%

10	NEt_3	16%
11	$CsOH•H_2O$	8%

[a] ^{19}F yields reported using fluorobenzene as internal standard.

Next, different solvents were screened (Table 14). Only acetonitrile, dichloromethane and ethyl acetate delivered any detectable product (Entry 1–3). Commonly used solvents like THF and dioxane yielded no product (Entry 4 and 5). DMSO and acetone might interfere with the reaction due to their C–H acidic nature leading to undesired side products (Entry 6 and 7). In a different project it was found that THF can be oxidized using PPTNOs producing the lactone. The formed lactone may lead to undesired side reactions inhibiting the reaction. Benzonitrile is likely a competitive substrate for this reaction and using it as solvent probably suppresses the formation of the desired product.

Table 14. Photocatalytic trifluoromethylation of arenes. Solvent screening. Reaction depicted in Scheme 39.

Entry	Solvent	Yield[a]
1	**CH_3CN**	**36%**
2	DCM	15%
3	Ethylacetate	13%
4	THF	<5%
5	Dioxane	<5%
6	DMSO	<5%
7	DMF	<5%
8	PhCN	<5%
9	Acetone	<5%

[a] ^{19}F yields reported using fluorobenzene as internal standard.

Next the equivalents of cesium carbonate were optimized (Table 15). Using an excess of 3 equivalents decreased the yield (Entry 1). Reducing the equivalents to a catalytic amount of 0.25 equivalents also had an adverse effect (Entry 4). 1.1 equivalents and 0.5 equivalents delivered 36% and 34% yield respectively (Entry 2 and 3). Indicating that the reaction is not as sensitive towards a small deviation of base if it is in this range. The obtained yields are not synthetically useful and further optimization of the system was necessary.

Table 15. Photocatalytic trifluoromethylation of arenes. Optimization, equivalents of base.

Entry	Equiv. Cs_2CO_3	Yield[a]
1	3.0	18%
2	1.1	**36%**
3	0.5	34%
4	0.25	23%

[19]F yields reported using fluorobenzene as internal standard.

Changing the concentration (Table 16) in an area of 83 mM to 200 mM had only a small impact on the yield. Many photoreactions are sensitive towards variation in concentration due to the dependency from the optical attenuation on the concentration (Lambert-Beer-Law). Fortunately, this system seems to be not sensitive towards this change.

Table 16. Photocatalytic trifluoromethylation of arenes. Optimization, change of molarity. Reaction depicted in Scheme 39.

Entry	Molarity (Volume)	Yield[a]
1	0.083 M (6 mL)	36%, 32%[b]
2	**0.100 M (5 mL)**	**36%**, 34%[b]
3	0.125 M (4 mL)	32%
4	0.200 M (2.5 mL)	31%

[a] [19]F yields reported using fluorobenzene as internal standard. [b] Using 0.5 equiv. Cs_2CO_3.

Since cesium carbonate is hygroscopic it was necessary to check if handling of this compound impacts the yield (Table 17).[83] Changing from cesium carbonate stored on the bench to cesium carbonate stored in the glovebox only a neglectable change in yield was observed (Entry 1 and 2). Heating cesium carbonate to 550°C in vacuum increased the yield by almost 10% (Entry 3). Importantly the cesium carbonate should not be heated with a stirring bar because decomposition of the stirring bar can be observed. Heating to 650°C should also be avoided since the cesium carbonate undergoes change in color and structure and to secure reproducibility and avoid forming new unknown intermediates a temperature of 550°C should be used. Lastly, experiments were conducted in which an aqueous workup was avoided due to the high water solubility of caffeine derivatives.

Therefore, it was important to verify if product is lost in the workup. No loss of product was observed.

Table 17. Photocatalytic trifluoromethylation of arenes. Optimization, handling of cesium carbonate. Reaction depicted in Scheme 39.

Entry	Deviation	Yield[a]
1	Cs_2CO_3 from Glovebox	32%
2	Cs_2CO_3 from Bench	34%, 34%[b]
3	**Cs_2CO_3 heated to 550°C**	42%, **43%**[c]

[a] ^{19}F yields reported using fluorobenzene as internal standard. [b] No aqueous workup. [c] Using 1.1 equiv. Cs_2CO_3

Next a photocatalyst screening was performed (Table 18). To verify that a photocatalyst is needed to perform this reaction the reaction was conducted without any catalyst. No product was found (Entry 1). Within the class of PPTNO based catalysts (Entry 3-6) PrPPTNO was the one giving the highest yield (Entry 3). Ruthenium and acridinium based catalysts delivered no product likely due to catalyst decomposition (Entry 7 and 8). Remarkably, the iridium-based catalyst delivered slightly higher yield than the PrPPTNO (Entry 2). But taking the high price of this catalyst into consideration PrPPTNO was chosen for further evaluation. When degassing the solution by freeze-pump-thaw the yield could be further improved to 52% yield. This positive effect can be observed in photoreactions with gaseous side products.[31, 84] Likely the product side of the equilibrium of the decarbonylation step is slightly favored when the reaction is fully degassed. When degassing the reaction by freeze-pump-thaw the reaction is typically refilled with argon after the last degassing cycle. It was tested if there is an influence in regassing the solution or performing the reaction under reduced pressure. No difference in yield was observed.

Table 18. Photocatalytic trifluoromethylation of arenes. Photocatalyst screening. Reaction depicted in Scheme 39.

Entry	Photocatalyst	mol %	Yield[a]
1	-	-	<5%
2	$[Ir(dFCF_3ppy)_2(bpy)]PF_6$	2	45%
3	**PrPPTNO**	**5**	43%, **52%**[b], 51%[c],
4	BuPPTNO	5	39%
5	MePPTNO	5	30%

6	PhPPTNO	5	30%
7	$MesAcrMeBF_4$	5	<5%
8	$Ru(bpy)_3(PF_6)_2$	2	<5%

[a] ^{19}F yields reported using fluorobenzene as internal standard. [b] Degassed, refilled with argon. [c] Degassed, vacuum.

Lastly some additional and control experiments were conducted (Table 18). Decreasing the equivalents of TFAA to 2.5 drastically decreased the yield (Entry 2). Using PrPPT instead of PrPPTNO also decreased the yield (Entry 3). This observation is different as compared to that on the hydroamination project were PrPPT was assumed to be the active catalyst. PrPPTNO or an intermediate derived from it seems to be the more active catalyst. Also possible is that PrPPTNO and PrPPT are both active but PrPPT decomposes more quickly than PrPPTNO. Considering the electrophilic nature of CF_3 radicals and the fact that PrPPT is more electron rich on the heterocyclic core this seems possible. Increasing the reaction time to 48 h was beneficial and delivered the product in 67% yield (Entry 4). Isolation by column chromatography gave the product in 62% yield indicating only a minor loss in the purification step. When the solution is not irradiated no product is obtained proving that this reaction is indeed a photoreaction (Entry 5).

Table 19. Photocatalytic trifluoromethylation of arenes. Additional experiments. Reaction depicted in Scheme 39.

Entry	Deviation	Yield[a]
1	-	43%, **52%**[b]
2	2.5 equiv. TFAA	28%[b]
3	Using PrPPT, 48h	48%[c]
4	**48h**	**62%**[c], 67%[b,d]
5	No light	<5%
6	No photocatalyst	<5%

[a] ^{19}F yields reported using fluorobenzene as internal standard. [b] Degassed, refilled with argon. [c] Isolated Yield. [d] average of 2 experiments.

5.3 Mechanistic Consideration

Having the optimized conditions in hand, initial mechanistic investigations were conducted. Two mechanistic proposals (Scheme 40 and 41) seemed reasonable. The first one includes the oxidation of caffeine (**32a**) by the excited state PrPPTNO (**2b-c**) (Scheme 40). The oxidative reaction of excited state PrPPTNO with caffeine is exergonic (E_{ox} < +1.66 V vs SCE[85], ΔG_{PET} < -14.8 kcal/mol) and therefore possible.

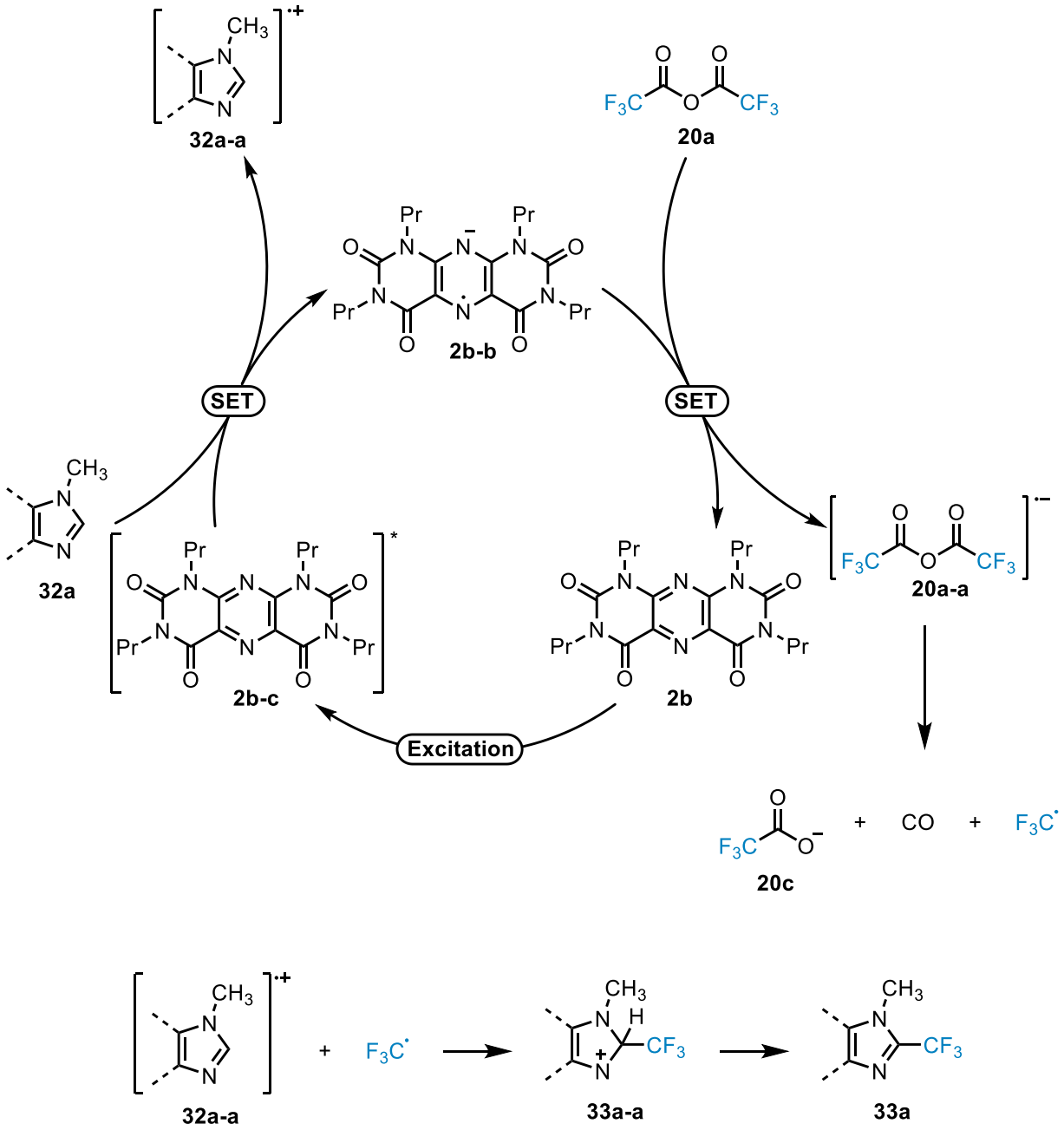

Scheme 40. Mechanistic proposal involving oxidation of caffeine.

The formed radical anion of PrPPTNO (**2b-b**) turns over with TFAA giving the radical anion of TFAA (**20a-a**) while closing the catalytic cycle. The TFAA radical anion will undergo fragmentation delivering CO and the CF_3 radical. Radical recombination of the radical cation of caffeine and the CF_3 radical will deliver intermediate **33a-a**. Deprotonation will lead to rearomatization delivering the product **33a**. The mechanism involving the oxidation of caffeine while being thermodynamically more feasible is unlikely to be present. The strongest argument against this mechanism is the fact that CF_3 radicals are strong electrophiles and recombination with a radical cation is probably not possible due to a nucleophile-electrophile mismatch. Furthermore, radical recombinations under

photocatalytic conditions are unlikely. Two highly reactive intermediates need to meet under dilute conditions without back electron transfer occurring.

More likely is a mechanism where the TFAA is reduced by the excited PrPPTNO (Scheme 41). The reductive reaction of excited state PrPPTNO with TFAA is also exergonic (E_{red} = -0.20 V vs SCE[30], ΔG_{PET} = -14.3 kcal/mol) and therefore also possible.

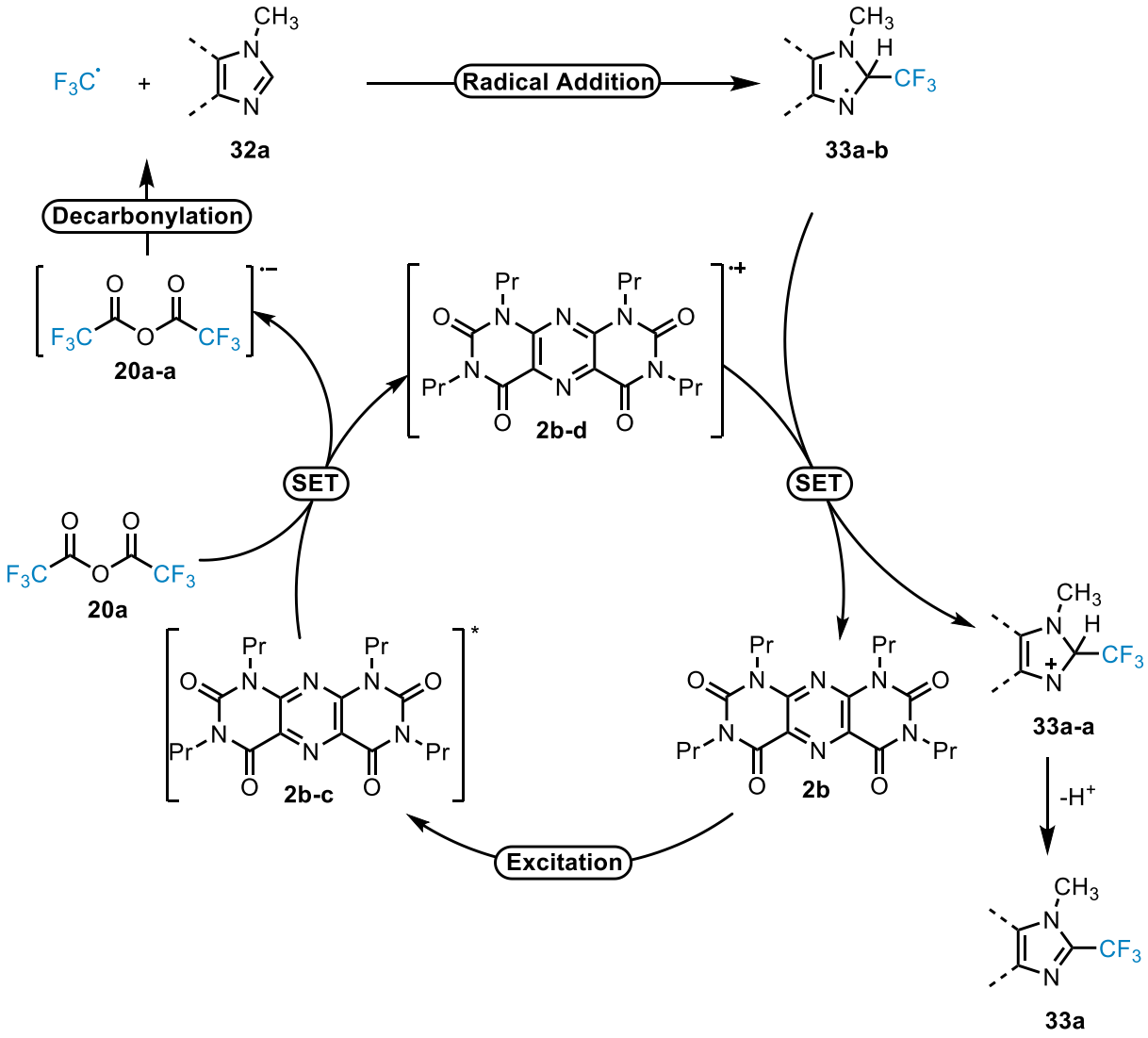

Scheme 41. Mechanistic proposal involving reduction of TFAA.

Excited state PrPPTNO (**2b-c**) will undergo reductive quenching with TFAA (**20a**) giving TFAA radical anion (**20a-a**) and the PrPPTNO radical cation (**2b-d**). This is different than the mechanism of the photocatalytic hydroamination were a PrPPTNO radical anion is formed after oxidative quenching. **20a-a** decarbonylates to give CF_3 radical and carbon monoxide. The CF_3 radical electrophilically attacks the caffeine giving radical intermediate **33a-b**. Oxidative turnover gives the cationic intermediate (**33a-a**) which will release a proton under rearomatization giving the product (**33a**). Notably the existence of CO was proven using a CO detector verifying a key decarbonylation step.

Next, the kinetic profile for the model reaction was recorded (Figure 16).

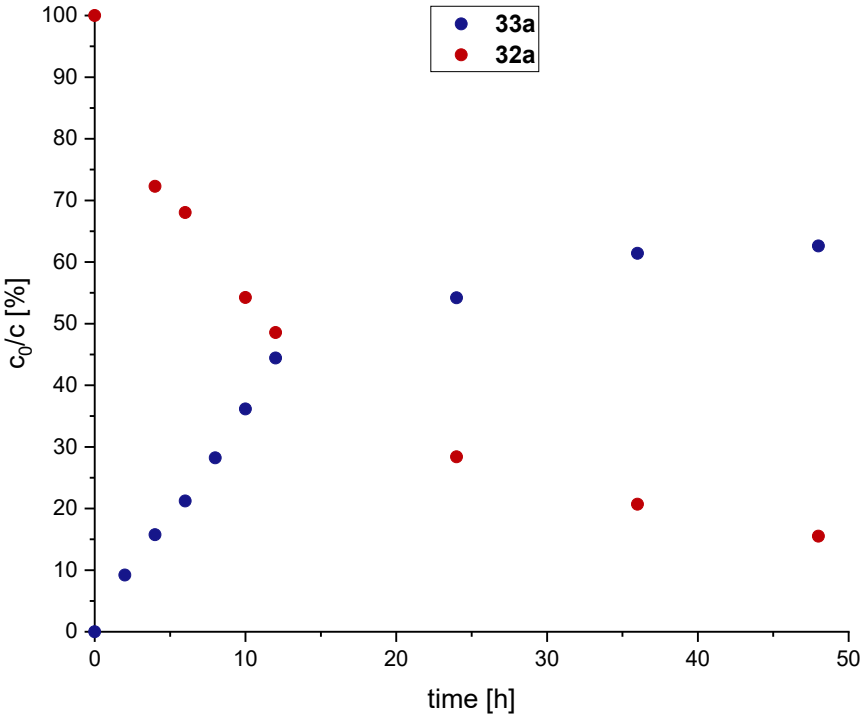

Figure 16. Kinetic profile for the model reaction.

The yield vs time course starts first linearly and then flattens after 14 h. Even after 48 h only 85% conversion and 62% yield are achieved. Since the conversion is higher than the yield, side products must be present. Analyzing the probes by GC/MS revealed the formation of two side products (Scheme 42). First a side product derived from a Friedel-Crafts type side reaction can be detected **34a**. It is unclear if this product is derived from a thermal background reaction or is formed by reaction with the trifluoroacyl radical before its decarbonylation. The second byproduct is derived from the Friedel-Crafts product and is a reductive trifluoromethylation product **35a**. The position of both the trifluoroacyl and the trifluoromethyl group is speculative and cannot be clearly assigned solely based on the MS data.

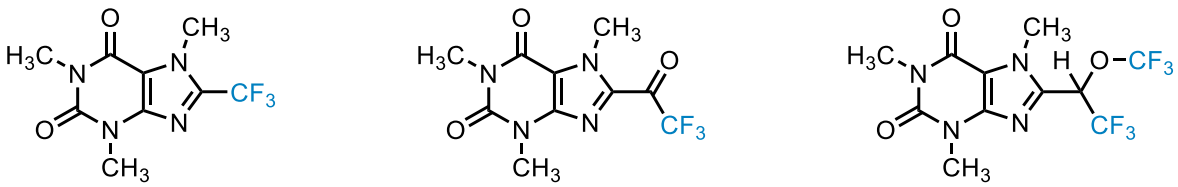

33a **34a** **35a**

Scheme 42. Reaction products detected by GC/MS. The constitution of **34a** and **35a** is hypothetical.

Since the product formation slows down faster than the product is consumed the photoreaction might slow down while the background Friedel-Crafts reaction maintains its speed. This observation indicates catalyst deactivation. The conversion-time course is

reminiscent of a reaction following a first order kinetics. No further kinetic investigations were performed.

5.4 Substrate scope for the photocatalytic trifluoromethylation of arenes

With the optimized conditions in hand the substrate scope was evaluated (Scheme 44). Xanthine derived theobromine (**32b**) and theophylline (**32c**) gave the products albeit in low yields (37% and 11% respectively). The present N–H bonds might not be tolerated due to a competitive oxidation inhibiting the reaction. Especially theophylline is more acidic then theobromine and very easily oxidized in its deprotonated form. This leads to a competitive pathway were theophylline is oxidized instead of TFAA being reduced by excited state PrPPTNO.[85a] Caffeine derived pentoxifylline (**33d**) also gave the product in reduced yield (31%). While no side products like O-acylation were found, a side reaction induced by the carbonyl group seems likely. Carbonyl group containing compounds like acetone are potent triplet quenchers. This feature might reduce the yield due to competitive quenching.[86] Dimethyl uracil (**33e**) and methyl thiophen-2-carboxylate (**33f**) also gave the products in poor yield (27% and 22% respectively) here a low conversion was found while the reaction was very selective (no side products found). This indicates that the reaction is either very slow or the catalyst is decomposing quickly. 4-substituted anisoles also gave products (**33g-33i**) in very poor yields (18-35%). Here the corresponding phenols were detected by GC/MS. The formation of phenols might be explained by water formed from cesium carbonate due to protonation. Since the benzene ring in anisoles is electron rich, oxidation of these is facilitated and can be easily achieved by PrPPTNO (E_{ox} *(4-methoxy anisole)* = +1.30 V vs SCE)[30]. The radical cation formed can then react with water under elimination of methanol (Scheme 43).[87]

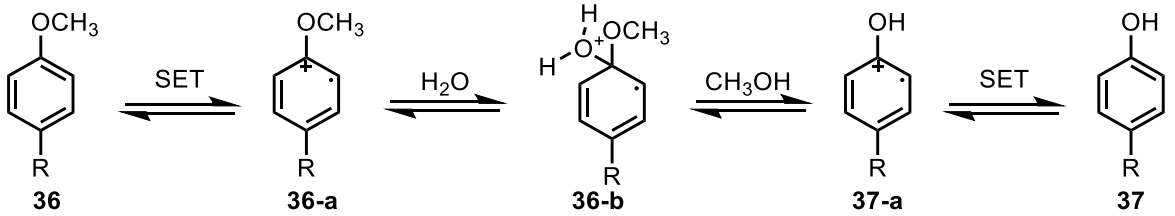

Scheme 43. Phenol formation of anisoles by water.

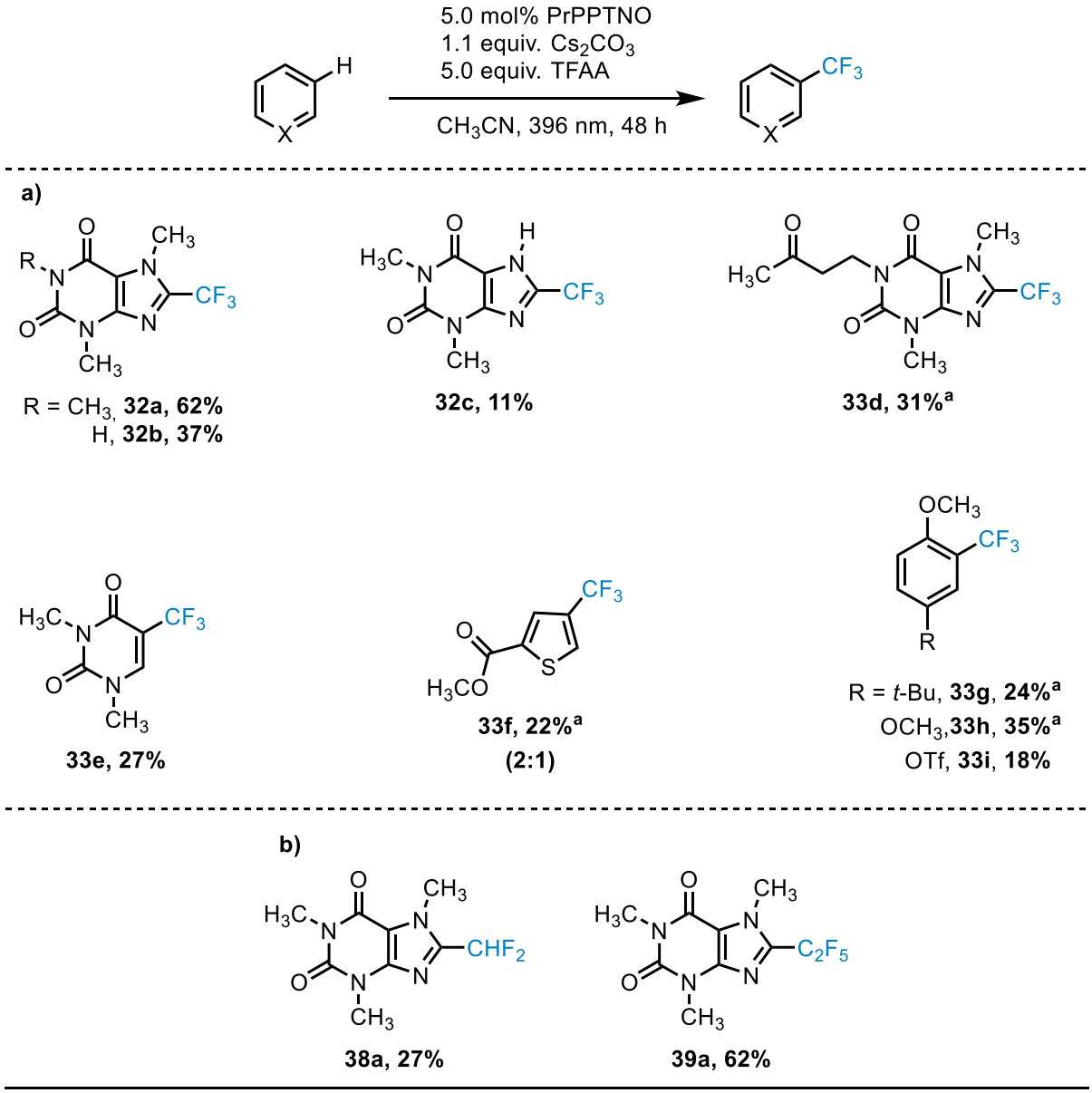

[a] Yields determined by ^{19}F-NMR spectroscopy.

Scheme 44. Substrate scope of the photocatalytic trifluoromethylation. a) scope of aromatic compounds, b) scope of anhydrides.

The methanol might be consumed by the TFAA forming the ester driving it out of the equilibrium. Since phenols are potent antioxidants the reaction slows down until no more substrate is converted. The second possibility is the direct oxidation of anisole in an oxygen atom transfer reaction (Scheme 45). This reaction was reported by Maki and might explain the formation of the phenol.[22] One product is the phenol, derived from the aromatic C–H oxidation, this product was not detected in the photocatalytic trifluoromethylation. The other oxidation product would be the C–H oxidation of the methyl group. The formed acetal will collapse releasing the phenol and formaldehyde. Isolation of the phenol might give more insight into this. If the yield is 5% or lower still both discussed pathways are

possible. Is the yield higher than the amount of used PrPPTNO (> 5%) the pathway including water is more likely. Still both pathways might be present but operating in parallel.

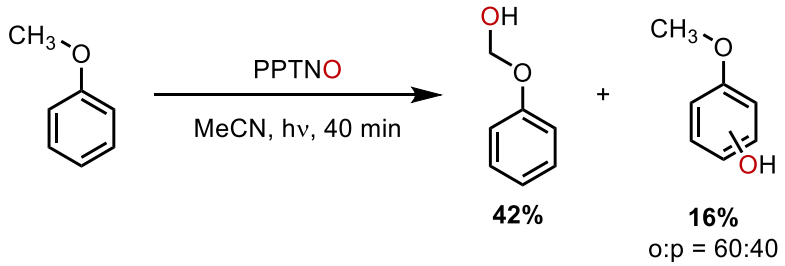

Scheme 45. Phenol formation from anisole by reaction with PPTNOs. Yields based on consumed PPTNO.[22]

Using different anhydrides for this reaction with caffeine as substrate was successful. Using the pentafluoro propionic acid anhydride gave the product (**38a**) in 62% showing that the chain length on the perfluorinated anhydride does not influence the yield. Changing from TFAA to the difluoroacetic acid anhydride also gave the product (**38b**) albeit in poor yield (27%). CF_2H radicals sometimes react as a nucleophile which might explain the low yield due to an electronic mismatch with the caffeine.[88] The fact that this reaction was heterogeneous might also be a reason for the reduced yield. Lastly the decarbonylation might be slower for the difluoro acyl radical compared to the trifluoro acyl radical. Using trichloroacetic acid anhydride was not successful. After addition of the anhydride to the reaction mixture a quick, exothermic decomposition occurred.

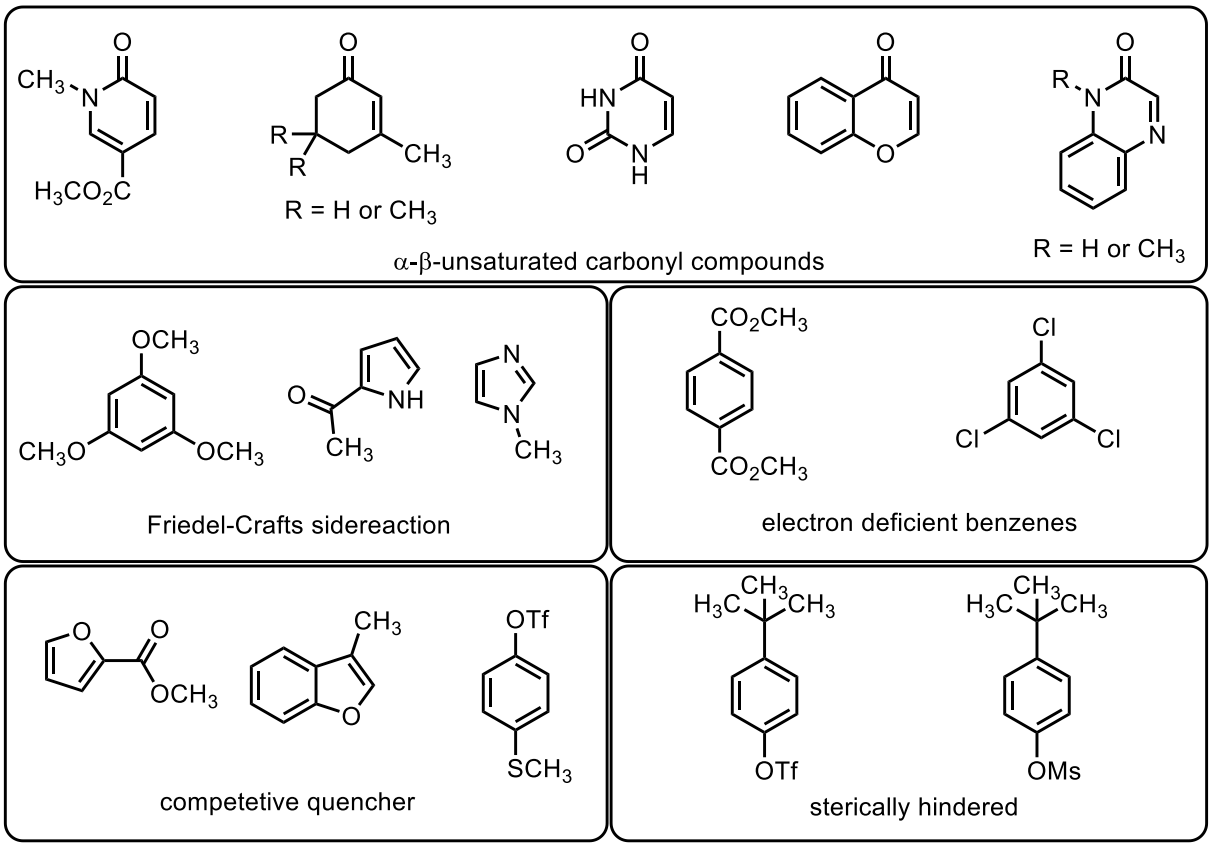

Figure 17. Unsuccessful substrates for the photocatalytic trifluoromethylation.

In Figure 17 a list of unsuccessful substrates is shown. α-β unsaturated carbonyl compounds are generally not tolerated, the only exception seems to be the dimethyl uracil. Triflyl and mesyl protected 4-tertbutyl phenol likely did not gave the product due to sterical hindrance. For these substrates, the position a CF_3 radical would attack would be ortho to the tert-butyl group. The tert-butyl group shields this position therefore inhibiting product formation. 1,3,5-trichlorobenzene and dimethyl terephthalate were likely not successful due their electron deficiency on the benzene ring. Thioanisole likely acts as competitive quencher (E_{ox} *(4-fluor thioanisole)* = +1.43 V vs SCE).[89] The reaction on Methyl furan-2-carboxylate showed many side products in the GC/MS. This is a known problem for furan derivatives.[90] 3-Methyl benzofuran showed no product formation and no side products were found by GC/MS even though this substrate is suitable for the reaction with CF_3 radicals.[91] Likely this benzofuran might also act as competitive quencher (E_{ox} = +1.94 V vs SCE)[92] which suppresses the formation of CF_3 radicals. 1-Methyl imidazole and trimethoxy benzene and 2-acyl pyrrole share the same problem. These compounds are so electron rich they undergo Friedel-Crafts acylation with TFAA. This side reaction is fast and cannot be suppressed.

To summarize, the main problem for this method is the fact that electron rich aromatic compounds are needed but if the aromatic ring is to electron rich unwanted Friedel-Crafts acylation occurs. If the aromatic ring is to electron deficient no conversion is observed. Benzylic positions and methoxy groups should be avoided. Especially methoxy groups due to the inevitable phenol formation. Catalyst decomposition could be observed for most reactions. Isolation of the photodecomposition products was not successful. Analysis by GC/MS revealed that many different species with a higher mass then PrPPTNO and PrPPT are formed. Most of the found signals could not be assigned to a PPT based structure. Only one assignment could be done which revealed that dealkylation might be a pathway of photodecomposition. To verify this, further analytical investigations like MS/MS are required.

To overcome some of the found problems and limitations additional experiments were conducted. For example, the utilization of triflyl anhydride instead of TFAA should theoretically also give the CF_3 radical under extrusion of SO_2 assuming that electron deficient anhydrides are easily reduced.[30] No reliable electrochemical characterization of Tf_2O was found in literature.[91] Utilization of Tf_2O would overcome the problem of Friedel-Crafts acylation. Unfortunately, the reaction using caffeine as substrate gave no product (Scheme 46, a). The utilization of the more expensive iridium based photocatalyst (1 mol%) was tested in the reaction using methyl thiophen-2-carboxylate (**32i**). With PrPPTNO, low conversion was the main problem likely due to catalyst deactivation. Unfortunately, using

the iridium catalyst resulted in a lower yield then PrPPTNO (Scheme 46, b). Increasing the catalyst loading might help getting higher yields when using the iridium catalyst. Considering the high price, the additional yield might not justify using more of the expensive catalyst.

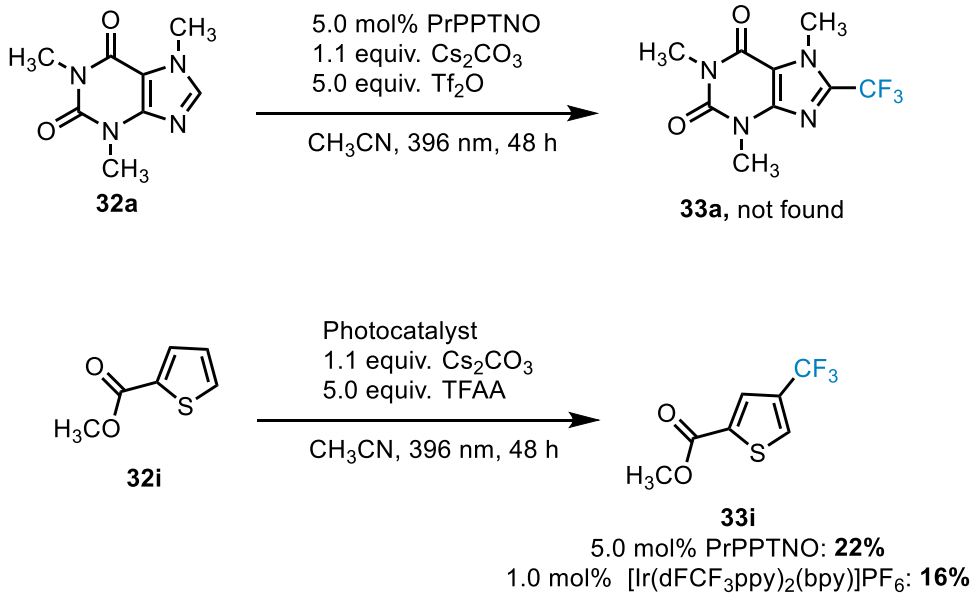

Scheme 46. Utilization of triflyl anhydride (top) and the usage of Iridium based photocatalyst (bottom).

The use of β-methyl styrene (**23a**) and phenylacetylene (**41a**) as substrates (Scheme 47) were also examined. While these substrates offer an aromatic ring for functionalization, a reaction on the C–C double and triple bond was envisioned (Scheme 48). After formation of the CF_3 radical, the addition to the olefin (**43**) may take place. Turnover gives the carbocation (**44-b**). This species can be trapped by nucleophiles like the trifluoroacetate giving access to new types of products (**44**).[91, 93]

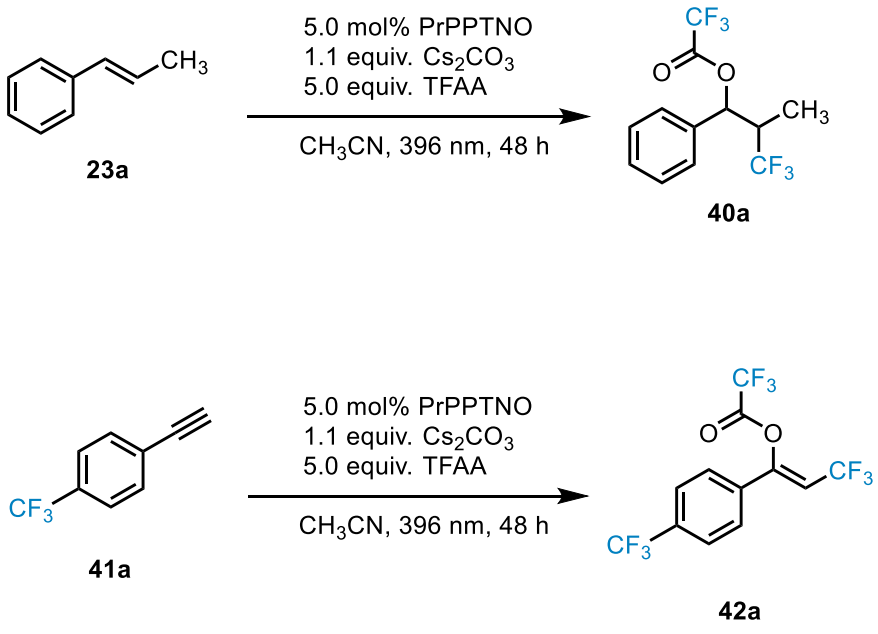

Scheme 47. Styrene and phenylacetylene derivatives under employed reaction conditions.

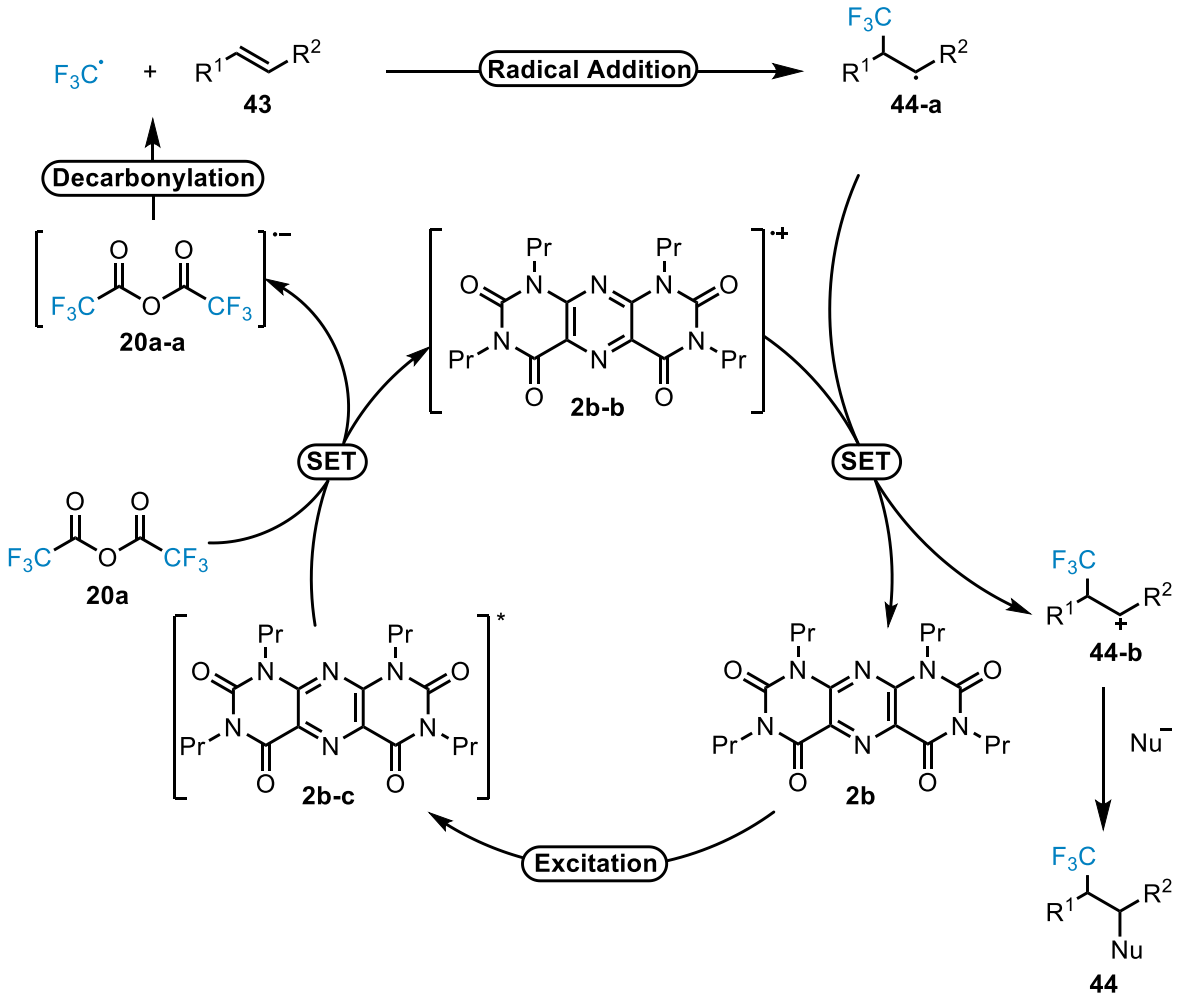

Scheme 48. Possible mechanism for the derivatization of olefins.

With phenylacetylene, the conversion was <5% indicating that here similar like the reaction with 3-methyl benzofuran the CF_3 radical formation was inhibited. Very fast catalyst decomposition might explain this. Using β-methyl styrene a broad spectrum of products was found. While in this reaction the starting material is fully consumed the reaction is very unselective. This is due to isomerization of the double bond, over substitution and a competitive hydroacetoxylation but these problems could be addressed by a thorough optimization of the reaction conditions. Changing to an alkyl chain bearing olefin like a fatty acid might help overcoming these problems.

Due to the low yields and low selectivity produced for most substrates the project was discontinued.

5.5 Summary and Outlook

A novel decarbonylative formation of CF_3 radicals using PPTNOs as photocatalyst was demonstrated. The utilization of aromatic compounds as substrates leads to the formation of trifluoromethylated products in low to medium yields. Kinetic investigations revealed

that catalyst deactivation seems to be a major problem, leading to low conversion. Furthermore, side reactions including Friedel-Crafts acylation and phenol formation were identified. In the reaction using β-methyl styrene full conversion was observed indicating that for olefins inhibition of the reaction does not occur or is slower than for aromatic compounds making this a promising reaction for further evaluation. Here the focus should be on the reduction of the equivalents of TFAA. Also, an olefin like styrene should be chosen to avoid isomerization as competing reaction. Moreover, Stern-Volmer quenching studies should be performed to gain more insight in the mechanism. The reaction using TFAA as anhydride with an olefin (Scheme 49) could give access to products (**40**) that can be functionalized further. For example, the hydrolysis gives access to alpha trifluoromethyl alcohols (**46**). Also possible is the formal elimination of TFA using a strong base to get the trifluoromethyl functionalized olefin (**45**). Furthermore, the utilization of mixed anhydrides could be attractive because they give access to a broad spectrum of different products.

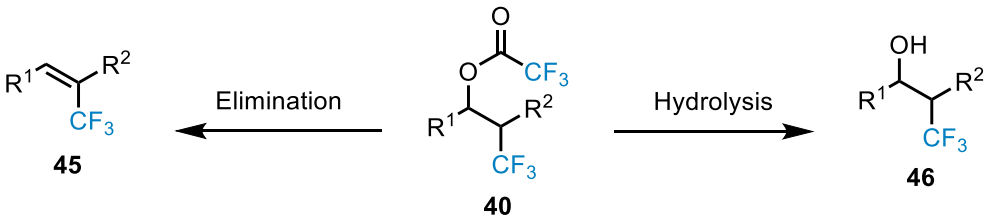

Scheme 49. Possible functionalization of **40**.

6 Experimental Section

6.1 General Remarks

All reactions involving moisture- or air-sensitive reagents or products were performed under an atmosphere of argon using standard Schlenk techniques and dried glassware. Syringes for handling of dry solvents or liquid reagents were flushed with argon prior to use. The synthesis of (*E*)-stilbenes was adapted from a literature procedure.[94] Substrates bought from commercial suppliers were used without further purification.

6.2 Solvents

All solvents for reactions containing moisture-sensitive reagents were stored under inert atmosphere (argon) according to following standard procedures.

Dry *N*,*N*-Dimethylformamide, dichloromethane, tetrahydrofuran, methanol, and *i*-propanol were purchased from Acros Organics and removed volume was replaced by argon.

Absolute methanol and ethanol were purchased from Fisher Chemical.

Dry Acetonitrile, toluene and *n*-hexane were taken from the solvent purification system.

Acetone, dichloromethane, ethylacetate, *n*-pentane, *c*-hexane and *n*-heptane used for chromatography were freshly distilled before use.

6.3 Chromatography

Analytical thin layer chromatography (TLC) was performed using TLC plates from MERCK (Geduran, Si 60, grain size 0.040-0.063 mm) with 254 nm fluorescence. Plates were visualized under ultraviolet light (254 nm or 366 nm) or developed by treatment with $KMnO_4$ solution (3.0 g $KMnO_4$, 20.0 g K_2CO_3 and 0.3 g KOH in 300 ml H_2O). Chromatographic purification of products was accomplished by flash column chromatography on MERCK silica gel, grade 60 (0.063-0.200 mm, 70–230 mesh ASTM).

6.4 Vacuum

Following pressures were measured on the used vaccuum pump and are not corrected: membrane pump vacuum (MPV): 10 mbar, oil pump vacuum (OPV): 0.01 mbar.

6.5 Infrared Spectroscopy

Infrared spectra were recorded using an Alpha FT-IR-Spectrometer (BRUCKER). Liquid probes were measured as film, solid probes were measured neat. Absorption is given in wave numbers (cm^{-1}). Spectra were recorded in the range of 4000–400 cm^{-1}. Following abbreviations were used for characterization: s (strong), m (medium), w (weak).

6.6 Nuclear Magnetic Resonance Spectroscopy

Nuclear magnetic resonance (NMR) spectra were recorded at 300 or 400 MHz (^{1}H-NMR) and 75 or 125 MHz (^{13}C-NMR), APT (Attached Proton Test) on AV 400 (BRUCKER), AV 300 (BRUCKER) or Fourier 300 (BRUCKER) instruments. Chemical shifts are reported as δ values in ppm relative to the residual proton peak of the deuterated solvent or its carbon atom, respectively.

	^{1}H-NMR	**^{13}C-NMR**
d_1-Chloroform	7.26 ppm	77.16 ppm
d_6-DMSO	2.50 ppm	39.52 ppm
d_2-Dichloromethane	5.32 ppm	53.84 ppm
d_3-Acetonitrile	1.94 ppm	1.32 ppm

For characterization of the observed signal multiplicities the following abbreviations were applied: s (singlet), d (doublet), t (triplet), q (quartet), m (multiplet). Coupling constants *J* are reported in Hertz (Hz).

6.7 Mass spectrometry

Mass spectra were measured on Agilent 6890/5973 (GC-MS), Agilent 7890/5977 (GC-MS), Agilent 1260/6130 Quadrupol (LC-MS), Agilent 1200/6210 (Time-of-Flight LC-MS). The ratio of mass to charge are indicated, intensities relative to the base peak (I = 100) are written in parentheses. High resolution mass spectras (HRMS) were recorded on Thermo Electron MAT 95-XP.

6.8 Melting Points

Melting points were measured using a Melting Point B-540 (BÜCHI).

6.9 Crystallographic Data

Crystallographic X-ray data were recorded with a BRUCKER KAPPA APEX II DUO diffractometer and a BRUKER D8 QUEST diffractometer. The structure was solved by direct methods and refined by fullmatrix least-squares procedures on F2 with the SHELXTL software package (Sheldrick, G. M. Acta Crystallogr. 2008, A64, 112.). For the data extraction, following software was used: publCIF (Westrip, S. P., J. Apply. Cryst. 2010, 43, 920-925). The documentation of the crystallographic data precedes according to the guidelines from Acta Crystallographica .The illustrations of the molecules were created with Mercury (Macrae, C. F., Bruno, I. J., Chisholm, J. A., Edgington, P. R., McCabe, P., Pidcock, E., Rodriguez-Monge, L., Taylor, R., van de Streek, J. & Wood, P. A. J. Appl. Cryst. 2008, 41, 466-470.).

6.10 Optical Rotations

Specific rotation values were recorded using an ANTON PAAR MCP 200 polarimeter, after the compound was dissolved in 10 ml CH_3CN, resulting in a concentration range of 0.3 to 0.6 mg/ml depending on the amount of substrate available. The given number is the average of three measurements.

6.11 Cyclovoltammetric and DPV measurements

All electrochemical investigations were performed at room temperature in dried acetonitrile p.A. (VWR) under an Argon atmosphere with 0.1 M tetrabutylammonium hexafluorophosphate (Fluka) as conducting salt using an Autolab (PGSTAT 204, Metrohm). A glassy carbon disk electrode (d = 2 mm) used as working electrode, a Pt-electrode as the counter electrode and an Ag/AgCl/LiClsat. in EtOH-system as the reference electrode (all electrodes: Metrohm). All potentials were measured with respect to this reference system and were checked by using the ferrocenium/ferrocene-internal reference system (potential of Fc^+ /Fc: 0.51 V [vs. Ag/AgCl/LiClsat. In EtOH]. The CV scans were done three times at a scan rate of 40 mV s^{-1}. The measurements were performed with 1 mM compound dissolved in the electrolyte.

6.12 DFT calculations

Computations were carried out using Gaussian 09[95] and visualized by Gaussview05[96]. All optimized structures were further characterized at the same level as energy minimums without imaginary frequencies by frequency calculations, which provided zero-point vibrational energies and thermal corrections to enthalpy and Gibbs free energy at 298.15 K under 1 atmosphere. The final Gibbs free energies for discussion include the thermal corrections to enthalpies and Gibbs free energies.

For the data presented in Figure 10:

Geometry optimization was carried out in gas phase using the hybrid functional B3LYP with the 6-31G(d,p)-basis set. The B3LYP method and 6-31G(d,p) basis set has been demonstrated to predict excellent geometries and energies for heteroaromatic-*N*-oxides and related compounds compounds.[97]

For the data presented in Figure 15:

Geometry optimization was carried out in gas phase at the B3PW91 level with the all-electron TZVP under the consideration of solvation effect of acetonitrile as solvent based on solute electron density (SMD) and van der Waals dispersion (GD3BJ).

6.13 UV-Vis spectroscopy

UV-Vis spectra were recorded using an UV5 Bio UV-Vis spectrophotometer from Mettler Toledo using 10mm quartz glass cuvette from Hellma Analytics (High Precision Cell). Acetonitrile was used as solvent and concentrations in a range of 10^{-4} M to 10^{-5} M were used typically resulting in optical densities of 0.8 to 1.2.

6.14 Fluorescence spectroscopy

Fluorescence spectra were recorded using a Cary Eclipse fluorescence spectrophotometer from Varian using 10mm quartz glass cuvette from Hellma Analytics (High Precision Cell). Acetonitrile was used as solvent and concentrations in a range of 10^{-5} M to 10^{-6} M were used typically resulting in optical densities of <0.10. The used excitation wavelength of PPT and PPTNO based compounds was λ = 350 nm. PPT compounds are much more fluorescent then their PPTNO analogues.

6.15 Determination of quantum yield of fluorescence

The emission spectra were detected with a FluoMax-4 (Horiba Scientific) spectrometer, the excitations wavelength was 350 nm in all cases. Acetonitrile (Fischer Scientic, HPLC grade) was used as solvent and the samples were placed in 10 mm quartz cuvettes (111-10-40, Hellma Analytics). The quantum yields were determined with the relative methot[98] using the fluorescence standard quinine hemisulfate dihydrate (Fluka Analytical) in sulfuric acid (0.05 M) as standard (ϕ_{st} = 0.52).[99] In all cases the optical densities were below 0.1 to prevent self-absorption. Due to the low fluorescence of the substances in comparison to the used standard, we attenuated the emissions signal of the quinine standard with a neutral density optical filter with an attenuation factor f_{att} of 94.0. The weak emission of BuPPTNO, PrPPTNO, MePPTNO and PhPPTNO, were overlaid by the Raman-bands of acetonitrile. The solvent Raman features were corrected by the blank solvent emission under identical excitation conditions, resulting in the corrected spectra. In case of the substances BuPPTNO, PrPPTNO and MePPTNO, the Raman contribution to the emission is reduced due to the stronger emission of the sample. As a result the correction by the plain solvent emission slightly overcorrects the Raman features. However, the applied routine is the best possible. The experimental error of the remaining Raman feature is estimated to be 3% and adds up to the common experimental error for quantum yield determination of 5 %, resulting in a total experimental error of 8%.

The quantum yields of the substances (ϕ_x) were calculated as follow:

$$\phi_x = \phi_{st} \cdot \frac{f_{st}}{f_x} \cdot \frac{F_x}{F_{st} \cdot f_{att}} \cdot \left(\frac{\eta_x}{\eta_{st}}\right)^2$$

Here, f_x and f_{st} are the absorption factors of the substances and the standard. F_x and F_{st} are the emitted relative integrated photon fluxes of the respective emission spectra. η_x and η_{st} are the refraction indices of the solvent of the sample (ACN, n_x=1.3442) and the standard (sulfuric acid, n_{st}=1.3380).

6.16 Chiral HPLC

Chiral HPLC was used to determine the enantiomeric excess. A HPLC-system 1200 with DAD-Detector from Agilent Technologies was used equipped with a ChiralCel OJ-H column. Samples were prepared using acetonitrile as solvent. The used eluent was a mixture of up to 5% EtOH in Heptane.

6.17 Experimental Procedures

6.18 General Procedures

General procedure A: Photocatalytic Hydroamination

Reactions were performed under Schlenk conditions using a 5 ml glass microwave vial equipped with a NS 14.5 rubber septum. The vial containing the corresponding stilbene (0.50 mmol, 1.0 equiv.) and the photoredox catalyst (5.0 mol%) was evacuated for 5 min and purged with argon. Acetonitrile (2.5 mL) was added and the corresponding amine (2.50 mmol, 5.0 equiv.) was added to the stirring solution. The walls of the microwave vial were rinsed with acetonitrile (2.5 mL). The reaction mixture was irradiated at 396 nm for 16-24 h. The reaction temperature was monitored in an adjacent microwave vial filled with oil and equipped with a thermal sensor. A constant temperature of 30 °C was measured due to heat emission of the LED. No extra heating or cooling was applied. After the indicated time, the reaction was quenched upon exposure to air and bubbling air through the solution using a pipette. The reaction was concentrated under reduced pressure and the crude product was purified by column chromatography.

General procedure B: Photocatalytic Trifluoromethylation

Reactions were performed under Schlenk conditions using a 10 or 25 ml Schlenk vessel equipped with a NS 14.5 rubber septum. To this flask was added cesium carbonate (0.55 mmol, 1.1 equiv.) and then evacuated and flushed with argon 3 times. Then the vacuum is applied, and the cesium carbonate is heated using a heatgun set at 550°C. The heating is applied until the pressure is constantly lower than 10^{-1} mbar. Then the vessel is cooled to room temperature and the corresponding aromatic compound (0.50 mmol, 1.0 equiv.), PrPPTNO (5.0 mol%) and the stir bar were added the solids were evacuated and purged with argon 3 times. Acetonitrile (5.0 mL) was added in one portion. Then the anhydride is added dropwise. When gas evolution ceased, the solution was degassed by freeze-pump-thaw. The reaction mixture was irradiated at 396 nm. After the indicated time, the reaction

was quenched upon exposure to air and bubbling air through the solution using a pipette. The reaction was concentrated under reduced pressure and the crude product was purified by column chromatography.

Reaction Set-up

Reactions following general procedure A and B were irradiated using 2 x 30 W LEDs from ONFURO in 5.7 to 10.4 cm distance (Figure 18). The emission spectra of the LED and the superimposed absorption spectra of PPT and PPTNO are shown in Figure 19.

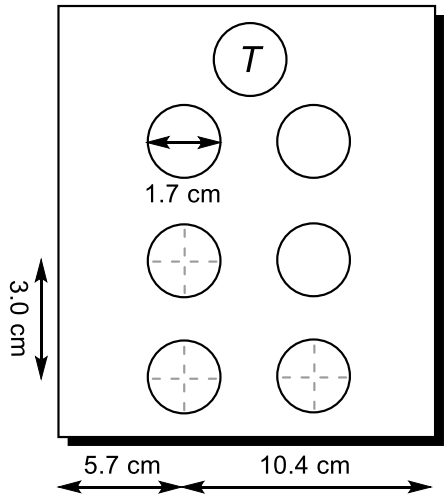

Figure 18. Reaction Set-up.

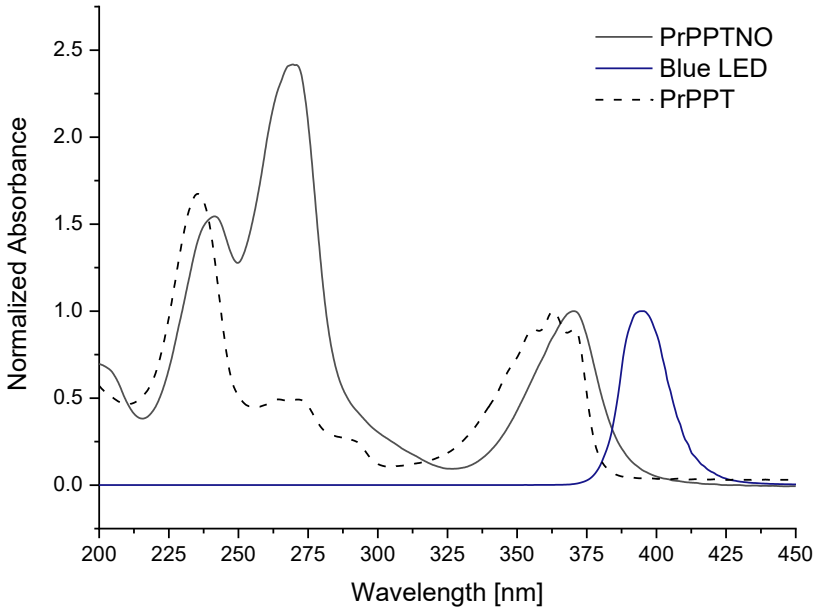

Figure 19. Absorption spectrum of PrPPTNO (black), PrPPT (dashed) and emission spectrum of the used ONFURO LED.

6.19 Synthesis and Characterization of PPT based Photocatalysts

Synthesis of 6-amino-1,3-di-*n*-propyl-5-nitrosouracil (1b):

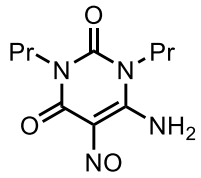

Sodium nitrite (0.65 g, 9.47 mmol) in water (4 mL) was added dropwise to a stirred homogeneous solution of 6-amino-1,3-dipropyluracil (**8b**) (1.00 g, 4.73 mmol) in 50 % aqueous acetic acid (24 mL) at 50 °C. After the addition was complete, the reaction mixture was allowed to cool to room temperature and stirred for 1 h. Subsequently, the suspension was cooled in ice bath for 30 mins, filtered and washed with water. The residue was dried to give **1b** (0.99 g, 4.12 mmol, 87 %) as a pink solid.

R_f = 0.3 (*n*-pentane/EtOAc/MeOH = 1:1:0.2, UV).

m.p. = 221–223 °C.

^{1}H NMR (400 MHz, DMSO-d_6) δ 13.18 (s, 1H), 9.12 (s, 1H), 3.83–3.86 (m, 2H), 3.75–3.79 (m, 2H), 1.47–1.64 (m, 4H), 0.85–0.90 (m, 6H).

^{13}C NMR (100 MHz, DMSO-d_6) δ 159.9, 149.0, 145.4, 138.9, 42.5, 42.4, 20.7, 19.7, 11.2, 10.6.

MS (EI): *m*/*z* (relative intensity) 240 (3) [M^+], 223 (100), 199 (32), 181 (10), 157 (11), 138 (12), 114 (12), 110 (21), 83 (10), 56 (9), 41 (13).

HRMS (EI): calcd. for $C_{10}H_{16}N_4O_3$ 240.1217; found 240.1212.

IR (ATR, neat, cm^{-1}): 3136 (w), 2961 (w), 2878 (w), 1717 (m), 1671 (m), 1406 (s), 1362 (m), 1230 (s), 1078 (s), 852 (m), 753 (s), 576 (m).

Synthesis of 1,3,7,9-tetra-*n*-propyl-2,4,6,8-tetraoxo-1,2,3,4,6,7,8,9-octahydropyrimido[5,4-g]pteridine 5-oxide, PrPPTNO (2b):

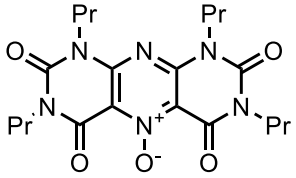

6-Amino-1,3-dipropyl-5-nitrosouracil (**1b**) (0.80 g, 3.33 mmol), glacial acetic acid (16 mL) and lead tetraacetate (1.62 g, 3.66 mmol) were stirred for 2 h at room temperature. Glycerol (0.8 mL) was added to quench unreacted lead tetraacetate and the mixture was stirred for an additional 10 min. The reaction mixture was poured into water and extracted with CH_2Cl_2. The combined organic layers were dried over anhydrous sodium sulfate, filtered and concentrated under reduced pressure. The solid mass was recrystallized from acetone/water = 3:1 to give the desired product. Subsequently, the supernatant was

concentrated under reduced pressure and recrystallized again. The title compound **2b** (551 mg, 1.27 mmol, 76%) was obtained as analytically pure fine yellow needles.

R_f = 0.2 (*n*-pentane/EtOAc = 3:2, UV).

m.p. = 208–210 °C.

^{1}H NMR (300 MHz, $CDCl_3$) δ 4.17–4.23 (m, 4H), 3.85–3.90 (m, 4H), 1.67–1.80 (m, 4H), 1.54–1.66 (m, 4H), 0.97 (t, *J* = 7.4 Hz, 6H), 0.90 (t, *J* = 7.4 Hz, 6H).

^{13}C NMR (75 MHz, $CDCl_3$) δ 153.4, 151.7, 149.5, 119.9, 45.3, 43.4, 21.2, 20.9, 11.3, 11.3.

MS (EI): *m*/*z* (relative intensity) 432 (1) [M^+], 416 (100), 374 (24), 332 (17), 302 (27), 290 (20), 249 (8), 232 (8), 43 (14).

HRMS (ESI-TOF, *m*/*z*): calcd. for $C_{20}H_{28}N_6O_5$ [M+Na^+] 455.2022; found 455.2019.

IR (ATR, neat, cm^{-1}): 2957 (w), 2876 (w), 1709 (m), 1667 (s), 1520 (s), 1106 (m), 885 (m), 746 (s), 568 (s), 464 (m).

Synthesis of 1,3-di-*n*-butylurea (7a):

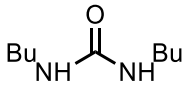

Butyl isocyanate (2.05 mL, 18 mmol) was added dropwise to a solution of butylamine (1.80 mL, 18 mmol) in CH_2Cl_2 (36 mL) at 0 °C. The reaction mixture was allowed to warm to room temperature and stirred for 1 h. Subsequently, the solvent removed under reduced pressure to give **7a** as an off-white solid (2.81 g, 16 mmol, 89 %,).

R_f = 0.5 (*n*-hexane/EtOAc/MeOH = 1:1:0.1, $KMnO_4$).

m.p. = 70–71 °C.[100]

^{1}H NMR (300 MHz, DMSO-d_6) δ 5.71 (t, *J* = 5.5 Hz, 2H) 2.92–2.98 (m, 4H), 1.18–1.37 (m, 8H), 0.85 (t, *J* = 7.2 Hz, 6H).

^{13}C NMR (75 MHz, DMSO-d_6) δ 158.0, 38.8, 32.2, 19.5, 13.6.

MS (EI): *m*/*z* (relative intensity) 172 (9) [M^+], 74 (8), 57 (11), 44 (27), 41 (43), 39 (13), 30 (100).

HRMS (EI): calcd. for $C_9H_{20}N_2O$ 172.1570; found 172.1570.

IR (ATR, neat, cm^{-1}): 3323 (m), 2956 (m), 2868 (m), 1570 (s), 1458 (s), 1278 (m), 1229 (s), 739 (m), 613 (s), 436 (m).

Synthesis of 6-amino-1,3-di-*n*-butyluracil (8a):

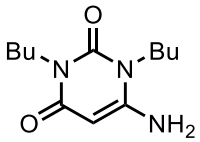

1,3-Dibutylurea (**7a**) (2.80 g, 16.2 mmol), cyanoacetic acid (1.59 g, 18.7 mmol) and acetic anhydride (2.5 mL) were heated at 60 ºC for 3 h under inert atmosphere. The reaction mixture was then concentrated under reduced pressure and dissolved methanol. A cold solution of 5% NaOH was slowly added until precipitation occurred, and the suspension was stirred at 0 °C for 1 hour. After the filtration, the crude product was purified by column chromatography (*n*-hexane:EtOAc:MeOH = 1:1:0 → 1:1:0.2) and dried in vacuo give **7a** (1.04 g, 4.35 mmol, 27 %) as a white solid.

R_f = 0.5 (*n*-hexane/EtOAc/MeOH = 1:1:0.2, UV).

m.p. = 91–93 °C.[101]

^{1}H NMR (300 MHz, DMSO-d_6) δ 6.78 (s, 2H), 4.64 (s, 1H), 3.66–3.79 (m, 4H), 1.37–1.52 (m, 4H), 1.16–1.33 (m, 4H), 0.83–0.90 (m, 6H).

^{13}C NMR (75 MHz, DMSO-d_6) δ 161.2, 154.2, 151.2, 75.1, 41.5, 39.5, 29.7, 29.7, 19.6, 19.2, 13.7, 13.6.

MS (EI): *m*/*z* (relative intensity) 239 (8) [M^+], 222 (77), 210 (15), 197 (14), 184 (26), 167 (36), 154 (13), 141 (90), 127 (100), 111 (33), 97 (39), 85 (17), 68 (42), 55 (13), 41 (19), 30 (11).

HRMS (ESI-TOF, *m*/*z*): calcd. for $C_{12}H_{21}N_3O_2$ [M+H^+] 240.1707; found 240.1708.

IR (ATR, neat, cm^{-1}): 3429 (w), 3139 (w), 2957 (w), 2872 (w), 1600 (s), 1496 (s), 1408 (s), 1288 (m), 787 (m), 526 (m).

Synthesis of 6-amino-1,3-di-*n*-butyl-5-nitrosouracil (1a):

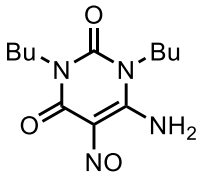

Sodium nitrite (0.62 g, 9.0 mmol) in water (1 mL) was added dropwise stirred homogeneous solution of 6-amino-1,3-dibutyluracil (**8a**) (0.95 g, 3.97 mmol) in 50 % aqueous acetic acid (17 mL) at 50 °C. After the addition was complete, the reaction mixture was allowed to cool to room temperature and stirred for 1 h. Subsequently, the suspension was cooled in ice bath for 30 mins, filtered and washed with water. The residue was dried to give **1a** (1.01 g, 3.76 mmol, 95 %) as a pink solid.

R_f = 0.3 (*n*-hexane/EtOAc/MeOH = 1:1:0.2, UV)

m.p. = 213–215 °C

^{1}H NMR (300 MHz, DMSO-d_6) δ 13.18 (s, 1H), 9.08 (s, 1H), 3.79–3.91 (m, 4H), 1.43–1.61 (m, 4H), 1.24–1.38 (m, 4H), 0.85–0.93 (m, 6H).

^{13}C NMR (75 MHz, DMSO-d_6) δ 159.8, 149.0, 145.4, 138.9, 41.0, 40.6, 29.5, 28.4, 19.6, 19.2, 13.7, 13.6.

MS (EI): *m/z* (relative intensity) 268 (9) [M^+], 251 (100), 213 (90), 197 (55), 157 (39), 141 (15), 127 (26), 114 (30), 97 (11), 82 (29), 70 (16), 55 (32), 43 (67).

HRMS (ESI-TOF, *m/z*): calcd. for $C_{12}H_{20}N_4O_3$ [M+H^+] 269.16082; found 269.16077.

IR (ATR, neat, cm^{-1}): 2956 (w), 2872 (w), 1715 (m), 1597 (s), 1513 (s), 1406 (s), 1234 (s), 1088 (m), 856 (m), 754 (s), 436 (m).

Synthesis of 1,3,7,9-tetra-*n*-butyl-2,4,6,8-tetraoxo-1,2,3,4,6,7,8,9-octahydropyrimido[5,4-g]pteridine 5-oxide, BuPPTNO (2a):

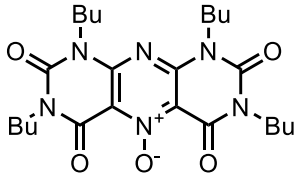

6-Amino-1,3-dibutyl-5-nitrosouracil (**1a**) (1.00 g, 3.73 mmol), glacial acetic acid (19 mL) and lead tetraacetate (1.82 g, 4.10 mmol) were stirred for 2 h at room temperature. Glycerol (0.5 mL) was added to quench unreacted lead tetraacetate and the mixture was stirred for additional 10 min. The reaction mixture was poured into water and extracted with CH_2Cl_2. The combined organic layers were dried over sodium sulfate, filtered and concentrated under reduced pressure. The oily residue was triturated with water and the formed solid mass was recrystallized from acetone/water = 3:1 to give the desired product. Subsequently, the supernatant was concentrated under reduced pressure and recrystallized again. The title compound **2a** (0.60 g, 1.23 mmol, 66 %) was obtained as yellow needles.

R_f = 0.4 (*n*-hexane/EtOAc = 1:1, UV).

m.p. = 163–164 °C.

^{1}H NMR (300 MHz, $CDCl_3$) δ 4.23–4.28 (m, 4H), 3.93–3.98 (m, 4H), 1.54–1.75 (m, 8H), 1.29–1.48 (m, 8H), 0.90–0.98 (m, 12H).

^{13}C NMR (75 MHz, $CDCl_3$) δ 153.3, 151.7, 149.4, 119.9, 43.8, 42.0, 30.1, 29.7, 20.4, 20.2, 13.9, 13.8.

MS (EI): *m/z* (relative intensity) 488 (7) [M^+], 472 (100), 430 (19), 417 (21), 361 (15), 249 (10), 41 (16).

HRMS (ESI-TOF, *m/z*): calcd. for $C_{24}H_{36}N_6O_5$ [M+H^+] 489.2820; found 489.2820.

IR (ATR, neat, cm^{-1}): 2955 (w), 2870 (w), 1666 (s), 1524 (s), 1318 (s), 920 (w), 793 (m), 754 (m), 556 (m), 420 (m).

Photocatalytic Isomerization of methyl cinnamate

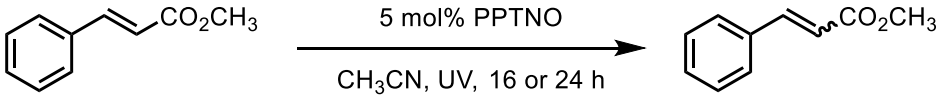

To a preheated microwave vessel under argon, (*E*)-methyl cinnamate (81 mg, 0.5 mmol) and photocatalyst (5.0 mol%) were added. The solids are evacuated for 5 min. Then CH_3CN (5.0 ml) was added and the mixture was stirred. The mixture is irradiated for 16 or 24h using 4 UVA lamps (Osram Dulux BL350). The mixture was purified by column chromatography (*n*-pentane:EtOAc = 5:1) and obtained as a mixture of the (E)- and (Z)-isomer. The results when varying the catalyst and reaction time are depicted in Table 3 and discussed in chapter 3.4.

6.20 Oxidative cyclization of 2-phenylbenzoic acid

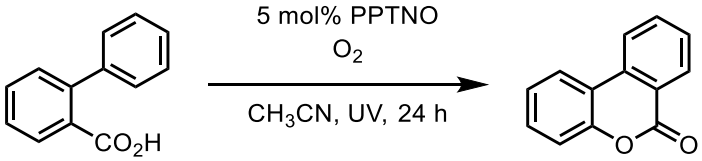

2-Phenylbenzoic acid (99 mg, 0.5 mmol) and PPTNO based photocatalyst (5.0 mol%) were dissolved in dry acetonitrile (5.0 ml) and irradiated using 4 UVA lamps (Osram Dulux BL350) under an oxygen atmosphere. The reaction mixture was concentrated and purified by flash chromatography (*n*-pentane:EtOAc = 20:1), yielding 3,4-benzocoumarin (**11a**) as a colorless solid. The results are depicted in Table 4 and discussed in chapter 3.5.

Synthesis of 3,4-benzocoumarin (11a):

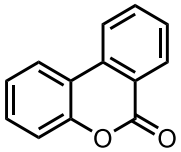

R_f = 0.4 (*n*-hexane/EtOAc = 10:1, UV).

m.p. = 90–91 °C.

^{1}H NMR (300 MHz, $CDCl_3$) δ 8.35 (ddd, *J* = 8.0, 1.4, 0.6 Hz, 1H), 8.11 – 8.03 (m, 1H), 8.00 (dd, *J* = 8.2, 1.4 Hz, 1H), 7.78 (ddd, *J* = 8.1, 7.3, 1.4 Hz, 1H), 7.54 (ddd, *J* = 8.2, 7.3, 1.1 Hz, 1H), 7.44 (ddd, *J* = 8.4, 7.0, 1.6 Hz, 1H), 7.30 (m, 2H).

^{13}C NMR (75 MHz, $CDCl_3$) δ 161.2, 151.3, 134.9, 134.8, 130.6, 130.5, 128.9, 124.6, 122.8, 121.7, 121.2, 118.0, 117.8.

MS (EI): *m/z* (relative intensity) 196 (100) [M^+], 168 (44), 139 (44), 113 (5), 70 (8).

HRMS (EI): calcd. for $C_{13}H_8O_2$ 196.0524; found 196.0525.

IR (ATR, neat, cm^{-1}): 1302 (m), 1262 (m), 1237 (m), 1203 (m), 1076 (s), 1031 (s), 895 (w), 743 (s), 717 (s), 679 (s).

Synthesis of 1,3-dicyclohexylpyrimidine-2,4,6(1H,3H,5H)-trione (12e)

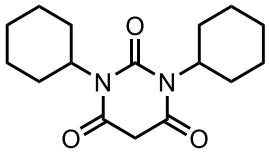

To dicyclohexylurea **7e** (2.24 g, 10.0 mmol) and malonic acid (1.04 g, 10.0 mmol) glacial acetic acid (60 ml) was added and stirred until everything had fully dissolved. The mixture was heated to 60°C, and acetic anhydride (40 ml) was added over 15 min. The reaction mixture was heated while stirring at 90°C for 4 h. The mixture was transferred to a separatory funnel using ethylacetate (150 ml). The organic layer was washed 3 times using water (100 ml) and once using $NaHCO_3$ (100 ml) solution. The organic layer was dried over sodium sulfate and all volatiles evaporated on vacuum at 60°C. The crude product was purified by multiple recrystallizations using acetone/water and obtained **12e** as slightly purple solid (1.78 g, 6.09 mmol, 61%).

m.p. = 200–204°C.

^{1}H NMR (300 MHz, $CDCl_3$) δ 4.57 (tt, *J* = 12.2, 3.7 Hz, 2H), 3.57 (s, 2H), 2.23 (qd, *J* = 12.3, 3.2 Hz, 4H), 1.81 (d, *J* = 13.2 Hz, 4H), 1.70 – 1.53 (m, 6H), 1.44 – 1.04 (m, 6H).

^{13}C NMR (75 MHz, $CDCl_3$) δ 165.1, 151.4, 55.4, 41.1, 29.2, 26.4, 25.2.

MS (EI): *m/z* (relative intensity) 212 (12), 211 (81), 129 (100), 98 (13), 86 (22), 83 (21), 82 (29), 81 (21), 79 (18), 70 (21), 69 (23), 67 (72), 56 (24), 55 (58), 54 (40), 53 (13), 43 (13), 42 (31), 41 (56), 39 (28).

Synthesis of 6-chloro-1,3-dicyclohexylpyrimidine-2,4(1H,3H)-dione (13e)

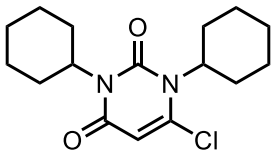

To **12e** (5.00 g, 17.1 mmol) and water (1 ml) was $POCl_3$ (30 mL) added dropwise under stirring at 0 °C over 20 min. After the addition the reaction mixture was stirred at 110 °C for 3h. The mixture is allowed to cool to room temperature and is then poured into a well

stirred mixture of crushed ice and ammonia solution and stirred at room temperature for 15 min. The crude mixture was extracted 3x with ethyl acetate, dried over sodium sulfate and purified by column chromatography (*c*-hexane:EtOAc = 20:1). **13e** was obtained as colorless solid (1.85 g, 5.95 mmol, 35%).

R_f = 0.3 (*c*-hexane:EtOAc = 10:1, UV).

m.p. = 96–98°C.

^{1}H NMR (300 MHz, $CDCl_3$) δ 5.78 (s, 1H), 4.69 (tt, *J* = 12.1, 3.7 Hz, 1H), 4.45 (s, 1H), 2.54 – 2.21 (m, 4H), 1.95 – 1.47 (m, 9H), 1.47 – 1.15 (m, 6H).

^{13}C NMR (75 MHz, $CDCl_3$) δ 161.3, 150.4, 145.6, 102.8, 61.2, 54.5, 29.4, 28.5, 26.5, 26.4, 25.3, 25.1.

IR (ATR, neat, cm^{-1}): 2942(w), 2925(m), 2916(m), 2879(w), 2851(m), 1712(m), 1664(s), 1609(m), 1594(m), 1521(w), 1470(w), 1417(s), 1383(m), 1357(w), 1330(s), 1268(w), 1253(w), 1198(w), 1168(w), 1111(m), 1072(w), 1056(w), 1042(w), 1024(w), 999(m), 961(w), 893(m), 853(w), 840(w), 816(w), 797(m), 759(s), 724(w), 706(w), 659(w), 597(w), 579(m), 536(w), 493(w), 475(w), 457(m).

Synthesis of 6-azido-1,3-dicyclohexylpyrimidine-2,4(1H,3H)-dione (14e)

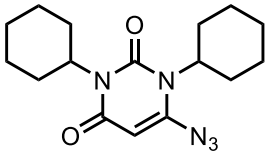

13e (1.69 g, 5.45 mmol) was dissolved in DMF (40 ml). Then NaN_3 (0.40g, 6.26 mmol) was added in one portion. The mixture was stirred for 90min and then transfer to a separatory funnel. The organic layer was extracted 3 times using DCM. The organic layer was dried over sodium sulfate and all volatiles evaporated. The product was purified by column chromatography using *c*-hexane:EtOAc (10:1) as eluent. The product **14e** was obtained as white solid (1.46g, 4.60 mmol, 84%).

R_f = 0.2 (*c*-hexane:EtOAc = 10:1, UV).

m.p. = 126–128°C.

^{1}H NMR (300 MHz, $CDCl_3$) δ 5.43 (s, 1H), 4.73 (tt, *J* = 12.0, 3.6 Hz, 1H), 4.46 (s, 1H), 2.35 (qd, *J* = 12.3, 3.4 Hz, 4H), 1.93 – 1.73 (m, 4H), 1.71 – 1.52 (m, 6H), 1.44 – 1.11 (m, 6H).

^{13}C NMR (75 MHz, $CDCl_3$) δ 162.1, 150.9, 150.8, 88.4, 57.9, 54.2, 29.9, 28.6, 26.6, 26.4, 25.4, 25.2.

HRMS (ESI-TOF, *m/z*): calcd. for $C_{16}H_{23}N_5O_2$ [M+H^+] 318.1930; found 318.1929.

IR (ATR, neat, cm^{-1}): 3066(w), 2976(w), 2932(m), 2875(w), 2853(w), 2659(w), 2130(m), 1707(m), 1649(s), 1605(s), 1529(w), 1493(w), 1469(m), 1435(s), 1391(m), 1364(m), 1334(s), 1288(m), 1266(s), 1195(w), 1179(m), 1133(w), 1080(w), 1056(w), 1044(m), 1031(w), 1010(w), 993(m), 894(m), 828(w), 803(w), 788(s), 763(s), 728(w), 699(w), 651(m), 598(w), 579(m), 544(m), 530(m), 492(m), 474(m), 459(m), 424(w), 407(w).

Synthesis of 6-amino-1,3-dicyclohexylpyrimidine-2,4(1H,3H)-dione (8e)

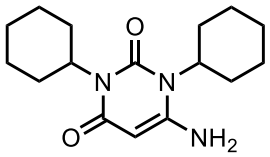

A suspension of $LiAlH_4$ (84 mg, 2.27 mmol) in dry THF (8 ml) was added dropwise to a homogeneous solution of **4e** (1.20 g, 3.78 mmol) in dry THF (16 ml) at 0 °C and the mixture was stirred for 30 min. The excess of $LiAlH_4$ was quenched by the careful addition of methanol until hydrogen evolution ceased. The mixture was then extracted using EtOAc. After evaporation of all volatiles the analytical pure product **8e** is obtained as white solid (1.09 g, 3.74 mmol, 99%).

m.p. = 158–160°C.

^{1}H NMR (300 MHz, $CDCl_3$) δ 5.22 (s, 1H), 4.88 (s, 1H), 4.71 (s, 1H), 2.53 – 2.08 (m, 4H), 1.95 – 1.47 (m, 10H), 1.46 – 1.00 (m, 6H).

^{13}C NMR (75 MHz, $CDCl_3$) δ 163.8, 154.5, 148.3, 79.3, 56.5, 52.6, 29.4, 27.7, 26.5, 25.9, 25.4, 23.9.

MS (EI): *m/z* (relative intensity) 291 (5), 210 (36), 195 (15), 128 (100), 127 (23), 111 (28), 98 (10), 85 (15), 83 (15), 82 (14), 81 (14), 68 (24), 67 (32), 56 (12), 55 (67), 54 (23), 42 (11), 41 (52), 39 (18).

HRMS (ESI-TOF, *m/z*): calcd. for $C_{16}H_{25}N_3O_2$ $[M+H^+]$ 291.1941; found 291.1944.

IR (ATR, neat, cm^{-1}): 3328(w), 3190(w), 2926(w), 2853(w), 1700(w), 1685(w), 1617(s), 1542(w), 1478(s), 1456(m), 1400(w), 1371(m), 1336(m), 1288(w), 1263(w), 1198(w), 1172(w), 1118(w), 1075(w), 1057(w), 1012(w), 997(w), 937(w), 895(w), 840(w), 785(m), 768(m), 734(w), 673(w), 651(w), 577(m), 495(w), 463(m), 419(w).

Synthesis of 6-amino-1,3-dicyclohexyl-5-nitrosopyrimidine-2,4(1H,3H)-dione (1e)

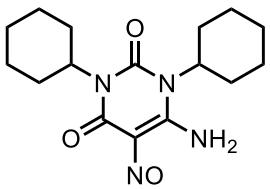

Sodium nitrite (108 mg, 1.57 mmol) in water (4 ml) was added to a stirred homogeneous mixture of **8e** (229 mg, 0.79 mmol) in 50% aqueous acetic acid (24 ml) at 50°C. After the addition was complete, the reaction mixture was allowed to cool to room temperature and stirred for 1h. Subsequently, the suspension was cooled in ice bath for 30 min, filtered and washed with water. The filtrate was dried in vacuo. The product **1e** was obtained was purple solid (227 mg, 0.71 mmol, 90%).

m.p. = 225°C (decomp).

^{1}H NMR (300 MHz, $CDCl_3$) δ 13.51 (s, 1H), 9.05 (s, 1H), 4.84 (t, *J* = 12.0 Hz, 1H), 4.28 (s, 1H), 2.37 (q, *J* = 11.6 Hz, 4H), 1.93 – 1.49 (m, 10H), 1.28 (dt, *J* = 39.3, 17.6 Hz, 6H).

^{13}C NMR (75 MHz, CDCl3) δ 161.7, 148.4, 146.8, 138.1, 56.8, 55.0, 29.1, 29.0, 26.5, 26.0, 25.3, 25.0.

MS (EI): *m*/*z* (relative intensity) 320 (1), 304 (9), 303 (16), 239 (62), 223 (26), 222 (18), 221 (20), 157 (100), 156 (21), 150 (42), 142 (12), 141 (37), 124 (10), 114 (12), 81 (20), 70 (10), 67 (11), 55 (33), 41 (23).

HRMS (ESI-TOF, *m*/*z*): calcd. for $C_{16}H_{24}N_4O_3$ [M+Na^+] 343.1740; found 343.1734.

IR (ATR, neat, cm^{-1}): 3189(w), 2926(m), 2854(w), 1727(w), 1667(m), 1623(s), 1496(s), 1453(m), 1424(m), 1401(m), 1373(m), 1340(m), 1282(m), 1254(m), 1222(s), 1178(s), 1121(s), 1058(m), 1017(m), 996(m), 944(w), 895(m), 880(w), 822(w), 804(m), 770(s), 754(m), 708(m), 685(m), 648(m), 604(m), 591(s), 576(s), 494(w), 463(s), 421(m).

Synthesis of 1,3,7,9-tetracyclohexyl-2,4,6,8-tetraoxo-1,2,3,4,6,7,8,9-octahydropyrimido[5,4-g]pteridine 5-oxide, CyPPTNO (2e)

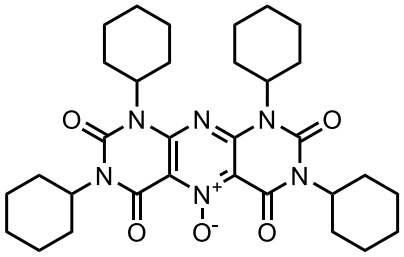

1e (800 mg, 2.50 mmol), glacial acetic acid (16 ml) and lead tetraacetate (1.22g, 2.75 mmol) were stirred for 2h at room temperature. Glycerol (0.8 ml) was added to complex unreacted lead tetraacetate and the mixture was stirred for additional 10 min. The reaction mixture was poured into water and extracted with DCM. The crude product was washed with minimal amount of EtOAc in an ultrasonic bath and **2e** was obtained a yellow solid (294 mg, 0.50 mmol, 40%).

m.p. = 258–261°C.

^{1}H NMR (300 MHz, $CDCl_3$) δ 5.13 (t, *J* = 11.4 Hz, 2H), 4.79 (t, *J* = 11.9 Hz, 2H), 2.60 – 2.26 (m, 8H), 2.02 – 1.51 (m, 20H), 1.50 – 1.14 (m, 12H).

^{13}C NMR (75 MHz, $CDCl_3$) δ 153.7, 151.4, 148.8, 119.8, 57.4, 55.5, 29.1, 28.6, 26.7, 26.3, 25.2, 25.2.

HRMS (ESI-TOF, *m*/*z*): calcd. for $C_{32}H_{44}N_6O_5$ [M^+] 593.3452; found 593.3455.

IR (ATR, neat, cm^{-1}): 2930(w), 2852(w), 1711(m), 1671(s), 1580(m), 1543(s), 1506(m), 1468(w), 1453(m), 1415(m), 1393(m), 1356(m), 1343(m), 1319(s), 1252(m), 1232(m), 1220(m), 1179(w), 1138(w), 1120(w), 1058(w), 1022(w), 993(w), 896(m), 872(w), 842(w), 793(m), 759(m), 726(w), 691(w), 667(w), 645(w), 596(m), 582(m), 528(w), 493(w), 459(m).

6.21 Oxidative decarboxylation of Boc-proline

To a preheated microwave vessel under argon, Boc-proline (108 mg, 0.5 mmol), PPTNO (1 mol%), and K_2HPO_4 (87 mg, 0.5 mmol) were added. The solids were evacuated for 5 min. Then O_2 sat. CH_3CN (5 ml) was added and the suspension was stirred. While stirring the solution was flushed once using an O_2 filled balloon. Then a freshly O_2 filled balloon was added. The mixture was irradiated for 20 h using 4 UVA lamps. The mixture was then transferred to a roundbottom flask using EtOAc. All volatiles were removed under reduced pressure and the residue was purified by column chromatography (DCM/Acetone = 50:1). The oxidation products were obtained as a mixture containing the aminal, amide and N-BOC-pyrroline and analyzed by NMR spectroscopy and GC/MS. The yields are determined assuming a molar mass of 185.22 g/mol.

The results are shown in Table 6 and discussed in chapter 3.7.

Synthesis of 1,3,7,9-tetra-*n*-butyl-4,6-dithioxo-4,6,7,9-tetrahydropyrimido[5,4-g]pteridine-2,8(1H,3H)-dione, (5g)

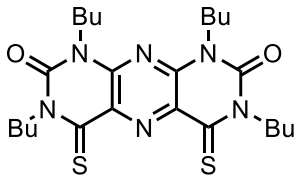

BuPPTNO (236 mg, 0.5 mmol) and Lawessons reagent (890 mg, 2.2 mmol) were added to a 25 ml Schlenk finger. While stirring toluene (5 ml) was added while rinsing the walls of the flask. The flask was equipped with a septum and the solution heated to 110 °C for 90 min. After cooling to room temperature the toluene was evaporated under reduced pressure and the residue dissolved in a little amount of DCM. This solution was directly transfered to a column and purified by chromatography (*n*-pentane:DCM 9:1 -> DCM). The product **5g** was obtained as an dark red solid (163 mg, 0.32 mmol, 65%). Crystals suitable for X-Ray analysis could be obtained by recrystallization from dry acetone.

R_f = 0.8 (DCM, not stainable by $KMnO_4$ or CAN, weak absorption under UV, red colored spot on TLC).

m.p. = 156–159°C.

^{1}H NMR (400 MHz, $CDCl_3$) δ 4.74 – 4.46 (m, 1H), 4.35 – 4.18 (m, 1H), 1.89 – 1.67 (m, 2H), 1.43 (tq, *J* = 14.9, 7.4 Hz, 2H), 0.98 (dt, *J* = 15.0, 7.4 Hz, 3H).

^{13}C NMR (101 MHz, $CDCl_3$) δ 186.1, 148.0, 145.7, 129.0, 48.8, 43.8, 29.8, 28.1, 20.4, 20.2, 13.9, 13.9.

HRMS (ESI-TOF, *m*/*z*): calcd. for $C_{24}H_{36}N_6O_2S_2$ [M+H^+] 505.2419; found 505.2418.

IR (ATR, neat, cm^{-1}): 2958(w), 2933(w), 2873(w), 1698(s), 1547(s), 1525(m), 1461(m), 1432(m), 1402(s), 1377(s), 1363(m), 1333(m), 1295(s), 1249(s), 1199(m), 1130(m), 1106(s), 1067(m), 1052(m), 1036(w), 1007(w), 945(w), 931(w), 907(w), 865(w), 810(w), 799(w), 745(m), 710(w), 677(m), 634(w), 622(w), 613(w), 543(w), 515(s), 488(w), 472(m), 432(w).

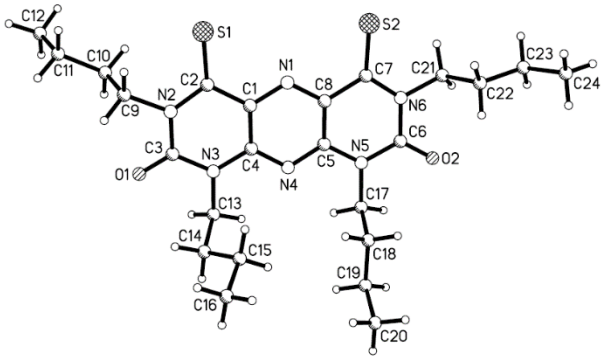

Table 20. Crystallographic Details

Empirical formula	$C_{24}H_{36}N_6O_2S_2$	
Formula weight	504.71	
Temperature	150(2) K	
Wavelength	0.71073 Å	
Crystal system	monoclinic	
Space group	$P2_1/c$	
Unit cell dimensions	a = 13.5983(8) Å	α= 90°.
	b = 9.4768(6) Å	β= 101.6668(12)°.
	c = 20.6279(13) Å	γ = 90°.
Volume	2603.4(3) $Å^3$	
Z	4	
Density (calculated)	1.288 g/cm^3	

Absorption coefficient	0.24 mm^{-1}
Reflections collected	63042
Independent reflections	6283 (R_{int} = 0.026)
Data / restraints / parameters	6283 / 0 / 311
Goodness-of-fit on F^2	1.04
Final R indices [$I>2\sigma(I)$]	R_1 = 0.032, wR_2 = 0.086
R indices (all data)	R_1 = 0.038, wR_2 = 0.091
Largest diff. peak and hole	0.36 and -0.23 e/$Å^3$

Synthesis of 6-amino-1,3-di-*n*-butyl-2-thioxo-2,3-dihydropyrimidin-4(1H)-one (8g)

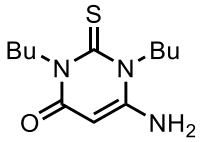

N,*N*'-Di-*n*-butylthiourea (7.53 g, 40.0 mmol) and cyanoacetic acid (3.91 g, 46.0 mmol) were added to a preheated 100 mL schlenk roundbottom flask under argon. The solids were evacuated for 5 minutes then flushed with argon. Acetic anhydride (16 ml) was added and the suspension stirred. The mixture turned homogeneous and yellow/orange over time. After 24 h solution was put in an ice bath. Then MeOH (20 ml) was added followed by the slow addition of aq. KOH (30 ml, 6M). The solution was stirred for 60 min at 0°C and then transferred to a separatory funnel filled with water and DCM. The organic phase was extracted once using 10% KOH and twice using dest. water. All volatiles were evaporated on the rotational evaporator. The crude product of **8g** was purified by column chromatography (DCM -> DCM:EtOAc = 3:1). A yellow analytically pure solid was obtained (6.77g, 26.5 mmol, 66%).

An optically clean product could be obtained by further purification. The yellow product was refluxed with cyclohexane (50 ml) and iPrOH (5 ml) then, when the solution is homogeneous, water (15 ml) is added quickly and the biphasic mixture is allowed to cool to room temperature. The precipitate was filtered of and washed 3 times with cyclohexane. **8g** is then dried on air over night and is obtained as white crystals suitable for X-Ray analysis.

R_f = 0.4 (DCM, UV).

m.p. = 127–129°C.

^{1}H NMR (300 MHz, DMSO-d_6) δ 7.01 (s, 2H), 4.98 (s, 1H), 4.37 – 4.16 (br, 4H), 1.66 – 1.48 (m, 4H), 1.39 – 1.18 (m, 4H), 0.88 (td, *J* = 7.3, 6.3 Hz, 6H).

^{13}C NMR (75 MHz, DMSO-d_6) δ 176.5, 159.1, 154.3, 79.8, 48.4, 46.8, 28.2, 28.2, 19.8, 19.2, 13.8, 13.8.

MS (EI): *m*/*z* (relative intensity) 255 (14) 199 (12), 198 (67), 182 (11), 166 (74), 157 (11), 144 (20), 143 (100), 127 (17), 115 (23), 111 (11), 110 (23), 97 (22), 86 (12), 85 (21), 84 (10), 72 (28), 70 (13), 69 (12), 68 (75), 60 (13), 57 (26), 56 (15), 55 (48), 44 (13), 43 (22), 42 (22), 41 (79), 39 (19), 30 (41), 29 (66).

HRMS (ESI-TOF, *m*/*z*): calcd. for $C_{12}H_{21}N_3O_1S_1$ [M^+] 255.1400; found 255.1406.

IR (ATR, neat, cm^{-1}): 3425(w), 3368(w), 3273(w), 3094(w), 2955(w), 2930(w), 2870(w), 1666(m), 1620(s), 1482(s), 1460(s), 1393(m), 1377(m), 1357(s), 1314(w), 1290(m), 1280(s), 1248(w), 1206(s), 1120(s), 1009(w), 957(w), 904(w), 872(w), 790(s), 729(m), 714(m), 695(m), 636(m), 591(m), 531(m), 481(s), 441(s).

Synthesis of 6-amino-1,3-di-*n*-butylpyrimidine-2,4(1H,3H)-dithione (8f)

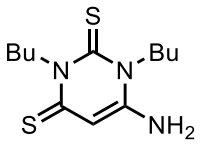

Lawessons reagent (2.09 g, 5.17 mmol) and **8g** (0.60 g, 2.35 mmol) were added to a preheated 25 ml Schlenk finger under argon. The solids were evacuated for 5min and then flushed with argon. While stirring toluene (24 ml) was added quickly. The mixture was heated to 110 °C for 16 h. After the indicated time all volatiles were removed under reduced pressure and the residue purified by twofold column chromatography (DCM -> DCM EtOAc = 10:1) and **8f** was obtained as off white solid (426 mg, 1.57 mmol, 67%).

R_f = 0.6 (DCM:EtOAc = 3:1).

m.p. = 178–180°C.

^{1}H NMR (400 MHz, DMSO-d_6) δ 7.58 (s, 2H), 6.20 (s, 1H), 5.61 – 3.68 (br, 4H), 1.78 – 1.51 (m, 4H), 1.31 (dq, *J* = 17.3, 7.5 Hz, 4H), 0.90 (td, *J* = 7.4, 3.2 Hz, 6H).

^{13}C NMR (101 MHz, DMSO-d_6) δ 179.0, 174.5, 148.8, 98.4, 53.6, 49.3, 39.9, 39.7, 39.5, 39.3, 39.1, 27.3, 27.0, 19.5, 19.2, 13.7. One carbon is not found, probably accompanying the signal at 13.7 ppm.

MS (EI): *m*/*z* (relative intensity) 271 (9), 215 (12), 214 (100), 182 (20), 159 (27), 126 (16), 86 (10), 84 (34), 72 (13), 67 (11), 57 (13), 55 (18), 41 (32), 39 (11), 30 (14), 29 (39).

HRMS (EI, *m*/*z*): calcd. for $C_{12}H_{21}N_3S_2$ [M^+] 271.1174; found 271.1174.

IR (ATR, neat, cm^{-1}): 3326(w), 3032(w), 2957(m), 2930(w), 2860(w), 1637(s), 1581(s), 1488(s), 1435(m), 1419(m), 1371(m), 1356(s), 1295(w), 1277(m), 1247(w), 1211(m),

1186(m), 1165(w), 1121(m), 1083(m), 1045(s), 975(w), 942(m), 892(m), 831(m), 804(m), 728(m), 702(m), 645(w), 606(w), 588(w), 550(w), 493(m), 460(m), 418(m).

Synthesis of 6-amino-1,3-di-*n*-butyl-5-nitroso-2-thioxo-2,3-dihydropyrimidin-4(1H)-one (1g)

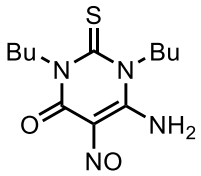

8g (515 mg, 2.01 mmol) and sodium nitrite (276 mg, 4.00 mmol) were suspended in HFIP (20 ml) at room temperature. Acetic acid was added dropwise (0.2 ml). The colorless suspension turns orange and later dark red. After 1h the solution was added to a separatory funnel filled with water/ice mixture and EtOAc, the color changes to purple. The organic layer was extracted 3 times using dest. water. The organic layer was dried over sodium sulfate and then all volatiles were evaporated under reduced pressure. The obtained purple solid was recrystallized from *i*PrOH. The product **1g** was obtained as purple amorph solid (456 mg, 1.60 mmol, 79%).

m.p. = 209–211°C.

^{1}H NMR (400 MHz, DMSO-d_6) δ 13.11 (s, 1H), 9.10 (s, 1H), 5.41 – 3.73 (m, 4H), 1.61 (dq, *J* = 45.1, 7.9 Hz, 4H), 1.34 (hept, *J* = 7.6 Hz, 4H), 0.91 (dt, *J* = 13.0, 7.3 Hz, 6H).

^{13}C NMR (101 MHz, DMSO-d_6) δ 177.5, 157.8, 143.2, 139.8, 47.5, 47.3, 28.1, 27.4, 19.7, 19.0, 13.7, 13.7.

HRMS (ESI-TOF, *m/z*): calcd. for $C_{12}H_{20}N_4O_2S_1$ [M+H$^+$] 285.1385; found 285.1391.

IR (ATR, neat, cm^{-1}): 3107(w), 2958(w), 2932(w), 2871(w), 1689(m), 1635(m), 1571(w), 1495(s), 1464(m), 1428(m), 1395(m), 1362(s), 1290(m), 1234(s), 1202(s), 1139(s), 1110(s), 1044(m), 944(m), 898(m), 872(m), 820(m), 750(m), 724(s), 698(m), 661(m), 651(m), 638(m), 621(m), 572(m), 541(m), 523(m), 453(m), 431(m).

Synthesis of 1,3,7,9-tetra-*n*-butyl-4,6-dioxo-2,8-dithioxo-1,2,3,4,6,7,8,9-octahydropyrimido[5,4-g]pteridine 5-oxide, (2g)

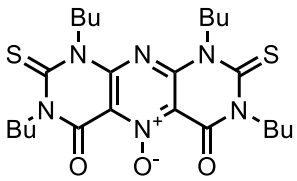

Method A: 1g (150 mg, 0.53 mmol) was dissolved in HFIP (5 ml) and $Pb(OAc)_4$ (296 mg, 0.67 mmol) added in one portion. The mixture was stirred at room temperature overnight. The solution was then transferred to a separatory funnel filled with EtOAc and water. The

organic layer was washed 3 times using water. Subsequently the organic layer was dried over sodium sulfate and all volatile compounds were evaporated under reduced pressure. The residue was dissolved in acetone and then slowly water was added until no precipitation is visible anymore. The solution was placed in a fridge and then filtered. The yellow solid was washed using water and then pentane. The product **2g** is obtained as yellow solid (43 mg, 0.08 mmol, 30%).

Method B: 1g (284 mg, 1.00 mmol) was suspended in AcOH (8 ml). PIDA (387 mg, 1.20 mmol) dissolved in AcOH (2 ml) was then added dropwise. The solution was stirred for 16 h and then water (5 ml) was added. The solution was transferred to a separatory funnel with sat. $NaHCO_3$ and EtOAc. The organic layer was washed 3 times using sat. $NaHCO_3$ solution. The organic layer was dried over sodium sulfate and all volatile compounds were evaporated under reduced pressure. The residue was dissolved in acetone (40 ml) and then slowly water (~20 ml) was added until no precipitation is visible anymore. The solution was placed in a fridge for 30 min and then filtered. The yellow solid was washed using water (2 x 10 ml) and then pentane (3 x 10 ml). The product **2g** was obtained as a yellow solid (44 mg, 0.08 mmol, 16 %).

R_f = 0.3 (DCM, p-anisaldehyde).

m.p. = 179–182°C.

^{1}H NMR (300 MHz, $CDCl_3$) δ 4.82 (s, 1H), 4.51 – 4.34 (m, 1H), 1.86 – 1.57 (m, 2H), 1.51 – 1.31 (m, 2H), 0.96 (td, *J* = 7.3, 5.0 Hz, 3H).

^{13}C NMR (75 MHz, $CDCl_3$) δ 239.9, 214.5, 214.3, 185.1, 113.5, 111.7, 92.1, 91.6, 83.5, 83.5, 77.2, 77.1.

HRMS (EI, *m/z*): calcd. for $C_{24}H_{36}N_6O_3S_2$ [M^+] 520.2285; found 520.2285.

IR (ATR, neat, cm^{-1}): 2956(m), 2932(w), 2870(w), 1696(s), 1674(s), 1587(m), 1538(s), 1504(m), 1465(m), 1421(s), 1386(s), 1360(s), 1313(s), 1282(s), 1244(s), 1219(m), 1203(s), 1127(s), 1071(m), 970(w), 937(w), 844(w), 809(w), 794(s), 755(m), 727(w), 679(w), 644(w), 618(w), 603(w), 565(m), 547(w), 520(m), 493(w), 433(m).

6.22 Photocatalytic hydroamination of stilbenes using monosubstituted amines

Synthesis of *N*-(1,2-diphenylethyl)butan-1-amine (29a)

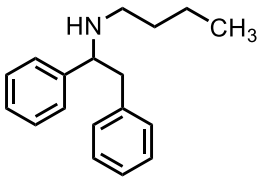

Compound **29a** was prepared following general procedure A. Purification by column chromatography (*n*-pentane:EtOAc = 20:1) yielded the title compound **29a** (63 mg, 0.25 mmol, 50%) as yellow oil.

R_f = 0.4 (*n*-pentane:EtOAc = 9:1, $KMnO_4$).

^{1}H NMR (300 MHz, $CDCl_3$) δ 7.22 (d, *J* = 4.3 Hz, 4H), 7.18 – 7.08 (m, 4H), 7.07 – 7.01 (m, 2H), 3.75 (dd, *J* = 8.0, 6.0 Hz, 1H), 2.93 – 2.72 (m, 2H), 2.41 – 2.15 (m, 2H), 1.39 (s, 1H), 1.33 – 1.19 (m, 2H), 1.19 – 1.01 (m, 2H), 0.72 (t, *J* = 7.2 Hz, 3H).

^{13}C NMR (75 MHz, $CDCl_3$) δ 144.1, 139.1, 129.4, 128.4, 128.4, 127.4, 127.1, 126.4, 65.0, 47.6, 45.5, 32.3, 20.4, 14.0.

MS (EI): *m*/*z* (relative intensity) 252 (1), 163 (12), 162 (100), 106 (17), 91 (10).

HRMS (ESI-TOF, *m*/*z*): calcd. for $C_{18}H_{23}N$ [M^+] 254.1908; found 254.1911.

IR (ATR, neat, cm^{-1}): 3062(w), 3028(w), 2956(w), 2928(w), 2869(w), 2795(w), 2727(w), 2565(w), 2461(w), 1721(w), 1674(w), 1601(w), 1585(w), 1494(w), 1454(m), 1377(w), 1314(w), 1244(w), 1212(w), 1141(w), 1127(w), 1072(w), 1028(w), 1001(w), 984(w), 922(w), 879(w), 839(w), 793(w), 770(w), 758(m), 739(m), 697(s), 613(w), 563(w), 507(w), 473(w), 447(w).

Synthesis of *N*-(1,2-diphenylethyl)-2-methylpropan-1-amine (29b)

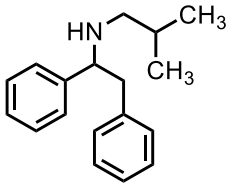

Compound **29b** was prepared following general procedure A. Purification by column chromatography (*n*-pentane:EtOAc = 20:1) yielded the title compound **29b** (80 mg, 0.32 mmol, 63%) as colorless oil.

R_f = 0.5 (*n*-pentane:EtOAc = 9:1, $KMnO_4$).

^{1}H NMR (400 MHz, $CDCl_3$) δ 7.26 – 7.08 (m, 8H), 7.08 – 7.02 (m, 2H), 3.72 (dd, *J* = 8.5, 5.6 Hz, 1H), 2.92 – 2.68 (m, 2H), 2.10 (d, *J* = 6.8 Hz, 2H), 1.53 (dp, *J* = 13.4, 6.7 Hz, 1H), 1.34 (s, 1H), 0.67 (t, *J* = 6.5 Hz, 6H).

^{13}C NMR (101 MHz, $CDCl_3$) δ 144.3, 139.2, 129.4, 128.4, 128.3, 127.4, 127.0, 126.4, 64.9, 55.9, 45.6, 28.3, 20.7.

MS (EI): *m*/*z* (relative intensity) 252 (1), 181 (13), 163 (12), 162 (100), 106 (29).

HRMS (ESI-TOF, *m*/*z*): calcd. for $C_{18}H_{23}N$ [$M+H^+$] 254.1908; found 254.1909.

IR (ATR, neat, cm^{-1}): 3084(w), 3062(w), 3026(w), 2952(w), 2869(w), 2800(w), 1946(w), 1877(w), 1806(w), 1602(w), 1585(w), 1493(w), 1453(m), 1386(w), 1364(w), 1307(w), 1240(w), 1213(w), 1179(w), 1144(w), 1115(w), 1070(w), 1050(w), 1028(w), 962(w), 912(w), 794(w), 756(m), 741(m), 696(s), 626(w), 556(m), 515(w), 482(w), 461(w).

Synthesis of *N*-(1,2-diphenylethyl)-2-methylpropan-2-amine (29c)

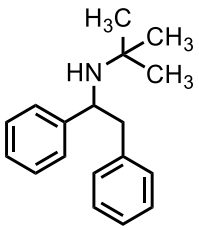

Compound **29c** was prepared following general procedure A. Purification by column chromatography (*n*-pentane:EtOAc = 20:1) yielded the title compound **29c** (68 mg, 0.27 mmol, 54%) as colorless oil.

$\mathbf{R_f}$ = 0.5 (*n*-pentane:EtOAc = 9:1, $KMnO_4$).

^{1}H NMR (400 MHz, $CDCl_3$) δ 7.34 – 7.27 (m, 2H), 7.23 – 7.14 (m, 4H), 7.14 – 7.08 (m, 2H), 7.08 – 7.03 (m, 2H), 3.90 (dd, *J* = 8.9, 5.5 Hz, 1H), 2.84 (dd, *J* = 13.5, 5.5 Hz, 1H), 2.63 (dd, *J* = 13.5, 8.9 Hz, 1H), 0.75 (s, 9H).

^{13}C NMR (101 MHz, $CDCl_3$) δ 147.6, 139.3, 129.3, 128.3, 128.1, 127.1, 126.5, 126.3, 59.3, 51.1, 47.2, 29.9.

MS (EI): *m*/*z* (relative intensity) 181 (10), 162 (58), 106 (100), 91 (11), 79 (11).

HRMS (ESI-TOF, *m*/*z*): calcd. for $C_{18}H_{23}N$ [$M+H^+$] 254.1908; found 254.1913.

IR (ATR, neat, cm^{-1}): 3084(w), 3062(w), 3026(w), 2958(w), 2861(w), 1602(w), 1585(w), 1493(w), 1453(m), 1388(w), 1364(w), 1306(w), 1227(m), 1213(w), 1155(w), 1096(w), 1069(w), 1027(w), 1004(w), 960(w), 910(w), 844(w), 799(w), 756(s), 697(s), 625(w), 600(w), 566(m), 555(m), 506(w), 491(w), 476(w), 445(w).

Synthesis of *N*-(1,2-diphenylethyl)cyclohexanamine (29d)

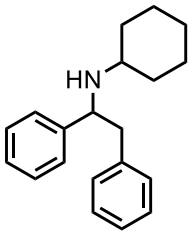

Compound **29d** was prepared following general procedure A. Purification by column chromatography (*n*-pentane:EtOAc = 20:1) yielded the title compound **29d** (73 mg, 0.25 mmol, 50%) as yellow oil.

R_f = 0.2 (*n*-pentane:EtOAc = 9:1, $KMnO_4$).

m.p. = 53–55°C.

^{1}H NMR (300 MHz, $CDCl_3$) δ 7.31 – 7.15 (m, 8H), 7.08 (ddt, *J* = 7.3, 1.5, 0.7 Hz, 2H), 4.02 (dd, *J* = 8.1, 6.0 Hz, 1H), 2.95 – 2.75 (m, 2H), 2.19 (tt, *J* = 10.0, 3.7 Hz, 1H), 1.82 (d, *J* = 12.4 Hz, 1H), 1.69 – 1.39 (m, 4H), 1.30 – 1.18 (m, 1H), 1.14 – 0.92 (m, 4H), 0.87 – 0.69 (m, 1H).

^{13}C NMR (75 MHz, $CDCl_3$) δ 144.7, 139.2, 129.4, 128.4, 128.3, 127.4, 126.9, 126.4, 61.3, 53.6, 45.8, 34.9, 32.8, 26.2, 25.3, 24.9.

MS (EI): *m*/*z* (relative intensity) 188 (100), 106 (67), 103 (11), 91 (50), 79 (14), 77 (13), 65 (10), 55 (15), 41 (13).

HRMS (ESI-TOF, *m*/*z*): calcd. for $C_{20}H_{25}N$ [M^+] 280.2065; found 280.2066.

IR (ATR, neat, cm^{-1}): 3083(w), 3061(w), 3026(w), 2922(m), 2850(w), 1602(w), 1584(w), 1493(w), 1451(m), 1359(w), 1345(w), 1307(w), 1259(w), 1181(w), 1143(w), 1120(w), 1070(w), 1028(w), 976(w), 911(w), 889(w), 846(w), 804(w), 779(w), 756(m), 696(s), 624(w), 565(m), 532(m), 500(w), 464(w), 417(w).

Synthesis of *N*-(1,2-diphenylethyl)adamantan-1-amine (29e)

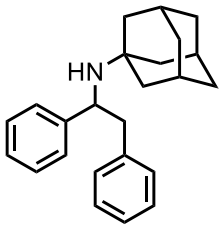

Compound **29e** was prepared following general procedure A. Purification by column chromatography (*n*-pentane:EtOAc = 20:1) yielded the title compound **29e** (99 mg, 0.30 mmol, 60%) as colorless solid.

R_f = 0.3 (*n*-pentane:EtOAc = 20:1, $KMnO_4$).

m.p. = 95–97°C.

^{1}H NMR (300 MHz, $CDCl_3$) δ 7.38 – 7.26 (m, 2H), 7.25 – 6.99 (m, 8H), 4.05 (dd, *J* = 8.8, 5.5 Hz, 1H), 2.83 (dd, *J* = 13.5, 5.5 Hz, 1H), 2.62 (dd, *J* = 13.5, 8.8 Hz, 1H), 1.81 (p, *J* = 3.3 Hz, 3H), 1.53 – 1.29 (m, 9H), 1.23 – 1.03 (m, 4H).

^{13}C NMR (75 MHz, $CDCl_3$) δ 147.9, 139.4, 129.4, 128.4, 128.1, 127.2, 126.5, 126.4, 57.2, 51.4, 47.4, 43.7, 36.7, 29.7.

MS (EI): *m*/*z* (relative intensity) 240 (21), 135 (21), 91 (100), 65 (13).

HRMS (ESI-TOF, *m*/*z*): calcd. for $C_{24}H_{29}N$ [$M+H^+$] 332.2378; found 332.2379.

IR (ATR, neat, cm^{-1}): 3082(w), 3061(w), 3025(w), 2898(w), 2844(w), 2655(w), 1947(w), 1875(w), 1601(w), 1493(w), 1474(w), 1452(m), 1356(w), 1343(w), 1307(w), 1289(w), 1268(w), 1211(w), 1184(w), 1137(m), 1097(m), 1065(w), 1027(w), 975(w), 948(w), 935(w), 910(w), 886(w), 848(w), 817(w), 801(w), 776(w), 755(s), 739(m), 697(s), 642(w), 621(w), 609(w), 565(m), 529(m), 496(w), 457(w), 439(w).

Synthesis of *N*-benzyl-1,2-diphenylethan-1-amine (29f)

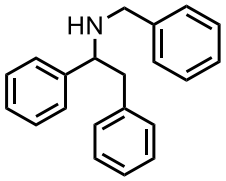

Compound **29f** was prepared following general procedure A. Purification by column chromatography (*n*-pentane:EtOAc = 20:1) yielded the title compound **29f** (95 mg, 0.33 mmol, 66%) as a colorless solid.

$\mathbf{R_f}$ = 0.3 (*n*-pentane:EtOAc = 9:1, $KMnO_4$).

m.p. = 52–54 °C.

^{1}H NMR (400 MHz, $CDCl_3$) δ 7.29 – 7.19 (m, 4H), 7.19 – 7.06 (m, 7H), 7.00 (dt, J = 7.9, 1.4 Hz, 4H), 3.79 (dd, *J* = 8.5, 5.5 Hz, 1H), 3.56 (d, *J* = 13.5 Hz, 1H), 3.36 (d, *J* = 13.5 Hz, 1H), 2.97 – 2.70 (m, 2H), 1.64 (s, 1H).

^{13}C NMR (101 MHz, $CDCl_3$) δ 143.8, 140.6, 138.9, 129.4, 128.5, 128.5, 128.4, 128.0, 127.5, 127.2, 126.8, 126.5, 63.7, 51.5, 45.4.

MS (EI): *m*/*z* (relative intensity) 286 (1), 197 (15), 196 (100), 91 (87).

HRMS (EI, *m*/*z*): calcd. for $C_{21}H_{21}N$ [$M+H^+$] 288.1752; found 288.1759.

IR (ATR, neat, cm^{-1}): 2704(w), 1952(w), 1871(w), 1813(w), 1601(w), 1582(w), 1491(m), 1452(m), 1398(w), 1357(w), 1315(w), 1288(w), 1269(w), 1227(w), 1195(w), 1179(w), 1162(w), 1153(w), 1120(m), 1068(m), 1028(m), 1000(w), 988(w), 946(w), 911(w), 832(w), 820(w), 793(w), 758(m), 741(m), 728(s), 695(s), 635(m), 619(w), 579(w), 547(s), 506(m), 460(m).

Synthesis of 1,2-diphenyl-*N*-(4-(trifluoromethyl)benzyl)ethan-1-amine (29g)

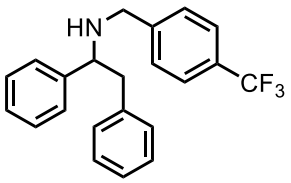

Compound **29g** was prepared following general procedure A. Purification by column chromatography (*n*-pentane:EtOAc = 20:1) yielded the title compound **29g** (109 mg, 0.31 mmol, 62%) as a colorless oil.

R_f = 0.5 (*n*-pentane:EtOAc = 9:1, $KMnO_4$).

^{1}H NMR (300 MHz, $CDCl_3$) δ 7.38 (d, *J* = 8.0 Hz, 2H), 7.30 – 7.05 (m, 10H), 7.05 – 6.86 (m, 2H), 3.75 (dd, *J* = 8.8, 5.3 Hz, 1H), 3.65 – 3.28 (m, 2H), 2.96 – 2.68 (m, 2H), 1.65 (s, 1H).

^{13}C NMR (75 MHz, $CDCl_3$) δ 144.6, 143.4, 138.8, 129.4, 129.3 (q, *J* = 22.7 Hz), 128.6, 128.6, 128.2, 127.5, 126.6, 125.3 (q, *J* = 3.8 Hz), 124.4 (q, *J* = 272.1 Hz), 63.8, 50.9, 45.4.

^{19}F NMR (282 MHz, $CDCl_3$) δ -62.30.

MS (EI): *m*/*z* (relative intensity) 354 (1), 265 (16), 264 (100), 159 (58).

HRMS (ESI-TOF, *m*/*z*): calcd. for $C_{22}H_{20}NF_3$ [M+H$^+$] 356.1626; found 356.1628.

IR (ATR, neat, cm^{-1}): 3062(w), 3027(w), 2920(w), 2843(w), 1807(w), 1618(w), 1602(w), 1585(w), 1494(w), 1454(m), 1417(w), 1322(s), 1161(m), 1118(s), 1065(s), 1028(w), 1017(m), 984(w), 948(w), 911(w), 887(w), 823(m), 795(w), 756(m), 742(m), 697(s), 643(w), 621(w), 593(w), 553(m), 516(m), 495(w).

Synthesis of N-(4-chlorobenzyl)-1,2-diphenylethan-1-amine (29h)

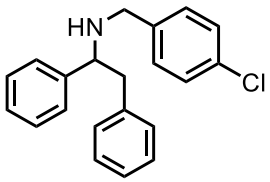

Compound **29h** was prepared following general procedure A. Purification by column chromatography (*n*-pentane:EtOAc = 20:1) yielded the title compound **29h** (101 mg, 0.31 mmol, 63%) as a colorless solid.

R_f = 0.4 (*n*-pentane:EtOAc = 9:1, $KMnO_4$).

m.p. = 70–72 °C.

^{1}H NMR (400 MHz, $CDCl_3$) δ 7.28 – 7.21 (m, 4H), 7.20 – 7.08 (m, 6H), 7.04 – 6.98 (m, 2H), 6.95 – 6.88 (m, 2H), 3.74 (dd, *J* = 8.8, 5.3 Hz, 1H), 3.58 – 3.45 (m, 1H), 3.32 (d, *J* = 13.8 Hz, 1H), 2.92 – 2.70 (m, 2H), 1.61 (s, 1H).

^{13}C NMR (101 MHz, $CDCl_3$) δ 143.6, 139.1, 138.8, 132.5, 129.4, 128.5, 128.5, 128.4, 127.4, 127.3, 126.5, 63.6, 50.7, 45.4.

MS (EI): *m*/*z* (relative intensity) 320 (1), 232 (33), 231 (15), 230 (99), 127 (32), 125 (100), 89 (10).

HRMS (ESI-TOF, *m*/*z*): calcd. for $C_{21}H_{20}NCl$ [M+H$^+$] 322.1362; found 322.1362.

IR (ATR, neat, cm^{-1}): 3311(w), 3083(w), 3062(w), 3027(w), 3005(w), 2929(w), 2910(w), 2873(w), 2847(w), 2796(w), 2702(w), 1601(w), 1572(w), 1488(w), 1453(w), 1438(w), 1400(w), 1356(w), 1317(w), 1286(w), 1266(w), 1229(w), 1209(w), 1191(w), 1177(w), 1160(w), 1120(m), 1090(m), 1070(m), 1029(w), 1014(m), 986(w), 941(w), 910(w), 831(w), 808(m), 789(m), 759(m), 741(m), 696(s), 674(m), 634(w), 612(m), 581(w), 556(s), 509(m), 482(s), 420(m).

Synthesis of *N*-(4-methylbenzyl)-1,2-diphenylethan-1-amine (29i)

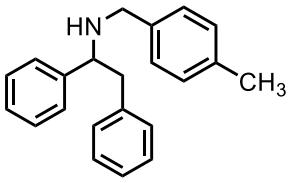

Compound **29i** was prepared following general procedure A. Purification by column chromatography (*n*-pentane:EtOAc = 20:1) yielded the title compound **29i** (80 mg, 0.27 mmol, 53%) as a colorless oil.

R$_f$ = 0.3 (*n*-pentane:EtOAc = 15:1, $KMnO_4$).

^{1}H NMR (300 MHz, $CDCl_3$) δ 7.30 – 7.20 (m, 4H), 7.20 – 7.06 (m, 4H), 7.04 – 6.86 (m, 6H), 3.80 (dd, *J* = 8.3, 5.7 Hz, 1H), 3.53 (d, *J* = 13.3 Hz, 1H), 3.34 (d, *J* = 13.4 Hz, 1H), 2.98 – 2.70 (m, 2H), 2.22 (s, 2H), 1.65 (s, 1H).

^{13}C NMR (75 MHz, $CDCl_3$) δ 143.9, 138.9, 137.5, 136.3, 129.4, 129.0, 128.5, 128.4, 128.0, 127.5, 127.2, 126.4, 63.7, 51.2, 45.4, 21.2.

MS (EI): *m*/*z* (relative intensity) 300 (1), 211 (13), 210 (80), 106 (12), 105 (100).

HRMS (ESI-TOF, *m*/*z*): calcd. for $C_{22}H_{23}N$ [M+H$^+$] 302.1909; found 302.1909.

IR (ATR, neat, cm^{-1}): 3324(w), 3083(w), 3060(w), 3025(w), 2919(w), 2849(w), 1947(w), 1894(w), 1804(w), 1602(w), 1584(w), 1514(w), 1494(w), 1452(m), 1355(w), 1307(w), 1198(w), 1179(w), 1155(w), 1106(w), 1070(w), 1027(w), 1001(w), 965(w), 911(w), 886(w), 844(w), 794(m), 755(m), 739(m), 696(s), 625(w), 578(w), 554(m), 537(m), 483(m).

Synthesis of *N*-(4-methoxybenzyl)-1,2-diphenylethan-1-amine (29j)

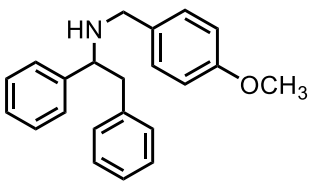

Compound **29j** was prepared following general procedure A. Purification by column chromatography (*n*-pentane:EtOAc = 20:1) yielded the title compound **29j** (59 mg, 0.19 mmol, 37%) as a colorless oil.

R_f = 0.2 (*n*-pentane:EtOAc = 9:1, $KMnO_4$).

^{1}H NMR (400 MHz, $CDCl_3$) δ 7.31 – 7.20 (m, 4H), 7.21 – 7.06 (m, 4H), 7.06 – 6.98 (m, 2H), 6.98 – 6.88 (m, 2H), 6.76 – 6.64 (m, 2H), 3.78 (ddd, *J* = 8.4, 5.5, 1.1 Hz, 1H), 3.68 (d, *J* = 0.7 Hz, 3H), 3.50 (dd, *J* = 13.2, 1.1 Hz, 1H), 3.31 (dd, *J* = 13.1, 1.2 Hz, 1H), 2.95 – 2.68 (m, 2H), 1.63 (s, 1H).

^{13}C NMR (101 MHz, $CDCl_3$) δ 158.5, 143.9, 138.9, 132.7, 129.4, 129.2, 128.5, 128.4, 127.5, 127.2, 126.4, 113.8, 63.6, 55.3, 50.8, 45.4.

MS (EI): *m*/*z* (relative intensity) 316 (1), 226 (38), 121 (100), 91 (7).

HRMS (EI, *m*/*z*): calcd. for $C_{22}H_{23}NO$ [M+H$^+$] 318.1858; found 318.1862.

IR (ATR, neat, cm^{-1}): 3327(w), 3060(w), 3026(w), 3001(w), 2916(w), 2833(w), 1963(w), 1882(w), 1810(w), 1610(w), 1584(w), 1510(s), 1494(m), 1453(m), 1355(w), 1300(w), 1243(s), 1200(w), 1173(m), 1104(m), 1070(w), 1032(m), 982(w), 913(w), 886(w), 820(m), 795(m), 754(s), 739(m), 697(s), 625(m), 581(m), 544(m), 516(m), 451(w).

Synthesis of *N*-(2-((tert-butyldimethylsilyl)oxy)ethyl)-1,2-diphenylethan-1-amine (29k)

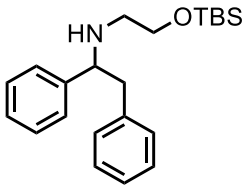

Compound **29k** was prepared following general procedure A. Purification by column chromatography (*n*-pentane:EtOAc = 20:1) yielded the title compound **29k** (70 mg, 0.20 mmol, 40%) as colorless solid.

R_f = 0.6 (*n*-pentane:EtOAc = 9:1, $KMnO_4$).

^{1}H NMR (300 MHz, $CDCl_3$) δ 7.28 – 7.05 (m, 10H), 3.81 (dd, *J* = 8.3, 5.6 Hz, 1H), 3.61 – 3.47 (m, 2H), 2.97 – 2.74 (m, 2H), 2.49 – 2.33 (m, 2H), 1.96 (s, 1H), 0.74 (d, *J* = 0.7 Hz, 9H), -0.08 – -0.16 (m, 6H).

^{13}C NMR (75 MHz, $CDCl_3$) δ 144.0, 138.9, 129.4, 128.5, 128.4, 127.5, 127.1, 126.5, 64.7, 62.4, 49.8, 45.6, 26.0, 18.3, -5.3.

MS (EI): *m*/*z* (relative intensity) 354 (1), 265 (36), 264 (100), 248 (14), 166 (10), 165 (10), 105 (13), 103 (14), 91 (25), 73 (21).

HRMS (EI, *m*/*z*): calcd. for $C_{22}H_{32}NOSi$ [M$^+$] 354.2239; found 354.2248.

IR (ATR, neat, cm^{-1}): 3084(w), 3062(w), 3027(w), 2952(w), 2927(w), 2855(w), 1602(w), 1494(w), 1462(w), 1453(m), 1388(w), 1360(w), 1309(w), 1253(m), 1226(w), 1085(m), 1020(w), 1006(w), 957(w), 939(w), 888(w), 832(s), 811(m), 775(s), 756(s), 697(s), 662(m), 629(w), 568(w), 548(w), 512(w), 450(w).

Synthesis of *N*-(1,2-diphenylethyl)prop-2-en-1-amine (29l)

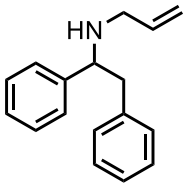

Compound **29l** was prepared following general procedure A. Purification by column chromatography (*n*-pentane:EtOAc = 20:1) yielded the title compound **29l** (40 mg, 169 mmol, 34%) as colorless oil.

R_f = 0.4 (*n*-pentane:EtOAc = 9:1, $KMnO_4$).

^{1}H NMR (300 MHz, $CDCl_3$) δ 7.28 – 7.09 (m, 8H), 7.08 – 7.01 (m, 2H), 5.68 (dddd, *J* = 17.6, 9.7, 6.6, 5.3 Hz, 1H), 5.00 – 4.86 (m, 2H), 3.82 (dd, *J* = 8.0, 6.1 Hz, 1H), 3.01 (ddt, *J* = 14.3, 5.3, 1.6 Hz, 1H), 2.93 – 2.76 (m, 3H), 1.46 (s, 1H).

^{13}C NMR (75 MHz, $CDCl_3$) δ 143.7, 138.9, 136.9, 129.4, 128.5, 128.4, 127.5, 127.2, 126.5, 115.7, 64.0, 50.1, 45.3.

MS (EI): *m*/*z* (relative intensity) 236 (1), 147 (13), 146 (100), 91 (17), 41 (17).

HRMS (EI, *m*/*z*): calcd. for $C_{17}H_{18}N$ [M^+] 236.1430; found 236.1434.

IR (ATR, neat, cm^{-1}): 3062(w), 3026(w), 2977(w), 2918(w), 2845(w), 1948(w), 1879(w), 1808(w), 1642(w), 1602(w), 1584(w), 1494(w), 1453(m), 1417(w), 1355(w), 1328(w), 1308(w), 1229(w), 1208(w), 1180(w), 1141(w), 1109(w), 1070(w), 1028(w), 993(w), 914(m), 844(w), 794(w), 756(m), 742(m), 696(s), 625(w), 591(w), 562(m), 547(m), 503(w), 444(w).

Synthesis of methyl (1,2-diphenylethyl)-*L*-phenylalaninate (29m)

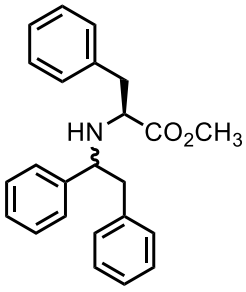

Compound **29m** was prepared following general procedure A. Purification by column chromatography (*n*-pentane:EtOAc = 20:1) yielded the diastereomers **29ma** (30 mg, 0.08 mmol, 17%) as a colorless oil and **29mb** (30 mg, 0.08 mmol, 17%) as a colorless solid.

29ma:

R_f = 0.3 (*n*-pentane:EtOAc = 15:1, $KMnO_4$).

^{1}H NMR (300 MHz, $CDCl_3$) δ 7.25 – 7.05 (m, 11H), 6.97 – 6.90 (m, 2H), 6.90 – 6.83 (m, 2H), 3.72 (dd, *J* = 7.6, 6.3 Hz, 1H), 3.33 (s, 4H), 2.93 – 2.65 (m, 4H), 1.92 (s, 1H).

^{13}C NMR (75 MHz, $CDCl_3$) δ 174.5, 143.1, 138.7, 137.2, 129.4, 129.2, 128.5, 128.4, 128.4, 127.7, 127.4, 126.6, 126.4, 63.8, 61.1, 51.6, 44.8, 38.8.

MS (EI): *m*/*z* (relative intensity) 358 (1), 269 (25), 268 (100), 208 (21), 181 (60, 166 (12), 165 (11), 117 (13), 103 (18), 91 (25), 77 (10).

HRMS (EI, *m*/*z*): calcd. for $C_{24}H_{24}NO_2$ [M^+] 358.1802; found 358.1801.

IR (ATR, neat, cm^{-1}): 3331(w), 3084(w), 3061(w), 3027(w), 2948(w), 2849(w), 1948(w), 1881(w), 1733(m), 1602(w), 1584(w), 1494(m), 1453(m), 1434(w), 1347(w), 1273(w), 1197(m), 1166(m), 1126(m), 1075(w), 1028(w), 981(w), 913(w), 844(w), 758(m), 743(m), 696(s), 620(w), 550(m), 518(w), 500(m).

$[\alpha]_D^{22}$ = +1.0° (c = 0.6, CH_3CN).

29mb:

R_f = 0.2 (n-pentane:EtOAc = 15:1, $KMnO_4$).

m.p. = 49–52°C.

^{1}H NMR (300 MHz, $CDCl_3$) δ 7.42 – 7.21 (m, 9H), 7.19 – 7.04 (m, 6H), 3.87 (dd, *J* = 8.2, 5.8 Hz, 1H), 3.57 (s, 3H), 3.31 (dd, *J* = 7.5, 6.4 Hz, 1H), 3.03 – 2.74 (m, 4H), 2.00 (d, *J* = 0.6 Hz, 1H).

^{13}C NMR (75 MHz, $CDCl_3$) δ 175.0, 142.8, 138.4, 137.5, 129.4, 129.4, 128.4, 128.3, 128.3, 127.6, 127.3, 126.6, 126.5, 62.7, 60.2, 51.5, 45.8, 40.2.

MS (EI): *m*/*z* (relative intensity) 358 (1), 269 (25), 268 (100), 208 (21), 181(51), 166 (12), 165 (11), 117 (13), 103 (18), 91 (24), 77 (11).

HRMS (EI, *m*/*z*): calcd. for $C_{24}H_{24}NO_2$ [M^+] 358.1802; found 358.1797.

IR (ATR, neat, cm^{-1}): 3318(w), 3082(w), 3060(w), 3026(w), 3002(w), 2948(w), 2920(w), 2850(w), 1731(w), 1602(w), 1584(w), 1492(w), 1477(w), 1452(m), 1434(w), 1344(w), 1333(w), 1307(w), 1276(m), 1229(w), 1189(m), 1161(s), 1124(m), 1091(w), 1072(w), 1026(w), 1004(w), 975(m), 937(w), 914(w), 895(w), 884(w), 842(w), 791(w), 751(s), 695(s), 625(w), 576(m), 556(m), 527(w), 495(m), 481(w), 450(w), 408(w).

$[\alpha]_D^{22}$ = -32.8° (c = 0.6, CH_3CN).

Synthesis of (*R*)-1,2-diphenyl-*N*-((*R*)-1-phenylethyl)ethan-1-amine (*R,R*-29n) and (*S*)-1,2-diphenyl-*N*-((*R*)-1-phenylethyl)ethan-1-amine (S,*R*-29n)

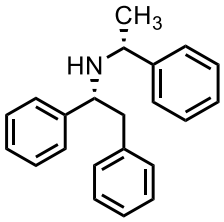
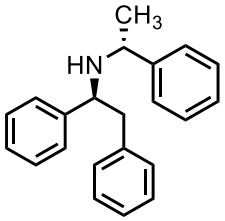

Compound **29n** was prepared following general procedure A. Purification by column chromatography (*n*-pentane:EtOAc = 20:1 (+0.1% NEt_3) yielded **(R,R)-29na** (54 mg, 0.18 mmol, 36%) as a colorless oil and **(S,R)-29nb** (48 mg, 0.16 mmol, 32%) as a colorless oil.

(*R*,*R*)-29n:

R_f = 0.23 (*n*-heptane:EtOAc = 10:1, $KMnO_4$).

^{1}H NMR (400 MHz, $CDCl_3$) δ 7.36 – 7.13 (m, 11H), 7.09 – 6.99 (m, 2H), 6.85 – 6.76 (m, 2H), 3.55 (dd, *J* = 9.2, 5.1 Hz, 1H), 3.45 (q, *J* = 6.7 Hz, 1H), 2.87 (dd, *J* = 13.6, 5.1 Hz, 1H), 2.78 (dd, *J* = 13.6, 9.3 Hz, 1H), 1.72 (s, 1H), 1.19 (d, *J* = 6.7 Hz, 3H).

^{13}C NMR (101 MHz, $CDCl_3$) δ 145.5, 144.3, 138.9, 129.4, 128.5, 128.4, 128.4, 127.5, 127.1, 126.7, 126.5, 126.4, 61.1, 55.0, 45.5, 25.0.

MS (EI): *m*/*z* (relative intensity) 302 (1), 210 (50), 106 (74), 105 (100), 104 (13), 103 (19), 91 (31), 79 (23), 77 (30), 65 (12).

HRMS (EI, *m*/*z*): calcd. for $C_{22}H_{23}N$ [M^+] 302.1909; found 302.1914.

IR (ATR, neat, cm^{-1}): 3082(w), 3061(w), 3025(w), 2959(w), 2922(w), 2850(w), 1962(w), 1947(w), 1875(w), 1807(w), 1743(w), 1601(w), 1584(w), 1492(m), 1466(w), 1452(m), 1368(w), 1306(w), 1271(w), 1200(w), 1180(w), 1155(w), 1132(w), 1109(w), 1069(w), 1028(w), 1016(w), 966(w), 942(w), 910(w), 844(w), 797(w), 758(s), 696(s), 628(w), 589(w), 573(w), 538(m), 518(w), 483(w), 439(w), 428(w), 410(w).

$[\alpha]_D^{24}$ = +64.4° (c = 0.3, CH_3CN).

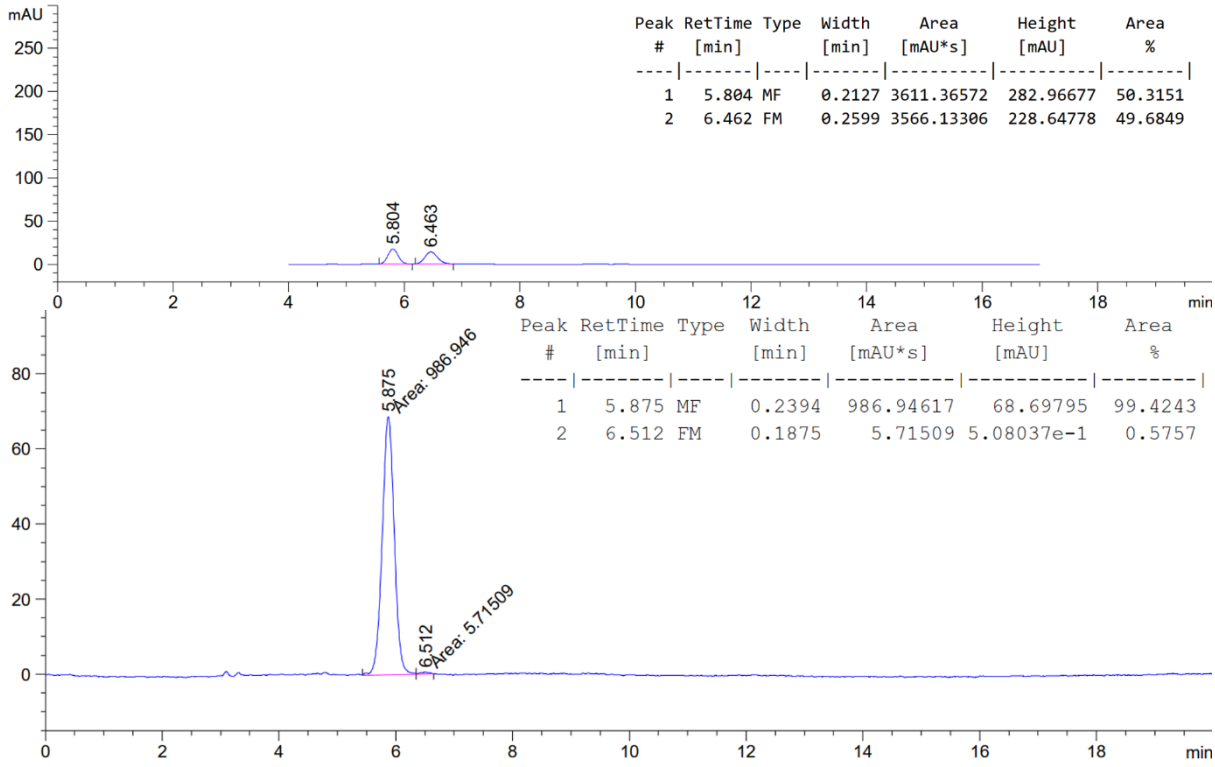

Figure 20. Chiral HPLC (ChiralCel, OJ-H, Heptan/EtOH 95:5, 1.0 mL/min flow rate, 210 nm): major enantiomer t_R = 5.9 min, minor enantiomer t_R = 6.5 min. Enantiomeric ratio: 99:1.

(S,*R*)-29n:

R_f = 0.20 (*n*-heptane:EtOAc = 10:1, $KMnO_4$).

^{1}H NMR (400 MHz, $CDCl_3$) δ 7.48 – 7.13 (m, 14H), 7.08 – 6.99 (m, 2H), 3.97 (t, *J* = 6.9 Hz, 1H), 3.72 (q, *J* = 6.5 Hz, 1H), 3.05 (dd, *J* = 13.3, 6.9 Hz, 1H), 2.94 (dd, *J* = 13.4, 6.9 Hz, 1H), 1.66 (s, 1H), 1.28 (d, *J* = 6.5 Hz, 4H).

^{13}C NMR (101 MHz, $CDCl_3$) δ 146.2, 143.9, 139.0, 129.5, 128.5, 128.3, 128.3, 127.4, 127.0, 126.9, 126.7, 126.2, 62.0, 55.0, 54.8, 44.6, 29.8, 22.4.

MS (EI): *m*/*z* (relative intensity) 211 (6), 210 (36), 106 (73), 105 (100), 104 (14), 103 (20), 91 (41), 79 (26), 78 (10), 77 (35), 65 (16), 51 (10).

HRMS (EI, *m*/*z*): calcd. for $C_{22}H_{23}N$ [M^+] 302.1909; found 302.1913.

IR (ATR, neat, cm^{-1}): 3083(w), 3060(w), 3025(w), 2963(w), 2922(w), 2852(w), 1947(w), 1875(w), 1806(w), 1741(w), 1601(w), 1584(w), 1544(w), 1492(m), 1464(w), 1452(m), 1369(w), 1327(w), 1305(w), 1204(w), 1179(w), 1154(w), 1125(w), 1070(w), 1027(w), 949(w), 911(w), 843(w), 782(w), 757(m), 695(s), 622(w), 609(w), 560(m), 548(m), 536(m), 515(m), 426(w).

$[\alpha]_D^{24}$ = +45.6° (c = 0.1, CH_3CN).

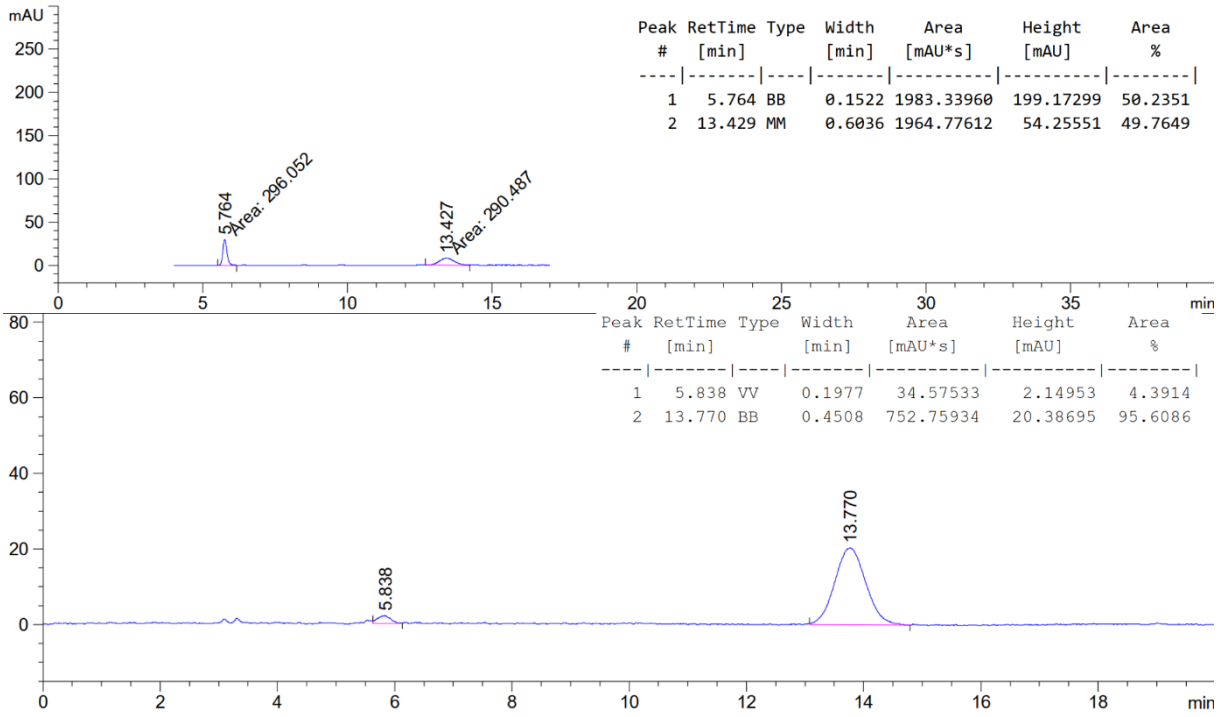

Figure 21. Chiral HPLC (ChiralCel, OJ-H, Heptan/EtOH = 95:5, 1.0 mL/min flow rate, 210 nm): minor enantiomer t_R = 5.8 min, major enantiomer t_R = 13.9 min. Enantiomeric ratio: 99:1

Synthesis of *N*-benzyl-1-(4-fluorophenyl)-2-(*p*-tolyl)ethan-1-amine (30ba) and *N*-benzyl-2-(4-fluorophenyl)-1-(*p*-tolyl)ethan-1-amine (30bb)

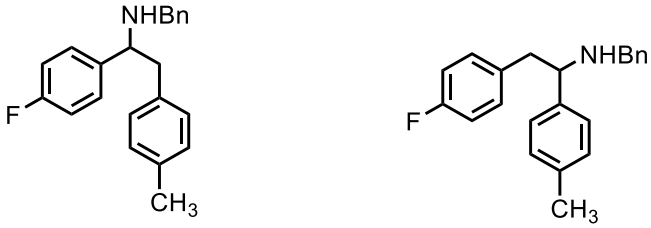

Compound **30b** was prepared following general procedure A. Purification by column chromatography (*n*-pentane:EtOAc = 20:1) yielded compound **30ba** (72 mg, 0.23 mmol, 46%) and compound **30bb** (45 mg, 0.14 mmol, 28%) as colorless oils.

30ba:

R_f = 0.3 (*n*-pentane:EtOAc = 20:1, $KMnO_4$).

^{1}H NMR (300 MHz, CD_3CN) δ 7.42 – 7.11 (m, 7H), 7.11 – 6.92 (m, 6H), 3.88 (t, *J* = 7.1 Hz, 1H), 3.59 (d, *J* = 13.4 Hz, 1H), 3.44 (d, *J* = 13.2 Hz, 1H), 3.03 – 2.74 (m, 2H), 2.28 (s, 3H), 2.04 – 1.67 (m, 1H).

^{13}C NMR (75 MHz, CD_3CN) δ 162.7 (d, *J* = 242.3 Hz), 141.8, 141.0 (d, *J* = 3.0 Hz), 136.6 (d, *J* = 12.5 Hz), 130.6, 130.1, 130.0, 129.8, 129.1, 128.9, 127.6, 115.7 (d, J = 21.2 Hz), 64.0, 51.9, 45.3, 21.2.

^{19}F NMR (282 MHz, CD_3CN) δ -114.58.

MS (EI): *m*/*z* (relative intensity) 318 (1), 215 (11), 214 (66), 105 (12), 91 (100), 65 (11).

HRMS (EI, *m*/*z*): calcd. for $C_{22}H_{21}NF$ [M^+] 318.1653; found 318.1651.

IR (ATR, neat, cm^{-1}): 3025(w), 2919(w), 2847(w), 1733(w), 1716(w), 1701(w), 1684(w), 1670(w), 1648(w), 1636(w), 1603(m), 1558(w), 1541(w), 1507(s), 1454(m), 1417(w), 1342(w), 1292(w), 1218(s), 1153(m), 1111(m), 1091(m), 1027(w), 1014(w), 976(w), 908(w), 833(s), 806(m), 781(m), 734(s), 697(s), 637(w), 619(w), 606(m), 546(s), 494(m), 478(m), 460(m).

30bb:

R_f = 0.2 (*n*-pentane:EtOAc = 20:1, $KMnO_4$).

^{1}H NMR (300 MHz, CD_3CN) δ 7.30 – 6.86 (m, 12H), 3.79 (t, *J* = 7.1 Hz, 1H), 3.63 – 3.49 (m, 1H), 3.42 (d, *J* = 13.5 Hz, 1H), 2.97 – 2.77 (m, 2H), 2.31 (s, 3H).

^{13}C NMR (75 MHz, CD_3CN) δ 162.3 (d, *J* = 241.6 Hz), 141.9, 141.7, 137.5, 136.4 (d, *J* = 3.2 Hz), 131.9 (d, *J* = 7.9 Hz), 129.8, 129.1, 128.9, 128.3, 127.6, 115.5 (d, *J* = 21.1 Hz), 64.3, 51.8, 44.6, 21.1.

^{19}F NMR (282 MHz, CD_3CN) δ -115.94.

MS (EI): *m*/*z* (relative intensity) 318 (1), 211 (10), 210 (58), 109 (17), 91 (100), 65 (12).

HRMS (EI, *m*/*z*): calcd. for $C_{22}H_{21}NF$ [M^+] 318.1653; found 318.1646.

IR (ATR, neat, cm^{-1}): 3026(w), 2920(w), 2852(w), 1601(w), 1508(s), 1453(m), 1415(w), 1348(w), 1305(w), 1220(s), 1177(w), 1157(m), 1096(m), 1028(w), 1018(w), 971(w), 908(w), 817(s), 782(m), 735(s), 720(m), 697(s), 642(w), 621(w), 607(w), 545(s), 531(m), 505(m), 472(m).

Synthesis of *N*-benzyl-1-(4-fluorophenyl)-2-phenylethan-1-amine (30ca) and *N*-benzyl-2-(4-fluorophenyl)-1-phenylethan-1-amine (30cb)

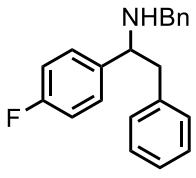

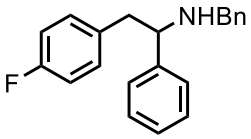

Compounds **30ca** and **30cb** were prepared following general procedure A with a reaction time of 16 h. Purification by column chromatography (*n*-pentane:EtOAc = 10:1) yielded the

title compounds (76 mg, 0.25 mmol, 50%, **30ca**:**30cb** = 61:39) as a colorless oil. Analytically pure samples were obtained by flash chromatography (*n*-pentane:EtOAc = 20:1). When the reaction was run for 24h the products (82 mg, 0.27 mmol, 54%, **30ca:30cb** = 61:39) were obtained as colorless oil.

30ca:

R_f = 0.4 (*n*-pentane:EtOAc = 5:1, $KMnO_4$).

^{1}H NMR (300 MHz, $CDCl_3$) δ 7.36 – 7.17 (m, 8H), 7.15 – 6.97 (m, 6H), 3.88 (t, *J* = 7.1 Hz, 1H), 3.65 (d, *J* = 13.5 Hz, 1H), 3.46 (d, *J* = 13.5 Hz, 1H), 3.00 – 2.83 (m, 2H), 1.98 (s, 1H).

^{13}C NMR (75 MHz, $CDCl_3$) δ 160.5 (d, *J* = 245.3 Hz), 138.5, 129.4, 129.0 (d, *J* = 7.9 Hz), 128.5, 128.5, 128.1, 127.0, 126.6, 115.3 (d, *J* = 21.2 Hz), 63.1, 51.4, 45.4.

^{19}F NMR (282 MHz, $CDCl_3$) δ -115.79.

MS (EI): *m*/*z* (relative intensity) 214 (36), 122 (3), 91 (100), 77 (3), 65 (15).

HRMS (EI, *m*/*z*): calcd. for $C_{21}H_{20}NF$ [M+H$^+$] 306.1658; found 3056.1665.

IR (ATR, neat, cm^{-1}): 3325(w), 3019(w), 2956(w), 2924(m), 2858(w), 2810(w), 1894(w), 1729(w), 1604(m), 1507(s), 1459(m), 1417(w), 1378(w), 1344(w), 1292(w), 1219(s), 1183(w), 1153(m), 1117(m), 1091(m), 1040(w), 1014(w), 960(w), 900(w), 833(s), 808(m), 780(m), 752(m), 718(m), 636(w), 575(m), 550(m), 507(w), 496(m), 475(w).

30cb:

R_f = 0.3 (*n*-pentane:EtOAc = 5:1, $KMnO_4$).

^{1}H NMR (400 MHz, CD_2Cl_2) δ 7.23 (d, *J* = 3.8 Hz, 4H), 7.19 – 7.08 (m, 4H), 7.06 (ddt, *J* = 7.3, 1.4, 0.7 Hz, 2H), 7.02 – 6.90 (m, 2H), 6.89 – 6.78 (m, 2H), 3.76 (dd, *J* = 7.4, 6.8 Hz, 1H), 3.53 (dd, *J* = 13.4, 0.7 Hz, 1H), 3.38 (d, *J* = 13.4 Hz, 1H), 2.81 (d, *J* = 7.1 Hz, 2H), 1.55 (s, 1H).

^{13}C NMR (101 MHz, CD_2Cl_2) δ 162.0 (d, *J* = 243.3 Hz), 144.0, 141.1, 135.2 (d, *J* = 3.3 Hz), 131.2 (d, *J* = 7.9 Hz), 128.7, 128.6, 128.3, 127.8, 127.5, 127.1, 115.3 (d, *J* = 21.1 Hz), 64.2, 51.7, 44.7.

^{19}F NMR (376 MHz, CD_2Cl_2) δ -117.80.

MS (EI): *m*/*z* (relative intensity) 304 (1), 196 (44), 109 (18), 91 (100), 65 (12).

HRMS (EI, *m*/*z*): calcd. for $C_{21}H_{20}NF$ [M+H$^+$] 306.1658; found 306.1660.

IR (ATR, neat, cm^{-1}): 3325(w), 3019(w), 2956(w), 2924(m), 2858(w), 2810(w), 1894(w), 1729(w), 1604(m), 1507(s), 1459(m), 1417(w), 1378(w), 1344(w), 1292(w), 1219(s), 1183(w), 1153(m), 1117(m), 1091(m), 1040(w), 1014(w), 960(w), 900(w), 833(s), 808(m), 780(m), 752(m), 718(m), 636(w), 575(m), 550(m), 507(w), 496(m), 475(w).

Synthesis of 4-(1-(benzylamino)-2-phenylethyl)benzonitrile (30da) and 4-(2-(benzylamino)-2-phenylethyl)benzonitrile (30db)

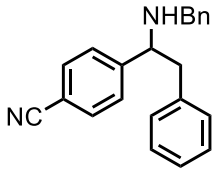

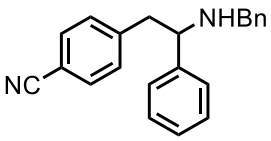

Compounds **30da** and **30db** were prepared following general procedure a with a reaction time of 24 h. Purification by column chromatography (*n*-pentane:EtOAc = 10:1) yielded the title compounds (46 mg, 0.15 mmol, 29%, **30da:30db** = 74:26) as a colorless oil. Analytically pure samples were obtained by flash chromatography (*n*-pentane:EtOAc = 20:1).

30da:

R_f = 0.3 (*n*-pentane:EtOAc = 9:1, $KMnO_4$).

^{1}H NMR (400 MHz, $CDCl_3$) δ 7.65 (d, *J* = 8.4 Hz, 2H), 7.50 (d, *J* = 8.3 Hz, 2H), 7.36 – 7.16 (m, 7H), 7.11 (ddt, *J* = 14.0, 5.5, 1.7 Hz, 4H), 3.98 (dd, *J* = 8.2, 6.0 Hz, 1H), 3.66 (d, *J* = 13.5 Hz, 1H), 3.49 (d, *J* = 13.5 Hz, 1H), 3.00 – 2.85 (m, 2H), 1.80 (s, 1H).

^{13}C NMR (101 MHz, $CDCl_3$) δ 149.6, 140.0, 137.8, 132.4, 129.3, 128.7, 128.5, 128.3, 127.9, 127.1, 126.9, 119.2, 111.0, 63.6, 51.6, 45.2.

MS (EI): *m*/*z* (relative intensity) 222 (16), 221 (82), 92 (15), 91 (100), 65 (24).

HRMS (ESI-TOF, *m*/*z*): calcd. for $C_{22}H_{21}N_2$ [M+H$^+$] 313.1705; found 313.1710.

IR (ATR, neat, cm^{-1}): 3326(w), 3084(w), 3061(w), 3027(w), 2919(w), 2840(w), 2226(m), 1950(w), 1808(w), 1647(w), 1605(w), 1583(w), 1494(m), 1453(m), 1411(w), 1349(w), 1301(w), 1200(w), 1177(w), 1155(w), 1103(w), 1076(w), 1028(w), 1019(w), 971(w), 909(w), 832(m), 733(s), 696(s), 647(w), 626(w), 605(w), 584(m), 562(s), 514(m), 479(m).

30db:

R_f = 0.1 (*n*-pentane:EtOAc = 9:1, $KMnO_4$).

^{1}H NMR (400 MHz, $CDCl_3$) δ 7.41 (d, *J* = 8.3 Hz, 1H), 7.30 – 7.09 (m, 11H), 7.09 – 6.99 (m, 4H), 3.78 (dd, *J* = 7.0 Hz, 1H), 3.73 (s, 1H), 3.58 (d, *J* = 13.4 Hz, 1H), 3.41 (d, *J* = 13.3 Hz, 1H), 3.00 – 2.83 (m, 2H).

^{13}C NMR (101 MHz, $CDCl_3$) δ 144.6, 142.7, 140.4, 140.3, 132.1, 130.3, 128.7, 128.5, 128.5, 128.3, 128.1, 127.6, 127.4, 127.1, 119.1, 110.3, 63.4, 53.3, 51.4, 45.2.

MS (EI): *m*/*z* (relative intensity) 221 (1), 197 (9), 196 (59), 116 (10), 91 (100), 89 (11), 65 (13).

HRMS (ESI-TOF, *m*/*z*): calcd. for $C_{22}H_{21}N_2$ [M+H$^+$] 313.1705; found 313.1705.

IR (ATR, neat, cm^{-1}): 3084(w), 3061(w), 3027(w), 2923(w), 2850(w), 2226(w), 1641(w), 1606(w), 1493(w), 1453(m), 1413(w), 1358(w), 1331(w), 1307(w), 1199(w), 1177(w), 1155(w), 1113(w), 1074(w), 1027(w), 1002(w), 970(w), 912(w), 848(w), 823(m), 733(m), 697(s), 616(w), 587(w), 562(m), 547(m), 486(w), 462(w), 426(w).

Synthesis of ethyl-4-(1-(benzylamino)-2-phenylethyl)benzoate (30ea) and ethyl-4-(2-(benzylamino)-2-phenylethyl)benzoate (30eb)

Compounds **30ea** and **30eb** were prepared following general procedure A with a reaction time of 24h. The products **30ea** and **30eb** (73 mg, 0.20 mmol, 40%, **30ea:30eb** = 66:34) were obtained after flash chromatography (*n*-pentane:EtOAc = 9:1) as colorless oil.

30ea:

R_f = 0.4 (*n*-pentane:EtOAc = 5:1, $KMnO_4$).

^{1}H NMR (300 MHz, $CDCl_3$) δ 8.11 – 8.01 (m, 2H), 7.51 – 7.41 (m, 2H), 7.33 – 7.20 (m, 6H), 7.17 – 7.05 (m, 4H), 4.42 (q, *J* = 7.1 Hz, 2H), 3.99 (dd, *J* = 7.9, 6.2 Hz, 1H), 3.68 (d, *J* = 13.5 Hz, 1H), 3.49 (d, *J* = 13.5 Hz, 1H), 3.04 – 2.89 (m, 2H), 1.91 (s, 1H), 1.44 (t, *J* = 7.1 Hz, 3H).

^{13}C NMR (75 MHz, $CDCl_3$) δ 168.3, 148.8, 141.3, 138.3, 129.9, 129.6, 129.4, 128.6, 128.5, 128.1, 127.6, 127.0, 126.7, 63.1, 58.4, 50.8, 43.2, 13.5.

MS (EI): *m*/*z* (relative intensity) 358 (1), 314 (1), 268 (42), 91 (100), 65 (9).

HRMS (ESI-TOF, *m*/*z*): calcd. for $C_{24}H_{25}NO_2$ [M+H^+] 360.1964; found 360.1969.

IR (ATR, neat, cm^{-1}): 3084(w), 3061(w), 3027(w), 2980(w), 2927(w), 2840(w), 1712(s), 1609(w), 1577(w), 1494(w), 1453(m), 1415(w), 1390(w), 1366(w), 1307(w), 1270(s), 1199(w), 1172(m), 1099(s), 1019(m), 979(w), 909(w), 858(w), 769(m), 742(m), 696(s), 657(w), 621(w), 604(w), 572(w), 550(m), 482(w).

30eb:

R_f = 0.3 (*n*-pentane:EtOAc = 5:1, $KMnO_4$).

^{1}H NMR (400 MHz, CD_2Cl_2) δ 7.93 – 7.86 (m, 2H), 7.38 – 7.10 (m, 12H), 4.34 (q, *J* = 7.1 Hz, 2H), 3.93 (dd, *J* = 7.4, 6.7 Hz, 1H), 3.64 (d, *J* = 13.4 Hz, 1H), 3.49 (d, *J* = 13.4 Hz, 1H), 3.07 – 2.94 (m, 2H), 1.68 (s, 1H), 1.37 (t, *J* = 7.1 Hz, 3H).

^{13}C NMR (101 MHz, CD_2Cl_2) δ 166.7, 144.8, 143.8, 141.0, 129.9, 129.7, 129.7, 129.1, 128.7, 128.6, 128.3, 127.8, 127.6, 127.1, 64.0, 51.7, 45.5, 14.5.

MS (EI): *m/z* (relative intensity) 358 (1), 314 (1), 197 (11), 196 (72), 91 (100), 65 (9).

HRMS (ESI-TOF, *m/z*): calcd. for $C_{24}H_{25}NO_2$ [M+H$^+$] 360.1964; found 360.1958.

IR (ATR, neat, cm^{-1}): 3327(w), 3061(w), 3027(w), 2980(w), 2926(w), 2850(w), 1947(w), 1809(w), 1714(s), 1610(w), 1575(w), 1493(w), 1453(m), 1415(w), 1391(w), 1366(w), 1309(w), 1274(s), 1199(w), 1178(m), 1103(s), 1022(m), 974(w), 912(w), 854(w), 762(m), 699(s), 651(w), 638(w), 612(w), 584(w), 553(w), 500(w), 462(w), 426(w).

Synthesis of *N*-benzyl-2-phenyl-1-(4-(trifluoromethyl)phenyl)ethan-1-amine (30fa) and *N*-benzyl-1-phenyl-2-(4-(trifluoromethyl)phenyl)ethan-1-amine (30fb)

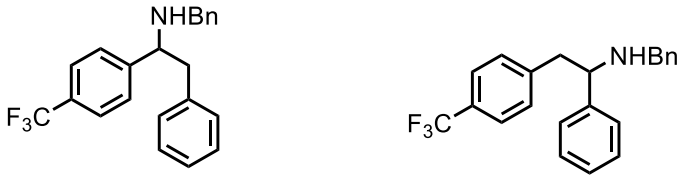

Compounds **23a** and **23b** were prepared following general procedure A, with a reaction time of 24 h. Purification by column chromatography (*n*-pentane:EtOAc = 20:1) yielded the title compound (49 mg, 0.14 mmol, 28%, **30fa:30fb** = 69:31) as colorless oil. Analytically pure samples were obtained by flash chromatography (*n*-pentane:EtOAc = 20:1).

30fa:

R$_f$ = 0.2 (*n*-pentane:EtOAc = 10:1, $KMnO_4$).

^{1}H NMR (300 MHz, $CDCl_3$) δ 7.61 (d, *J* = 8.1 Hz, 2H), 7.50 (d, *J* = 8.1 Hz, 2H), 7.27 (dqt, *J* = 5.5, 3.8, 1.9 Hz, 6H), 7.18 – 7.02 (m, 4H), 3.97 (dd, *J* = 8.4, 5.7 Hz, 1H), 3.66 (d, *J* = 13.5 Hz, 1H), 3.47 (d, *J* = 13.6 Hz, 1H), 3.05 – 2.81 (m, 2H).

^{13}C NMR (75 MHz, $CDCl_3$) δ 148.1, 140.2, 138.2, 129.4, 129.3, 128.7, 128.5, 128.0, 127.9, 127.0, 126.8, 125.5, 125.5, 63.4, 51.5, 45.3.

^{19}F NMR (282 MHz, $CDCl_3$) δ -62.30.

HRMS (ESI-TOF, *m/z*): calcd. for $C_{22}H_{20}NF_3$ [M+H$^+$] 356.1626; found 356.1631.

IR (ATR, neat, cm-1): 3330(w), 3085(w), 3063(w), 3028(w), 2920(w), 2846(w), 1948(w), 1807(w), 1618(w), 1603(w), 1585(w), 1495(w), 1454(w), 1417(w), 1322(s), 1161(m), 1118(s), 1065(s), 1029(w), 1017(m), 976(w), 909(w), 834(m), 734(m), 696(s), 649(w), 609(m), 565(w), 543(m), 515(w), 473(w).

30fb:

R$_f$ = 0.1 (n-pentane:EtOAc = 10:1, $KMnO_4$).

^{1}H NMR (300 MHz, $CDCl_3$) δ 7.53 – 7.45 (m, 2H), 7.38 – 7.21 (m, 9H), 7.15 (dddd, *J* = 9.5, 7.6, 1.8, 1.1 Hz, 4H), 3.88 (t, *J* = 7.0 Hz, 1H), 3.67 (d, *J* = 13.4 Hz, 1H), 3.49 (d, *J* = 13.4 Hz, 1H), 2.99 (d, *J* = 7.0 Hz, 2H).

^{13}C NMR (75 MHz, $CDCl_3$) δ 143.1, 140.4, 129.8, 128.6, 128.5, 128.1, 127.5, 127.5, 127.0, 125.3, 125.3 (q, *J* = 3.8 Hz), 63.5, 51.5, 45.1.

^{19}F NMR (282 MHz, $CDCl_3$) δ -62.30.

MS (EI): *m*/*z* (relative intensity) 354 (1), 196 (50), 91 (100), 65 (10).

HRMS (ESI-TOF, *m*/*z*): calcd. for $C_{22}H_{20}NF_3$ [M+H$^+$] 356.1626; found 356.1631.

IR (ATR, neat, cm^{-1}): 3085(w), 3063(w), 3028(w), 2920(w), 2846(w), 1948(w), 1807(w), 1618(w), 1603(w), 1585(w), 1495(w), 1454(w), 1417(w), 1322(s), 1161(m), 1118(s), 1065(s), 1029(w), 1017(m), 976(w), 909(w), 834(m), 734(m), 696(s), 649(w), 609(m), 565(w), 543(m), 515(w), 473(w).

Synthesis of *N*-benzyl-1-phenyl-2-(*p*-tolyl)ethan-1-amine (30ga) and *N*-benzyl-2-phenyl-1-(p-tolyl)ethan-1-amine (30gb)

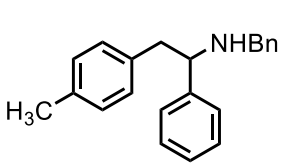

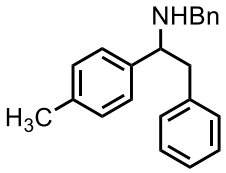

Compounds **30ga** and **30gb** were prepared following general procedure A with a reaction time of 24 h. Purification by column chromatography (*n*-pentane:EtOAc = 10:1) yielded the title compounds as inseparable mixture (101 mg, 0.34 mmol, 67%, **30ga**:**30gb** = 61:39) as a colorless oil.

R_f = 0.3 (*n*-pentane:EtOAc = 9:1, $KMnO_4$).

^{1}H NMR (300 MHz, CD_2Cl_2) δ 7.46 – 7.00 (m, 14H), 3.91 (ddd, *J* = 8.0, 6.0, 4.0 Hz, 1H), 3.65 (dd, *J* = 13.5, 0.8 Hz, 1H), 3.49 (dd, *J* = 13.4, 1.7 Hz, 1H), 3.03 – 2.83 (m, 2H), 2.36 (d, *J* = 12.5 Hz, 3H), 1.71 (s, 1H).

^{13}C NMR (75 MHz, CD_2Cl_2) δ 144.6, 141.3, 141.3, 139.6, 137.0, 136.2, 129.7, 129.5, 129.4, 129.4, 128.7, 128.7, 128.6, 128.3, 127.8, 127.7, 127.4, 127.0, 126.6, 64.3, 63.9, 51.8, 51.7, 45.6, 45.2, 21.3, 21.2. Collection of peaks of both isomers.

MS (EI): *m*/*z* (relative intensity) 300 (1), 210(27), 197 (12), 196 (76), 105 (11), 91 (100), 65 (11).

Synthesis of *N*-benzyl-2-(4-methoxyphenyl)-1-phenylethan-1-amine (30ha) and *N*-benzyl-1-(4-methoxyphenyl)-2-phenylethan-1-amine (30hb)

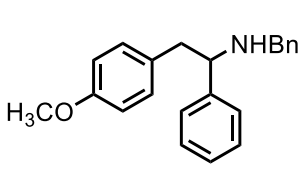

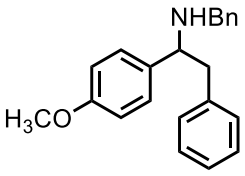

Compound **30h** was prepared following general procedure A with a reaction time of 24 h. Purification by column chromatography (*n*-pentane:EtOAc = 10:1) yielded the title compounds (33 mg, 0.10 mmol, 20%, **30ha:30hb** = 84:16) as a colorless oil.

R_f = 0.1 (*n*-pentane:EtOAc = 10:1, $KMnO_4$).

^{1}H NMR (300 MHz, $CDCl_3$) δ 7.30 – 7.06 (m, 8H), 7.06 – 6.87 (m, 4H), 6.82 – 6.65 (m, 2H), 3.83 – 3.62 (m, 4H), 3.57 (d, *J* = 13.5 Hz, 1H), 3.37 (d, *J* = 13.5 Hz, 1H), 2.96 – 2.54 (m, 2H), 1.65 (s, 1H).

^{13}C NMR (75 MHz, $CDCl_3$) δ 172.1, 171.2, 159.4, 153.9, 152.3, 149.9, 144.2, 143.6, 142.7, 141.8, 141.6, 141.3, 140.8, 140.4, 140.1, 139.7, 128.1, 77.2, 75.9, 68.2, 64.8, 64.7, 58.8, 57.8. Collection of peaks of both isomers.

MS (EI): *m*/*z* (relative intensity) 316 (1), 226 (5), 197 (15), 196 (100), 194 (9), 121 (6), 91 (67).

HRMS (ESI-TOF, *m*/*z*): calcd. for $C_{22}H_{23}NO$ [M+H^+] 318.1858; found 318.1858.

IR (ATR, neat, cm^{-1}): 3322(w), 3083(w), 3060(w), 3027(w), 3001(w), 2931(w), 2913(w), 2834(w), 1947(w), 1885(w), 1810(w), 1611(w), 1583(w), 1510(s), 1493(m), 1453(m), 1356(w), 1300(m), 1245(s), 1176(m), 1109(m), 1073(w), 1034(m), 975(w), 912(w), 822(m), 738(m), 698(s), 619(w), 597(w), 548(m), 519(w), 466(w), 442(w).

Synthesis of *N*-benzyl-2-(4-methoxyphenyl)-1-(4-(trifluoromethyl)phenyl)ethan-1-amine (30i)

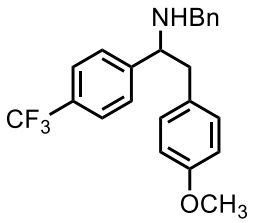

Compound **30i** was prepared following general procedure A. Purification by column chromatography (*n*-pentane:EtOAc = 20:1) yielded the title compound **30i** (40 mg, 0.13 mmol, 26%, 95:5) as a colorless oil.

R_f = 0.3 (*n*-pentane:EtOAc = 10:1, $KMnO_4$).

^{1}H NMR (300 MHz, $CDCl_3$) δ 7.54 – 7.43 (m, 2H), 7.42 – 7.34 (m, 2H), 7.23 – 7.08 (m, 3H), 7.05 – 6.97 (m, 2H), 6.95 – 6.87 (m, 2H), 6.75 – 6.65 (m, 2H), 3.81 (dd, *J* = 8.4, 5.6 Hz, 1H),

3.69 (s, 3H), 3.54 (d, *J* = 13.5 Hz, 1H), 3.35 (d, *J* = 13.5 Hz, 1H), 2.91 – 2.59 (m, 2H), 1.67 (s, 1H).

^{13}C NMR (101 MHz, $CDCl_3$) δ 158.4, 148.1, 140.1, 130.2, 130.1, 129.3 (q, *J* = 32.3 Hz), 128.4, 127.9, 127.8, 126.9, 125.4 (q, *J* = 3.7 Hz), 124.3 (q, *J* = 272.2 Hz), 113.9, 63.5, 55.3, 51.5, 44.4.

^{19}F NMR (282 MHz, $CDCl_3$) δ -62.20.

MS (EI): *m*/*z* (relative intensity) 384 (1), 265 (13), 264 (79), 262 (12), 121 (11), 91 (100).

HRMS (ESI-TOF, *m*/*z*): calcd. for $C_{23}H_{22}F_3NO$ [M+H$^+$] 386.1732; found 386.1727.

IR (ATR, neat, cm^{-1}): 3023(w), 3003(w), 2938(w), 2911(w), 2843(w), 1611(m), 1581(w), 1510(s), 1462(m), 1440(w), 1416(w), 1321(s), 1304(m), 1244(m), 1196(w), 1158(m), 1119(s), 1100(s), 1065(s), 1035(m), 1015(m), 953(w), 913(w), 887(w), 839(s), 802(m), 770(w), 731(m), 714(m), 696(s), 644(m), 602(m), 552(m), 539(m), 512(m).

Synthesis of *N*-benzyl-9,10-dihydrophenanthren-9-amine (30j)

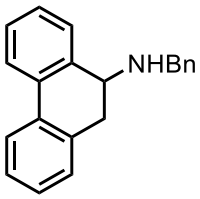

Compound **30j** was prepared following general procedure A. Purification by column chromatography (*n*-pentane:EtOAc = 20:1) yielded the title compound (43 mg, 0.15 mmol, 29%) as colorless solid.

R_f = 0.3 (*n*-pentane:EtOAc = 9:1, $KMnO_4$).

^{1}H NMR (300 MHz, $CDCl_3$) δ 7.70 (dd, *J* = 7.6, 5.4 Hz, 2H), 7.39 – 7.01 (m, 11H), 3.81 – 3.54 (m, 3H), 3.15 – 2.89 (m, 2H), 1.56 (s, 1H).

^{13}C NMR (75 MHz, $CDCl_3$) δ 140.5, 138.0, 134.3, 133.7, 133.5, 129.6, 128.4, 128.4, 128.2, 128.1, 127.9, 127.4, 127.3, 126.9, 124.4, 123.7, 54.6, 50.9, 35.4.

MS (EI): *m*/*z* (relative intensity) 285 (23), 284 (18), 206 (10), 194 (46), 180 (29), 179 (79), 178 (100), 177 (12), 176 (14), 165 (23), 152 (14), 106 (30), 91 (39).

HRMS (EI, *m*/*z*): calcd. for $C_{21}H_{19}N$ [M$^+$] 285.1507; found 285.1512.

IR (ATR, neat, cm^{-1}): 3334(w), 3061(w), 3025(w), 2922(w), 2848(w), 1946(w), 1915(w), 1811(w), 1642(w), 1601(w), 1583(w), 1493(w), 1483(w), 1452(m), 1361(w), 1319(w), 1265(w), 1240(w), 1202(w), 1157(w), 1130(w), 1102(w), 1075(w), 1046(w), 1027(w), 1005(w), 973(w), 945(w), 908(w), 872(w), 817(w), 782(w), 735(s), 695(s), 619(m), 602(m), 577(m), 562(m), 531(w), 511(w), 463(m).

Synthesis of *N*-(9,10-dihydrophenanthren-9-yl)adamantan-1-amine (30k)

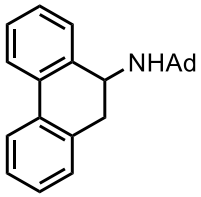

Compound **30k** was prepared following general procedure A. Purification by column chromatography (*n*-pentane:EtOAc = 20:1) yielded the title compound (43 mg, 0.14 mmol, 27%) as off-white solid.

$\mathbf{R_f}$ = 0.3 (*n*-pentane:EtOAc = 9:1, $KMnO_4$).

^{1}H NMR (400 MHz, $CDCl_3$) δ 7.72 (d, *J* = 7.5 Hz, 1H), 7.72 – 7.64 (m, 1H), 7.61 (ddd, *J* = 5.3, 2.8, 1.3 Hz, 1H), 7.32 – 7.22 (m, 3H), 7.21 – 7.17 (m, 2H), 4.05 (dd, *J* = 8.7, 4.8 Hz, 1H), 2.95 (dd, *J* = 14.8, 4.8 Hz, 1H), 2.82 (dd, *J* = 14.8, 8.7 Hz, 1H), 2.02 (p, *J* = 2.7 Hz, 3H), 1.66 (d, *J* = 2.8 Hz, 6H), 1.64 – 1.53 (m, 6H), 1.01 (s, 1H).

^{13}C NMR (101 MHz, $CDCl_3$) δ 142.1, 135.6, 134.5, 133.9, 129.1, 127.8, 127.5, 127.3, 127.2, 127.2, 124.0, 123.7, 51.4, 48.3, 44.1, 39.7, 36.9, 29.8.

MS (EI): *m*/*z* (relative intensity) 329 (8), 180 (15), 179 (60), 178 (100), 176 (10), 151 (10), 95 (15), 94 (95), 93 (14), 79 (14), 41 (12).

HRMS (EI, *m*/*z*): calcd. for $C_{24}H_{27}N$ [M^+] 329.2138; found 329.2137.

IR (ATR, neat, cm^{-1}): 3064(w), 3029(w), 2899(s), 2845(m), 2655(w), 2323(w), 1913(w), 1805(w), 1696(w), 1624(w), 1601(w), 1565(w), 1479(w), 1450(m), 1356(m), 1343(w), 1309(m), 1287(w), 1250(w), 1201(w), 1183(w), 1145(m), 1097(m), 1076(w), 1045(w), 1005(w), 990(w), 977(w), 938(w), 907(m), 873(w), 814(w), 781(w), 752(s), 736(s), 665(m), 640(m), 619(m), 555(w), 521(m), 503(m), 473(m), 457(m), 443(m), 418(m).

Synthesis of 1,2-diphenylethan-1-amine (24d)

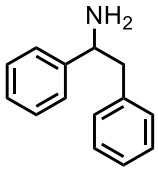

29f (287 mg, 1.00 mmol) and palladium on carbon (5wt% Pd on C, 107 mg, 0.05 mmol, 5.0 mol%) was suspended in absolute methanol (10 ml). The solution is flushed with a hydrogen filled balloon three times. The heterogeneous solution was heated to 50 °C for 3 h under hydrogen atmosphere. The mixture is cooled to room temperature and then filtered through a plug of celite and washed with methanol (20 mL). The filtrate was concentrated under reduced pressure and purified by column chromatography

(CH_2Cl_2:NH_4OH (10%, in MeOH) = 100:1). The title compound **24d** (165 mg, 0.84 mmol, 84%) was isolated as a colorless oil.

R_f = 0.3 (CH_2Cl_2:NEt_3 = 20:3, $KMnO_4$).

^{1}H NMR (300 MHz, CD_2Cl_2) δ 7.46 – 7.07 (m, 10H), 4.20 (dd, *J* = 8.7, 5.2 Hz, 1H), 3.01 (dd, *J* = 13.3, 5.2 Hz, 1H), 2.82 (dd, *J* = 13.3, 8.7 Hz, 1H), 1.46 (s, 2H).

^{13}C NMR (75 MHz, CD_2Cl_2) δ 146.8, 140.0, 129.9, 128.8, 128.8, 127.4, 127.0, 126.8, 58.1, 47.1.

MS (EI): *m*/*z* (relative intensity) 196 (1), 107 (11), 106 (100), 91 (21), 79 (37), 77 (28), 65 (14), 51 (11).

HRMS (EI, m/z): calcd. for $C_{14}H_{14}N$ [M^+] 196.1121; found 196.1129.

IR (ATR, neat, cm^{-1}): 3083(w), 3060(w), 3026(w), 2916(w), 2849(w), 1601(w), 1584(w), 1493(m), 1452(m), 1373(w), 1342(w), 1273(w), 1181(w), 1155(w), 1069(w), 1028(w), 1001(w), 984(w), 896(w), 821(w), 784(w), 756(s), 739(m), 695(s), 628(w), 608(w), 537(m), 502(w), 464(w).

Stability of α-stereogenic centers

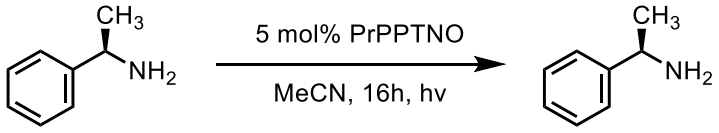

99:1 *e.r.* 99:1 *e.r.*

A solution containing enantiomeric pure (*R*)-1-phenylethan-1-amine (303 mg, 2.5 mmol) and **PrPPTNO** (11 mg, 5.0 mol%) in acetonitrile (5.0 mL) was irradiated at 396 nm for 16 h. The comparison of the HPLC traces before and after the reaction did not indicate any racemization of the α-stereogenic center of (*R*)-1-phenylethan-1-amine.

HPLC (ChiralCel, OJ-H, Heptan/EtOH 99:1, 0.5 mL/min flow rate, 210 nm): major enantiomer $\underline{t}_R$ = 25.4 min, minor enantiomer t_R = 31.0 min. Enantiomeric ratio: 99:1.

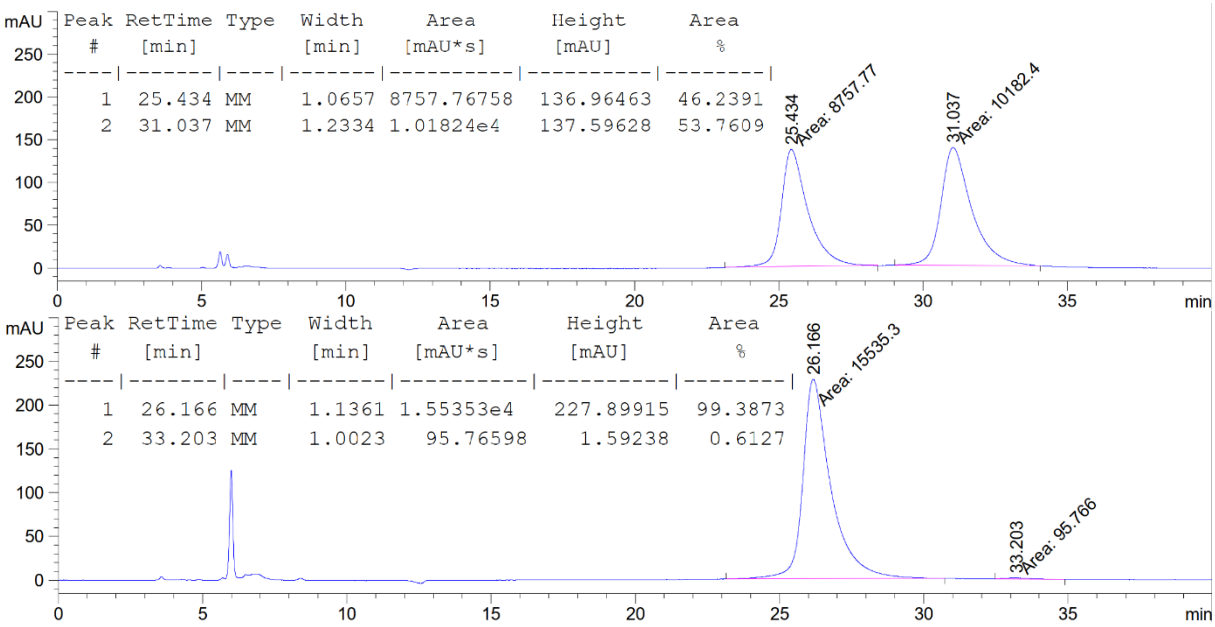

Stern-Volmer Experiments

Stern-Volmer quenching experiments were run with freshly prepared solutions of **PrPPT** (0.02 mM in dry CH_3CN) at room temperature under an inert atmosphere. The solutions were degassed by "freeze-pump-thaw" technique and then flushed with argon directly before measurement. The solutions were irradiated at 350 nm and luminescence was measured at 385 nm.

The data shows that *E*-stilbene (**(*E*)-26a**) (K_{SV} = 40.0 M^{-1}) and benzylamine (K_{SV} = 27.8 M^{-1}) are competent quencher for the excited state of **PrPPT**. For all tabular data, see Table 21 and 22 below.

Table 21. Fluorescence quenching data with solutions of PrPPT and E-stilbene (**(*E*)-26a**).

I_x [a.u.]	I_0/I_x [a.u.]	Q [mM]
I_0 = 848.2724	1	0
I_1 = 835.1589	1.0157	0.4975
I_2 = 824.2144	1.0292	0.9900
I_3 = 777.5056	1.0910	2.4390
I_4 = 703.3204	1.2061	4.7620
I_5 = 624.5875	1.3581	9.0909

Table 22. Fluorescence quenching data with solutions of PrPPT and benzylamine.

I_x [a.u.]	I_0/I_x [a.u.]	Q [mM]
I_0 = 869.5162	1	0

I_1 = 833.4047	1.0433	2.4752
I_2 = 780.9609	1.1134	4.9020
I_3 = 680.7875	1.2772	11.9048
I_4 = 549.2914	1.5830	22.7273
I_5 = 394.16885	2.2060	41.6667

EPR spectroscopy

EPR spectra were recorded on an X-band Bruker EMX CW-micro EPR spectrometer equipped with an ER4119HS high-sensitivity resonator using a microwave power of Ca 6.9 mW, modulation frequency of 100 kHz and modulation amplitude up to 5 G. For low temperature measurements, the EPR spectrometer was equipped with a temperature controller and liquid N2 cryostat. The hν =gβB_0 equation was used to calculate g values with ν and B_0 being the frequency and resonance field, respectively. 2,2-Diphenyl-1-picrylhydrazyl g values calibration was performed using 2,2-Diphenyl-1-picrylhydrazyl as a standard (g = 2.0036 ± 0.0004). EPR spectrum simulation was done by Bruker SimFonia software.

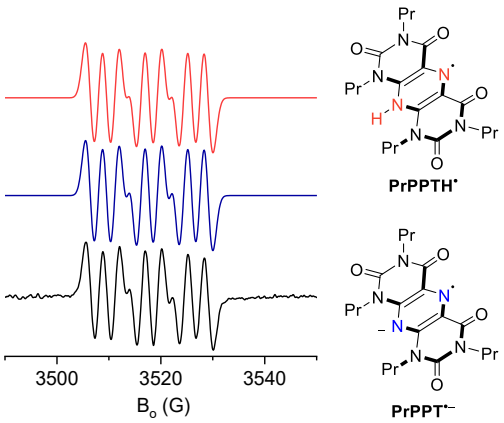

Figure 22. EPR spectrum of benzylamine and PrPPT (black line); blue and red lines are simulated spectra considering a hyperfine splitting from two nonequivalent N (blue line, AN1 = 8.25 G and AN2 = 3.25 G) and two nonequivalent N and one hydrogen (red line, AN1 = 8.25 G and AN2 = 3.25 G AH = 0.4 G).

6.23 Photocatalytic trifluoromethylation of arenes

Synthesis of 1,3,7-trimethyl-8-(trifluoromethyl)-3,7-dihydro-1H-purine-2,6-dione (32a)

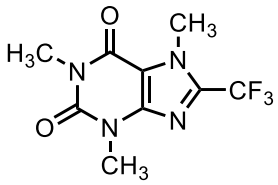

Compound **32a** was prepared following general procedure B with a reaction time of 48 h. Purification by column chromatography (*n*-pentane:EtOAc = 2:1) yielded **32a** as a (82 mg, 0.31 mmol, 62%) pale yellow solid.

R_f = 0.5 (*n*-pentane:EtOAc = 2:1, UV).

m.p. = 127–128 °C.

^{1}H NMR (300 MHz, $CDCl_3$) δ 4.14 (q, *J* = 1.2 Hz, 1H), 3.58 (s, 1H), 3.40 (s, 1H).

^{13}C NMR (75 MHz, $CDCl_3$) δ 155.6, 151.4, 146.6, 138.8 (q, *J* = 40.2 Hz), 116.5 (q, *J* = 271.3 Hz), 109.8, 33.3 (q, *J* = 1.9 Hz), 30.0, 28.3.

^{19}F NMR (282 MHz, $CDCl_3$) δ -62.41.

MS (EI): *m/z* (relative intensity) 262 (95), 243 (14), 193 (15), 177 (65), 82 (33), 81 (20), 69 (20), 67 (100), 66 (14), 56 (24), 55 (28), 54 (12), 42 (15), 40 (11).

HRMS (EI, *m/z*): calcd. for $C_9H_9N_4O_2F_3$ [M^+] 262.0672; found 262.0672.

IR (ATR, neat, cm^{-1}): 2966(w), 1705(m), 1661(s), 1607(m), 1543(m), 1508(m), 1468(m), 1426(m), 1408(m), 1385(w), 1339(m), 1288(m), 1247(m), 1219(m), 1201(m), 1175(s), 1123(s), 1098(s), 1036(m), 972(m), 944(m), 803(w), 763(m), 744(s), 733(m), 685(m), 605(m), 552(w), 496(m), 475(m), 440(m), 405(s).

3,7-dimethyl-8-(trifluoromethyl)-3,7-dihydro-1H-purine-2,6-dione (32b)

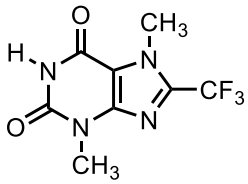

Compound **32b** was prepared following general procedure B with a reaction time of 48 h. Purification by column chromatography (DCM:MeOH = 100:3) yielded **32b** (46 mg, 0.19 mmol, 38%) as a pale yellow solid.

R_f = 0.2 (DCM:MeOH = 100:3, UV).

m.p. = 215 °C (decomp).

^{1}H NMR (300 MHz, DMSO-d_6) δ 11.47 (s, 1H), 4.08 – 3.98 (m, 5H), 3.34 (s, 3H).

^{13}C NMR (75 MHz, DMSO-d_6) δ 155.7, 151.1, 148.0, 137.5 (q, *J* = 40.3 Hz), 118.7 (q, *J* = 270.8 Hz), 110.4, 33.6, 29.0.

^{19}F NMR (282 MHz, DMSO-d_6) δ -61.29.

MS (EI): *m*/*z* (relative intensity) 248 (10), 428 (100), 229 (15), 177 (42), 82 (30), 81 (12), 70 (16), 69 (15), 67 (77), 66 (11), 55 (30).

HRMS (EI, *m*/*z*): calcd. for $C_8H_7N_4O_2F_3$ [M^+] 248.0516; found 248.0520.

IR (ATR, neat, cm^{-1}): 3155(w), 3118(w), 3018(w), 2962(w), 2922(w), 2852(w), 2831(w), 1696(s), 1595(m), 1546(m), 1506(m), 1462(m), 1424(m), 1407(m), 1381(m), 1350(m), 1292(m), 1245(m), 1215(m), 1187(s), 1167(s), 1138(s), 1122(s), 1098(s), 955(m), 865(m), 789(m), 767(m), 746(s), 740(s), 725(m), 700(m), 677(w), 637(w), 589(m), 552(w), 520(m), 473(s), 445(s).

Synthesis of 1,3-dimethyl-5-(trifluoromethyl)pyrimidine-2,4(1H,3H)-dione (33e)

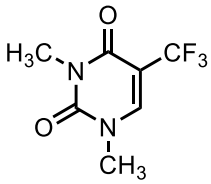

Compound **33e** was prepared following general procedure B with a reaction time of 48 h. Purification by column chromatography (*n*-pentane:EtOAc = 2:1) yielded **33e** (28 mg, 0.14 mmol, 28%) as a pale yellow solid.

R_f = 0.2 (*n*-pentane:EtOAc = 2:1, UV).

m.p. = 98–100 °C.

^{1}H NMR (300 MHz, $CDCl_3$) δ 7.68 (q, *J* = 1.2 Hz, 1H), 3.48 (s, 3H), 3.36 (s, 3H).

^{13}C NMR (75 MHz, $CDCl_3$) δ 158.7, 150.9, 143.6 (q, *J* = 5.8 Hz), 121.9 (q, *J* = 270.6 Hz), 104.1 (q, *J* = 32.8 Hz), 37.8, 28.0.

^{19}F NMR (282 MHz, $CDCl_3$) δ -63.81.

MS (EI): *m*/*z* (relative intensity) 208 (34), 189 (10), 188 (10), 150 (13), 123 (13), 75 (15), 69 (15), 60 (11), 56 (19), 53 (11), 42 (100).

HRMS (EI, *m*/*z*): calcd. for $C_7H_7N_2O_2F_3$ [M^+] 208.0454; found 208.0453.

IR (ATR, neat, cm^{-1}): 3083(w), 3045(w), 2994(w), 2923(w), 2853(w), 1774(w), 1721(m), 1658(s), 1641(s), 1564(w), 1519(w), 1495(s), 1458(s), 1440(m), 1402(m), 1386(s), 1355(m), 1324(s), 1210(s), 1159(m), 1116(s), 1070(s), 1018(s), 973(m), 962(s), 863(m), 815(w), 781(s), 758(s), 713(m), 699(s), 532(m), 499(s), 461(w).

Synthesis of 8-(difluoromethyl)-1,3,7-trimethyl-3,7-dihydro-1H-purine-2,6-dione (38a)

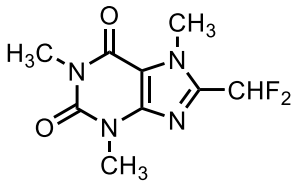

Compound **38a** was prepared following general procedure B with a reaction time of 48 h using difluoroaceticacid anhydride. Purification by column chromatography (DCM:MeOH = 200:3, UV) yielded **38a** (33 mg, 0.14 mmol, 28%) as a pale yellow solid.

R_f = 0.3 (DCM:MeOH = 100:3, UV).

m.p. = 159–161 °C.

^{1}H NMR (300 MHz, $CDCl_3$) δ 6.74 (t, *J* = 52.3 Hz, 1H), 4.14 (t, *J* = 1.2 Hz, 3H), 3.55 (s, 3H), 3.39 (s, 3H).

^{13}C NMR (75 MHz, $CDCl_3$) δ 155.7, 151.5, 147.0, 142.9 (t, *J* = 27.4 Hz), 109.9 (t, *J* = 238.0 Hz), 109.6, 33.0, 29.9, 28.2.

^{19}F NMR (282 MHz, $CDCl_3$) δ -115.02 (dd, *J* = 52.3, 1.1 Hz).

MS (EI): *m*/*z* (relative intensity) 244 (100), 193 (11), 159 (44), 67 (24), 55 (13).

HRMS (EI, *m*/*z*): calcd. for $C_9H_{10}N_4O_2F_2$ [M^+] 244.0766; found 244.0768.

IR (ATR, neat, cm^{-1}): 3028(w), 2959(w), 1706(m), 1664(s), 1603(m), 1548(m), 1504(w), 1457(m), 1428(m), 1409(m), 1387(w), 1364(w), 1337(m), 1289(m), 1255(w), 1224(m), 1164(w), 1089(s), 1037(s), 977(m), 954(w), 864(w), 820(s), 799(m), 762(m), 744(s), 732(s), 688(w), 620(w), 573(w), 544(m), 498(m), 460(s), 439(w), 422(m).

Synthesis of 1,3,7-trimethyl-8-(perfluoroethyl)-3,7-dihydro-1H-purine-2,6-dione (39a)

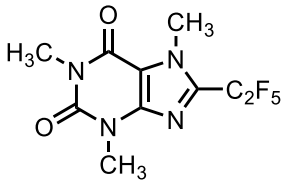

Compound **39a** was prepared following general procedure B with a reaction time of 48 h using pentafluoropropionicacid anhydride. Purification by column chromatography (*n*-pentane:EtOAc = 5:1) yielded **39a** (96 mg, 0.31 mmol, 62%) as a colorless solid.

R_f = 0.2 (*n*-pentane:EtOAc = 5:1, UV).

m.p. = 102–105 °C.

^{1}H NMR (300 MHz, $CDCl_3$) δ 4.16 (t, J = 1.8 Hz, 1H), 3.55 (s, 1H), 3.38 (s, 1H).

^{13}C NMR (75 MHz, $CDCl_3$) δ 155.5, 151.4, 147.0, 138.2, 137.8, 137.4, 120.6, 120.1, 119.7, 117.1, 116.3, 115.4, 112.8, 112.2, 110.1, 109.7, 109.1, 106.3, 105.8, 33.7, 30.0, 28.2.

^{19}F NMR (282 MHz, $CDCl_3$) δ -82.73 (t, *J* = 2.7 Hz, 3F), -111.41 – -111.54 (m, 2F).

MS (EI): *m*/*z* (relative intensity) 312 (100), 293 (12), 243 (14), 227 (57), 193 (24), 82 (26), 81 (13), 69 (10), 67 (80), 56 (12), 55 (35), 42 (13).

HRMS (EI, *m*/*z*): calcd. for $C_7H_7N_2O_2F_3$ [M^+] 312.0640; found 312.0634.

IR (ATR, neat, cm^{-1}): 2966(w), 1705(m), 1661(s), 1607(m), 1543(m), 1508(m), 1468(m), 1426(m), 1408(m), 1385(w), 1339(m), 1288(m), 1247(m), 1219(m), 1201(m), 1175(s), 1123(s), 1098(s), 1036(m), 972(m), 944(m), 803(w), 763(m), 744(s), 733(m), 685(m), 605(m), 552(w), 496(m), 475(m), 440(m), 405(s).

Kinetic Investigations for the photocatalytic trifluoromethylation

A reaction was set up using caffeine and TFAA as substrates following general procedure B. When the reaction solution was degassed, butylacetate (40 µl) was added in on portion. After 2, 4, 6, 8, 10, 12, 24, 30, 36, 48 h samples (0.1 ml) were taken and filtered through a plug of silica using methanol. The obtained curves are depicted in Figure 16 and discussed in chapter 5.3. The resulting calibration curve is presented Figure 21.

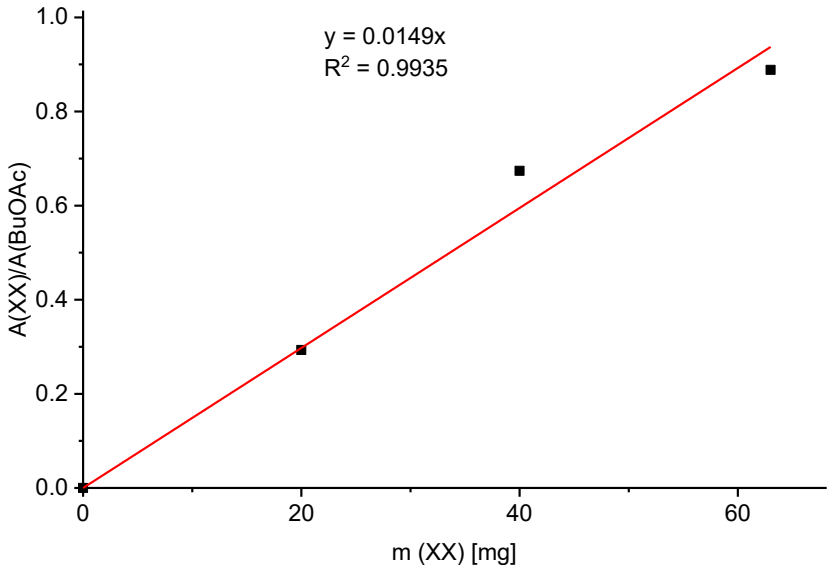

Figure 23. Calibration of GC/FID

Detection of CO

A reaction following general procedure B was set up using caffeine as substrate. After 48h the reaction was removed from the reactor. The reaction vessel was opened, and the CO detector was held approximately 30 cm above the neck. Then a stream of argon was used to drive the gaseous products out of the flask. The detector reacted fast with a loud sound showing the presence of CO.

6.24 Geometries obtained by DFT methods

Table 23. B3PW91 computed total electronic energy (HF, au), zero-point vibrational energies (ZPOE, au), number of imaginary frequencies (NImag), thermal corrected enthalpies (Htot, au) and Gibbs free energies (Gtot, au) under the consideration of van der Waals dispersion correction (GD3BJ) and solvation effect (SMD) of acetonitrile as solvent as well as the optimized coordinates of the equilibrium geometries (B3PW91-SMD-GD3BH//TZVP)

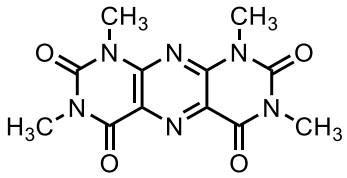	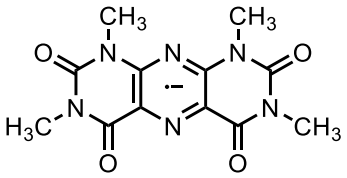
HF=-1094.0543315 ZPE=0.253986 NImag=0 Htot=-1093.779532 Gtot=-1093.850848	HF=-1094.1653212 ZPE=0.251072 NImag=0 Htot=-1093.893340 Gtot=-1093.963957
C,0,0.0430205681,-1.1406626907,1.0371580091 C,0,-0.0492883827,-1.1281858799,-0.3701942386 N,0,-0.0689044406,0.0060586894,-1.057810965 C,0,0.0023711528,1.1323557809,-0.3606110391 N,0,0.1134682379,-0.0098663827,1.7156075213 C,0,0.0951979267,1.1286691921,1.0467574796 N,0,-0.0165175395,2.3097426278,-1.0463085068 N,0,-0.1215581228,-2.2976338144,-1.0658566695 C,0,0.1729147119,2.3924654251,1.7900755581 C,0,0.0619846626,-2.4129254276,1.7697756708 O,0,0.140173208,-2.4962341277,2.9794509265 O,0,0.254680375,2.4618594559,3.0003923354 C,0,0.0534679349,3.5392801034,-0.4022016185 C,0,-0.1088442535,-3.5344787276,-0.4321471733 O,0,0.0362565376,4.5863323925,-1.0167160437 O,0,-0.1739311152,-4.5744018448,-1.0554981529 N,0,0.1449097811,3.5264717228,0.9836947748 N,0,-0.0183210291,-3.5375800319,0.9538637877 C,0,0.2164614941,4.8376392439,1.6207700143 H,0,-0.6768082701,5.4152804838,1.3860317666 H,0,1.0961898543,5.3753617395,1.2691229082 H,0,0.2835920838,4.6800468981,2.6923192028 C,0,-0.1133559469,2.2826774297,-2.5027782636 H,0,-1.0351331136,1.785188935,-2.8022055749 H,0,0.7387656766,1.7468798714,-2.919501932 H,0,-0.1144181127,3.3086844214,-2.85405457 C,0,-0.2159642356,-2.2538486523,-2.5220798643 H,0,-1.1144873954,-1.7133699381,-2.817687254 H,0,-0.2623158765,-3.27575648,-2.882138483	C,0,0.0442245144,-1.1597505472,1.072505924 C,0,-0.0468468719,-1.130569018,-0.3198034524 N,0,-0.0679400055,0.0059241625,-1.0315585335 C,0,0.0052356597,1.1341899786,-0.3102271667 N,0,0.1187862587,-0.0103724184,1.8070349116 C,0,0.0973639077,1.1473831987,1.082255847 N,0,-0.0153165659,2.3115357981,-1.027059732 N,0,-0.1212311329,-2.2996274123,-1.0465656526 C,0,0.172222189,2.4051577192,1.780282985 C,0,0.0607505591,-2.4254846189,1.7598821934 O,0,0.1380485794,-2.56583759,2.9794636518 O,0,0.2558420001,2.5314907469,3.0009796757 C,0,0.0528773737,3.5499708773,-0.4184828018 C,0,-0.110076005,-3.5449895475,-0.4484964275 O,0,0.0343827013,4.5951502182,-1.0587736428 O,0,-0.1762858388,-4.5827685075,-1.0976073856 N,0,0.1437004253,3.5509560942,0.9541286338 N,0,-0.0203627012,-3.5617340487,0.9240859364 C,0,0.2150998643,4.8610688473,1.5833004172 H,0,-0.6766363747,5.4437444397,1.3501983645 H,0,1.0929865128,5.4040557134,1.231913729 H,0,0.2831488529,4.7035024084,2.6552751275 C,0,-0.1122696679,2.2559250812,-2.4794512404 H,0,-1.0320523775,1.7523844363,-2.7764220218 H,0,0.7373659585,1.712939978,-2.8930357895 H,0,-0.1138488173,3.2763799196,-2.8485952451 C,0,-0.2149209916,-2.2273522525,-2.498437753 H,0,-1.1103177279,-1.6793322773,-2.7911410978 H,0,-0.263526243,-3.2434950775,-2.8761800397

H,0,0.6594641493,-1.7528836967,-2.9337696683 C,0,-0.0079730257,-4.8559718203,1.5798663407 H,0,-0.9259707683,-5.3903716837,1.3382699544 H,0,0.0635755224,-4.7106369532,2.6528608934 H,0,0.8472978052,-5.4301861008,1.2255429796	H,0,0.6590762858,-1.7207705085,-2.9074343076 C,0,-0.0096979664,-4.8790073349,1.542168674 H,0,-0.9263062455,-5.4187229347,1.3022934694 H,0,0.0629458571,-4.7337481481,2.6155789925 H,0,0.8435780874,-5.4581972158,1.1879238627
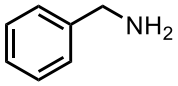	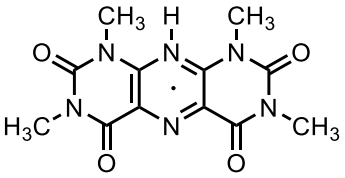
HF=-326.9350375 ZPE=0.145704 NImag=0 Htot=-326.781119 Gtot= -326.821509	HF=-1094.6265578 ZPE=0.263953 NImag=0 Htot=-1094.341155 Gtot= -1094.413940
H,0,-0.1908641546,0.1104189789,-0.0205400722 C,0,-0.1124248,0.0751935254,1.0616292666 C,0,0.0911262529,-0.0138306801,3.82643033 C,0,0.0059777175,-1.1587310566,1.6962204036 C,0,-0.1321908475,1.2565216026,1.7975109491 C,0,-0.0301996121,1.2146487898,3.1820333168 C,0,0.1093084713,-1.1891227243,3.0882053614 H,0,-0.2255839021,2.2091119888,1.2871678892 H,0,-0.045282129,2.13312393,3.7585481105 H,0,0.2060327141,-2.1446527526,3.5934453722 H,0,0.1675956145,-0.0535201793,4.9077819352 C,0,0.0476094361,-2.4349933957,0.8996842592 H,0,-0.2492777524,-2.2138419098,-0.1339938999 H,0,-0.6890848497,-3.1363384224,1.3025184718 N,0,1.3652571972,-3.0711621461,1.0002933533 H,0,1.3552086924,-3.9489766918,0.4905329443 H,0,2.0576276653,-2.4842592867,0.5448068748	C,0,0.052937162,-1.16087329,1.037213029 C,0,-0.0394852606,-1.1830063753,-0.3384251904 N,0,-0.051223917,0.0054987208,-1.0191889442 C,0,0.0157451372,1.1863826155,-0.3284289837 N,0,0.1298362395,-0.0104444542,1.7594941584 C,0,0.1062154482,1.1483798241,1.046988065 N,0,-0.010355097,2.3417028668,-1.0463429465 N,0,-0.1196026611,-2.329754728,-1.0660191653 C,0,0.1769614383,2.4088742575,1.7677358115 C,0,0.0666422699,-2.4293845092,1.7471627676 O,0,0.1461095936,-2.5335917281,2.9606385692 O,0,0.2598000739,2.4990045366,2.9821169712 C,0,0.0530523545,3.5796484748,-0.4129925002 C,0,-0.1115590955,-3.574669859,-0.4433069869 O,0,0.0292832945,4.6222374442,-1.0432906238 O,0,-0.1808301498,-4.6097250455,-1.0825951722 N,0,0.1434286361,3.5580372502,0.9605293303 N,0,-0.0212928576,-3.5688563226,0.930379292 C,0,0.2086383261,4.8632467372,1.6078393276 H,0,-0.6880549273,5.4391461388,1.380167776 H,0,1.084118819,5.4105422315,1.2593483061 H,0,0.2788375999,4.6956464525,2.6777277445 C,0,-0.1093437886,2.3137469526,-2.502462869 H,0,-1.0394301617,1.8327410559,-2.8106133652 H,0,0.7513115738,1.797803085,-2.9317381919 H,0,-0.1126848117,3.3416414087,-2.8484579412 C,0,-0.217289911,-2.284975098,-2.5218073348 H,0,-1.1218262639,-1.7547782864,-2.8252328944 H,0,-0.2732468922,-3.3085196083,-2.876095342 H,0,0.6683050742,-1.8100220974,-2.9476707813

	C,0,-0.0155940716,-4.8811152122,1.5665892867 H,0,-0.931111373,-5.418952877,1.3219227475 H,0,0.0473280883,-4.7256031416,2.6387663165 H,0,0.8422815131,-5.4597590724,1.2246509178 H,0,-0.1290558023,0.0115570526,-2.0253611839
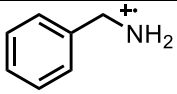	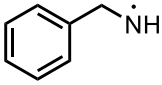
HF=-326.7192894 ZPE=0.143316 NImag=0 Htot=-326.567560 Gtot= -326.608526	HF=-326.2654655 ZPE=0.130612 NImag=0 Htot=-326.126750 Gtot= -326.167621
H,0,-0.4690100001,0.1899244561,-0.0294202539 C,0,-0.2628000473,0.1341283087,1.0337744145 C,0,0.283579542,-0.0196610176,3.758333239 C,0,0.0663581754,-1.0925212524,1.6096737965 C,0,-0.3181068795,1.2766263374,1.8177196367 C,0,-0.0424139547,1.2022399291,3.1797271053 C,0,0.3333085725,-1.1659065901,2.979176178 H,0,-0.5732833798,2.2283052137,1.3660388399 H,0,-0.089239492,2.0959437994,3.7915648771 H,0,0.559437304,-2.1230499889,3.4379123423 H,0,0.4866629513,-0.0819753023,4.8211817898 C,0,0.0973163228,-2.323241615,0.769966666 H,0,0.1062159306,-2.0794157997,-0.3133242984 H,0,-0.8232844253,-2.9245303607,0.863173277 N,0,1.1866858522,-3.174520229,1.01022325 H,0,1.1687566675,-4.1400505811,0.6870944652 H,0,2.0206525744,-2.8527057377,1.4994595411	H,0,-0.3301433976,0.1397530012,-0.0104160074 C,0,-0.1870589569,0.0943354558,1.064820089 C,0,0.1964283823,-0.0140850606,3.8093687621 C,0,0.0933174016,-1.1304573464,1.6676847333 C,0,-0.2766848848,1.2551562929,1.8243127305 C,0,-0.0852590831,1.2042892854,3.2003854175 C,0,0.2822620649,-1.1732868854,3.0478789188 H,0,-0.4917198151,2.2014205894,1.33970479 H,0,-0.1523987566,2.1088701238,3.7947500025 H,0,0.5047420817,-2.1215982946,3.5244733114 H,0,0.3472672507,-0.0621828207,4.8824934457 C,0,0.1497761758,-2.3865899112,0.8406980047 H,0,0.3503953306,-2.1342431679,-0.2130295645 H,0,-0.8517996422,-2.852801437,0.8140183751 N,0,1.1007559194,-3.3469726616,1.3047354994 H,0,1.0243039295,-4.1541111631,0.6780464919

7 References

[1] H. Trommsdorff, *Liebigs Ann.* **1834**, *11*, 190-207.
[2] A. Albini, M. Fagnoni, *ChemSusChem* **2008**, *1*, 63-66.
[3] H. D. Roth, *Pure Appl. Chem.* **2001**, *73*, 395-403.

[4] a) R. G. W. Norrish, F. W. Kirkbride, *J. Chem. Soc.* **1932**, 1518-1530; b) G. Ciamician, P. Silber, *Chem. Ber.* **1902**, *35*, 4128-4131.
[5] T. Matsuura, Y. Sata, K. Ogura, M. Mori, *Tetrahedron Lett.* **1968**, *9*, 4627-4630.
[6] J. W. Verhoeven, *Pure Appl. Chem.* **1996**, *68*, 2223-2286.
[7] M. Kasha, *Faraday Discuss.* **1950**, *9*, 14-19.
[8] A. Jablonski, *Nature* **1933**, *131*, 839-840.
[9] N. A. Romero, D. A. Nicewicz, *Chem. Rev.* **2016**, *116*, 10075-10166.
[10] D. Ravelli, D. Dondi, M. Fagnoni, A. Albini, *Chem. Soc. Rev.* **2009**, *38*, 1999-2011.
[11] H. Gerischer, *J. Electrochem. Soc.* **1978**, *125*, 218C.
[12] S. Protti, D. Dondi, M. Fagnoni, A. Albini, *Pure Appl. Chem.* **2007**, *79*, 1929-1938.
[13] M. Neumann, S. Füldner, B. König, K. Zeitler, *Angew. Chem. Int. Ed.* **2011**, *50*, 951-954.
[14] C. K. Prier, D. A. Rankic, D. W. C. MacMillan, *Chem. Rev.* **2013**, *113*, 5322-5363.
[15] a) Y. Lee, M. S. Kwon, *Eur. J. Org. Chem.* **2020**, *n/a*; b) S. Fukuzumi, K. Ohkubo, *Org. Biomol. Chem.* **2014**, *12*, 6059-6071.
[16] a) D. Ravelli, M. Fagnoni, A. Albini, *Chem. Soc. Rev.* **2013**, *42*, 97-113; b) J. M. R. Narayanam, C. R. J. Stephenson, *Chem. Soc. Rev.* **2011**, *40*, 102-113; c) T. P. Yoon, M. A. Ischay, J. Du, *Nat. Chem.* **2010**, *2*, 527-532.
[17] Y. Maki, M. Sako, E. C. Taylor, *Tetrahedron Lett.* **1971**, *12*, 4271-4274.
[18] M. Sako, S. Ohara, K. Hirota, K. Kano, Y. Maki, E. C. Taylor, *J. Org. Chem.* **1991**, *56*, 6302-6306.
[19] Adapted from Miguel A. Argüello Corderos master thesis.
[20] a) M. Sako, K. Shimada, K. Hirota, Y. Maki, *Tetrahedron Lett.* **1986**, *27*, 3877-3880; b) Y. Maki, K. Shimada, M. Sako, Y. Kitade, K. Hirota, *Chem. Pharm. Bull.* **1988**, *36*, 1714-1720; c) Y. Maki, I. Oyabu, S. Ohara, M. Sako, Y. Kitade, K. Hirota, *Chem. Pharm. Bull.* **1989**, *37*, 3239-3242.
[21] M. Sako, K. Shimada, K. Hirota, Y. Maki, *J. Am. Chem. Soc.* **1986**, *108*, 6039-6041.
[22] M. Sako, S. Ohara, K. Shimada, K. Hirota, Y. Maki, *Perkin Trans.* **1990**, 863-868.
[23] Y. Maki, K. Shimada, M. Sako, K. Hirota, *Tetrahedron* **1988**, *44*, 3187-3194.
[24] a) M. Sako, S. Ohara, K. Hirota, Y. Maki, *Tetrahedron* **1990**, *46*, 4171-4178; b) M. Sako, S. Ohara, K. Hirota, Y. Maki, *Chem. Pharm. Bull.* **1990**, *38*, 2676-2680; c) M. Sako, K. Hirota, Y. Maki, *Chem. Pharm. Bull.* **1990**, *38*, 2069-2071; d) Y. Maki, M. Sako, I. Oyabu, T. Murase, Y. Kitade, K. Hirota, *ChemComm* **1989**, 1780-1782.
[25] J. J. Warren, T. A. Tronic, J. M. Mayer, *Chem. Rev.* **2010**, *110*, 6961-7001.
[26] A. Petrosyan, R. Hauptmann, J. Pospech, *Eur. J. Org. Chem.* **2018**, *2018*, 5237-5252.
[27] D. M. Arias-Rotondo, J. K. McCusker, *Chem. Soc. Rev.* **2016**, *45*, 5803-5820.
[28] J. B. G. LAMBERT, *Spektroskopie: Strukturaufklärung in der Organischen Chemie*, Pearson Deutschland, **2012**.
[29] F. Scholz, *ChemTexts* **2015**, *1*, 17.
[30] H. G. Roth, N. A. Romero, D. A. Nicewicz, *Synlett* **2016**, *27*, 714-723.
[31] N. P. Ramirez, B. König, J. C. Gonzalez-Gomez, *Org. Lett.* **2019**, *21*, 1368-1373.
[32] A. Kotaki, K. Yagi, *J. Biochem.* **1970**, *68*, 509-516.
[33] K. A. Margrey, D. A. Nicewicz, *Acc. Chem. Res.* **2016**, *49*, 1997-2006.
[34] A. N. Masayuki Kuzuya, Yoshifumi Maki, Magoichi Saki, *Chem. Pharm. Bull.* **1991**, *39*, 3110-3113.
[35] M. Sowmiya, A. K. Tiwari, Sonu, S. K. Saha, *J. Photochem. Photobiol. A* **2011**, *218*, 76-86.
[36] A. Mallick, S. Maiti, B. Haldar, P. Purkayastha, N. Chattopadhyay, *Chem. Phys. Lett.* **2003**, *371*, 688-693.
[37] T. S. Pokidova, E. T. Denisov, A. F. Shestakov, *Pet. Chem.* **2008**, *48*, 174-185.
[38] Z. W. Zuo, D. W. C. MacMillan, *J. Am. Chem. Soc.* **2014**, *136*, 5257-5260.
[39] T. Niyazkhonov, A. Y. Veveris, L. B. Kuznetsova, *Chem. Nat. Compd.* **1983**, *19*, 467-469.
[40] X. Shao, Y. Zheng, L. Tian, I. Martín-Torres, A. M. Echavarren, Y. Wang, *Org. Lett.* **2019**, *21*, 9262-9267.

[41] F. El-Hage, C. Schöll, J. Pospech, *J. Org. Chem.* **2020**.
[42] a) J. W. Kuck, R. M. Reich, F. E. Kuhn, *Chem. Rec.* **2016**, *16*, 349-364; b) M. Crucianelli, R. Saladino, F. De Angelis, *ChemSusChem* **2010**, *3*, 524-540.
[43] C. Coperet, H. Adolfsson, T. A. V. Khuong, A. K. Yudin, K. B. Sharpless, *J. Org. Chem.* **1998**, *63*, 1740-1741.
[44] S. Caron, N. M. Do, J. E. Sieser, *Tetrahedron Lett.* **2000**, *41*, 2299-2302.
[45] S. Rozen, A. Shaffer, *Org. Lett.* **2017**, *19*, 4707-4709.
[46] H. T. Liu, L. Zhang, Y. L. Guo, C. Cheng, L. J. Yang, L. Jiang, G. Yu, W. P. Hu, Y. Q. Liu, D. B. Zhu, *J. Mater. Chem. C* **2013**, *1*, 3104-3109.
[47] M. Jesberger, T. P. Davis, L. Barner, *Synthesis* **2003**, *2003*, 1929-1958.
[48] a) J. D. Coyle, *Tetrahedron* **1985**, *41*, 5393-5425; b) A. Maciejewski, R. P. Steer, *Chem. Rev.* **1993**, *93*, 67-98.
[49] a) *Org. Process Res. Dev.* **2005**, *9*, 1016-1016; b) R. D. Taylor, M. MacCoss, A. D. G. Lawson, *J. Med. Chem.* **2014**, *57*, 5845-5859; c) D. O'Hagan, *Nat. Prod. Rep.* **2000**, *17*, 435-446.
[50] a) X. Lin, G. D. Artman, D. Stien, S. M. Weinreb, *Tetrahedron* **2001**, *57*, 8779-8791; b) T. M. Nguyen, D. A. Nicewicz, *J. Am. Chem. Soc.* **2013**, *135*, 9588-9591; c) A. J. Musacchio, L. Q. Nguyen, G. H. Beard, R. R. Knowles, *J. Am. Chem. Soc.* **2014**, *136*, 12217-12220; d) J. Davies, S. G. Booth, S. Essafi, R. A. W. Dryfe, D. Leonori, *Angew. Chem.* **2015**, *54*, 14017-14021; e) J. Davies, T. D. Svejstrup, D. Fernandez Reina, N. S. Sheikh, D. Leonori, *J. Am. Chem. Soc.* **2016**, *138*, 8092-8095; f) A. J. Musacchio, B. C. Lainhart, X. Zhang, S. G. Naguib, T. C. Sherwood, R. R. Knowles, *Science* **2017**, *355*, 727-730; g) M. D. Kärkäs, *ACS Catal.* **2017**, *7*, 4999-5022.
[51] L. Stella, *Angew. Chem.* **1983**, *22*, 337-350.
[52] J. H. Horner, F. N. Martinez, O. M. Musa, M. Newcomb, H. E. Shahin, *J. Am. Chem. Soc.* **1995**, *117*, 11124-11133.
[53] a) C. Grohmann, H. Wang, F. Glorius, *Org. Lett.* **2012**, *14*, 656-659; b) J.-C. Guillemin, J.-M. Denis, *Tetrahedron* **1988**, *44*, 4431-4446.
[54] J. Seayad, A. Tillack, C. G. Hartung, M. Beller, *Adv. Synth. Catal.* **2002**, *344*, 795-813.
[55] V. P. Andreev, V. V. Vapirov, Y. P. Nizhnik, L. A. Aleshina, T. A. Semenova, *Russ. J. Gen. Chem.* **2008**, *78*, 973-983.
[56] M. Yasuda, T. Isami, J. Kubo, M. Mizutani, T. Yamashita, K. Shima, *J. Org. Chem.* **1992**, *57*, 1351-1354.
[57] N. A. Romero, K. A. Margrey, N. E. Tay, D. A. Nicewicz, *Science* **2015**, *349*, 1326-1330.
[58] H.-B. Yang, A. Feceu, D. B. C. Martin, *ACS Catal.* **2019**, *9*, 5708-5715.
[59] S. Fukuzumi, K. Shimoosako, T. Suenobu, Y. Watanabe, *J. Am. Chem. Soc.* **2003**, *125*, 9074-9082.
[60] a) K. Nakajima, Y. Miyake, Y. Nishibayashi, *Acc. Chem. Res.* **2016**, *49*, 1946-1956; b) O. Kei, N. Takashi, F. Shunichi, *Bull. Chem. Soc. Jpn.* **2006**, *79*, 1489-1500.
[61] a) B. Huang, C. Yang, J. Zhou, W. Xia, *Chem. Commun.* **2020**, *56*, 5010-5013; b) B. Nyasse, L. Grehn, H. L. S. Maia, L. S. Monteiro, U. Ragnarsson, *J. Org. Chem.* **1999**, *64*, 7135-7139.
[62] K. Saito, A. Kawamura, T. Kanie, Y. Ueda, S. Kondo, *Heterocycles* **2001**, *55*, 1071-1080.
[63] R. R. Bodalia, R. S. Duran, *J. Am. Chem. Soc.* **1993**, *115*, 11467-11474.
[64] a) P. M. Wojciechowski, W. Zierkiewicz, D. Michalska, P. Hobza, *The Journal of Chemical Physics* **2003**, *118*, 10900-10911; b) X. Chen, X. Wang, Y. Sui, Y. Li, J. Ma, J. Zuo, X. Wang, *Angew. Chem. Int. Ed.* **2012**, *51*, 11878-11881.
[65] J. S. D. Kumar, S. Das, *Res. Chem. Intermed.* **1997**, *23*, 755-800.
[66] J. B. Metternich, D. G. Artiukhin, M. C. Holland, M. von Bremen-Kühne, J. Neugebauer, R. Gilmour, *J. Org. Chem.* **2017**, *82*, 9955-9977.
[67] M. Padilla, F. Peccati, J. L. Bourdelande, X. Solans-Monfort, G. Guirado, M. Sodupe, J. Hernando, *Chem. Commun.* **2017**, *53*, 2126-2129.
[68] A. Adenier, M. M. Chehimi, I. Gallardo, J. Pinson, N. Vilà, *Langmuir* **2004**, *20*, 8243-8253.
[69] a) D. H. Waldeck, *Chem. Rev.* **1991**, *91*, 415-436; b) G. S. Hammond, J. Saltiel, *J. Am. Chem. Soc.* **1962**, *84*, 4983-4984.

[70] a) O. E. Edwards, D. H. Paskovich, A. H. Reddoch, *Can. J. Chem.* **1973**, *51*, 978-980; b) S. Terabe, R. Konaka, *J. Am. Chem. Soc.* **1969**, *91*, 5655-5657.
[71] a) G. Landelle, M. Bergeron, M. O. Turcotte-Savard, J. F. Paquin, *Chem. Soc. Rev.* **2011**, *40*, 2867-2908; b) S. Arimori, N. Shibata, *Org. Lett.* **2015**, *17*, 1632-1635.
[72] a) J. Wang, M. Sánchez-Roselló, J. L. Aceña, C. del Pozo, A. E. Sorochinsky, S. Fustero, V. A. Soloshonok, H. Liu, *Chem. Rev.* **2014**, *114*, 2432-2506; b) K. Müller, C. Faeh, F. Diederich, *Science* **2007**, *317*, 1881-1886.
[73] W. K. Hagmann, *J. Med. Chem.* **2008**, *51*, 4359-4369.
[74] J. Charpentier, N. Früh, A. Togni, *Chem. Rev.* **2015**, *115*, 650-682.
[75] S. Barata-Vallejo, A. Postigo, *Chem. Eur. J.* **2020**, *26*, 11065-11084.
[76] Price per mole was calculated from the largest quantitiy avalable from Sigma Aldrich in april 2020.
[77] V. N. Andreev, V. A. Grinberg, A. G. Dedov, A. S. Loktev, N. A. Mayorova, I. I. Moiseev, A. A. Stepanov, *Russ. J. Electrochem.* **2013**, *49*, 996-1000.
[78] J. Lin, Z. Li, J. Kan, S. J. Huang, W. P. Su, Y. D. Li, *Nat. Commun.* **2017**, *8*.
[79] a) M. M. Maricq, J. J. Szente, G. A. Khitrov, T. S. Dibble, J. S. Francisco, *J. Phys. Chem. A* **1995**, *99*, 11875-11882; b) M. R. Nimlos, J. A. Soderquist, G. B. Ellison, *J. Am. Chem. Soc.* **1989**, *111*, 7675-7681.
[80] a) K. S. Egorova, V. P. Ananikov, *Organometallics* **2017**, *36*, 4071-4090; b) S. J. Stohs, D. Bagchi, *Free Radical Biol. Med.* **1995**, *18*, 321-336.
[81] a) A. Steinmetz, *ACROS ORGANICS*; b) T. Flessner, S. Doye, *J. Prakt. Chem.* **1999**, *341*, 186-190.
[82] R. Rabie, M. M. Hammouda, K. M. Elattar, *Res. Chem. Intermed.* **2017**, *43*, 1979-2015.
[83] F. Lehmann, *Synlett* **2004**, *2004*, 2447-2448.
[84] S. Crespi, S. Jäger, B. König, M. Fagnoni, *Eur. J. Org. Chem.* **2017**, *2017*, 2147-2153.
[85] a) N. Spătaru, B. V. Sarada, D. A. Tryk, A. Fujishima, *Electroanalysis* **2002**, *14*, 721-728; b) The oxidationpotential is strongly affected by pH value. No oxidationvalue in acetonitrile was found in literature. The used value was measure in aqueous buffer solution. .
[86] a) G. Porter, R. W. Yip, J. M. Dunston, A. J. Cessna, S. E. Sugamori, *J. Chem. Soc. Faraday Trans.* **1971**, *67*, 3149-3154; b) R. E. Rebbert, P. Ausloos, *J. Am. Chem. Soc.* **1965**, *87*, 5569-5572.
[87] a) M. Brandys, R. E. Sassoon, J. Rabani, *J. Phys. Chem. A* **1987**, *91*, 953-962; b) N. V. Raghavan, S. Steenken, *J. Am. Chem. Soc.* **1980**, *102*, 3495-3499; c) S. Steenken, P. O'Neill, *J. Phys. Chem. A* **1977**, *81*, 505-508.
[88] A. F. Garrido-Castro, A. Gini, M. C. Maestro, J. Aleman, *Chem. Commun.* **2020**, *56*, 3769-3772.
[89] X. Lu, X.-X. Li, Y.-M. Lee, Y. Jang, M. S. Seo, S. Hong, K.-B. Cho, S. Fukuzumi, W. Nam, *J. Am. Chem. Soc.* **2020**, *142*, 3891-3904.
[90] L. A. Badovskaya, L. V. Povarova, *Chemistry of Heterocyclic Compounds* **2009**, *45*, 1023.
[91] Y. Ouyang, X. H. Xu, F. L. Qing, *Angew. Chem.* **2018**, *57*, 6926-6929.
[92] S. Lips, B. A. Frontana-Uribe, M. Dörr, D. Schollmeyer, R. Franke, S. R. Waldvogel, *Chem. Eur. J.* **2018**, *24*, 6057-6061.
[93] J. W. Beatty, J. J. Douglas, K. P. Cole, C. R. J. Stephenson, *Nat. Commun.* **2015**, *6*, 7919.
[94] T. M. Shaikh, F.-E. Hong, *Beilstein J. Org. Chem.* **2013**, *9*, 1578-1588.
[95] G. W. T. M. J. Frisch, H. B. Schlegel, G. E. Scuseria, M. A., J. R. C. Robb, G. Scalmani, V. Barone, G. A. Petersson, H. Nakatsuji, X. Li, M., A. M. Caricato, J. Bloino, B. G. Janesko, R. Gomperts, B. Mennucci, H. P. Hratchian, J., A. F. I. V. Ortiz, J. L. Sonnenberg, D. Williams-Young, F. Ding, F. Lipparini, F. Egidi, J., B. P. Goings, A. Petrone, T. Henderson, D. Ranasinghe, V. G. Zakrzewski, J. Gao, N. Rega,, W. L. G. Zheng, M. Hada, M. Ehara, K. Toyota, R. Fukuda, J. Hasegawa, M. Ishida, T., Y. H. Nakajima, O. Kitao, H. Nakai, T. Vreven, K. Throssell, J. A. Montgomery, Jr., J. E., F. O. Peralta, M. Bearpark, J. J. Heyd, E. Brothers, K. N. Kudin, V. N. Staroverov, T. Keith,, J. N. R. Kobayashi, K. Raghavachari, A. Rendell, J. C.

Burant, S. S. Iyengar, J. Tomasi, M., J. M. M. Cossi, M. Klene, C. Adamo, R. Cammi, J. W. Ochterski, R. L. Martin, K., O. F. Morokuma, J. B. Foresman, and D. J. Fox, , *Gaussian, Inc., Wallingford CT,* **2016**.

[96] J. M. M. T. A. Keith, *Semichem Inc., Shawnee Mission, KS,* **2016**.

[97] a) R. Głaszczka, J. Jaźwiński, *J. Mol. Struct.* **2014**, *1061*, 150-159; b) T. Tandarić, R. Vianello, *J. Phys. Chem. A* **2018**, *122*, 1464-1471; c) N. V. Belova, G. V. Girichev, V. E. Kotova, K. A. Korolkova, N. H. Trang, *J. Mol. Struct.* **2018**, *1156*, 210-215.

[98] C. Würth, M. Grabolle, J. Pauli, M. Spieles, U. Resch-Genger, *Nat. Protoc.* **2013**, *8*, 1535-1550.

[99] K. Suzuki, A. Kobayashi, S. Kaneko, K. Takehira, T. Yoshihara, H. Ishida, Y. Shiina, S. Oishic, S. Tobita, *Phys. Chem. Chem. Phys.* **2009**, *11*, 9850-9860.

[100] N. D. Ca', P. Bottarelli, A. Dibenedetto, M. Aresta, B. Gabriele, G. Salerno, M. Costa, *J. Catal.* **2011**, *282*, 120-127.

[101] H. O. Kim, X.-d. Ji, N. Melman, M. E. Olah, G. L. Stiles, K. A. Jacobson, *J. Med. Chem.* **1994**, *37*, 3373-3382.

8 Anhang

Curriculum Vitae

Name:	**Richy, Hauptmann M.Sc.**
Date of birth:	April 15th, 1992
Current Address:	Brahestraße 23 D-18059 Rostock.
E-mail:	rix_190@hotmail.de

Education

Since 09/2017	**PhD Thesis** in Chemistry Advisor: Prof. Dr. J. de Vries / Dr. J. Pospech Leibniz Institute for Catalysis, Rostock, Germany.
10/2015-09/2017	**Master of Science** in Chemistry Advisor: Prof. Dr. Dr. h.c. mult. P. Langer University of Rostock, Germany.
10/2012-09/2015	**Bachelor of Science** in Chemistry Advisor: Prof. Dr. A. Schulz University of Rostock, Germany.
10/2011-09/2012	**Bachelor of Science** in Physics University of Rostock, Germany.
06/2011	**Highschool Graduation** Thomas-Mann-Oberschule, Berlin, Germany.

Additional Volunteering & Practical Experiences

2018-2019	**Guided Tours** "*Lange Nacht der Wissenschaft"* Rostock.
04/2016-10/2016	**Research Assistant** Advisor: Dr. R. Francke University of Rostock, Germany.

Poster Presentations:

07/2019	**26th International symposium: Synthesis in organic chemistry**, Cambridge, UK **R. Hauptmann**, J. Pospech. *"Photo-mediated intermolecular Hydroamination of activated Olefins using Primary Amines"*
09/2018	**26. Lecture Conference on Photochemistry**, Munich, Germany **R. Hauptmann**, J. Pospech. *"Oxyfunctionalization through Photoinduced Oxygen Atom Transfer"*
07/2018	**Alumni Meeting LIKAT,** Rostock, Germany **R. Hauptmann**, A. Petrosyan, J. Pospech. *"Oxyfunctionalization through Photoinduced Oxygen Atom Transfer using, N-substituted Pyrimio[5,4-g]pteridines"*
04/2018	JCF-Posterparty, University Rostock, Rostock, Germany **R. Hauptmann**, A. Petrosyan, J. Pospech. *"Oxyfunctionalization through Photoinduced Oxygen Atom Transfer using, N-substituted Pyrimio[5,4-g]pteridines"*

1. R. Hauptmann, A. Petrosyan, F. Fennel, M. A. Cordero, A. Surkus, J. Pospech, *Chem. Eur. J.* **2019**, 25, 4325–4329 *"Pyrimidopteridine N-Oxide Organic Photoredox Catalysts: Characterization, Application and Non-Covalent Interaction in Solid State"*
2. A. Petrosyan, R. Hauptmann, J. Pospech, *Eur. J. Org. Chem.* **2018**, 73, 5237–5252. *„Heteroarene N-Oxides as Oxygen Source in Organic Reactions"*
3. H. H. Do, R. Hauptmann, A. Villinger, A.Surkus, S. Lochbrunner, P. Ehlers, P. Langer, *Tetrahedron*, **2017**, 38, 3407–3414. "*Palladium-catalyzed synthesis and fluorescence study of 2,3-diaryl-5-ethynylbenzo[e]indoles"*